port No. FHWA/RD-81/087

ETECTION OF FLAWS IN REINFORCING STEEL IN PRESTRESSED CONCRETE BRIDGE MEMBERS

April 1981
Final Report

Document is available to the public through
the National Technical Information Service,
Springfield, Virginia 22161

Prepared for
FEDERAL HIGHWAY ADMINISTRATION
Offices of Research & Development
Structures and Applied Mechanics Division
Washington, D.C. 20590

FOREWORD

This report presents the development of a practical nondestructive
evaluation (NDE) device to detect loss of section and/or breaks in
reinforcing steel in prestressed concrete bridge members. In the
course of the research fifteen NDE methods were assessed. The magnetic
field disturbance method reported here was selected as having the best
chance for success in achieving the objective of the study.

This report is being distributed by memorandum to research engineers
concerned with the deterioration of prestressed concrete bridge members.

Research in bridge inspection and evaluation is included in the Federally
Coordinated Program of Highway Research and Development as Task 2
"Structural Integrity of Inservice Bridges" of Project 5L, "Safe Life
Design for Bridges." Mr. Charles H. McGogney is the Task Manager.

Charles F. Scheffey
Director, Office of Research
Federal Highway Administration

NOTICE

This document is disseminated under the sponsorship of the Department
of Transportation in the interest of information exchange. The United
States Government assumes no liability for its contents or use thereof.
The contents of this report reflect the views of the contractor, who is
responsible for the accuracy of the data presented herein. The contents
do not necessarily reflect the official views or policy of the Depart-
ment of Transportation. This report does not constitute a standard,
specification, or regulation.

The United States Government does not endorse products or manufacturers.
Trade or manufacturers' names appear herein only because they are con-
sidered essential to the object of this document.

Technical Report Documentation Page

1. Report No. FHWA/RD-81/087	2. Government Accession No.	3. Recipient's Catalog No.

4. Title and Subtitle DETECTION OF FLAWS IN REINFORCING STEEL IN PRESTRESSED CONCRETE BRIDGE MEMBERS	5. Report Date April 1981
	6. Performing Organization Code

7. Author(s) F. N. Kusenberger, J. R. Barton	8. Performing Organization Report No. 15-4543

9. Performing Organization Name and Address Southwest Research Institute Division of Instrumentation 6220 Culebra Road, P.O. Drawer 28510 San Antonio, Texas 78284	10. Work Unit No. (TRAIS) 35F1-042
	11. Contract or Grant No. DOT-FH-11-8999
12. Sponsoring Agency Name and Address Office of Research Federal Highway Administration U.S. Department of Transportation Washington, D.C. 20590	13. Type of Report and Period Covered Final Report April 1976–February 1979
	14. Sponsoring Agency Code S01136

15. Supplementary Notes

FHWA Contract Manager: C. H. McGogney (HRS-11)

DEPARTMENT OF TRANSPORTATION

FEB 20 1982

LIBRARY

16. Abstract

The long-range objective of the research summarized in this report is the development of a practical nondestructive (NDE) method for detecting deterioration in the reinforcement of prestressed concrete bridge structural members in situ. A detailed definition of the problem is presented and the technical approach is summarized. The basis for selecting and assessing fifteen NDE methods is reviewed, and the results of a limited laboratory investigation of the magnetic method prior to developing inspection equipment are summarized. Development of a preliminary magnetic inspection equipment is described and many records are presented from laboratory evaluations using a 20-ft. (6m) section of Texas Type "C" beam and from field evaluations on the Sixth South Street Viaduct at Salt Lake City, Utah. Similarities between laboratory and field inspection signatures are indicated; other prominent anomalous signatures are shown which correlated with steel elements neither known to be present nor shown on the plans; still other field signatures are shown which indicated the stirrup configuration in the post-tension girders was not in accordance with the plans. Correlation investigations are described which illustrate promising electronic signature enhancement and recognition methods for discriminating between steel artifacts and deterioration. Recommendations for further development are outlined.

17. Key Words Corrosion Fracture Concrete Bridges Prestressing Reinforcing Steel Nondestructive Testing	18. Distribution Statement No restrictions. This document is available to the public through the National Technical Information Service Springfield, Virginia 22161

19. Security Classif. (of this report) Unclassified	20. Security Classif. (of this page) Unclassified	21. No. of Pages 197	22. Price

Form DOT F 1700.7 (8-72)   Reproduction of completed page authorized

TABLE OF CONTENTS

LIST OF ILLUSTRATIONS

LIST OF ILLUSTRATIONS (Cont'd)

LIST OF ILLUSTRATIONS (Cont'd)

I. INTRODUCTION

A. The Overall Problem

About 25 years ago, a new bridge structural design called prestressed concrete was introduced. In recent years, the use of prestressed concrete bridges has been widespread and such design now incorporates a variety of structural configurations. Basically, prestressed concrete bridge structural members are of two general types, pretensioned and post-tensioned. Current pretensioned construction usually consists of 7-wire strand, on the order of 1/2-in. (1.3cm) diameter, arranged in a matrix on 2-in. (5cm) centers and the strands are tensioned prior to casting the concrete members. Pretensioned members are produced at a plant site because of the special fabrication facilities and tooling required. In the case of the post-tensioned configuration, ducts, usually metal, are cast in a specified location and configuration in the concrete member; subsequently, the reinforcing strand, rod, or bar is tensioned, usually at the bridge site, and grouting material is introduced to fill the space between the reinforcement and the duct.

The load-carrying capability of prestressed bridge structural members is directly dependent upon the strength of the steel reinforcement rods, bars, or strands; hence, the integrity of this steel is of primary concern and is influenced by one or more of the following factors:

(1) Quality of manufactured reinforcement material - governed by dimensional tolerances, strength, ductility, metallurgical type flaws such as voids or impurities, and mechanical damage such as nicks, gouges, etc.

(2) Corrosion deterioration as a result of field environment.

(3) Fracture - failure as a result of over stress (caused by loss of section due to corrosion deterioration) or by impact loading (as a result of construction or vehicular impact).

(4) Bond between steel and concrete, associated corrosion of post-tensioned members due to voids in duct grouting collecting moisture.

1

In recent years, there is conclusive evidence that deterioration of the steel as a result of corrosion does occur; furthermore, such deterioration does critically affect the structural strength.[1,2,3] Currently used inspection procedures rely heavily on rust staining, cracking, and spalling of the concrete as an indicator that a problem exists in the reinforcing steel.[2,4] (A more detailed discussion of the corrosion deterioration of steel in prestressed concrete is presented in Section I.C. of Appendix I) Apparently, deterioration and even fracture of the reinforcement can occur without being preceded by visual evidence on the external surfaces of the concrete members. For example, the Sixth South Street Viaduct structure in Salt Lake City consisting of 192 beams, presently, has more than 21 bars suspected to be fractured. A photograph of two such fractures is shown in Figure 1. In this case, the presence of corroded and fractured post-tensioning bars was determined only from i) the loose bars and end-nuts during a visual inspection, and ii) the loud noise generated by one of the bars breaking which was overheard by people in the area who reported it to the State. There are no cracks or significant rust stains visible on the exterior surfaces of these particular girders. Spalling of the end-grouting, when bar looseness or significant extension is not present, is considered an indication of possible bar fracture.

1.   Gould, R. W., Hummel, R. E., and Lewis, R. O., "Electrical Resistance as a Measure of Reinforcing Bar Continuity Sunshine Skyway Bridge," Progress Report 1, Dept. of Materials Science and Engineering, University of Florida, Gainesville, Florida 32611, June 29, 1973.

2.   Lewis, D. A., and Copenhagen, W. J., "The Corrosion of Reinforcing Steel in Concrete in Marine Atmospheres," The South African Industrial Chemist, Oct. 1957.

3.   Rehm, G., "Corrosion of Prestressing Steel," General Report submitted at FIP Symposium on Steel for Prestressing, Madrid 1968.

4.   Moore, D. G., Klodt, D. T., and Hensen, R. J., "Protection of Steel in Prestressed Concrete Bridges," Research sponsored by American Assoc. of State Highway Officials in cooperation with the Bureau of Public Roads; Highway Research Board, Div. of Engineering, National Research Council, National Academy of Sciences - National Academy of Engineering, 1970

Samples supplied through the
courtesy of Utah Department
of Transportation

1 inch
2.54 cm

FIGURE 1.   OVERALL VIEW OF TWO FRACTURES FROM SIXTH
SOUTH VIADUCT STRUCTURE IN SALT LAKE CITY

It is evident that presently available inspection methods for assessing the condition of reinforcing steel, in situ, in prestressed concrete bridge members are not adequate. The long-range objective of the research summarized in this report is the development of a practical nondestructive method for detecting deterioration in the reinforcement steel of prestressed concrete highway bridge structural members in situ.

B.   Detailed Definition of the Problem

The above overall objective of the program requires the consideration of the several flaw categories and an accompanying broad spectrum of mechanisms as follows:

(1)   voids - manufacturing and processing flaws

(2)   corrosion deterioration - loss of material by electrolytic processes, stress corrosion cracking, and hydrogen embrittlement

(3)   fracture - overload due to impact, gross loss of section, notch sensitivity, brittle fracture mechanisms such as stress corrosion cracking and hydrogen embrittlement

(4)   fatigue

From an overall point of view, the problem is extremely broad since the mechanisms contributing to the decrease or loss of structural integrity are complicated and also because of a wide variety of structural designs. Therefore, before a logical and valid assessment of nondestructive inspection (NDE) methods with possible applicability to the problem could effectively be undertaken, it was necessary to more precisely define the problem, to detail immediate goals, and to establish priorities according to both mechanisms and structural design categories.

Accordingly, a detailed definition of the problem was undertaken based on:

i)   A review of current literature relating to the corrosion of steel in reinforced concrete structures.

ii)   Personal contacts with highway and bridge engineers in several states where corrosion problems were known to exist.

iii)   Conferences with cognizant FHWA personnel.

4

A review of the current literature and personal contacts with bridge and highway engineers in Utah and Florida indicated that emphasis should be placed on the detection of loss-of-section by corrosion or fracture of the prestressing steel rods, strands, wires, and bars. In conference with cognizant FHWA personnel, the following goals were established for subsequent efforts under the subject contract:

(1) Type of Deterioration - primary emphasis on the detection of i) 10% or greater loss of area due to corrosion of steel, ii) fracture of rod or strand, iii) fracture of one or more wires in a strand, iv) low priority on the detection of voids, of the order of 1/8-in. (3mm) diameter in steel bars (this void size is within cross-sectional area tolerance band for manufacture of the bars).

(2) Type of Steel Configurations - both ducted and non-ducted steel configurations (pretensioned and post-tensioned).

(3) Type of Structural Members - emphasize the inspection of the steel prestressing elements adjacent to and essentially parallel to the lower surface of the tension flange in "I" and box beams as illustrated in Figure 2.

It was recognized that, for most applicable nondestructive inspection methods, a reduction in deterioration detection sensitivity is anticipated for those steel elements buried deeper within the concrete beam.

C.   The Approach

A state-of-the-art literature search and review was conducted pertaining to the detection of reinforcing steel deterioration in prestressed concrete structures. Based on information contained in the documents identified and input from Southwest Research Institute personnel having a broad background in related nondestructive inspection problems, fifteen (15) NDE methods with possible applicability to the subject inspection problem were identified. The formal assessment of these fifteen methods was undertaken based upon the detailed definition of the problem (presented in the previous section), analysis of information from the published literature, NDE background of the assessment team members, and information input by the Contract Manager and from other cognizant FHWA personnel. It was the concensus of the assessment team that none of the fifteen methods offered more than marginal promise for detecting steel deterioration (flaws)

5
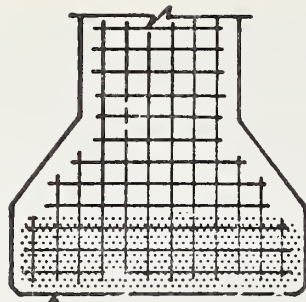
Pretension Beam
(Section, lower region)

Inspection of region of straight strands parallel to and within ~6 inches (15 cm) of bottom surface of flange
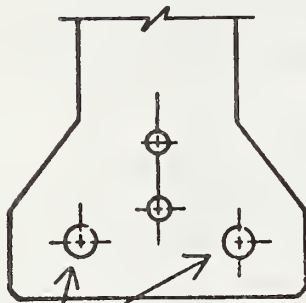
Post-tension Beam
(Section, lower region)

Inspection of straight bars parallel (or nearly parallel to bottom surface of flange
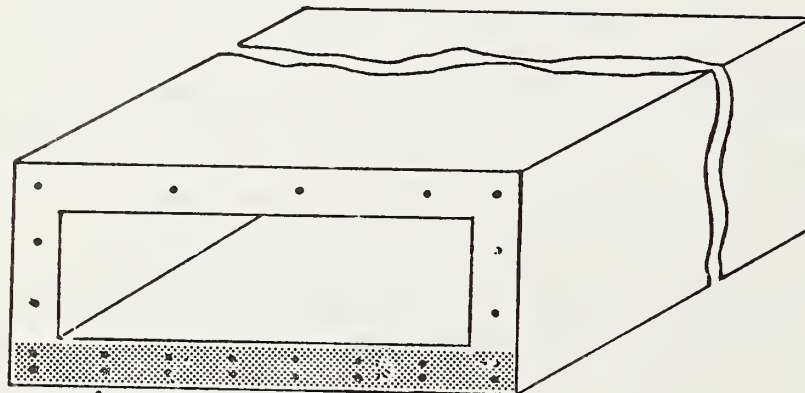
Box Beam
(Section)

Inspection of region of straight strands within ~6 inches (15cm) of bottom surface

FIGURE 2.   TYPE OF STRUCTURAL MEMBERS AND REGIONS GIVEN PRIORITY

6

for the case of the reinforcing steel inside a steel duct. A magnetic field method was the most promising one, and a limited experimental evaluation of the method was conducted. The experimental results were unexpectedly good, even with the test bar inside a steel tube; accordingly, it was decided to undertake a comprehensive laboratory evaluation of the magnetic field method.

The magnetic field method consists of applying a steady-state magnetic field to the beam under inspection and scanning a magnetic field sensor along the length of the beam, essentially parallel to each element of the prestressing steel, to detect perturbances in the applied field caused by anomalies such as deterioration or other types of flaws. A section of simulated beam consisting of a wooden superstructure in which a matrix of steel bar or strand specimens containing manufactured flaws and un-flawed steel elements arranged in various configurations was used for laboratory evaluation of the method. The magnetizing field was produced by a dc excited electromagnet; a Hall-effect device was used as the magnetic field sensor. Experiments were conducted to determine the influence of a range of conditions and test parameters on the detectability of simulated loss-of-section and fracture. The experiments included varying degrees of deterioration, influence of adjacent unflawed steel elements, type of duct, type of reinforcing steel, transverse rebar configuration, etc. Selected records are shown in Figure 3 which illustrate typical magnetic response for several different steel configurations and degrees of deterioration. The vertical excursion in each record of Figure 3 is proportional to the magnetic disturbance generated at the probe by the steel configuration and attendant flaw conditions; generally, there is a large vertical excursion at each end of scan (see record C) caused by the demagnetizing effect of the specimen ends. The horizontal scale in each record is proportional to distance along the specimen, a typical scale of which is shown at the bottom of record A. The results of the laboratory evaluation indicated good over-all sensitivity to loss-of-section and excellent sensitivity to fracture with minimal degradation of signal response in the presence of steel duct. *

---

* Detailed results of the laboratory assessment of the magnetic field method, as well as the detailed rating and assessment of the many NDE methods considered, problem background, discussions related to the definition of the problem, etc., are contained in an Interim Report dated March 1977 and entitled "Detection of Flaws in Reinforcing Steel in Pre-stressed Concrete Bridge Members," and which is included as Appendix I in this Final Report.
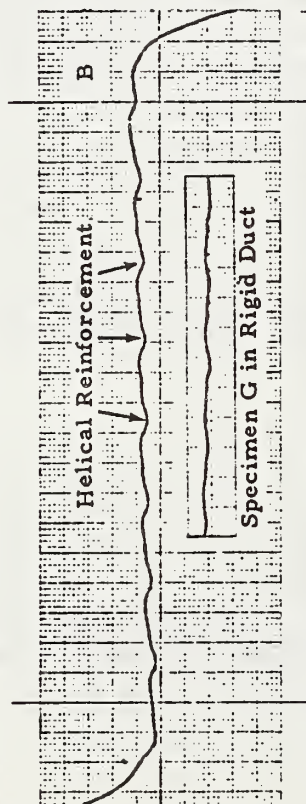
D

Rebar

86% × 0.13 in. Rebar
Section Loss

2.0 V

Rebar

NO 11:701:-7

1/2 in. ϕ strand (Specimen A), 3/8 in. ϕ rebars 20 in. apart and
above specimen, 1.5 in. probe-to-specimen spacing, 2 amp.

E

Rebar

Rebar

2-5/8 in. rigid duct, no specimen, 3/8 in. ϕ rebars 20 in. apart
and above duct, 2.5 in. probe-to-duct spacing, 3 amp.

F

Rebar

94% × 0.13 in. Rebar
Section Loss
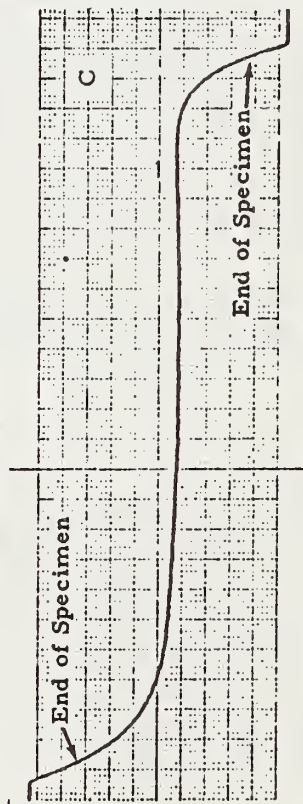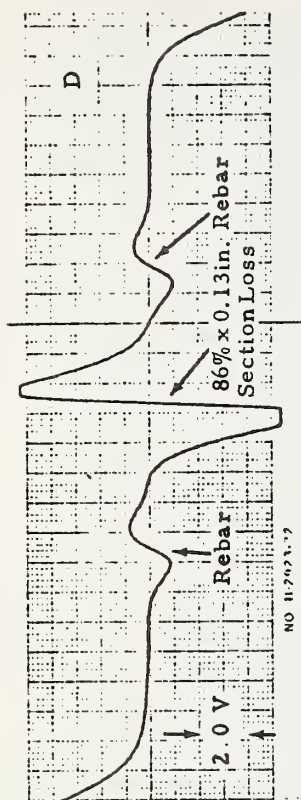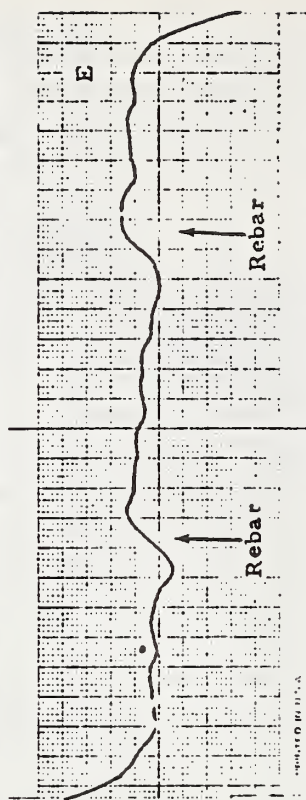
Rebar

1 in. ϕ bar (Specimen D), rigid duct, 3/8 in. ϕ rebars 20 in.
apart and above duct, 2.5 in. probe-to-specimen spacing, 3 amp.

1 in. = 2.54cm

A

Arrows indicate waviness in flexible duct

1.0 V Typ.

2 in. typical

2-5/8 in. flexible duct, no specimen, 2.5 in. probe-to-duct
spacing, 3 amp.

B

Helical Reinforcement

Specimen G in Rigid Duct

2-5/8 in. rigid duct, no specimen (insert with specimen), 2.5
in. probe-to-duct spacing, 3 amp.

C

End of Specimen

End of Specimen

1 in. ϕ A722 Type II bar (Specimen K), no duct, 2.5 in. probe-
to-bar spacing, 4 amp.

FIGURE 3.   SELECTED MAGNETIC RECORDS OBTAINED DURING INITIAL LABORATORY EVALUA-
TION ILLUSTRATING TYPICAL SIGNATURES

8

Based on the very encouraging results obtained in the laboratory, design and development of a preliminary magnetic field inspection equipment was undertaken. Laboratory evaluation work conducted in parallel with the development of the preliminary inspection equipment using a 20-ft. (6m) section of Texas Type "C" beam produced such encouraging results that field evaluations were undertaken on the Sixth South Street Viaduct in Salt Lake City, Utah, in mid-November 1977 (several views of the equipment in the field are presented in Figure 4). Field records showed signatures with features similar to those observed for the laboratory beam and also several prominent anomalous indications. From analyses of records and field excavation at selected locations to establish possible signature sources, it was determined that steel elements ("chairs") were present in the field structure which were completely unanticipated and were not indicated on the construction drawings. Furthermore, subsequent simulation of the field configurations and associated signatures in the laboratory produced results which confirmed the characteristic signatures attributed to the presence of unanticipated elements (chairs) and, in addition, showed that the transverse steel configuration in the field girders was not in accordance with the construction drawings. As a result of these findings from the limited field evaluations, it has become apparent that an expanded program is required to provide solutions for accommodating the variety of signature interpretation problems anticipated to be encountered in the field. Limited electronic signature enhancement and recognition investigations conducted in conjunction with the laboratory simulation efforts have produced results that show very promising prospects for the development of methods to discriminate between configurational steel artifacts and the deterioration and fracture of prestressing steel.

A more detailed presentation and discussion of the field results and their interpretation, as well as pre-field laboratory evaluation results and a description of the equipment are presented in Section II of this report. A summary of the technical basis for the selection and development of the magnetic field method is presented in Section III and recommendations for continued development of the magnetic field method are presented in Section IV. Importantly, if the fifteen candidate NDE methods were currently reassessed, the magnetic method would still be selected as the best approach for detecting steel deterioration and fracture in prestressed concrete members. For nearly all methods other than the magnetic approach even more difficult (perhaps insoluble in some cases) signature interpretation problems associated with the overall configuration of steel in field structural members would be anticipated.

9
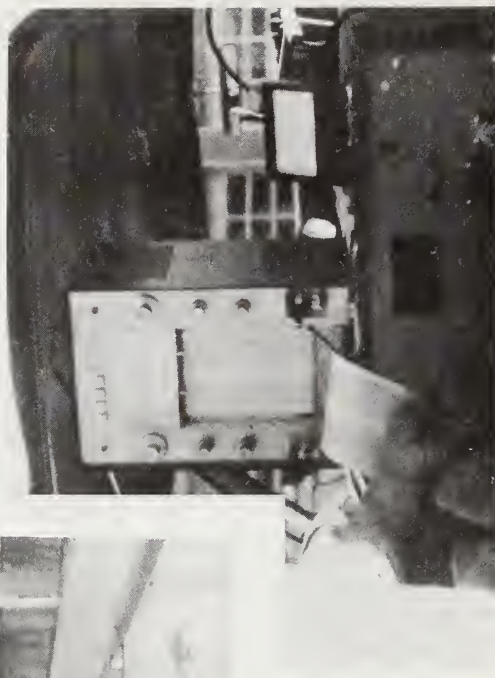
Closeup View of Operator Controls and Readout (Remote)

Closeup View of Inspection Cart

Overall View of Track Assembly and Inspection Cart

FIGURE 4. SEVERAL VIEWS OF MAGNETIC INSPECTION EQUIPMENT IN THE FIELD (Salt Lake City, Utah)

II.   SUMMARY OF PRELIMINARY EQUIPMENT DEVELOPMENT

A.   Description of Equipment

An overall view of the magnetic field inspection equipment was previously presented in Figure 4. For purposes of a more detailed description of the system, the reader is referred to Figures 5 through 8. Figure 5 shows another overall view of the equipment with the inspection cart, track, and hangers attached to a Texas Type "C" beam (20-ft. test section) in the laboratory. The closeup view in Figure 6 illustrates several details of the inspection cart, the size of which is commensurate with the 22-in. width (56cm) of the beam; the hangers are designed such that the cart assembly can pass through the hanger, unobstructed, and can scan regions of the beam along the entire track length. The total weight of the inspection hardware attached to the beam (i.e., inspection cart, track assembly, and hangers) is approximately 460 lbs. (209kg). Figure 7 illustrates many of the functional elements of the inspection cart. The electromagnetic-sensor assembly (which is demountable to facilitate setup of the equipment for inspection) may be positioned to different transverse locations across and the entire assembly driven along the beam by remote control. The capability to use the cantilevered sections of track for inspection is significant because it facilitates the inspection of steel elements in the vicinity of diaphragm attachment regions and end blocks. Figure 8 shows a view of the remote location equipment used by the operator during actual inspection; the remote site equipment is shown in the rear of a pickup truck for illustrative purposes. A small gasoline engine-driven generator (auxiliary equipment) is used to supply the power required by the inspection system and all inspection data are recorded on a strip-chart recorder (auxiliary equipment). The functional relationship between the various system inspection cart and remote site electronic, electrical, and control elements is shown by the block diagram in Figure 9. The elements which comprise the present inspection system consist of the following:

Subsystem	Approximate Size (in)			Approximate Weight (lb)
	L	W	H	
Inspection Cart (less electromagnet/sensor)	36	38	8	170
Electromagnet/Sensor	22	8-1/2	12-1/2	91

11

Inspection
Cart

Track
Hanger

Track Rail
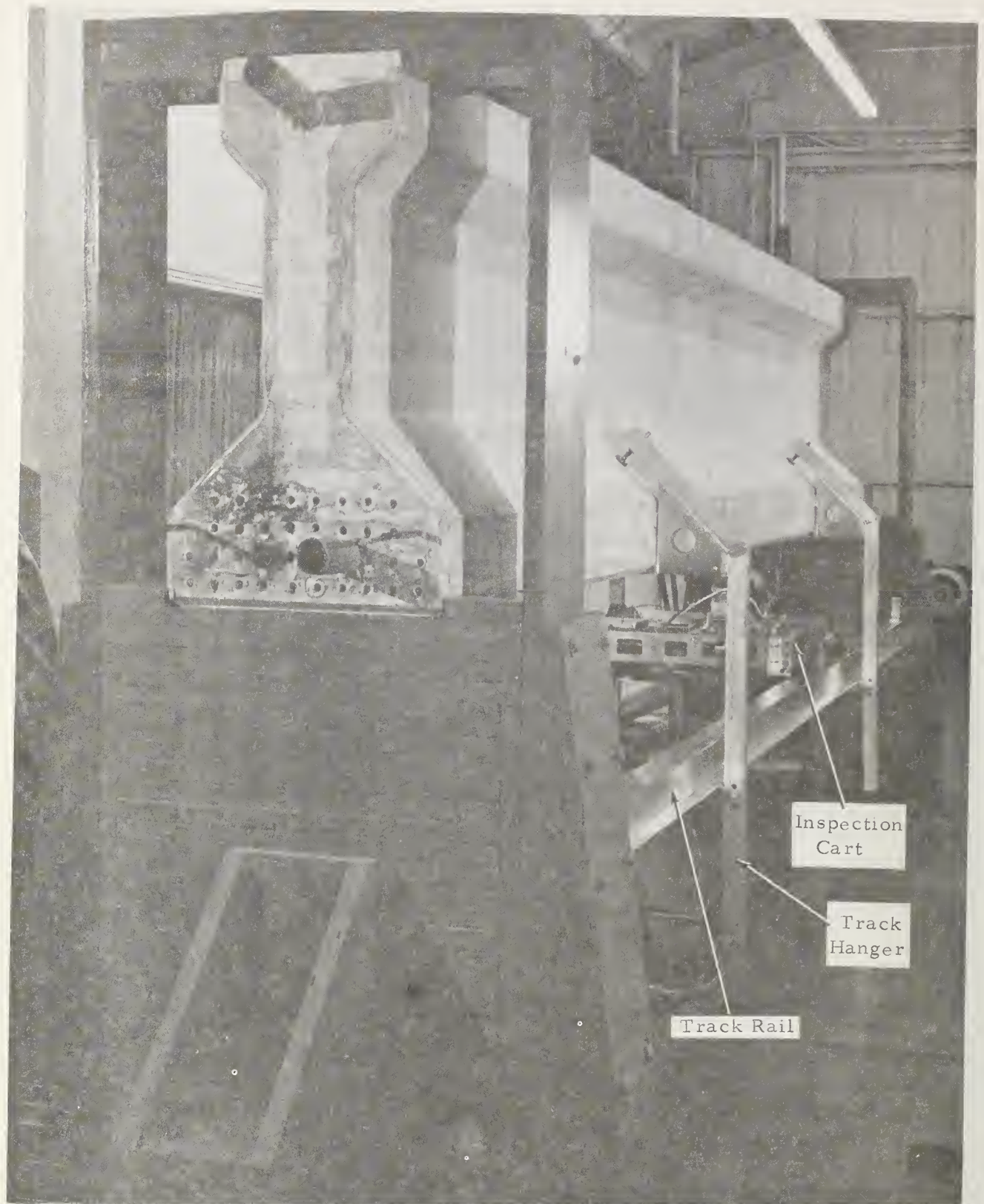
FIGURE 5. OVERALL VIEW OF TRACK ASSEMBLY AND INSPECTION
CART INSTALLED ON TEST BEAM IN THE LABORATORY

12
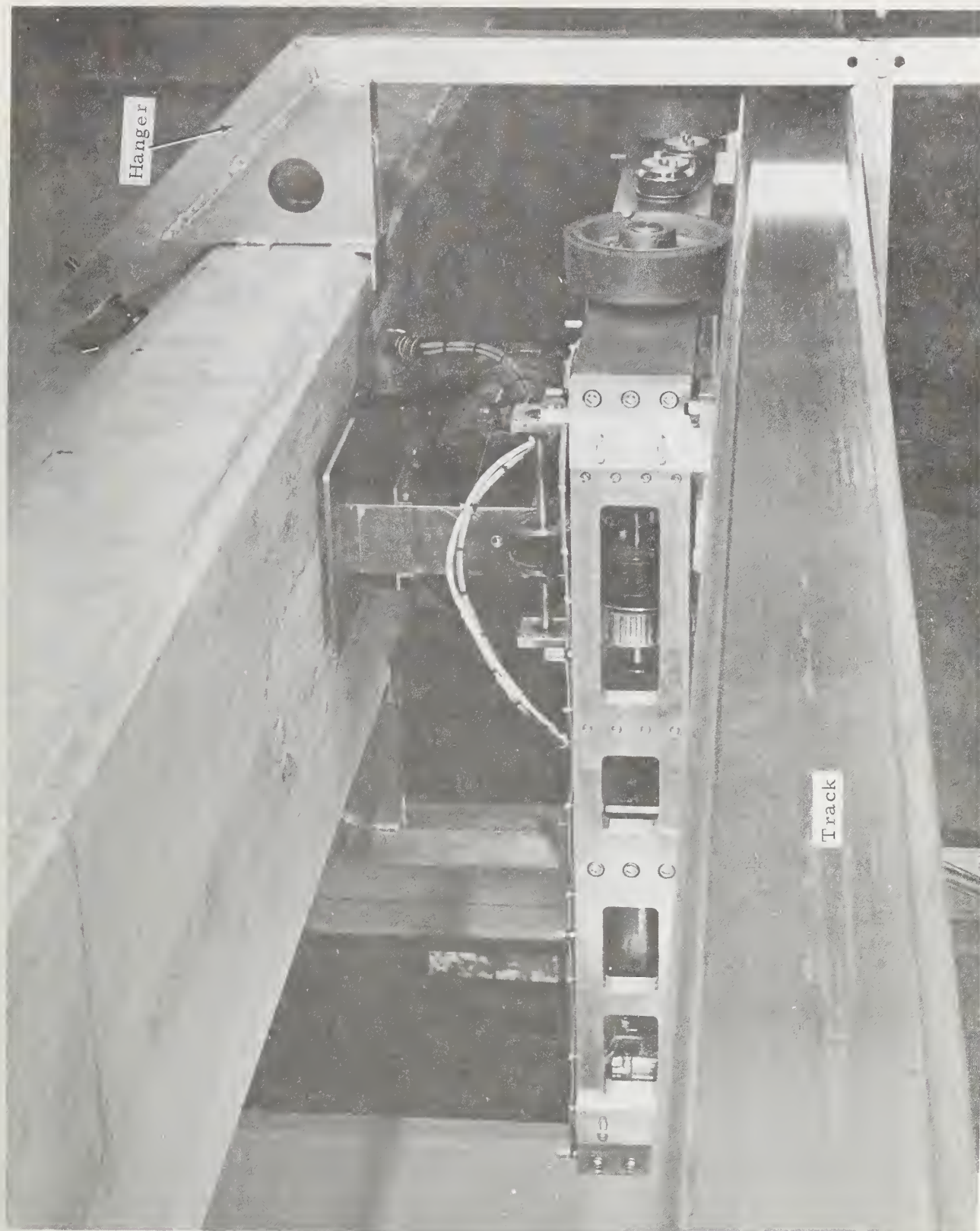
FIGURE 6. CLOSEUP VIEW OF INSPECTION CART IN THE LABORATORY

13
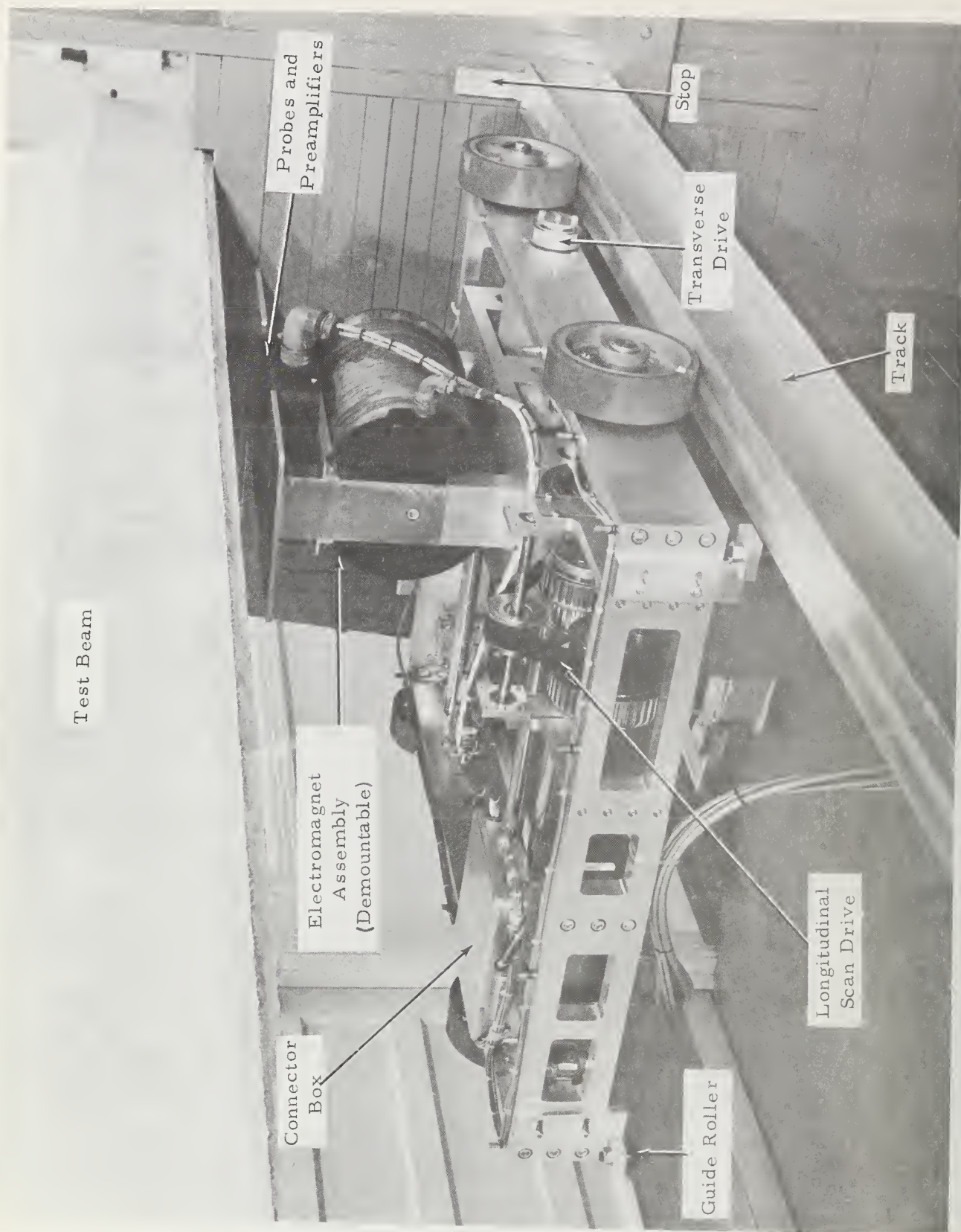
FIGURE 7. CLOSEUP VIEW OF INSPECTION CART

14

Strip Chart Recorder

Transverse Position Readout

Longitudinal and Tranverse Drive Controls

Electromagnet Current Source

Portable AC Power Source

Interconnecting Cable to Inspection Cart
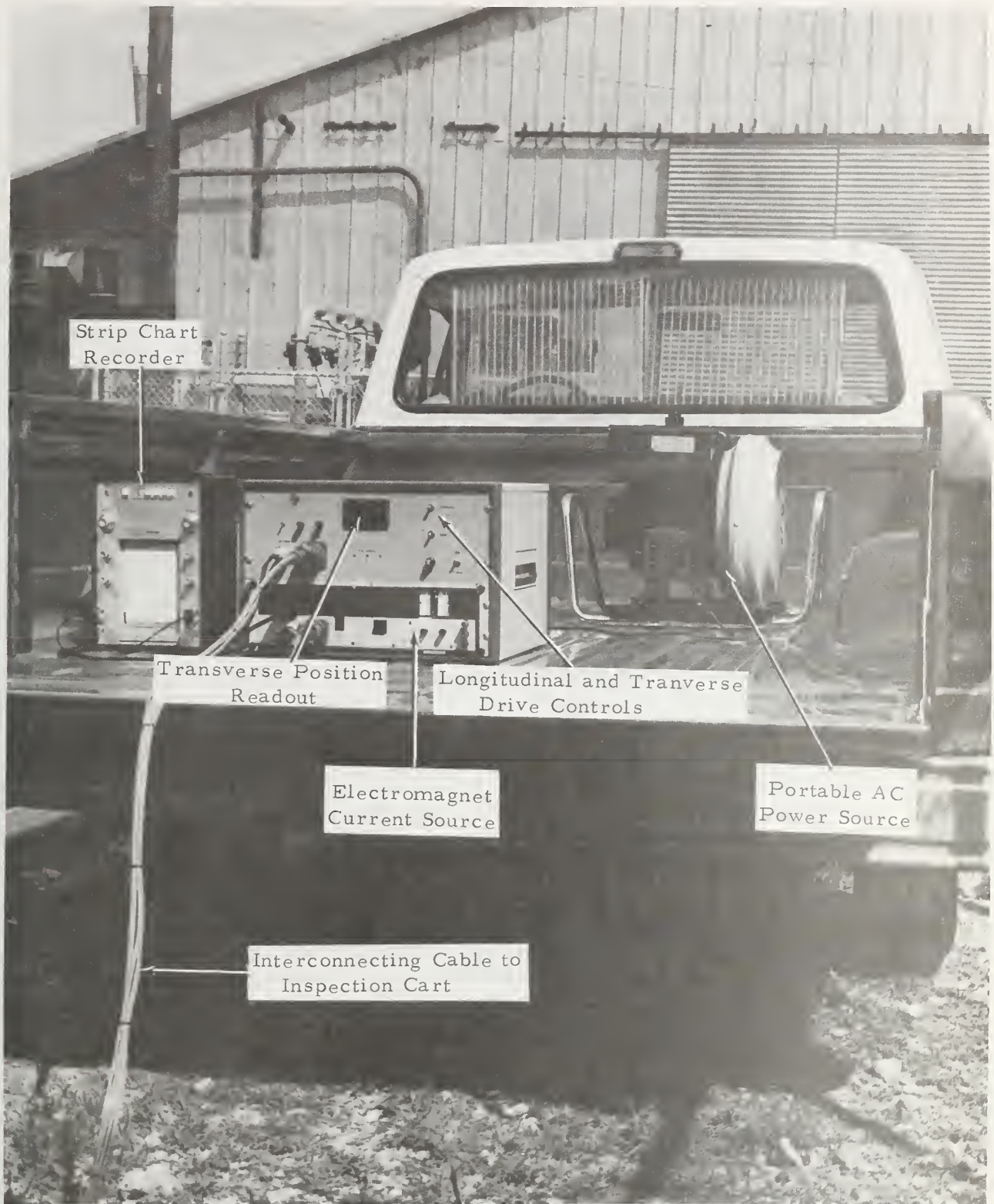
FIGURE 8. VIEW OF "REMOTE" EQUIPMENT AT OPERATOR'S LOCATION

15
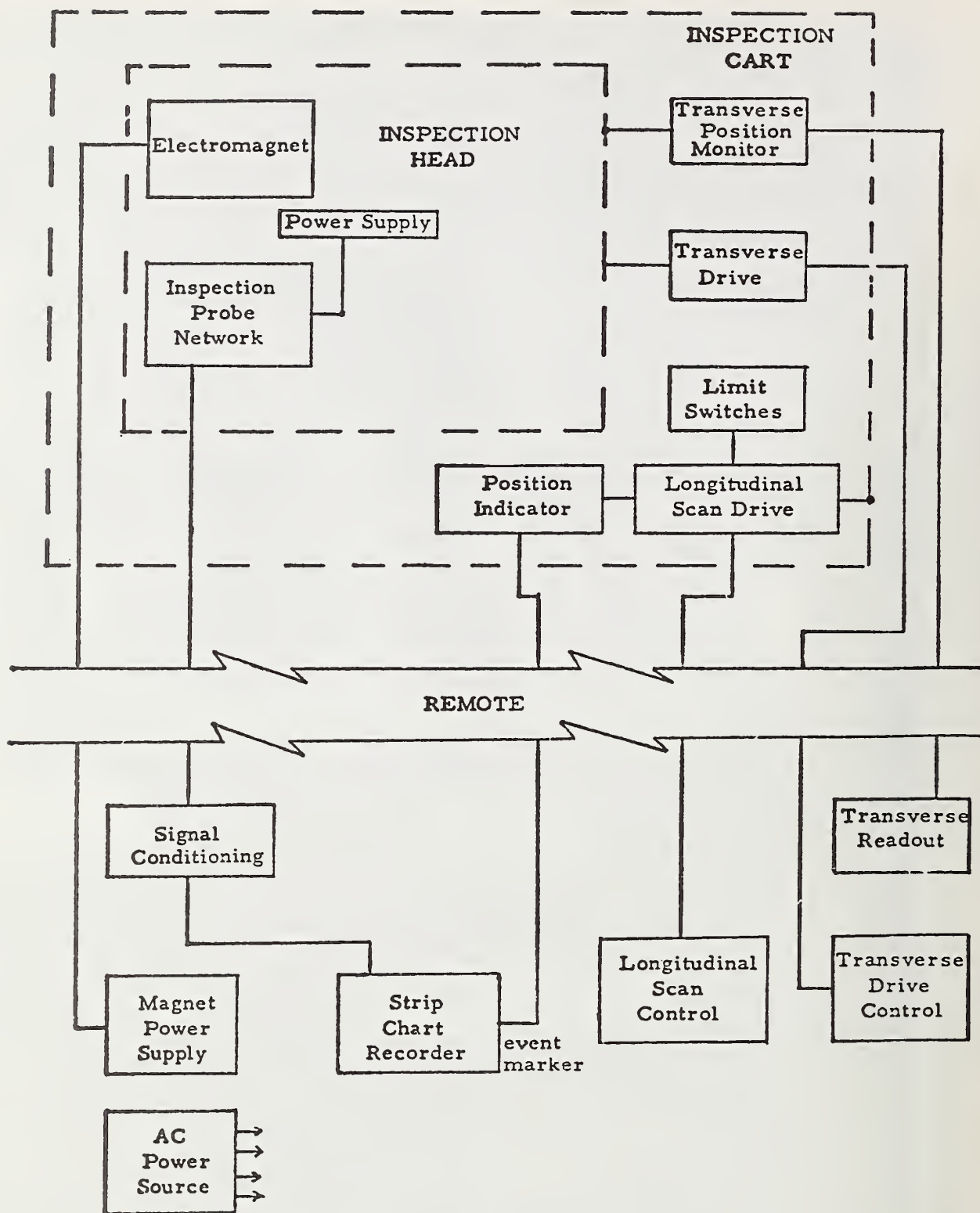
FIGURE 9.   FUNCTIONAL BLOCK DIAGRAM FOR PRELIMINARY
MAGNETIC INSPECTION EQUIPMENT

16

Subsystem	Approximate Size (in)			Approximate Weight (lb)
	L	W	H	
Signal/Control Rack	23	19-3/4	13-1/4	88
Recorder (Auxiliary equipment)	10	9	13-1/2	26
Signal/Control Cable	120ft.	-	-	33
Hangers (each)	3-1/2	40	52-1/2	50
Track Rails (each)	12-1/2, 15 ft.	3	5	43, 52
Portable AC Source (Auxiliary equipment)	25	19	21	130

1 in. = 2.54cm
1 lb. = 0.45kg
1 ft. = 0.3m

The magnetic equipment can be adapted to inspect the lower regions on a wide variety of prestressed concrete girders and box beams via the track approach. For example, box beams of various widths can be accommodated via track attachment brackets (coupled to the box beams by inserting anchors) or movable transverse support members.

B.   Laboratory Evaluations

1.   Test Specimen

Laboratory evaluation of the preliminary magnetic inspection equipment was conducted using a 20-ft.(6m) section of Texas Type "C" prestressed concrete beam. The test beam was fabricated by McDonough Brothers, Inc. of San Antonio in conjunction with the production of Type "C" beams. To facilitate the later mockup of flawed and unflawed pretension strands, PVC tubing was placed on a typical 2-in. (5cm) matrix spacing; two pretensioned strands were cast in place to achieve adequate dead load strength. In addition, metal ducts were cast in place so that post-tensioned bar configurations could be simulated using flawed and unflawed bars. Plans for the beam specimen are shown in Figure 10. Typical stirrup and "holddown" steel configurations were included in the

17
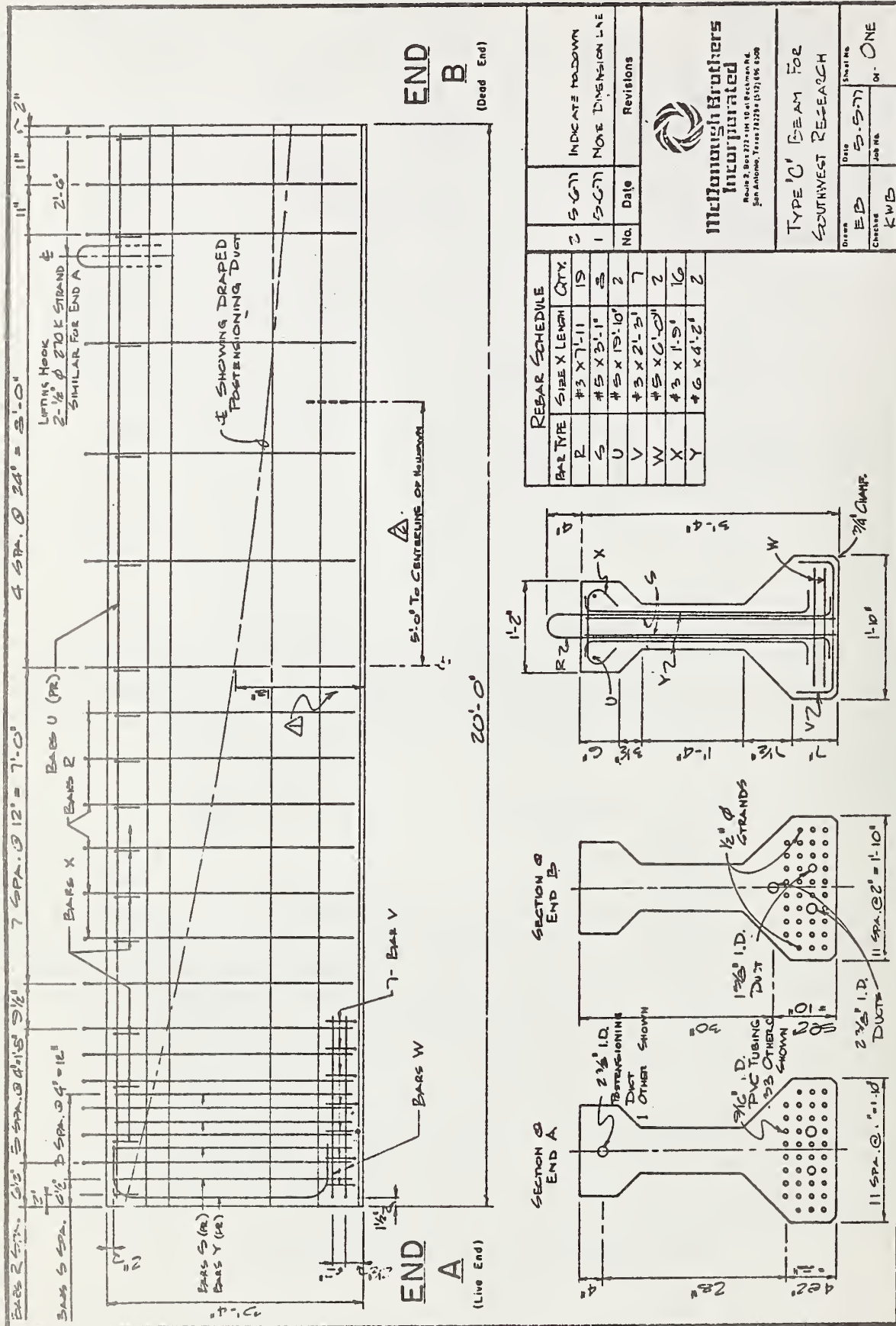
FIGURE 10. CONSTRUCTION DRAWING FOR TEXAS TYPE "C" TEST BEAM

beam design. Many detailed photographs of the steel "tie-up" were obtained prior to pouring the test beam; several of these showing the internal details of the beam are presented in Figures 11 through 13. Figure 14 presents a photograph of the completed beam near the NDE laboratory at SwRI; Figure 5 previously presented a view of the beam installed inside the laboratory with the preliminary magnetic inspection equipment attached. Tests with selected configurations of flawed and unflawed sections of prestressed steel elements were facilitated by the fabrication of a set of flawed bars and strands such as those illustrated in Figure 15. Simulation of a range of flaw sizes and types of bars was accomplished by cutting a 25-ft. (7.5m) length of bar approximately 7-ft. (2.1m) from one end, threading the two mating ends, and generating ferromagnetic and nonferromagnetic inserts of different diameters and thicknesses; a typical set of such inserts is shown in Figure 16. The flaw condition is set up in the bar by selecting the proper insert and using a threaded stud, assemblying the two sections of bar with the insert in place; for example, a fractured bar with 2-in. (5cm) separation is obtained by using a 2-in.-long (5cm) brass insert and a length of 300 Series stainless steel threaded stud stock (see Figure 16). Flawed strand was produced by cutting and removing one or more wires over the desired length of the flaw; several examples are shown in the closeup view of Figure 17. Table I summarizes the range and type of flaws simulated.

Pretensioned strand configuration tests were conducted by placing one or more flawed strands in a selected position of the 2-in. (5cm) x 2-in. (5cm) matrix of PVC tubes and filling the remaining matrix with the desired configuration of unflawed strands as illustrated by Figure 18. Post-tensioned bar testing was facilitated in a manner similar to the strand testing; either 1-in. (2.5cm) diameter of 1-3/8-in. (3.5cm) diameter flawed and unflawed bars were placed in one or more of the three metal ducts cast in place in the test beam (see Figure 19).

2. Test Procedures and Results

Laboratory tests were undertaken utilizing the preliminary inspection equipment in a manner similar to that envisioned for field testing; the results were recorded on a strip chart recorder. Inspections were conducted on various configurations of unflawed and flawed strand and bar specimens by inserting the specimens in the Texas Type "C" test beam and documenting the flaw location longitudinally along the beam via mechanical measurements. The signatures were recorded for a number of adjacent scan tracks, magnetizing field strengths (different electromagnet excitation currents), scan speeds, etc. Figure 20 illustrates the method used to identify the strand or bar configuration in each
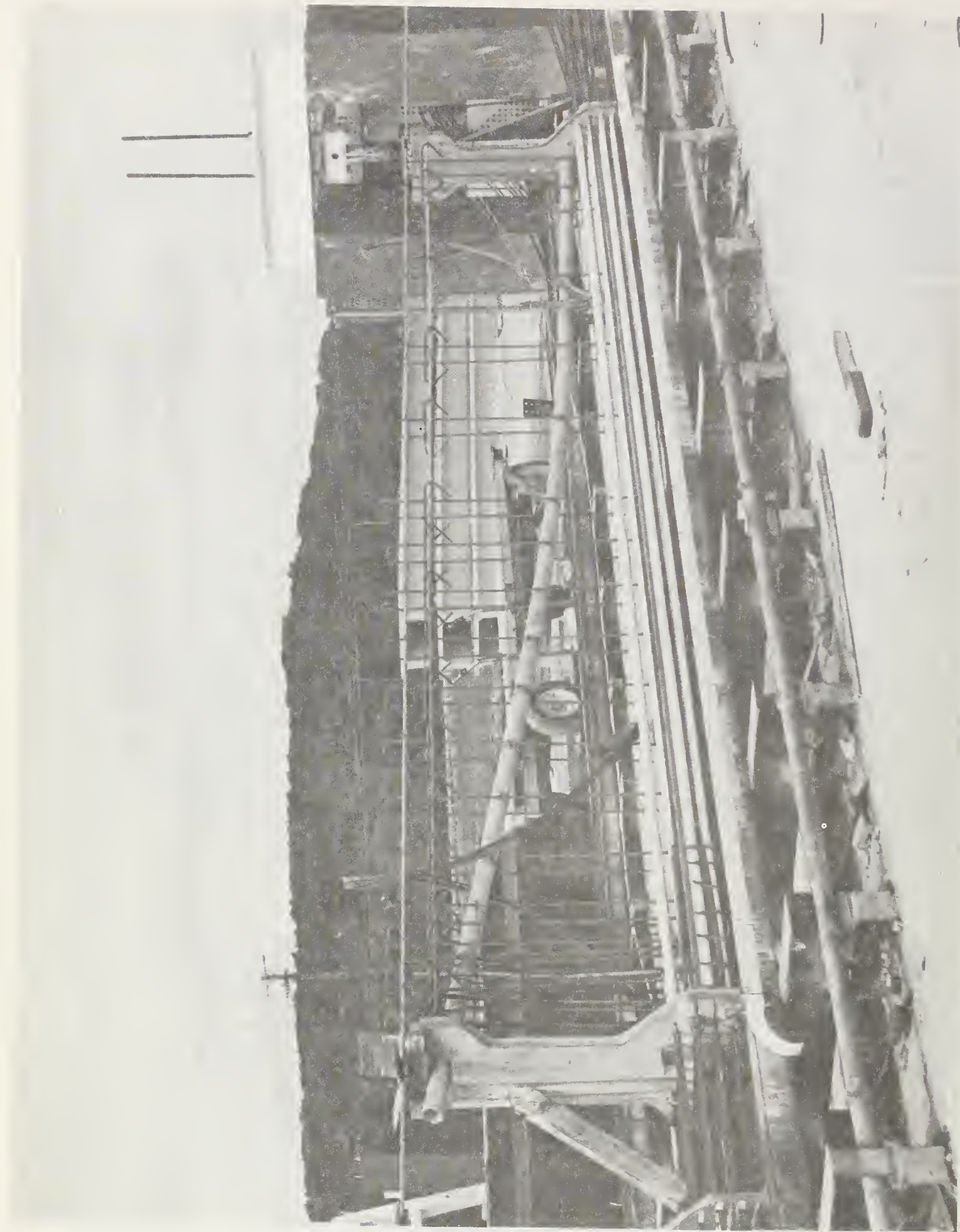
FIGURE 11. OVERALL VIEW OF TEST BEAM PRIOR TO SETTING FORMS
(Note 1-ft stations marked along edge of soffit)
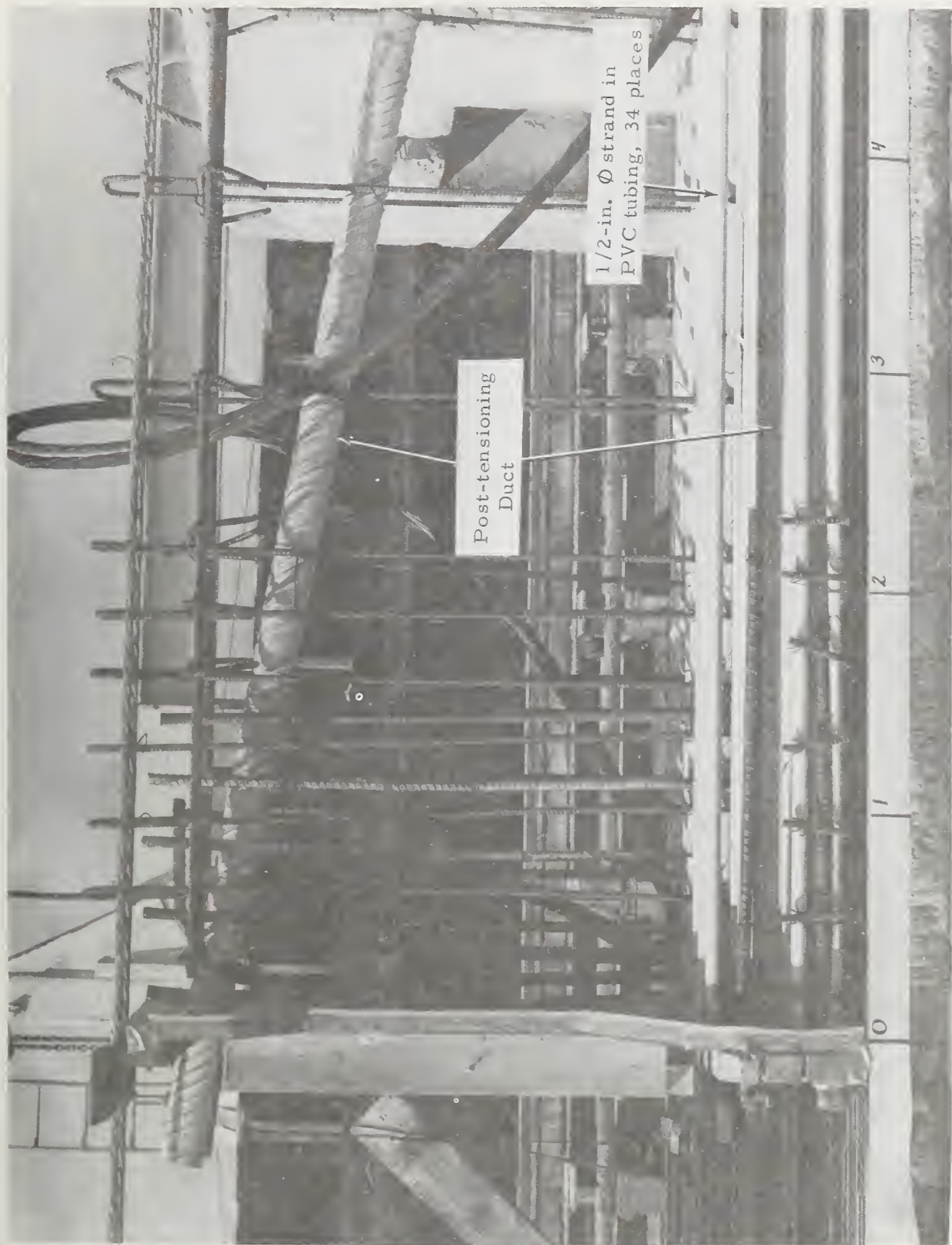
FIGURE 12. CLOSEUP VIEW OF STEEL CONFIGURATION NEAR END "A" OF BEAM (0 to 4-ft station)

21
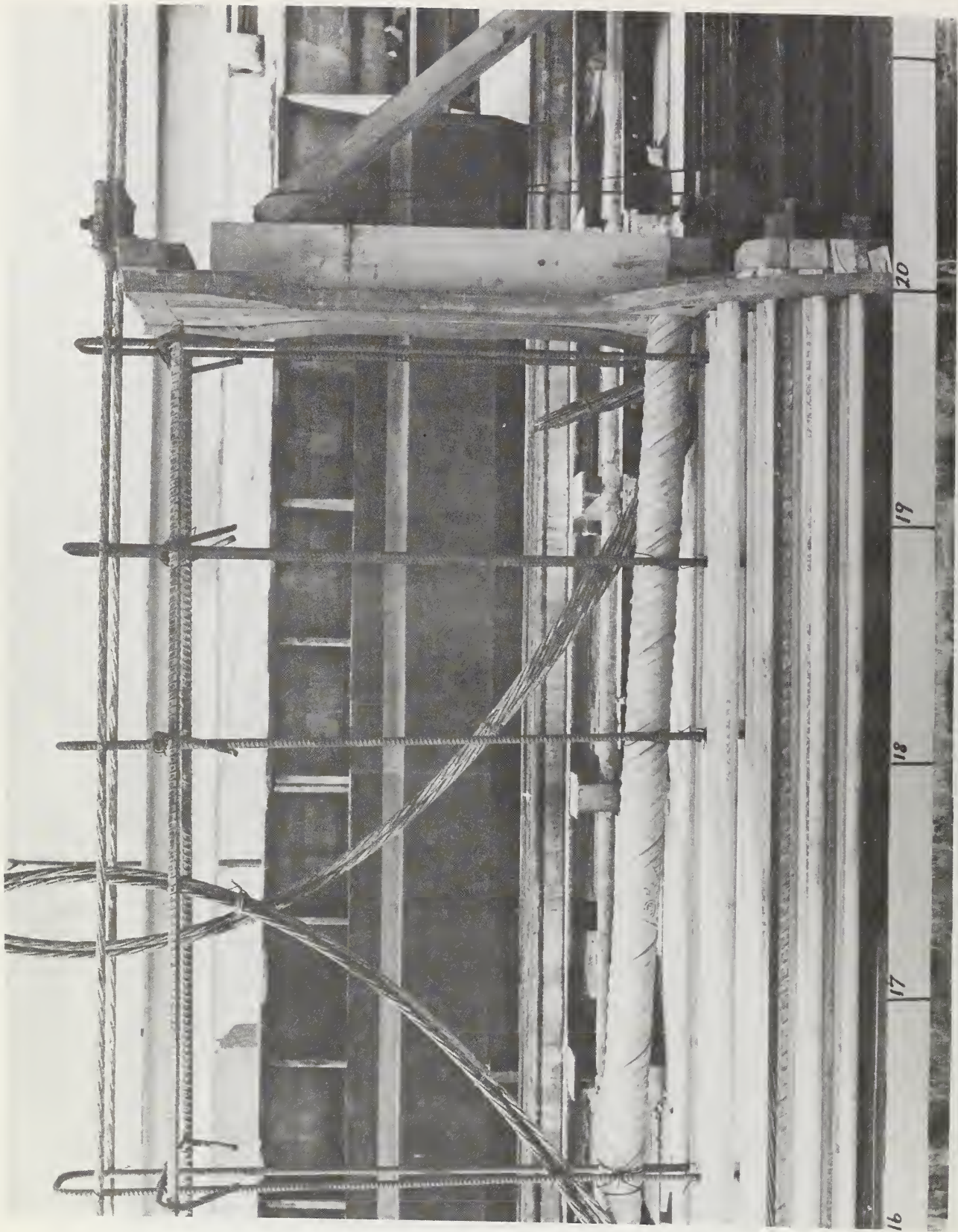
FIGURE 13. CLOSEUP VIEW OF STEEL CONFIGURATION NEAR END "B" OF BEAM (16 to 20-ft station)

22
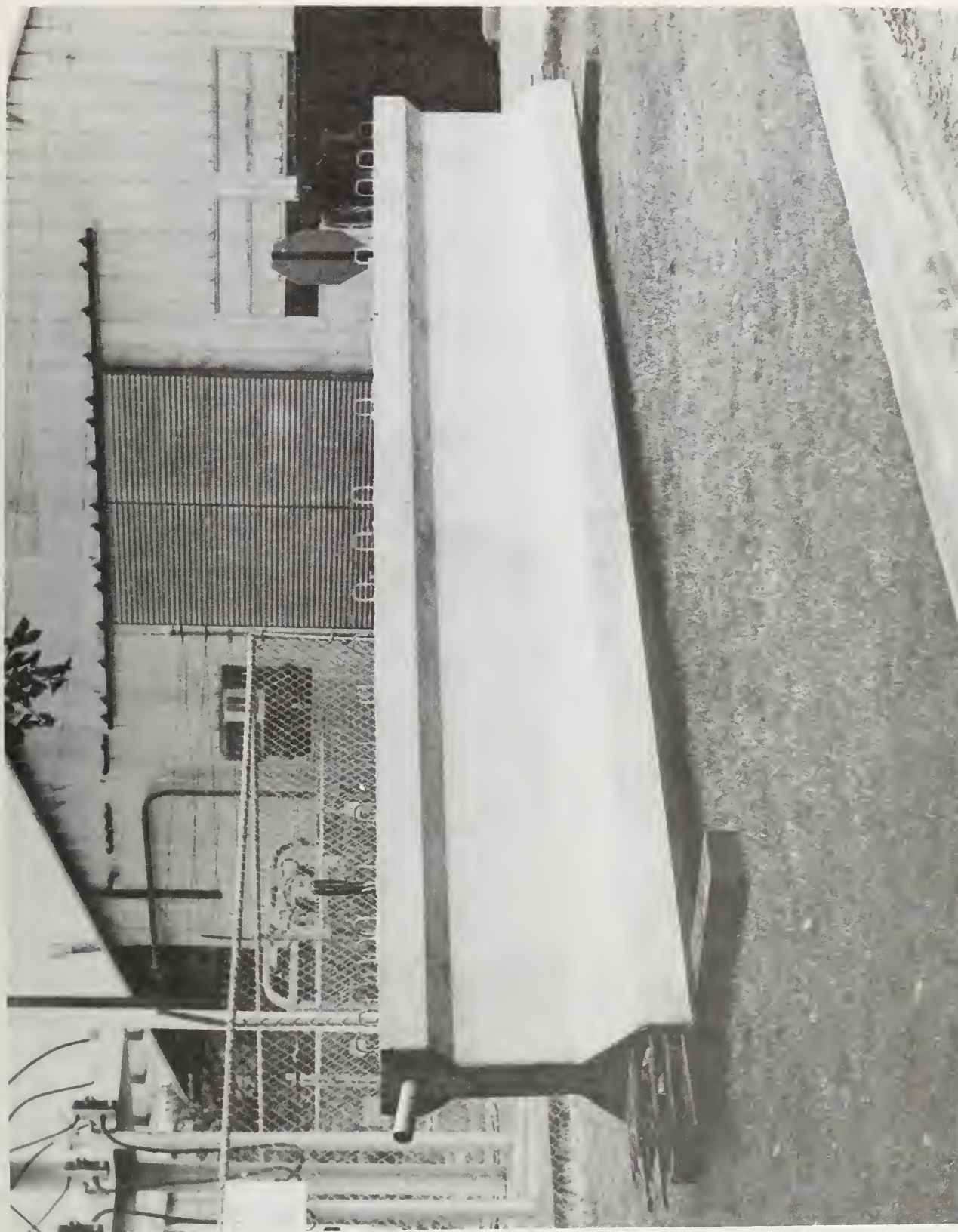
FIGURE 14. OVERALL VIEW OF COMPLETED TEST BEAM

23
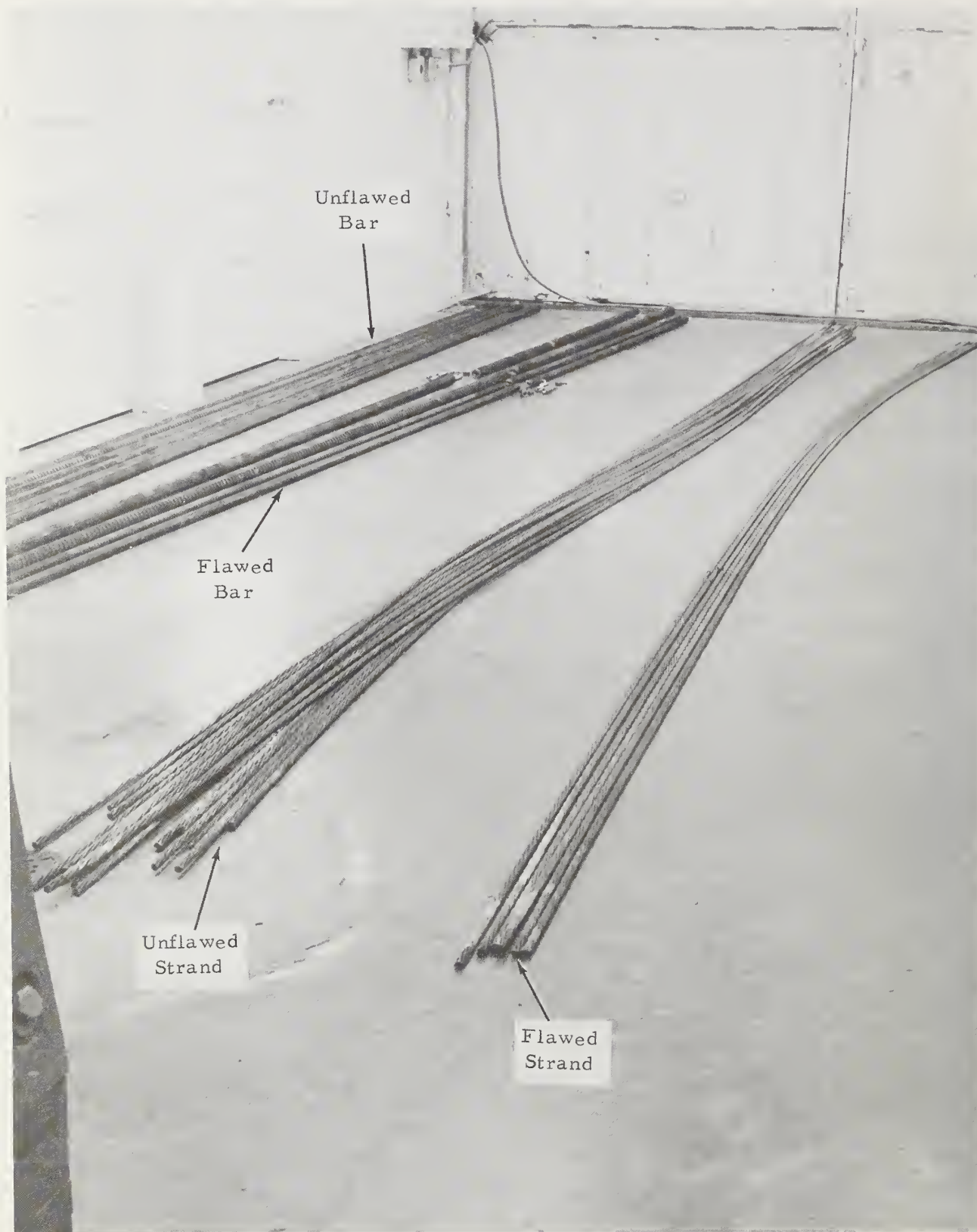
FIGURE 15. "FLAWED" AND "UNFLAWED" STRAND AND
BAR SPECIMENS
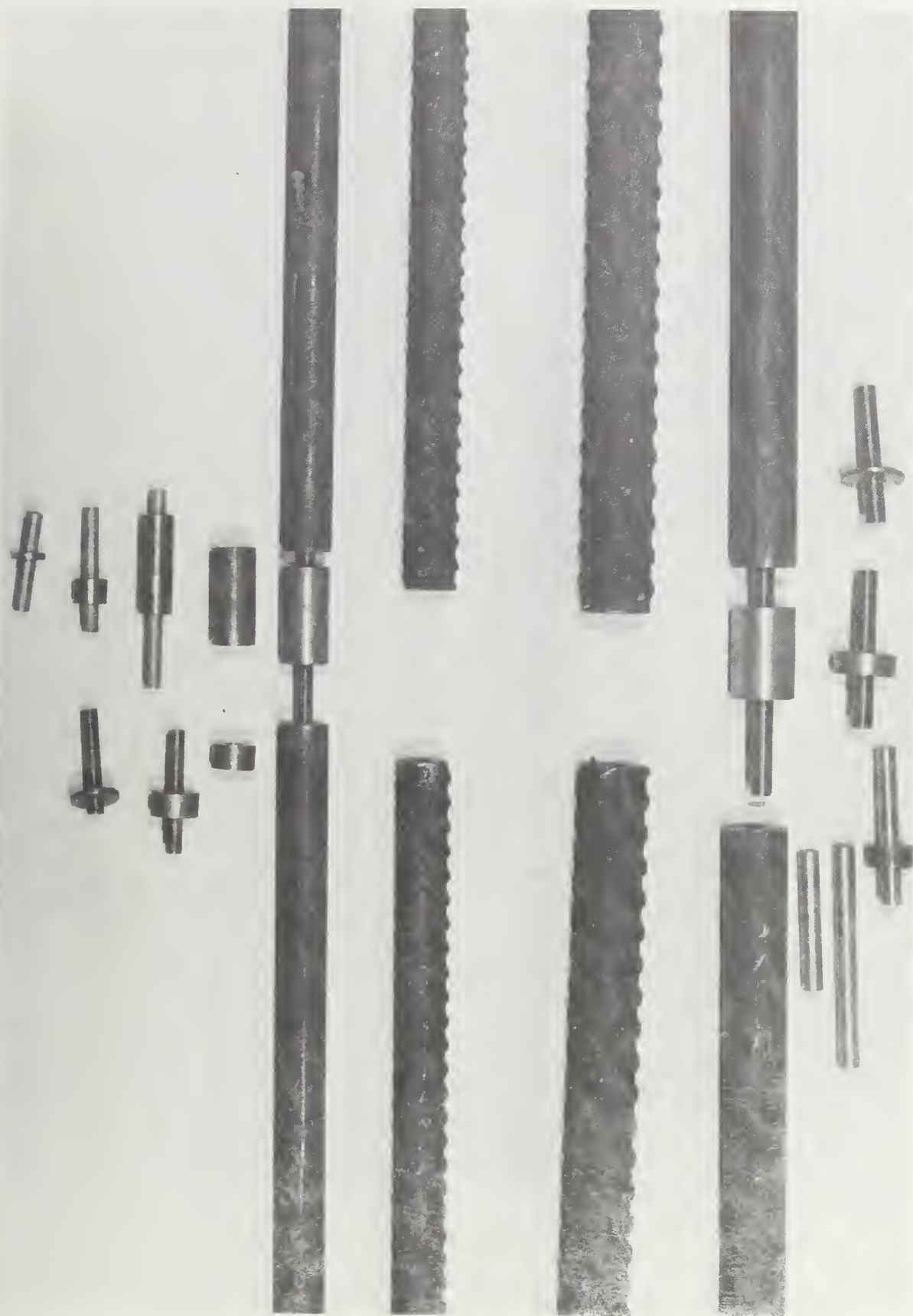
FIGURE 16. CLOSEUP VIEW SHOWING DETAILS OF FLAW SIMULATION IN HIGH STRENGTH STEEL BARS

FIGURE 17. CLOSEUP VIEW OF SIMULATED FLAWS IN STRANDS

26

TABLE I. BAR AND STRAND FLAW SPECIMEN

Type	Material	Loss-of-Section (%)	X Length (in)	Remarks
H.S.S. *Strand	1/2 in. Ø x 7 wire	14	0.12	1 wire removed
		14	2.0	1 wire removed
		43	0.12	3 wires removed
		43	2.0	3 wires removed
		86	0.12	6 wires removed
		86	2.0	6 wires removed
		100 (fracture)		--
H.S.S. Bar	1 in. Ø, A722	19	0.5	--
	Type I, Type II	19	2.0	--
		51	0.12	--
		51	0.5	--
		51	2.0	--
		100	0.015	fracture
		100	0.12	
		100	0.5	
		100	2.0	
	1-3/8 in. Ø, A722	47	0.5	--
	Type I, Type II	100	0.015	fracture
		100	0.12	
		100	0.5	
		100	2.0	

*H.S.S. - High Strength Steel
1 in. = 2.54cm

27
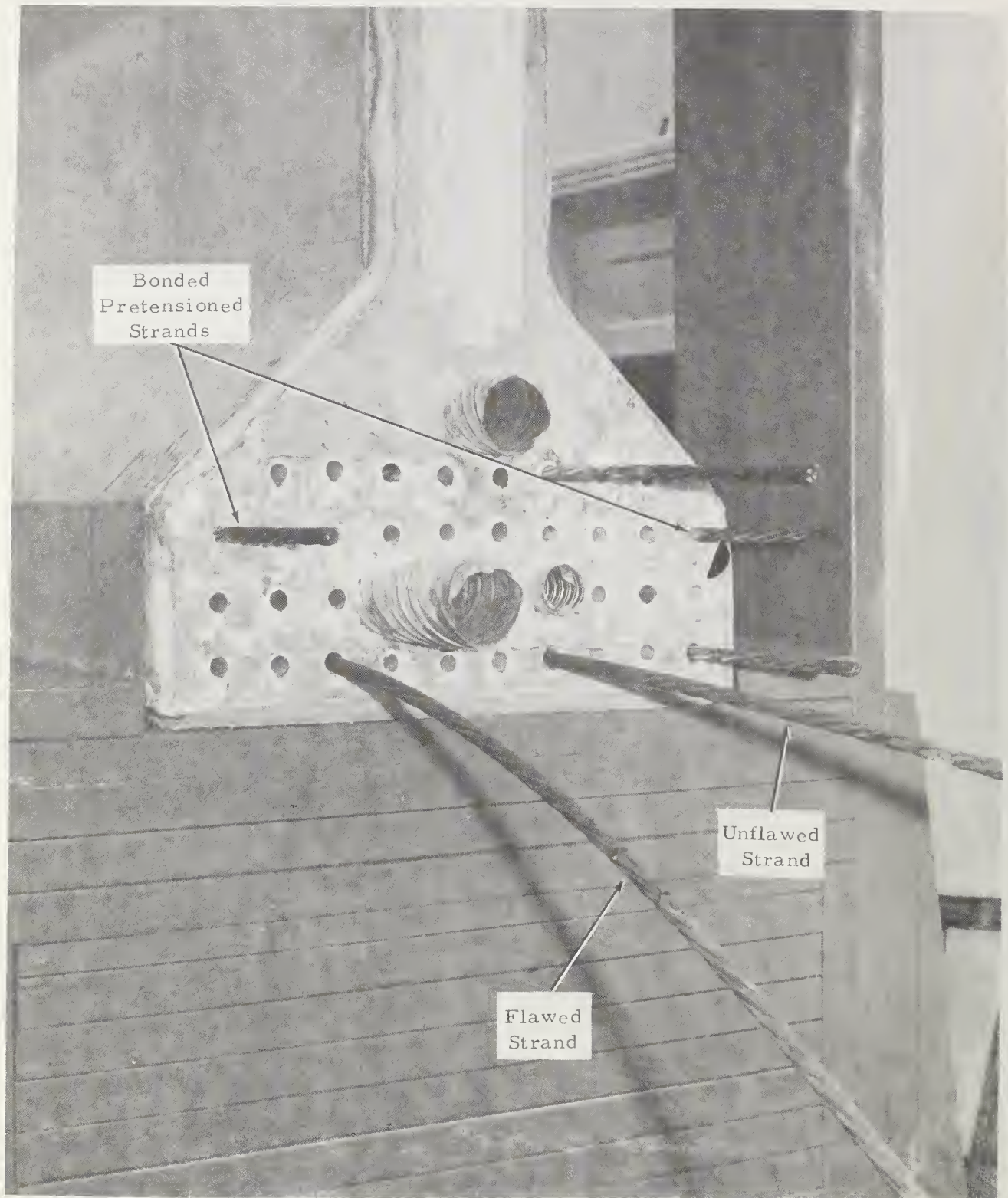
FIGURE 18. INSERTION OF STRAND IN TEXAS-TYPE "C" TEST BEAM

Bar with
Simulated
Fracture
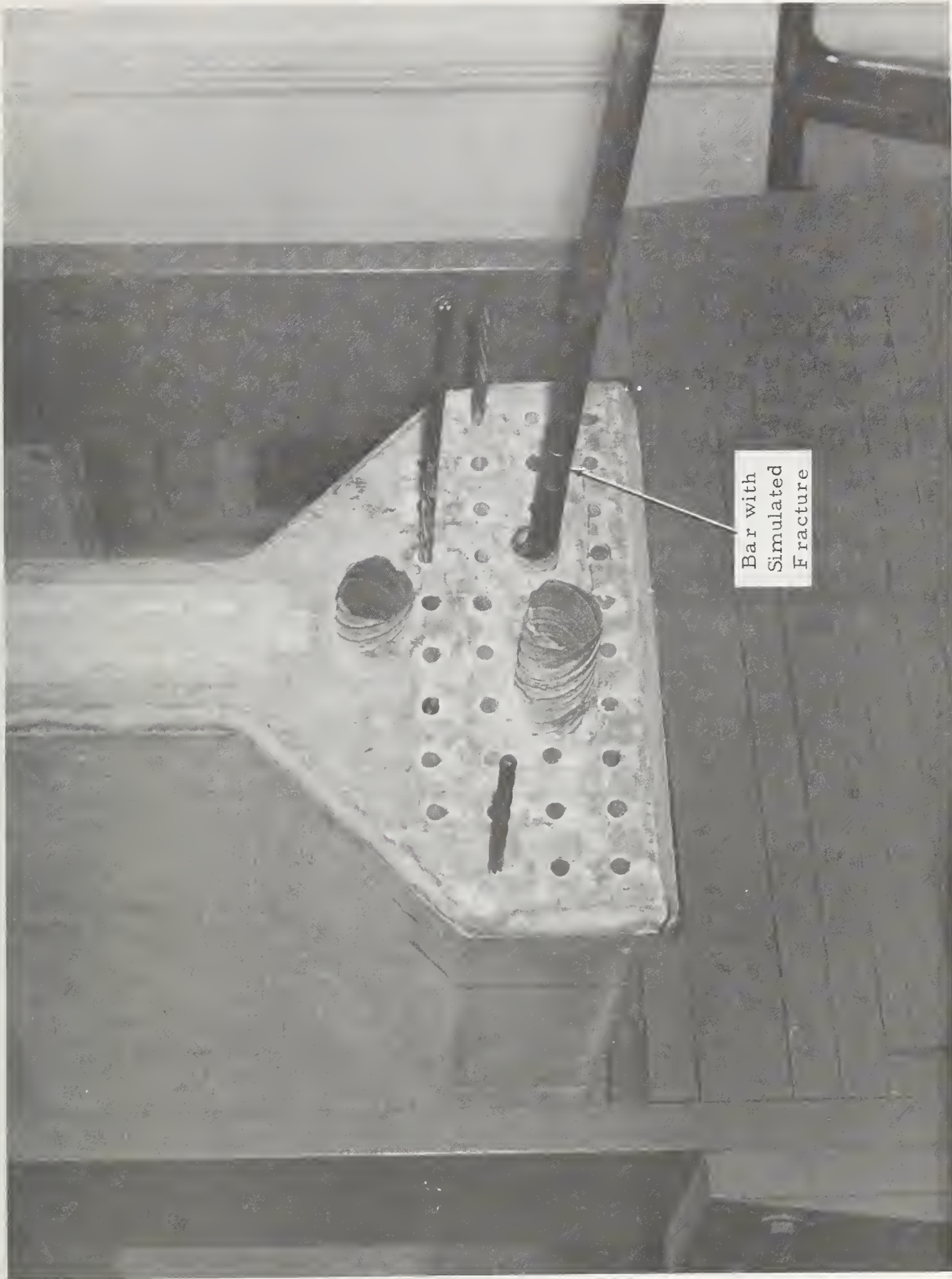
FIGURE 19. INSERTION OF HIGH-STRENGTH BAR, CONTAINING SIMULATED
FRACTURE, IN TEXAS-TYPE "C" TEST BEAM

29

View from End "A"
(Reference Figure 10)

Draped

Legend:

o Contains no prestressing steel
• Contains unflawed steel
⊠ Contains flawed steel

Longitudinal
Scan

Transverse | Location

Strand or Bar Location
#21 and #30 pretensioned strands
  are permanently bonded for
  dead load strength
#33 Strand is not removable
#14 Duct 1-5/8 in. ∅, flexible
#17 Duct 2-3/8 in. ∅, rigid
Draped Duct 2-3/8 in. ∅, rigid

1 in. = 2.54cm.
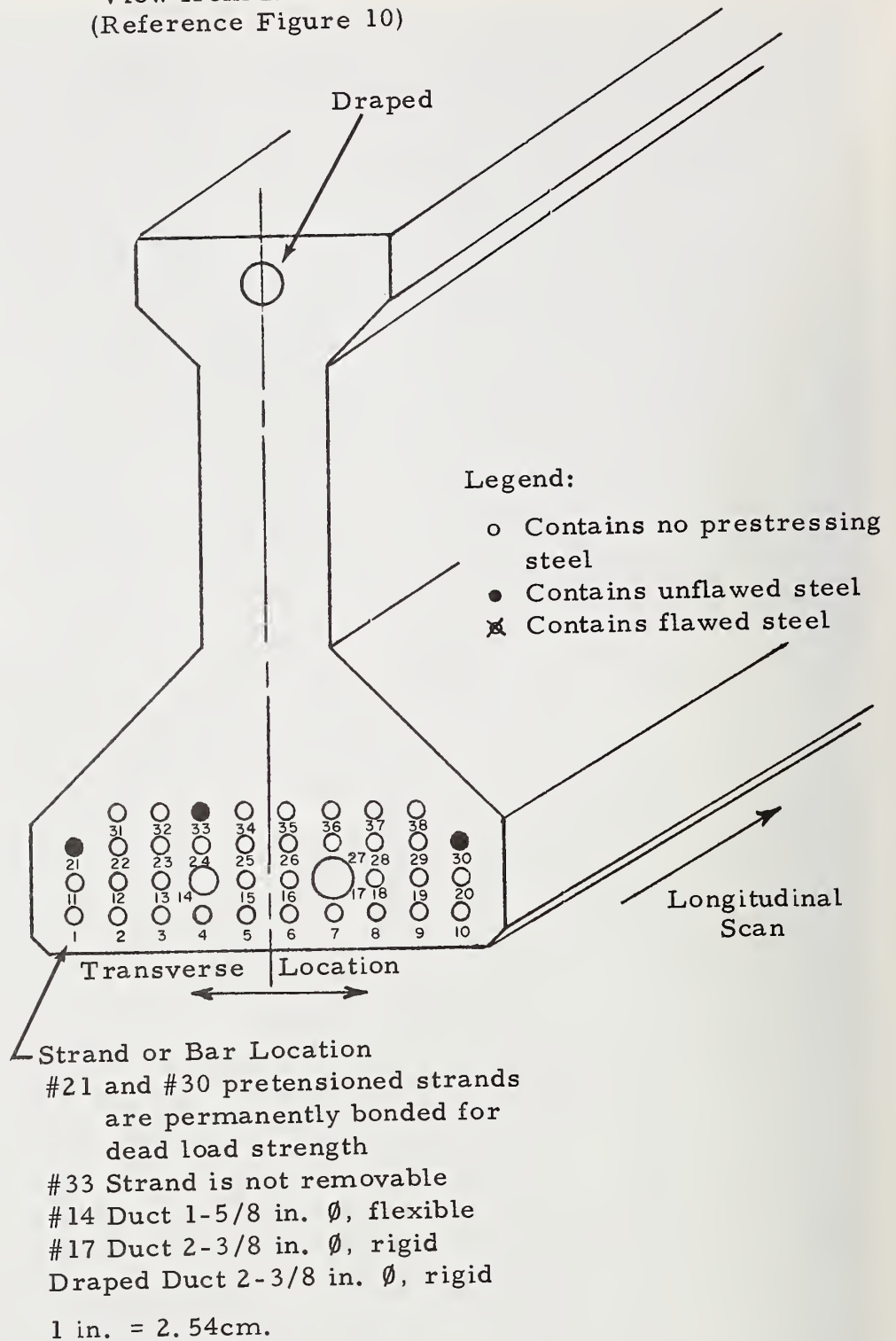
FIGURE 20. SKETCH OF END OF TEXAS TYPE "C" TEST BEAM
ILLUSTRATING PROCEDURE FOR IDENTIFYING PRE-
STRESSING STEEL CONFIGURATION INSPECTED

inspection. Selected magnetic inspection records are presented in
Figures 21 through 26 which illustrate typical experimental results. A
brief discussion of each of these figures follows.

Figure 21 presents results which indicate the signature
response from a 1-3/8-in. (3.5cm) diameter high-strength steel bar for a
simulated fracture with varying degrees of separation between the
fractured ends. The data shown in Figure 21 are for the centerline of the
flawed bar 3.7-in. (9.4cm) beneath the concrete surface of the test beam
being scanned; the clearance between the magnet pole faces (and Hall-
effect sensor and the concrete surface of the beam was 0.5-in (1.3cm).
It is pointed out that the signature from the simulated fracture for 0.5-in.
(1.3cm) separation and greater can be readily recognized from those
produced by the transverse stirrups. Furthermore for the cases in which
the simulated fracture is located between stirrups, end separations as
small as 0.015-in. (0.4mm) can be discerned because of the large hori-
zontal extent of the signature. For the record at the top of Figure 21, the
horizontal distance between the upward-going and downward-going peaks
of both the stirrup and fracture signatures have been indicated. This
separation between the peaks is proportional to the distance between the
sensor and the flaw and/or steel configuration causing the signature and
is a parameter which can be used to identify the depth of the element
causing the signature. It is noted that the separation of the peaks for the
stirrups is approximately one-third of that for the simulated fracture;
correspondingly, the lower arm of the stirrups is approximately 1.5-in.
(3.8cm) from the surface of the girder while the post-tensioned bar is
approximately 3.7-in.(9.4cm) from the surface. This peak separation
feature of the signatures will be referred to throughout this report since
it is a parameter which can be extremely helpful in the interpretation of
inspection results. A comparison of corresponding stirrup signatures in
the four records of Figure 21 show excellent repeatability even though bars
were removed and replaced to set up the various flaw conditions. Also,
it is pointed out that stirrup signatures could be monitored to assess
possible deterioration in the stirrup regions and to detect missing stirrups.

Signature responses from varying degrees of reduction
in cross-sectional area (simulation of loss-of-section due to corrosion)for a
1-in. (2.5cm) diameter high-strength steel bar are shown in Figure 22.
The upper record (Figure 22) shows the response from a 50-percent re-
duction in area over a 1/2-in (1.3cm) length in 1-in. (2.5cm) diameter
bar; the insert shows similar response from a slightly lower percentage
reduction in area for a 1-3/8-in (3.5cm) diameter bar. In all records of
Figure 22 for the 1-in. (2.5cm) diameter bar, the bar centerline is approxi-
mately 3.5-in. (9cm) from the face of the concrete beam. Evaluation of

31

FIGURE 21. MAGNETIC INSPECTION RECORDS ILLUSTRATING SIGNA-
TURES FROM SIMULATED FRACTURES OF 1-3/8 IN. (34mm)
Ø BAR WITH SEVERAL DEGREES OF FRACTURE END
SEPARATION WITH 3.7 IN. (9.4cm) CONCRETE COVER

Bar Flaw - 50% Area Reduction x 0.5 in. (12.5mm) Length

Bar Flaw = 50% Area Reduction x 0.12 in. (3mm) Length

Bar Flaw = 20% Area Reduction x 2 in. (5cm) Length

Bar Flaw = 20% Area Reduction x 0.5 in. (12.5mm) Length
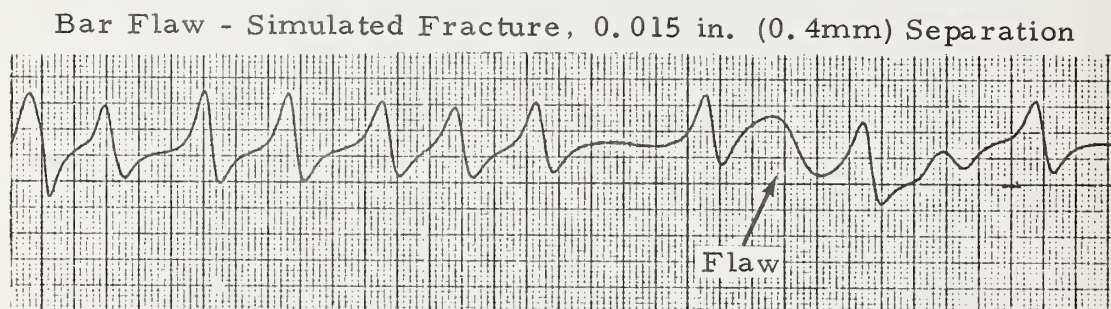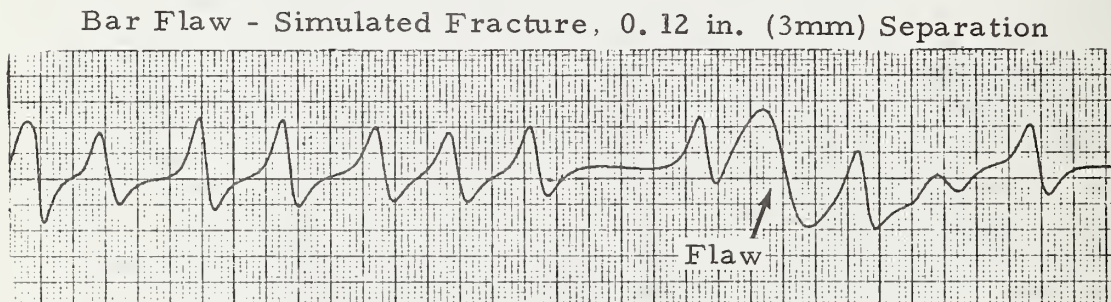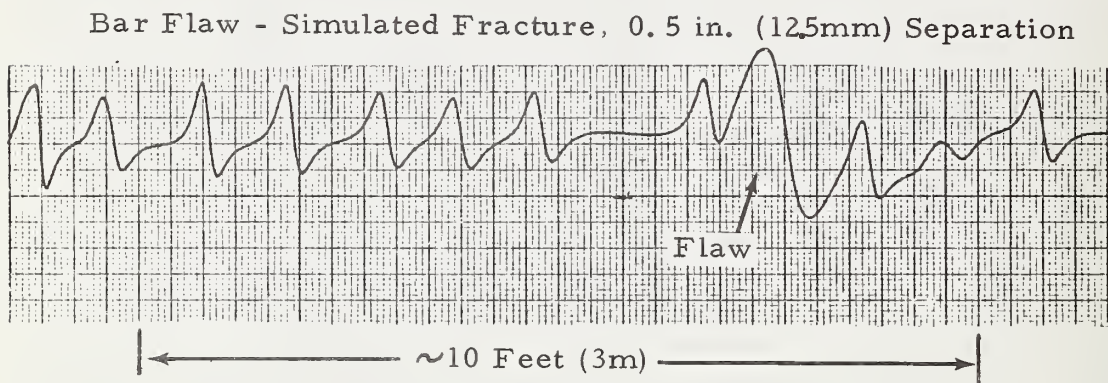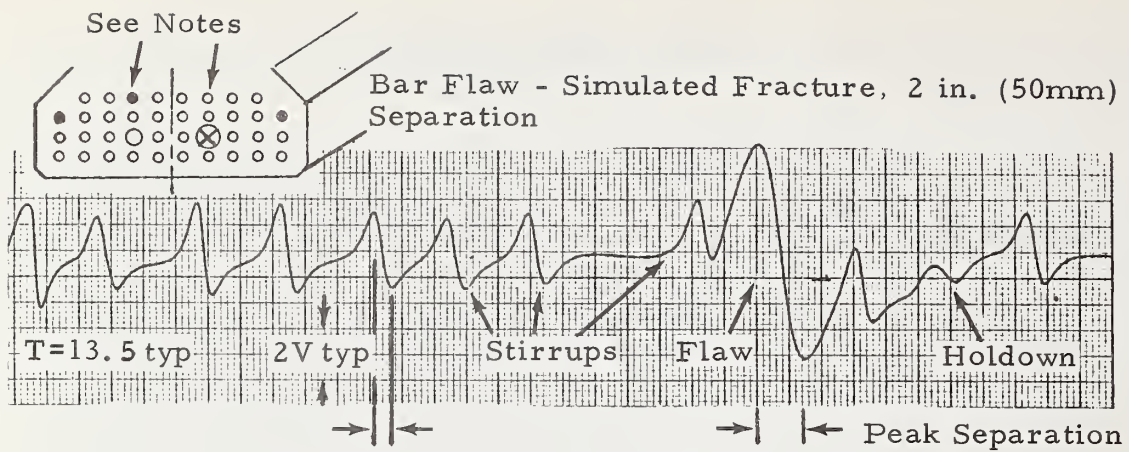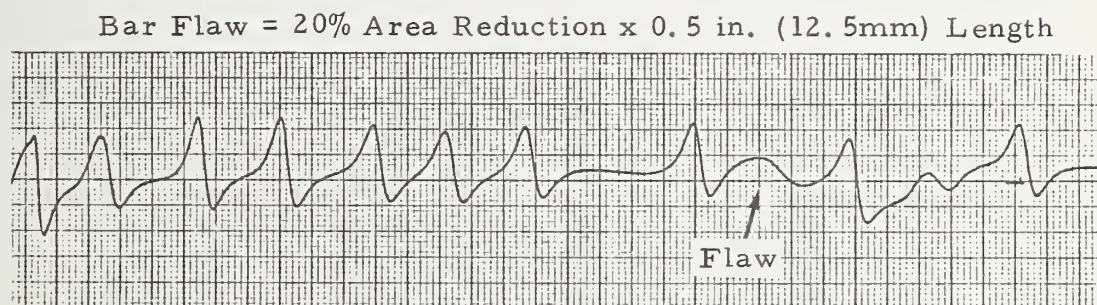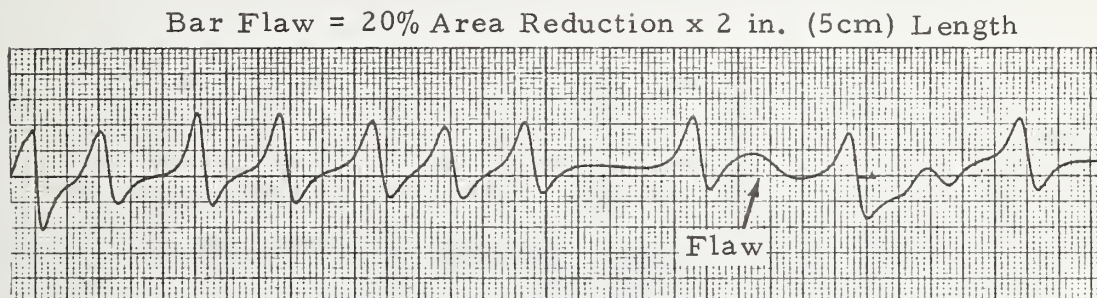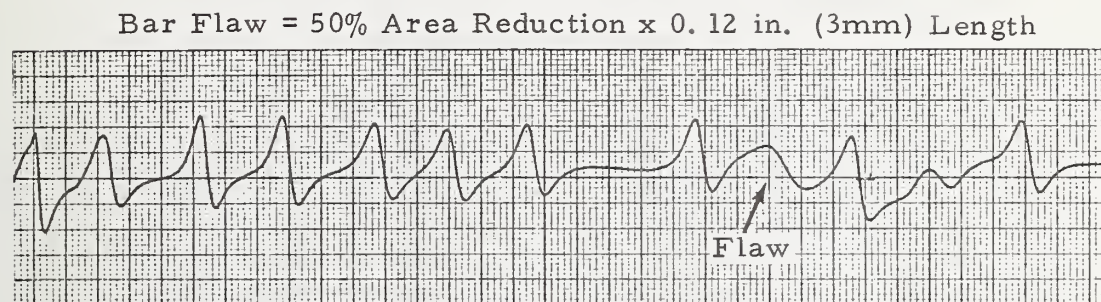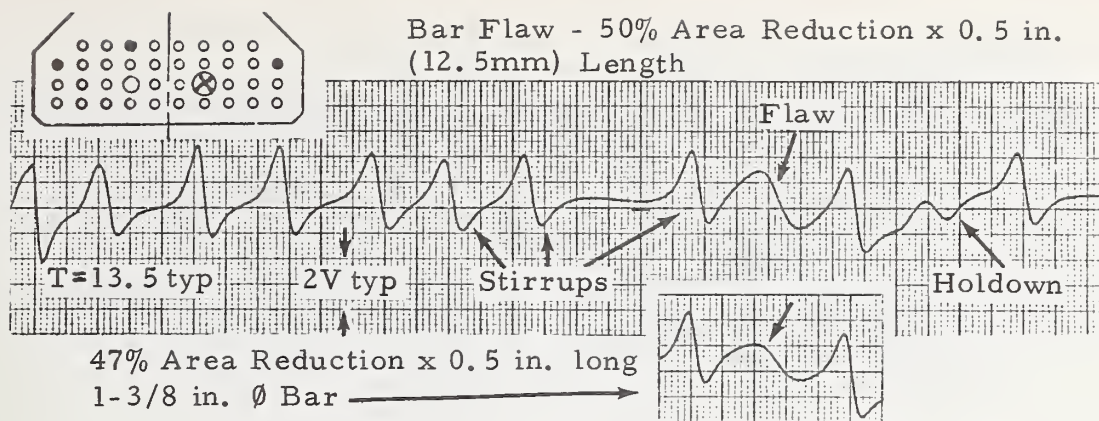
Notes: x Flawed bar, ● unflawed bar, T - transverse scan reading

FIGURE 22. MAGNETIC INSPECTION RECORDS ILLUSTRATING SIGNA-
TURES FROM SEVERAL FLAW SIZES IN 1 IN. (2.5cm) Ø
HIGH STRENGTH STEEL BAR (Texas Type "C" Test Beam)
WITH 3.5 IN. (9cm) CONCRETE COVER

33

*Strand Flaw - 3 Wires Removed Over 2 in. (5cm)
Length, First Row

T=10.5 typ   2V typ   Flaw   Holdown

←————————— ~10 Feet (3m) —————————→
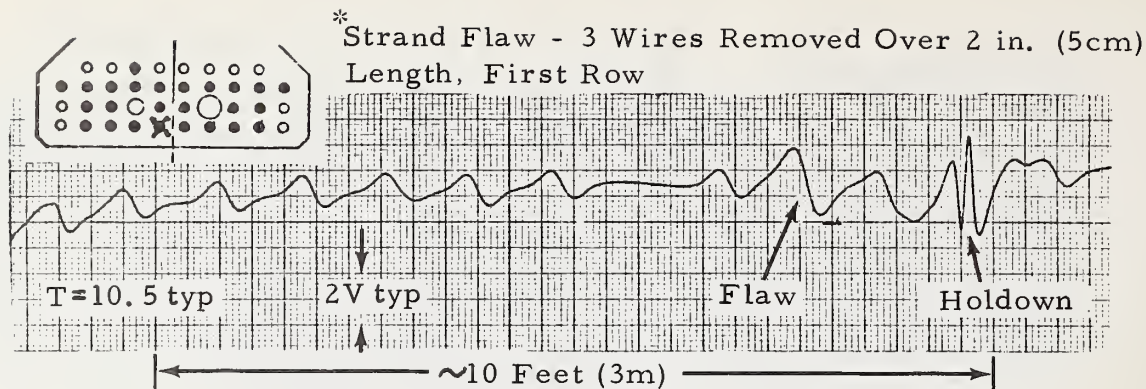
*Strand Flaw = 1 Wire Removed Over 2 in. (5cm) Length, First Row
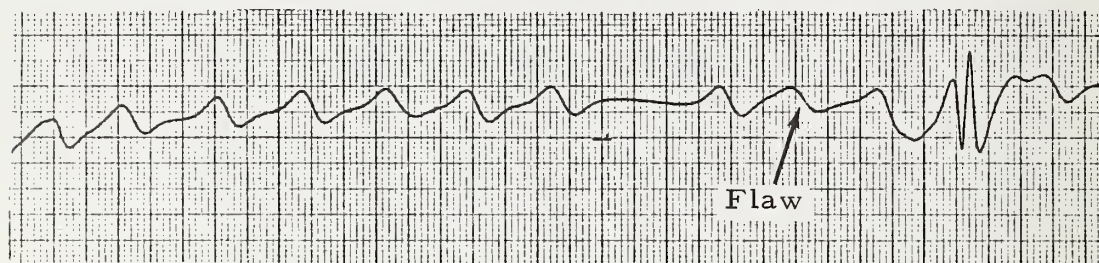
Flaw

*Strand Flaw = 1 Wire Removed Over 0.12 in. (3mm) Length, First Row
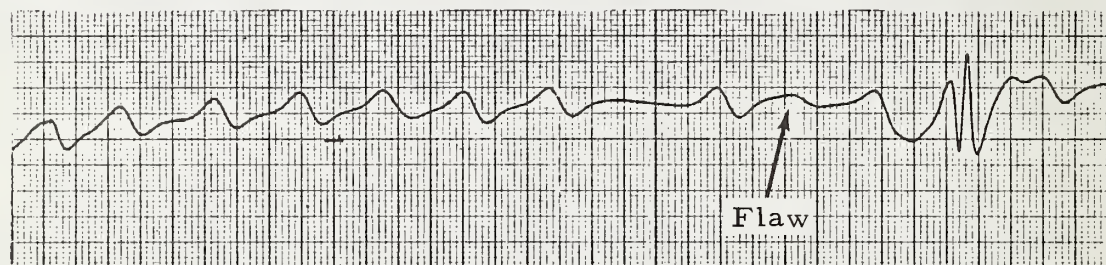
Flaw

Notes: x Flawed strand, ● unflawed strand, T - transverse scan reading
         Strand Matrix 2 in. (5cm) x 2 in. (5cm) typically
      * 1 wire of 7-wire strand removed (14% reduction)
         3 wire of 7-wire strand removed (42% reduction)

FIGURE 23.   MAGNETIC INSPECTION RECORDS ILLUSTRATING SIGNA-
             TURES FROM SEVERAL SIZES OF FLAWS IN STRAND [0.5 in.
             Ø (1.3cm) x 7 wire] (Texas Type "C" Test Beam)
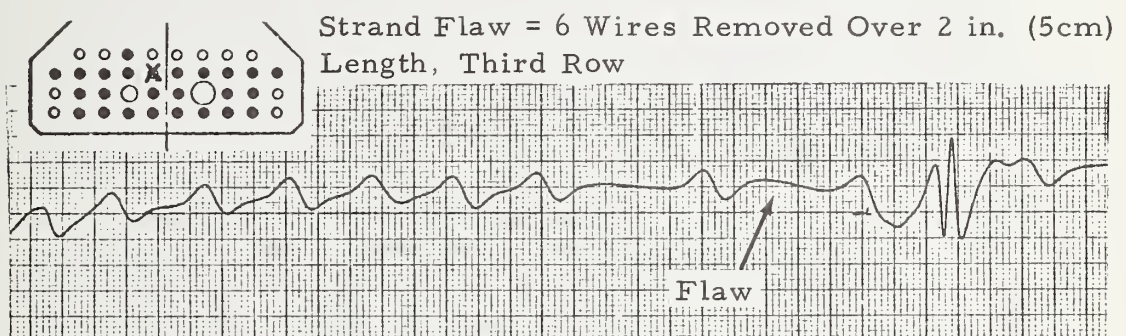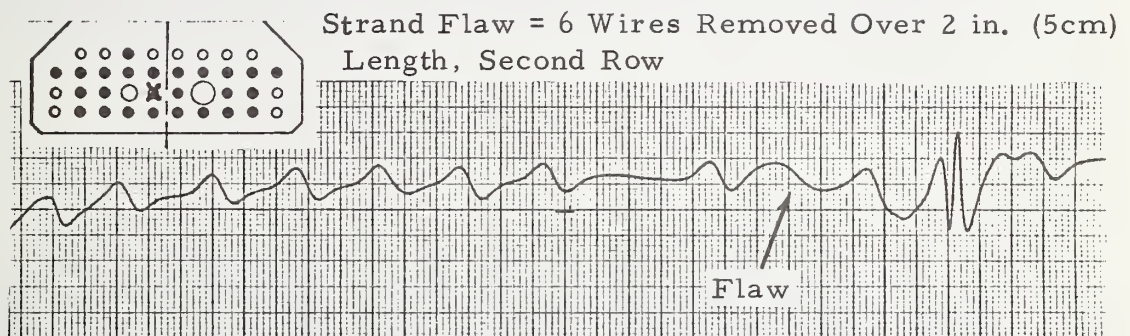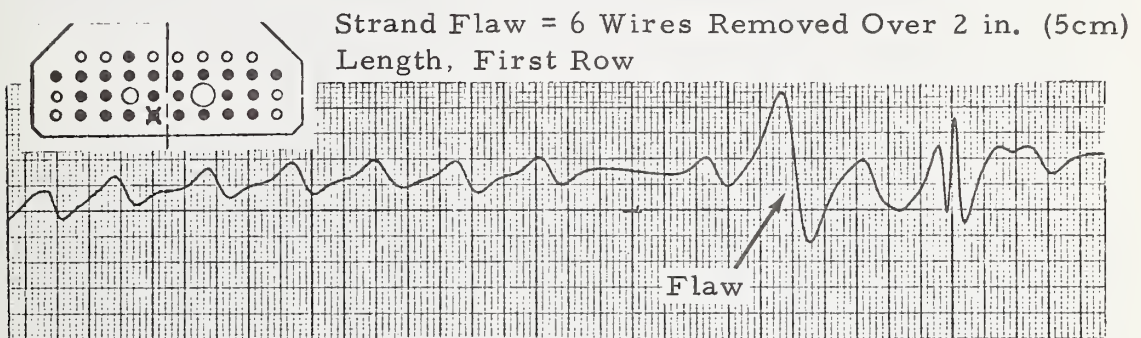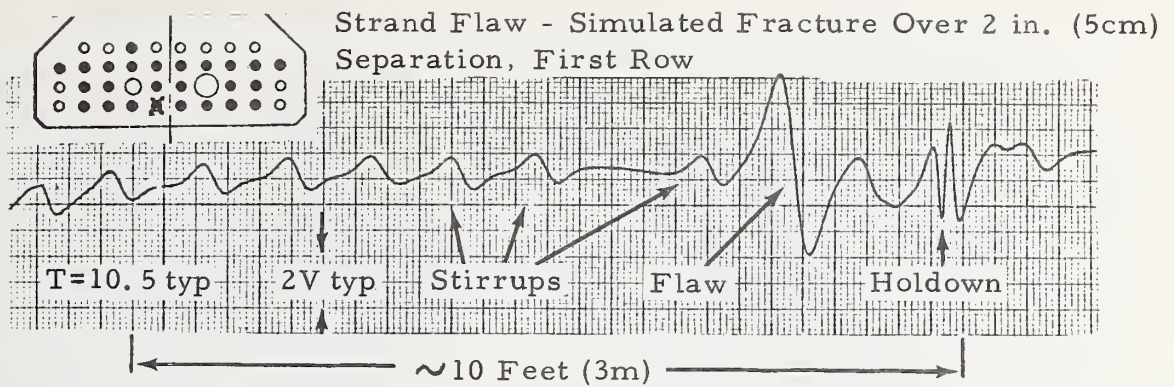
34

Strand Flaw - Simulated Fracture Over 2 in. (5cm) Separation, First Row

T=10.5 typ   2V typ   Stirrups   Flaw   Holdown

$\sim$10 Feet (3m)

Strand Flaw = 6 Wires Removed Over 2 in. (5cm) Length, First Row

Flaw

Strand Flaw = 6 Wires Removed Over 2 in. (5cm) Length, Second Row

Flaw

Strand Flaw = 6 Wires Removed Over 2 in. (5cm) Length, Third Row

Flaw

Notes: x Flawed strand, • unflawed strand, T - transverse scan reading
        Strand Matrix 2 in. (5cm) x 2 in. (5cm) typically

FIGURE 24. MAGNETIC INSPECTION RECORDS ILLUSTRATING SIGNA-
            TURES FROM FLAWED STRAND [0.5 in. Ø (1.3cm) x 7 wire]
            WITH SEVERAL DEPTHS OF CONCRETE COVERAGE (Texas
            Type "C" Test Beam)

35

Simulated Fracture (0.5 in. separation, 1.3cm)
at 13 Ft. Longitudinal Position

Stirrup

T=14.5 typ   2V typ   Flaw

Simulated Fracture at 12 Ft. -6 in. Location

Stirrup

Flaw

Simulated Fracture at 12 Ft. Location
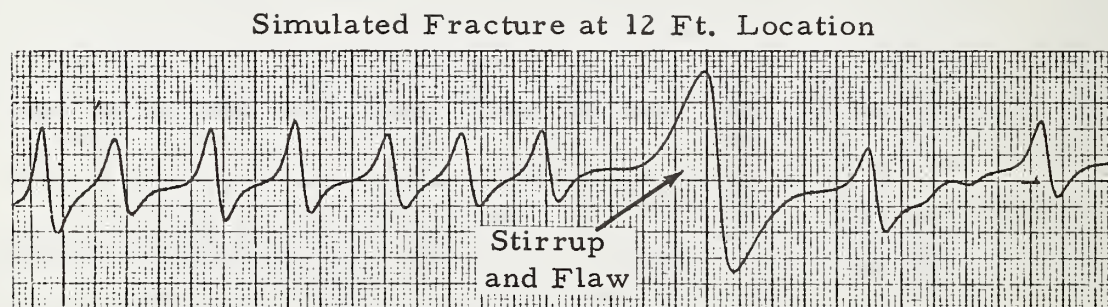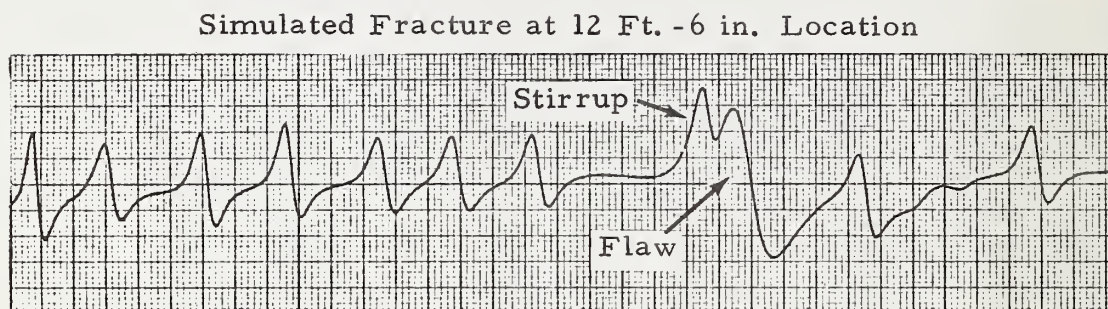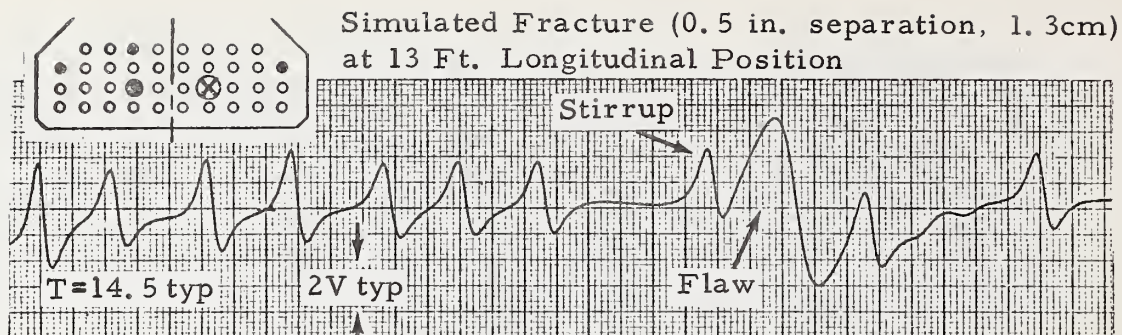
Stirrup
and Flaw

Notes: x Flawed bar, ● Unflawed bar, T - transverse scan reading
        1 in. = 2.54cm

FIGURE 25.   MAGNETIC INSPECTION RECORDS ILLUSTRATING COMBINED
             SIGNATURES FROM A STIRRUP AND FLAW (simulated fracture,
             0.5 in. separation) AS A FUNCTION OF RELATIVE POSITION
             (Texas Type "C" Test Beam) FOR 1-3/8 in. (3.5cm) ∅ BAR
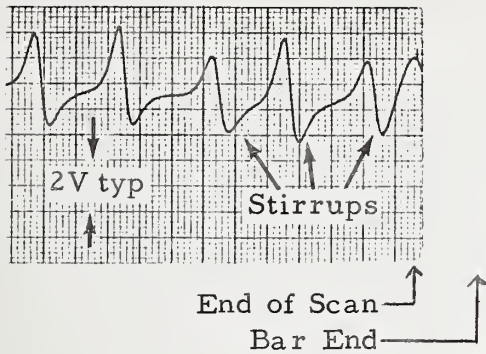
36
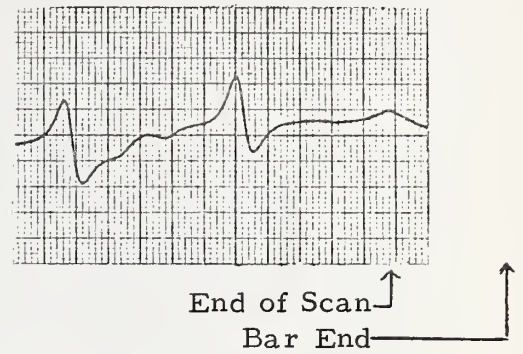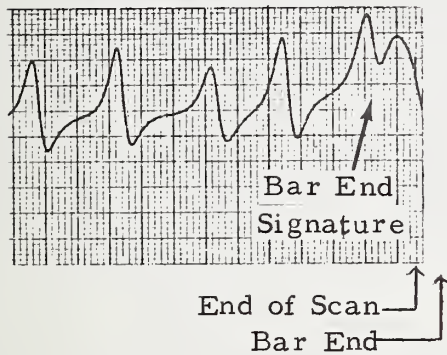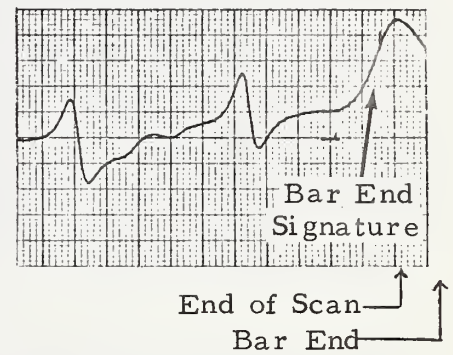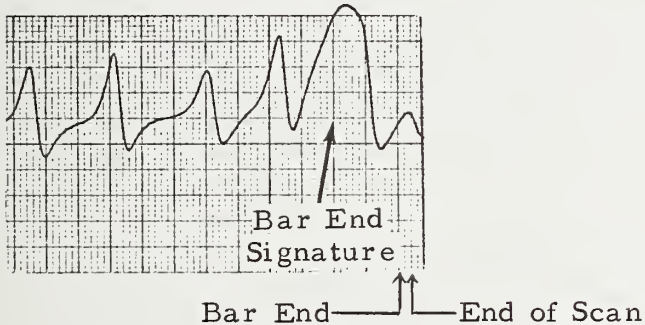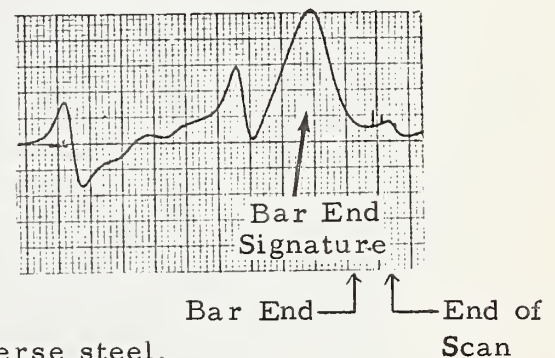
FIGURE 26. MAGNETIC INSPECTION RECORDS ILLUSTRATING SIGNA-
TURE RESPONSE FROM END OF A BAR NEAR THE END
OF SCAN

37

the signatures for the 20-percent area reduction for this concrete coverage condition indicates a good probability for the detection of a 10% reduction in area provided adequate stirrup signature discrimination could be developed. The need for such discrimination against configurational steel artifact signatures is discussed in considerable detail later in this section of the report.

Figures 23 and 24 present results from simulated flaws in 1/2-in. (1.3cm) diameter x 7-wire strand arranged in a typical 2-in. (5cm) by 2-in. (5cm) matrix. Figure 23 presents results for varying degrees of strand deterioration with the flawed strand in the first row of the matrix (see partial cross-sectional view of the girder at the upper left record). Analysis of the lower two records (Figure 23) indicates that detection of a 14% reduction in cross-sectional area would probably be marginal. The records in Figure 24 show a rapid decrease in signature amplitude from the same size flaw for increasing depths of the flawed strand in the matrix. The second, third, and fourth records from the top of Figure 24 present flaw signature data from an 86% reduction in area over a 2-in. (5cm) length [removal of six wires from the 7-wire strand over a 2-in. (5cm) length] with this flawed strand 2-in. (5cm), 4-in. (10cm), and 6-in. (15cm), respectively, beneath the surface; unflawed strands adjacent to the flawed strand are present in all cases as indicated by the cross-section at the upper left in each record. The results in Figure 24 indicate that detection of an 86% x 2 in. (5cm) loss of section deeper than the first row of the matrix would probably be marginal.

The influence of signatures from reinforcement steel details, such as stirrups, holdowns, etc., on flaw signature recognition is illustrated by Figure 25. The center and lower records in this figure indicate that the field perturbances from the combined steel and flaw configurations are essentially cumulative. The combined effects can significantly modify the amplitude and shape of the resulting signal; for example, note the greater amplitude and significantly reduced horizontal separation between the upward-going and downward-going peaks (peak separation) of the combined stirrup and flaw signature in the lower record of Figure 25 as compared with that for the flaw signature only in the upper record of the same figure. Importantly, the outstanding signature from the simulated fracture (0.5-in. separation, 1.3cm), illustrated in Figure 25, for a concrete coverage of approximately 3.7-in. (9.4cm) indicates that such a condition should be readily detectable. Other examples will be presented later in this report, however, from field data which indicate that the presence of other types of steel details as well as other complicating factors can significantly influence the interpretation of inspection data.

38

Figure 26 presents numerous magnetic records illustrating detection near the end of scan as related to the detection of deterioration (flaw condition) near the end of a girder which is resting on a bent (such that an inspection scan to the end of the girder is not possible). The results in Figure 26 indicate the presence of a significant flaw (such as a bar fracture with 0.5-in. (1.3cm) separation can be detected even though the scan does not fully extend to the flaw location. Based on these results, it is estimated that a significant flaw can be detected when it is approximately 6-in. (15cm) beyond the end of scan. For example, with a 1-ft. (0.3m) footing over the bent, fracture could be detected almost within 2-ft. (0.6m) of the end of the girder. If detailed inspection near the ends of girders is of critical concern, with special-purpose inspection equipment design, closer approach to the girder ends may be possible.

Figure 27 summarizes signature response data as a function of concrete coverage for several types of simulated deterioration. It is pointed out that the electronic noise level of the equipment is two orders of magnitude below the amplitude range of the dominating signatures. Importantly, realization of the potential capability of the magnetic inspection method is heavily dependent on development of techniques for discriminating between signatures from deterioration and those from reinforcement steel details. The significance of the discrimination problem will become clearer in the subsequent discussion of the field evaluation efforts.

C. Field Evaluation

1. Site Selection and Planning

As a parallel effort to the design, fabrication, and laboratory evaluation of the preliminary magnetic inspection equipment, site selection and planning for field evaluations were conducted. Through discussions with FHWA personnel, personal contacts by SwRI personnel, and personal contacts by Mr. A. Leone, Consultant, two candidate sites were selected.

a. One site was the Sunshine Skyway Bridge at Tampa, Florida, which was selected on the basis that known corrosion deterioration currently exists in that structure. Considerable information about the structure was made available through the excellent cooperation of Mr. Roger Hove, Director, Office of Bridges, FHWA, Atlanta, Georgia, and Mr. Jack Roberts and Mr. Rene Rodriguez, Bridge Maintenance, Tampa District, Florida Department of Transportation.

39
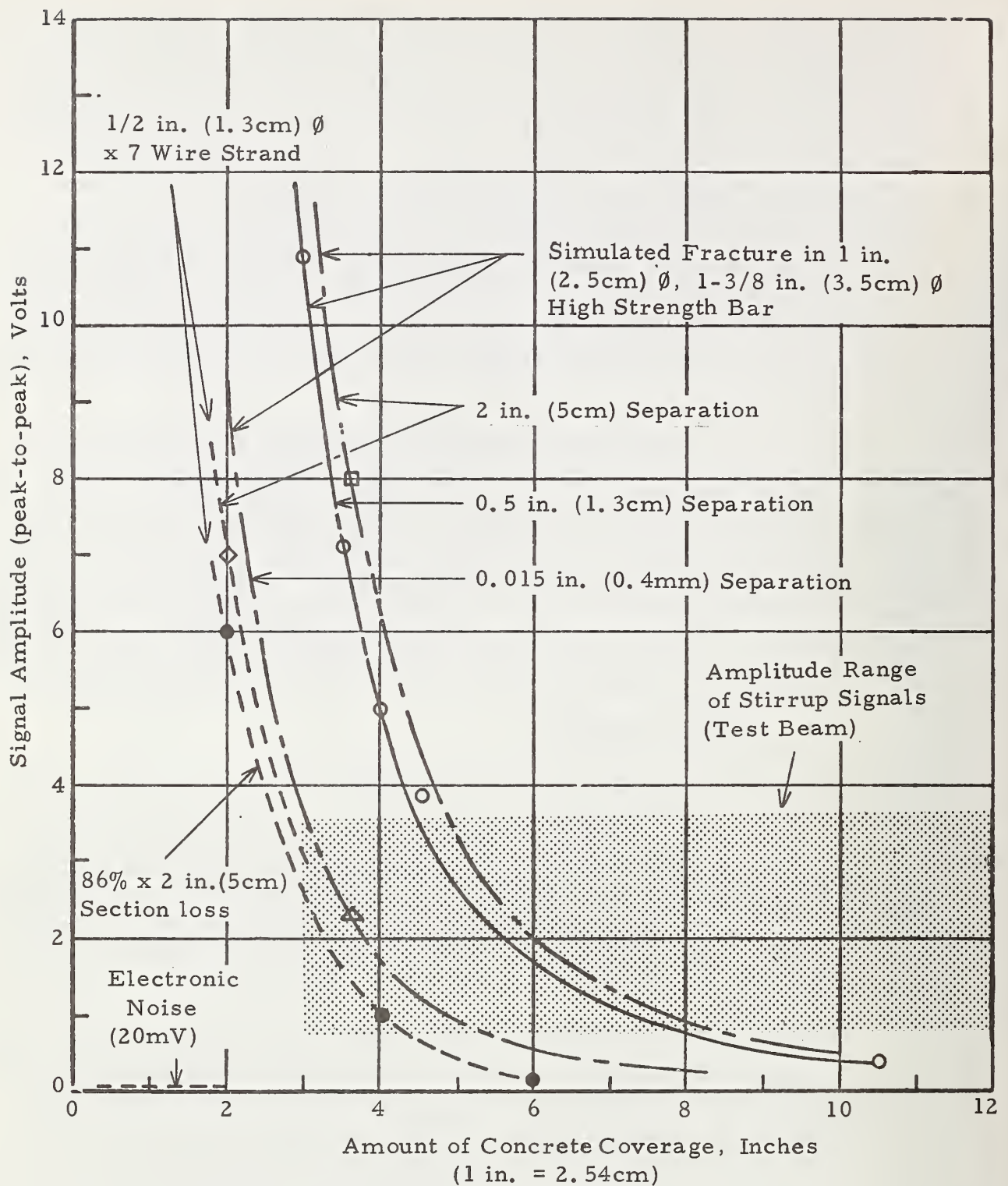
FIGURE 27. GRAPH PRESENTING SIGNATURE RESPONSE FROM SEVERAL
TYPES OF SIMULATED DETERIORATION AS A FUNCTION OF
CONCRETE COVERAGE

40

b.   The other test site was the Sixth South Street
Viaduct in Salt Lake City, Utah, which was considered a prime field
test site since there are known deteriorated members (fractured
1-3/8-in. (3.5cm) ∅ post-tensioned bars) and members which were
perhaps questionable. Photographs of and construction drawings for
this structure were made available through the efforts of Mr. A. Leone
and through the excellent aid and cooperation of Mr. Ray Behling, Chief
Structural Engineer, Utah Department of Transportation, as well as
Mr. Robert Frost, Bridge Engineer, FHWA, Utah Division. The
Sixth South Street Viaduct was selected for the first field trip which
was conducted during the week of 7-11 November 1977.

Handling equipment requirements, accessability,
inspection procedures, etc. at the Utah site were discussed by Messrs.
C. McGogney, Contract Manager, R. Behling, Chief Structural Engineer,
Utah DOT, A. Leone, Consultant, and F. Kusenberger, Principal Investigator
at the FCP meeting in Atlanta on 3-4 October 1977 and in subsequent telecons.
Also, photographs of the inspection setup (installed on the test beam at SwRI)
and a brief description of the equipment and installation procedures were
forwarded to Mr. Behling. The inspection plan consisted of first verifying
detection of the ends of fractured bars in situ; the location of bar ends should
be known since one end of a fractured bar had been removed in each of
two girders. Subsequently, it was planned to proceed to bars suspected
to be fractured.

c.   As will become evident to the reader, the Utah
field evaluation records showed several prominent anomalous signatures
which subsequent field excavations established to be the result
of unanticipated steel elements (chairs). Following the Utah tests, labora-
tory simulation of the field configurations confirmed the features of the
anomalous signatures. Subsequently, it was decided to conduct a second
field evaluation on beams having a configuration of steel more nearly
approximating that of the laboratory test beam - desirably a Texas Type
"C" girder. Accordingly, it was decided to inspect a group of 80-ft. (24m)
Type "C" girders available at Manufactured Concrete, Inc. (formerly
McDonough Brothers, Inc.) San Antonio, Texas. The inspection sig-
natures obtained from stirrups and simulated fractures (fabricated in a
reject girder) on 80-ft. (24m) girders were in agreement with those
obtained from the laboratory test beam. The "holdown" fixture on the
80-ft. (24m) girders was different from that incorporated in the 20-ft.

41

(6m) test beam and corresponding signature responses were observed.
Still other small amplitude signatures obtained on the production girders
(not observed on the test beam) were correlated with "tie wire" scrap
located on the lower surface of some girders. The results of this most
recent field work at Manufactured Concrete, Inc. are presented in
detail in Appendix IV of this report.

2. Utah Site Description

Figure 28 shows several views of the Sixth South Street
Viaduct. It is noted that the area beneath the bridge was used as a con-
trolled parking area during normal business hours. It was necessary to
make arrangements to clear parking from those areas required to gain
access to the girders being inspected. Figure 29 shows typical views of
the inspection equipment installed on a girder and the remote control
equipment located at ground level in a station wagon. Figure 30 shows
plans of the structural details for both post-tensioned and pretensioned
girder designs used in the structure. Particular attention is called to
the "L"-shaped stirrups specified for both types of prestressing. It is
also pointed out that the exterior dimensions of the lower flange region
of the girders are identical to those of the Texas Type "C" test beam
used in the laboratory evaluations. Later discussions in this report
will make reference to the "L" stirrups and associated magnetic signa-
tures. Details pertaining to the placement of the post-tension bars are
presented in Figure 31. Magnetic inspections were limited to the two
lower bars and no attempt was made to inspect the "draped" bars. While
inspections were limited to those elements previously defined in Section
I.B of this report, with appropriately designed fixtures, the draped
elements could also be inspected. Referring to Figure 31, it is pointed
out that the lower two post-tension bars are not precisely parallel to the
lower concrete surface of the girder. The distance from the centerline
of the bar to the lower concrete surface varies from a minimum of
3.5-in. (9cm) at mid-span to a maximum of 6-in. (15cm) at the ends
of the girder. The influence of this "slight drape" on the magnetic sig-
natures will be pointed out later in this section. The sketch in Figure 32
references the location of the girders inspected.

3. Inspections and Data Analyses in the Field

As indicated earlier, a logical inspection sequence
was planned. Initially, a region known to contain the end of a fractured
bar was to be inspected to provide a signature from a known field condition

Overall View of
Inspection Site
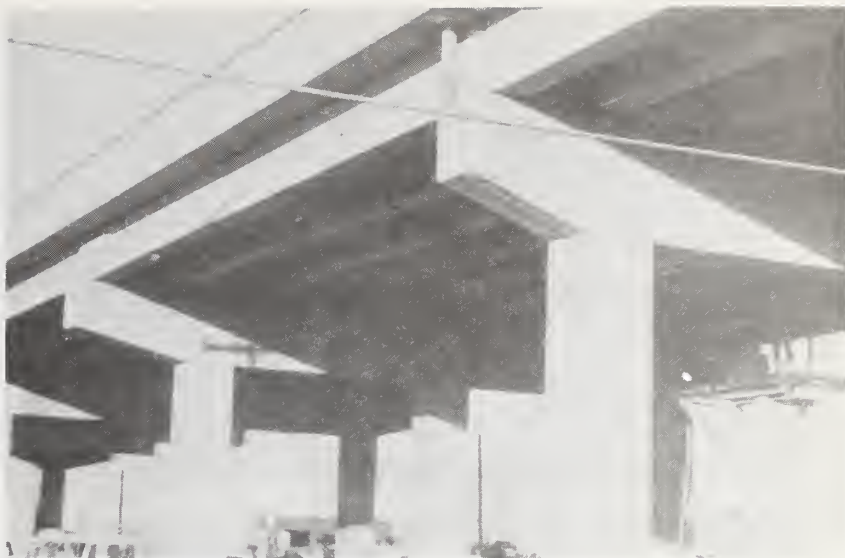
Installation via
Hydraulically
Actuated
Scissor-Lift

Installation via
Reusable
Scaffolding

FIGURE 28.   VIEWS OF FIELD TEST SITE AT SIXTH SOUTH STREET VIADUCT
IN SALT LAKE CITY, UTAH

43

Overall View of
Inspection Cart and
Track Assembly
Installed on Girder

Track

Hangers

Inspection Cart
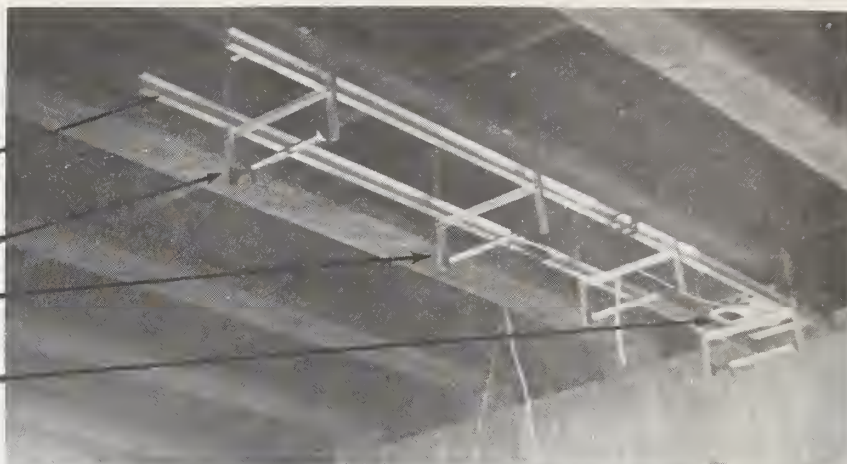
Closeup View of
Inspection Cart and
Track Assembly
Installed on Girder

View of Remote
Site Signal and
Control Equipment

FIGURE 29. VIEWS OF PRELIMINARY MAGNETIC INSPECTION EQUIPMENT
AT SIXTH SOUTH STREET VIADUCT, SALT LAKE CITY, UTAH

44

FIGURE 30. GIRDER DRAWINGS FOR SIXTH SOUTH STREET VIADUCT (Salt Lake City, Utah)

FIGURE 31. POST-TENSIONING BAR LAYOUT FOR SIXTH SOUTH STREET VIADUCT (Salt Lake City, Utah)
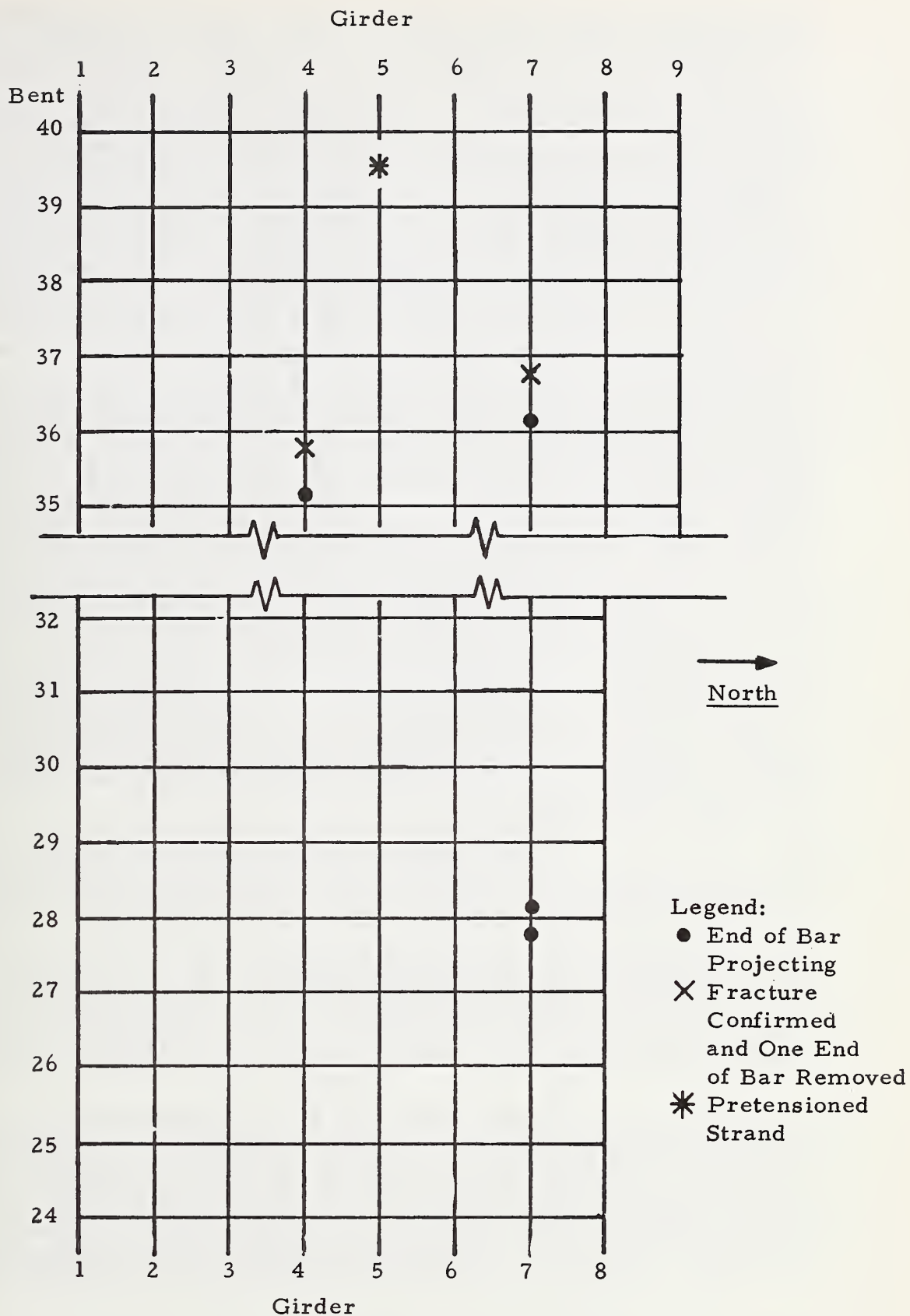
FIGURE 32.   LAYOUT OF SIXTH SOUTH STREET VIADUCT SPANS SHOWING
LOCATION OF GIRDERS INSPECTED

47

for comparison with signatures from similar conditions obtained during previous laboratory investigations. Such conditions existed in girder 4 between bents 35 and 36 (Span 35-36) and girder 7 between bents 36 and 37 (Span 36-37) since one end of the fractured bars had been pulled out of the duct in each case (see Figure 32). This plan was not followed; Mr. Pete Panos, Bridge Maintenance, Utah DOT, indicated problems of gaining access to the girders with the fracture bad ends using available equipment (a scaffold/flat-bed truck configuration) because of existing curbing in these areas of interest. Mr. Panos suggested that initial inspections be conducted on girder 7 of the span between bents 27 and 28 of the Sixth South Street Viaduct. This location was selected on the basis of a possible bar fracture based on the loss of end grouting and a slight projection at the bent 28 end of the lower post-tension bar (North bar). It was indicated that the longitudinal location of the suspect fracture would probably be near the end of the girder opposite that showing the projection (i. e., bent 27 end). This rationale was based on previous observations made when fractured bars were physically removed from two other locations in the viaduct. Accordingly, inspection of girder 7, Span 27-28, was initiated near the bent 27 end, but was extended over almost the entire length of the girder; transverse locations in the region of both lower bars were inspected. Five inspection scans were recorded; approximately 2-in. (5cm) outboard of the nominal location of each lower bar, at the nominal location of each bar, and midway between the two lower bars. This scan procedure was typically followed in all girder inspections. A composite scan over approximately 52-ft. (15.8m) of the nominal 60-ft. (18m) long girder was carried out in three adjacent (end-to-end) setups of the track assembly with a slight overlap of longitudinal coverage of each scan.

Next, girder 7 of adjacent Span 28-29 was inspected. One of the lower bars (North bar) was suspected as fractured because the retaining nut was not seated in the end retaining plate at the bent 28 end. The inspection was initiated adjacent to the bent 29 end of the span and progressed towards the bent 28 end. A very outstanding signature was obtained approximately 14.5-ft. (4.4m) from the end containing the bar extension (bent 28 end), and a reference mark was spray-painted on the beam corresponding to this signature location.

Finally, inspections were conducted on three other girders. On two of the girders (girder 7 of Span 36-37 and girder 4 of Span 35-36), one end of each fractured bar had been previously removed. The location of the end of the remaining bar in each case was independently measured using "plumber's" and "electricians's snakes"; subsequently, signature recordings were obtained in the vicinity of the

48

fractured end of each of the bars of these two girders. Several pre-
tensioned strand girders were also used in the Sixth South Street
Viaduct and signatures from a typical section were recorded on one
of these beams (girder 5, Span 39-40). Signatures obtained from the
four post-tensioned girders inspected will now be discussed briefly
from the standpoint of analyses made in the field based on information
known at the time of the field site visit. Following this discussion,
a retrospective interpretation of the same data will be presented on
the basis of results from subsequent correlation investigations. This
"before and after" type of data presentation will better acquaint the
reader with the overall data interpretation problem.

        Figure 33 shows a composite record over ∼52-ft.
(15.8m) of the nominal 60-ft. (18m) long girder 7, Span 27-28 in the
region of the two lower bars. The numbers above each trace (Figure 33)
identify outstanding signatures from corresponding longitudinal loca-
tions for scans of the two adjacent lower bars. The lower amplitude
signatures in the two scans (see arrows in Figure 33) appear similar
to those obtained from stirrups in the Texas Type "C" laboratory test
beam (Figure 21); it is pointed out that the signatures in Figure 33,
attributed to the stirrup structure, appear inverted to those of Figure 21
because of the relative direction of travel of the inspection cart. In
nearly all cases, the outstanding signatures numbered in Figure 33 are
opposite in polarity to the stirrup signatures (i.e., from left to right,
the numbered signatures are upward-going and then downward going
versus downward-going and then upward-going for the stirrup signatures);
the peak separation of the numbered and stirrup signatures is similar.
A review of signature characteristics from simulated fractures in the
laboratory (refer to Figure 21) in conjunction with examination of the
recordings from the two lower bars (see Figure 33) of girder 7, Span 27-
28 of the Sixth South Street Viaduct indicates no evidence of fracture in
the North bar of girder 7 based on the following rationale:

        i)   None of the signatures from the North bar of
girder 7, Span 27-28 have the combined features of the laboratory sig-
natures indicated for a bar fracture; namely, the same polarity as the
stirrup signatures and a peak separation of the order of 6-in. (15cm).

        ii)   In nearly all cases, the outstanding signatures
from girder 7, Span 27-28 appear on both the North bar and South bar
scans at approximately the same longitudinal locations. The coincident
occurrence of such similar signatures in two adjacent bars located 6-in.
(15cm) apart (transversely) cannot be interpreted, logically, as indica-
tive of fracture in one bar only, and fracture of both bars at the same
longitudinal location is highly improbable.

49
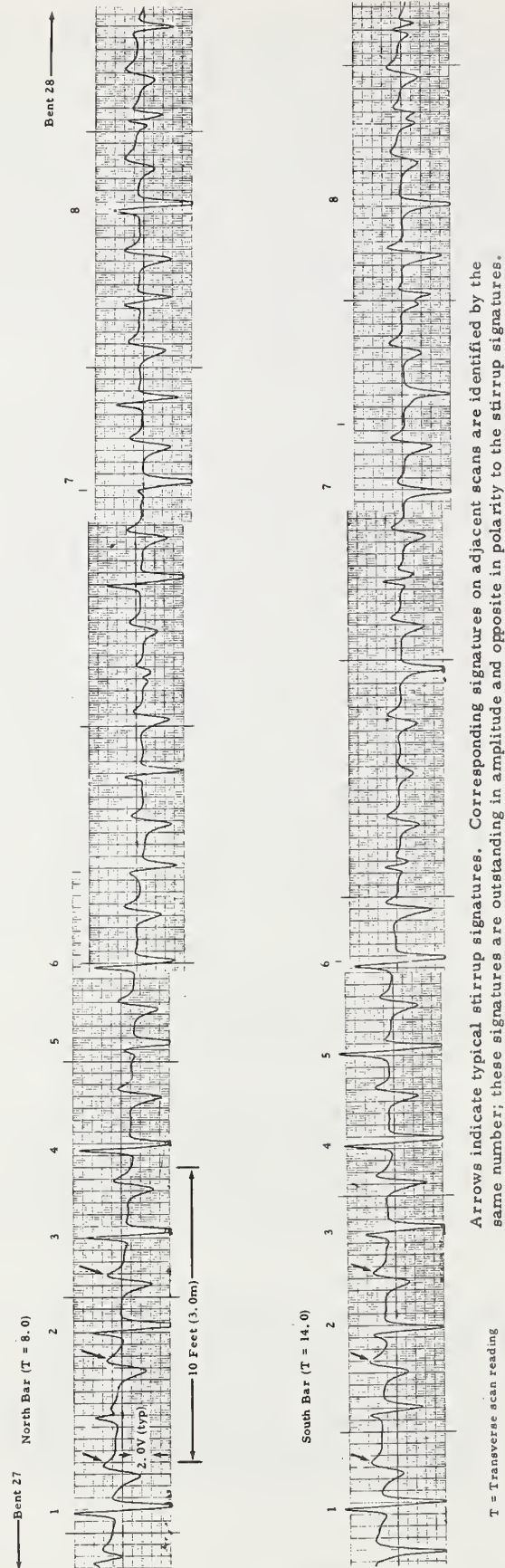
FIGURE 33. MAGNETIC RECORDS FROM AN INSPECTION SCAN BENEATH EACH OF THE TWO LOWER BARS ON GIRDER 7 BETWEEN BENTS 27 AND 28, SIXTH SOUTH STREET VIADUCT (Salt Lake City, Utah)

Arrows indicate typical stirrup signatures. Corresponding signatures on adjacent scans are identified by the same number; these signatures are outstanding in amplitude and opposite in polarity to the stirrup signatures.

T = Transverse scan reading

iii) If any one of the outstanding signatures for the
North bar of girder 7, Span 27-28 corresponds to fracture, then the
presence of other signatures having the same features would indicate
multiple fractures within a single bar; this is highly improbable.

Signature recordings obtained in the vicinity of the
fracture of the remaining end of the fractured bar in girder 4, Span 35-36
and in girder 7, Span 36-37 as well as the one in the region of the outstanding
signature in girder 7, Span 28-29 are presented in Figure 34.

Referring to the second and third records from the top
in Figure 34, the regions from which signatures 1 and 2 were obtained
coincide with the bar ends in girder 7 of Span 36-37 and girder 4 of Span
35-36, respectively, as measured from one end of the girder using an
"electrician's snake" (on girder 7, Span 36-37 measurement confirmation
was obtained using both plumber's and electrician's snakes). Notice the
similarities in the two signatures; namely, i) both signatures have a
polarity opposite to that of the surrounding signals attributed to stirrups,
ii) both signatures are bipolar, i.e., downward- and then upward-going,
and iii) the spacing between the downward- and upward going peaks
corresponds to approximately 5-6 in. (13-15cm). It is pointed out that
laboratory results indicate the signature from the end of the bar should be
unipolar, i.e., only upward-going or downward-going; for an example,
refer to the lower right record in Figure 26. Despite these differences
between the laboratory and field results, independent physical measure-
ments of the location of the end of the bar for both girders 7, Span 36-37,
and girder 4, Span 35-36, confirmed the end of the bar in each case to be
coincident with the outstanding signatures (signatures 1 and 2, respectively,
Figure 34). Accordingly, during the field evaluation, the results from these
two cases associated with the known end of the bar were used as a basis
to examine the other outstanding signatures A, B and C (Figure 34) which
are similar in shape and amplitude. A detailed discussion of the results
presented in Figure 34 was conducted during a meeting on the last day of
the Utah field evaluation at the State Offices of the Utah Department of
Transportation.* From these discussions, it was decided to excavate
the regions corresponding to the prominent signatures A and C (Figure 34).
The results of the excavation efforts are discussed next in conjunction with
the results of subsequent work in the laboratory regarding simulation of
the steel configuration in the Utah girders.

_____
* See Appendix II for a list of attendees at this meeting.
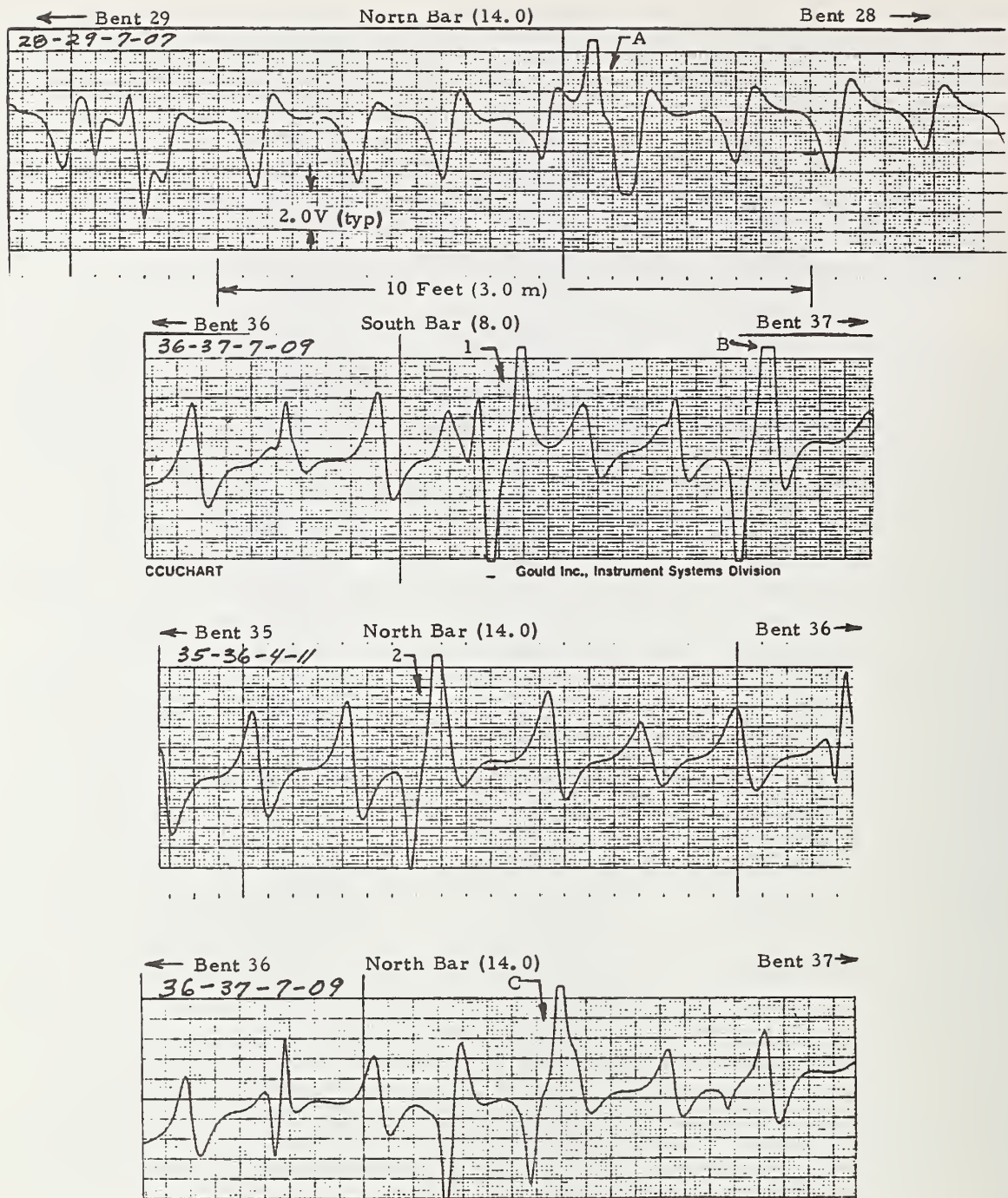
Note: Signatures 1 and 2 coincide with location of known bar ends of two fractured bars. Signatures A, B, and C are suspect fractures based on similarity to Signatures 1 and 2.

FIGURE 34. SELECTED SIGNATURES FROM SIXTH SOUTH STREET VIADUCT GIRDERS

52

4.   Correlation Investigations

As previously indicated, field evaluation of the inspection equipment was followed by excavation of one signature location each in girder 7, Span 28-29, North bar (see signature A, Figure 34) and in girder 7, Span 36-37, North bar (signature C, Figure 34) by Utah DOT. An air hammer was used to remove the concrete in the regions of interest, and the duct was penetrated to determine the condition of the post-tension bar in each case. In neither case was the bar fractured. However, a "bar-duct support high-chair" was disclosed at each location coincident with the signature of interest (see Figures 35, 36, and 37). A "high-chair" is a steel structure, usually several inches (cm) in length and height (available in a range of sizes), having four support feet which are normally flush with the lower surface of the girder; high-chairs, not shown on the bridge drawings or otherwise known to be present, were used, apparently, to hold the steel in position and off the bottom of the form during pouring of the girders. Correlation between the signatures of interest and the high-chairs was excellent. For example, analysis of the second and fourth inspection records from the top in Figure 34 indicates signature C to be 10 in. (25cm) toward bent 37 from signature 1 (corresponding to the end of a bar); the measurement in Figure 36 shows the chair position to be 10 in. (25cm) from the mark, corresponding to signature 1, towards bent 37 (the line painted on the bottom surface of the girder corresponding to signature 1 was painted during inspection, before excavation).

A cursory analysis of the characteristic signature anticipated from the high-chair indicates a shape similar to that observed for signatures 1, 2, A, B, and C in Figure 34. Since it is known (from the measured distance using a snake) that the end of the bar was coincident with signatures 1 and 2 (Figure 34), it is anticipated that the signature from the end of the bar is "masked" by the high-chair signature. In order to clarify and better define the problems of data interpretation encountered in evaluating the Utah field results, laboratory investigations were conducted using a mockup steel configuration simulating that of the Utah girder, according to the construction drawing, and including other constructional artifacts such as high-chairs. Figures 38 and 39 present overall and close-up photographs of the laboratory simulation setup. The initial stage of the investigation was aimed at confirming the typical signature shapes obtained from the stirrup configuration of the Utah girders in the field before adding the additional complexity of the high-chair. This initial step was prompted because of the similarity in shape of stirrup signatures obtained from the Texas Type "C" test beam in the laboratory and those obtained from the Utah girder in the field (see Figures 21 and 34); examination of the plans
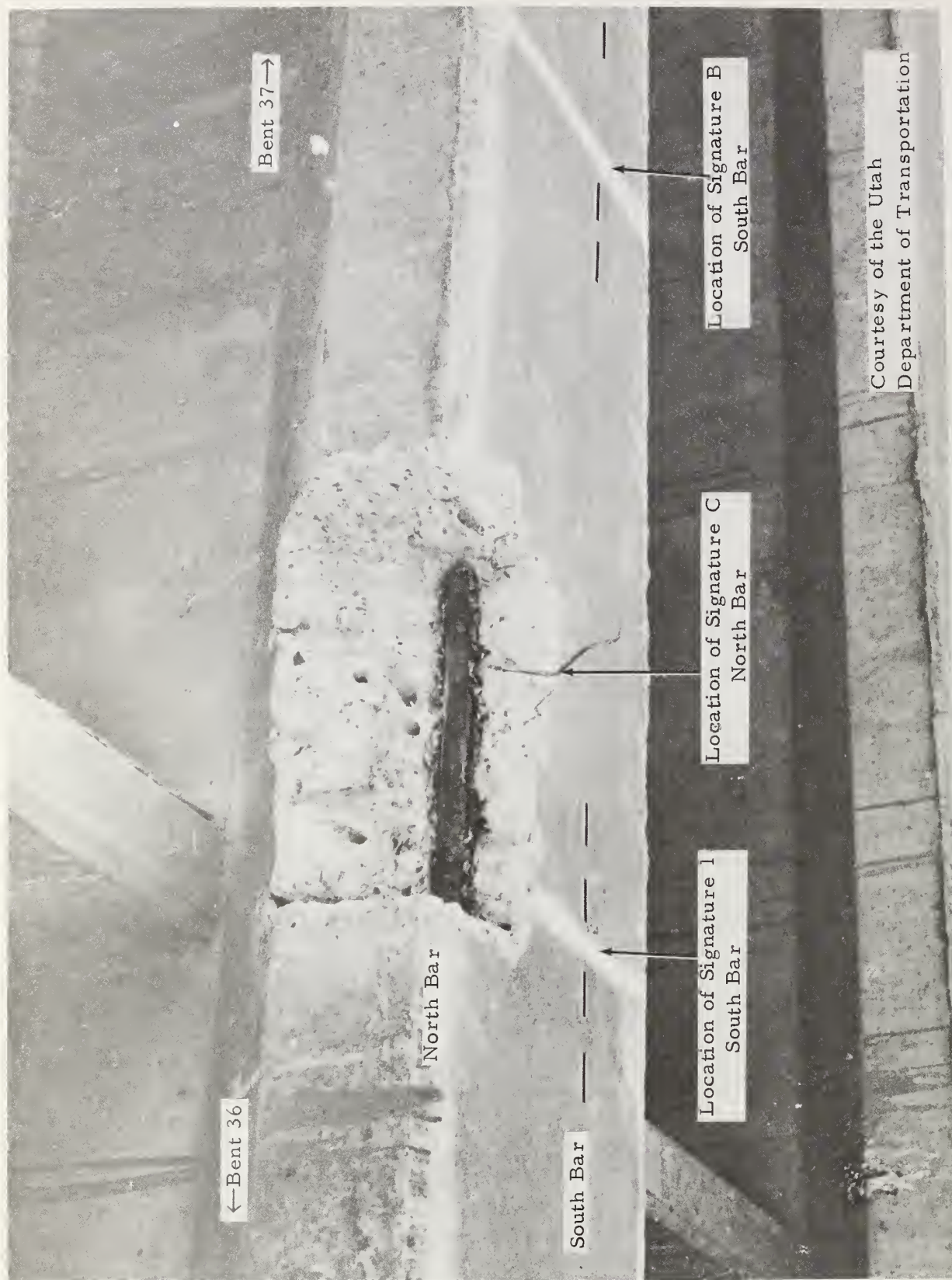
FIGURE 35. OVERALL VIEW, AFTER EXCAVATION, IN REGION OF
INTEREST ON GIRDER 7, BENTS 36-37

54

Location of
Signature C,
North Bar

Location of
Signature 1,
South Bar
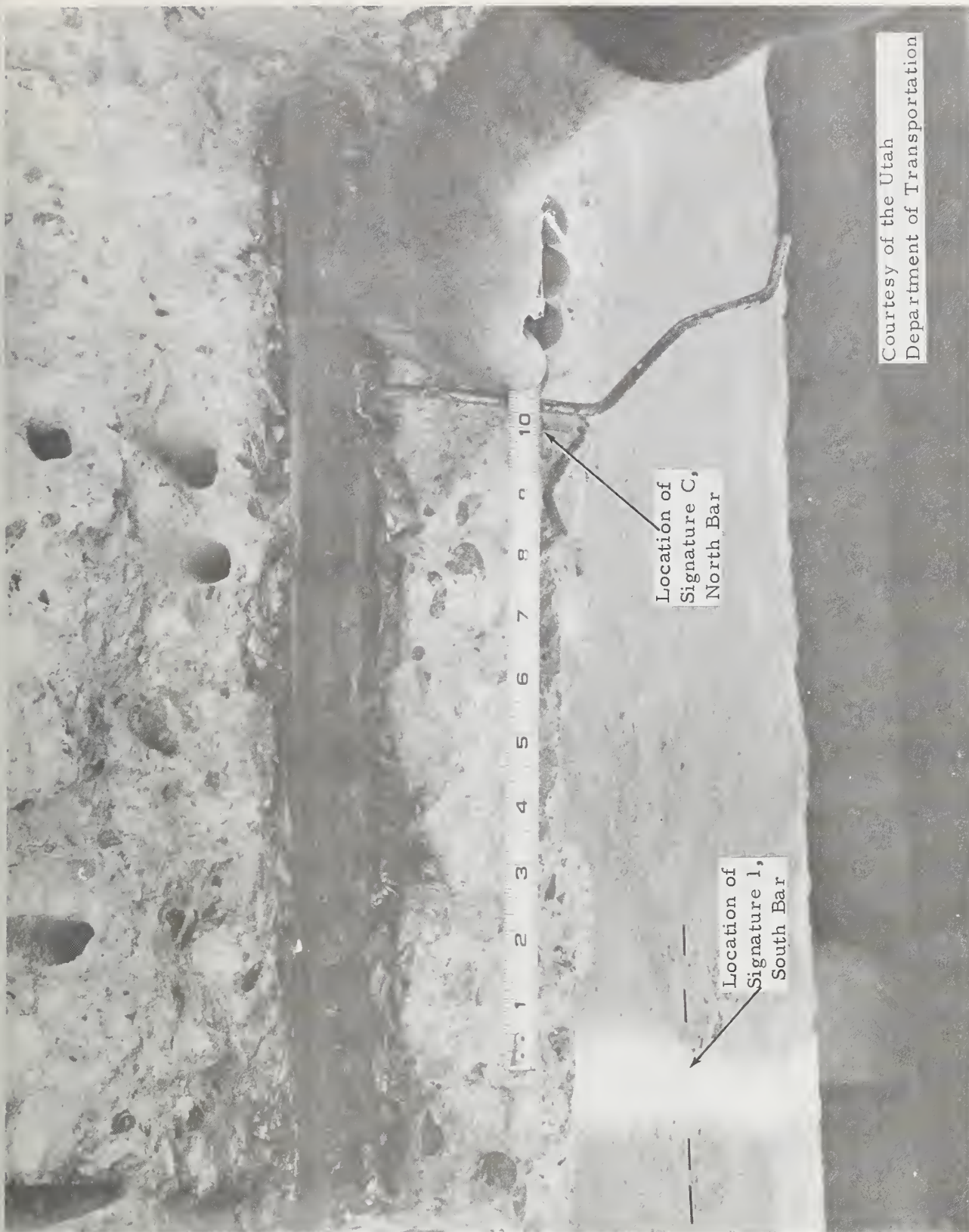
FIGURE 36. CLOSEUP VIEW IN REGION OF SIGNATURE C,
GIRDER 7, BENTS 36-37

55
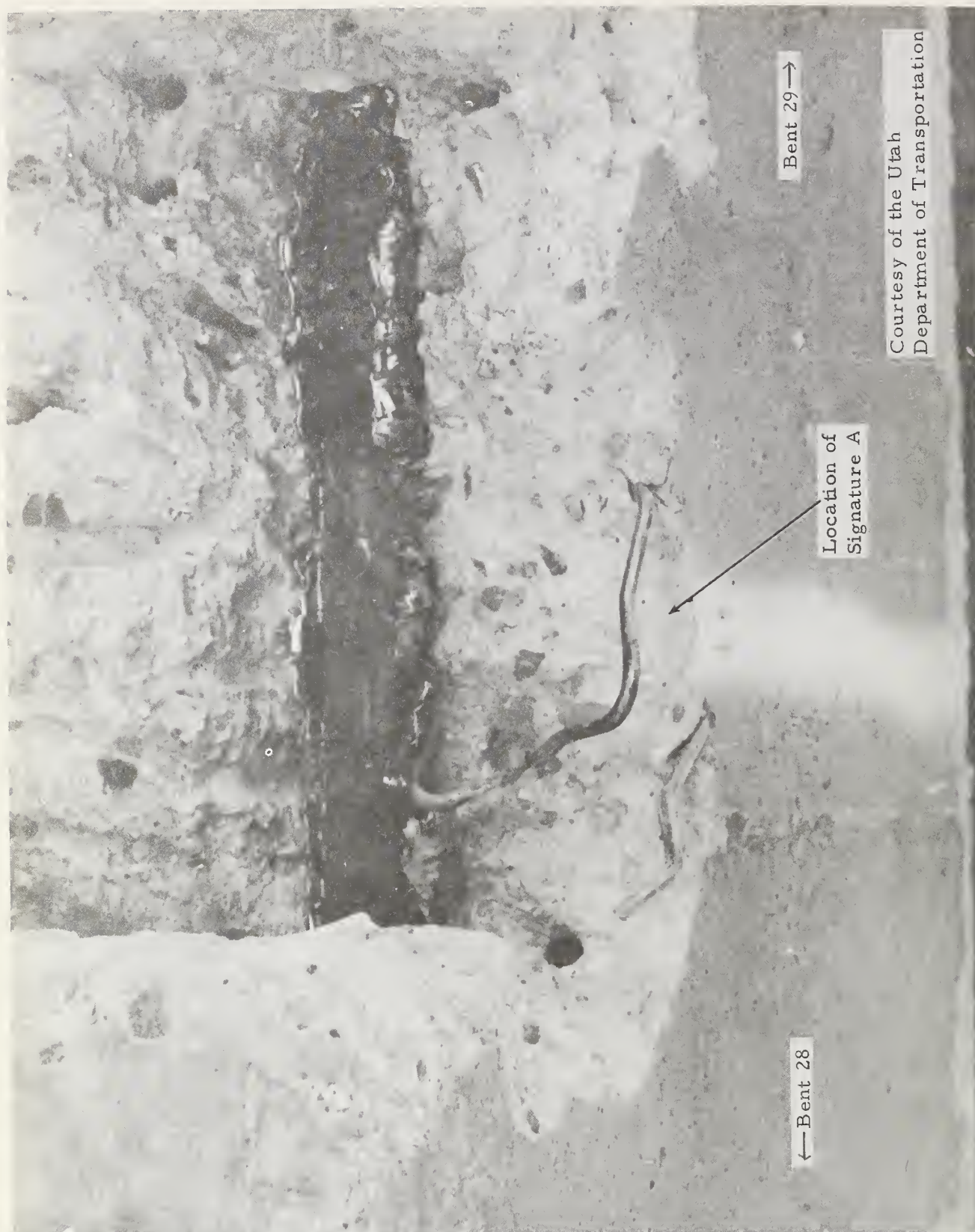
FIGURE 37. CLOSEUP VIEW, AFTER EXCAVATION, IN REGION OF SIGNATURE A, GIRDER 7, BENTS 28-29

56

Stirrups

1-3/8-in. Ø
Bar

Flexible
Duct

Inspection
Cart

Longitudinal
"L" Stirrup

Transverse
"L" Stirrup

Flexible
Duct
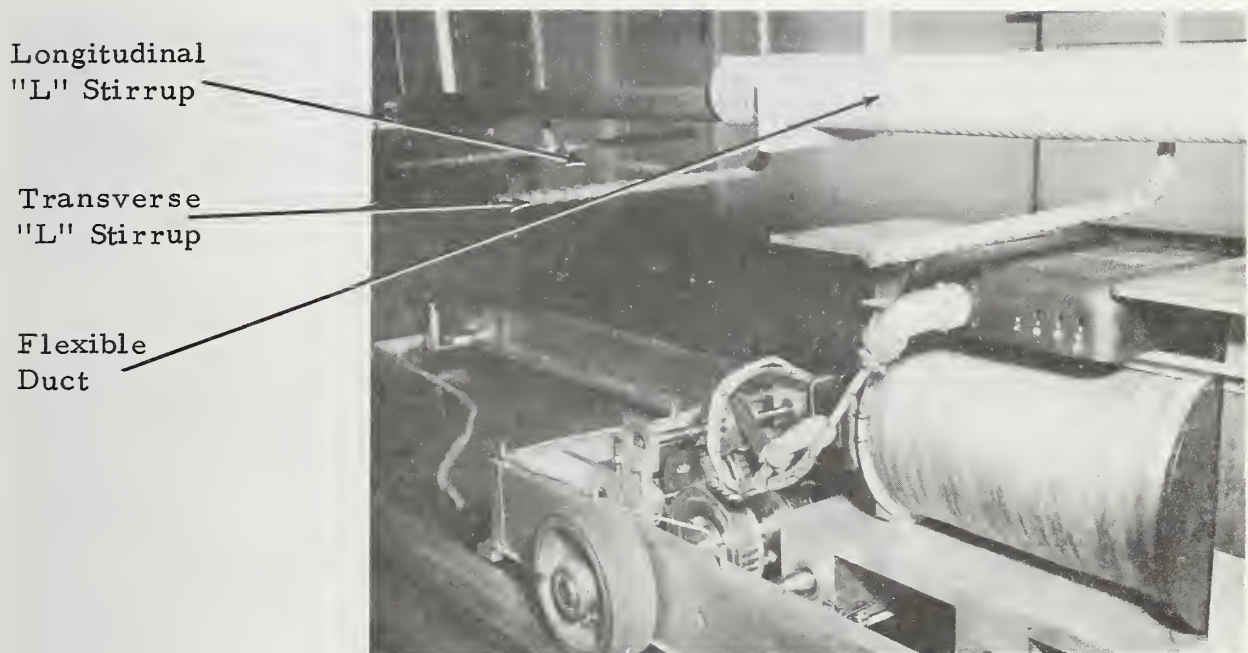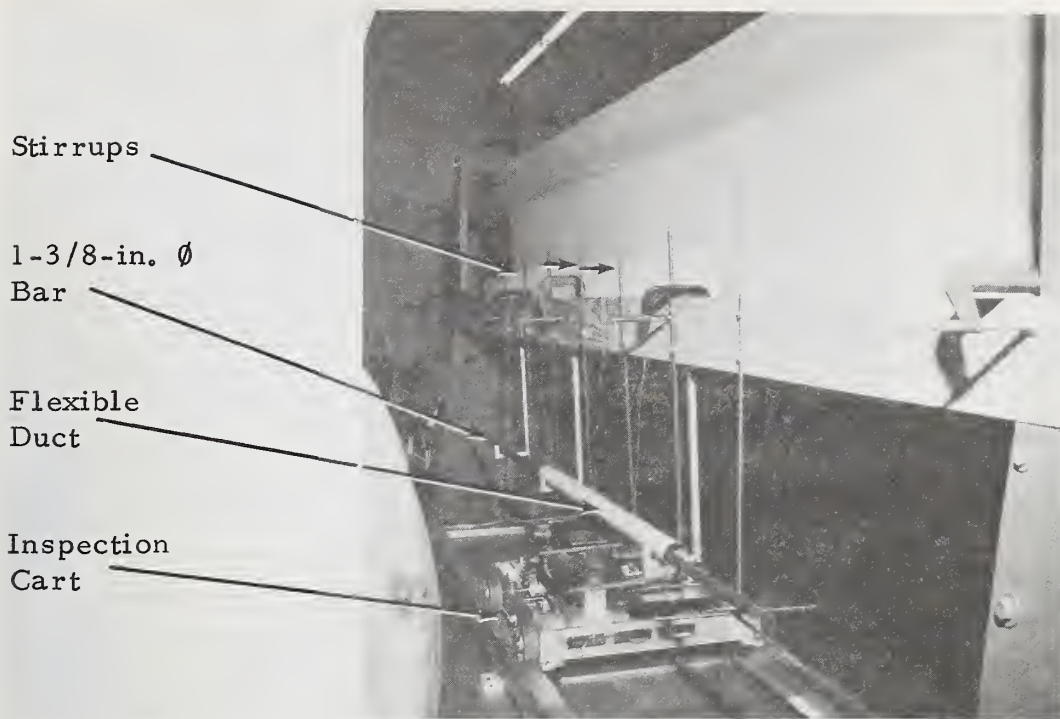
FIGURE 38. OVERALL AND CLOSEUP VIEWS OF LABORATORY MOCKUP
OF UTAH BRIDGE (S. L. C. Sixth South St.) GIRDER STEEL
CONFIGURATION

57
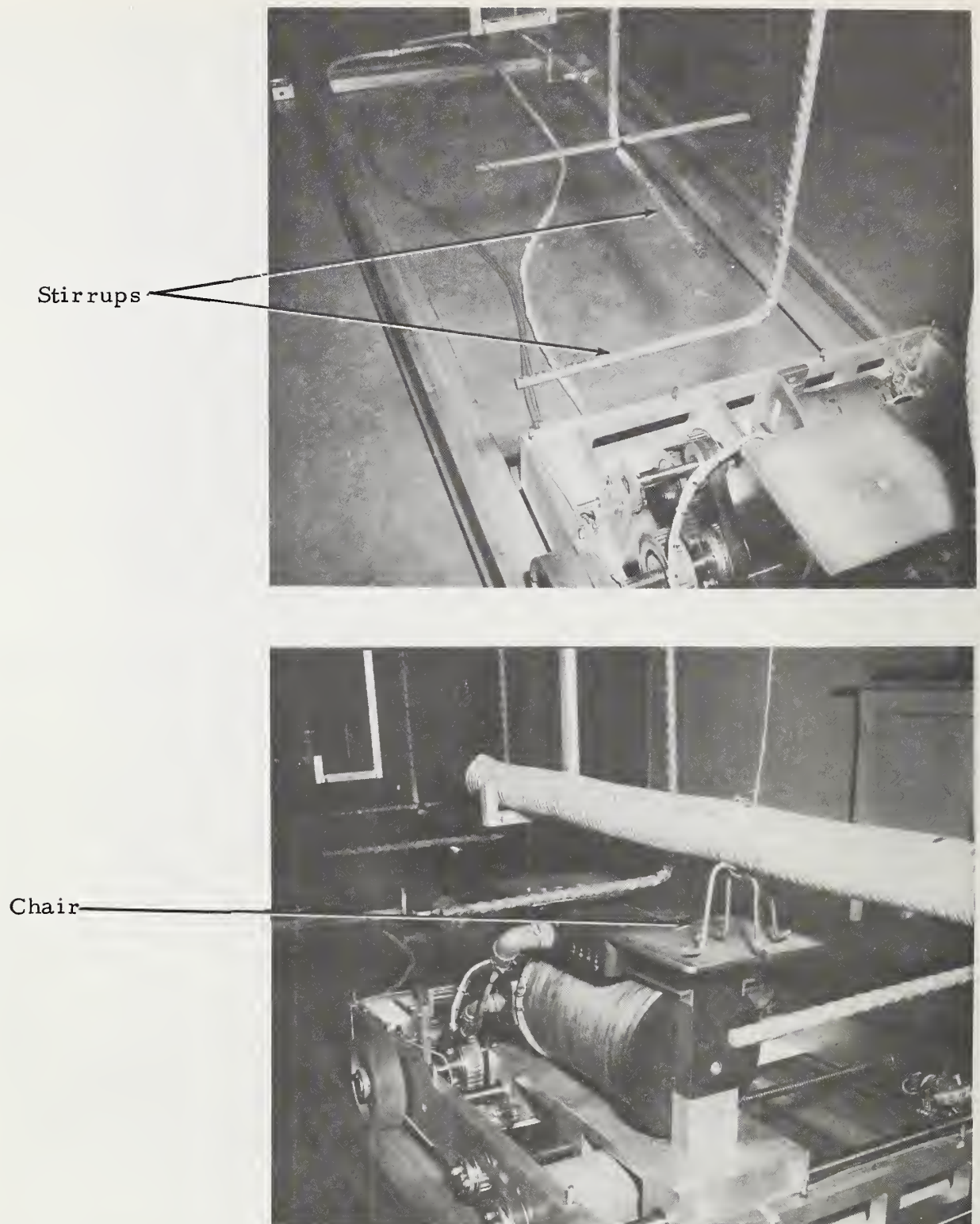
Stirrups

Chair

FIGURE 39. CLOSEUP VIEWS OF LABORATORY MOCKUP OF UTAH
BRIDGE (S. L. C. Sixth South St.) GIRDER STEEL
CONFIGURATION SHOWING STIRRUPS AND A CHAIR
(without high-strength bar)

58

for each of these structural members indicate similar shaped stirrup signatures would not be anticipated (refer to Figures 10 and 30 for details of the stirrup design). According to the plans, the lower portion of the stirrup in the Texas Type "C" beam is "L" shaped similar to that in the Utah girder, but the foot of the "L" in the Texas beam is oriented transverse to the axis of the beam while in the Utah beam it is oriented parallel to the axis of the beam. Figure 40 shows typical inspection signatures for each stirrup orientation in the laboratory and typical signatures obtained from the Sixth South Street Viaduct. In the left column of records in Figure 40, the stirrup signatures for a scan of one pretensioned strand configuration girder (girder 5, Span 39-40) in the Sixth South Street Viaduct are presented along with signatures from the laboratory mockup of "L" stirrups oriented longitudinally according to the bridge plans - a high degree of similarity is evident. The right column of records in Figure 40 shows a high degree of similarity between stirrup signatures from a laboratory mockup of the "L" stirrups oriented transverse to the beam axis and those typically obtained from the post-tensioned bar girder configurations in the Sixth South Street Viaduct. Furthermore, a comparison between the left and right columns of records (Figure 40) clearly establishes the different magnetic inspection signature response for the "L"-shaped stirrups in the two different orientations. The results of this phase of the laboratory simulation efforts strongly indicate that the stirrup configuration for the post-tensioned girders in the Sixth South Street Viaduct in Salt Lake City, Utah, is not in accordance with the construction plans which specify stirrups with the leg oriented along the beam; the pretensioned stirrup configuration appears to be in agreement with the plans. Accordingly, subsequent signature simulation efforts in the laboratory to determine the influence of stirrups and chairs on simulated fracture signatures were conducted using the transverse orientation of the "L" stirrup.

Selected inspection records in Figure 41 (low three recordings) from laboratory mockup tests illustrate signatures from:

- a high-chair and a smooth continuous bar specimen inside flexible duct,

- a high-chair which is located coincident with the end of a bar, and

- a high-chair which is located coincident with a simulated fracture 1-in. (2.5cm) separation.

A reproduction of the bar-end signature region from girder 4, Span 35-36, North bar of the Sixth South Street Viaduct (see third record from the top, Figure 34) is included at the top of Figure 41 to facilitate comparison.
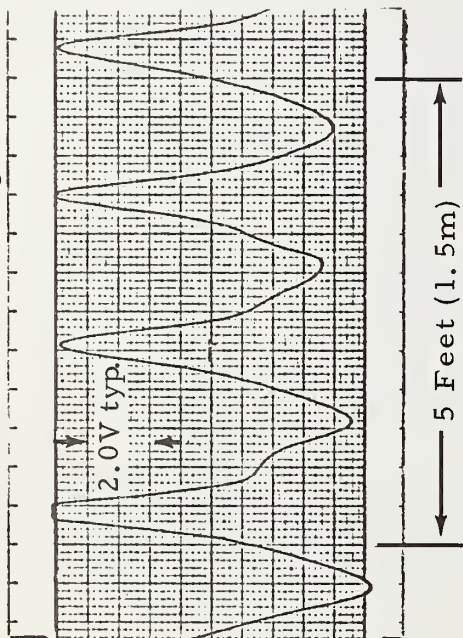
59
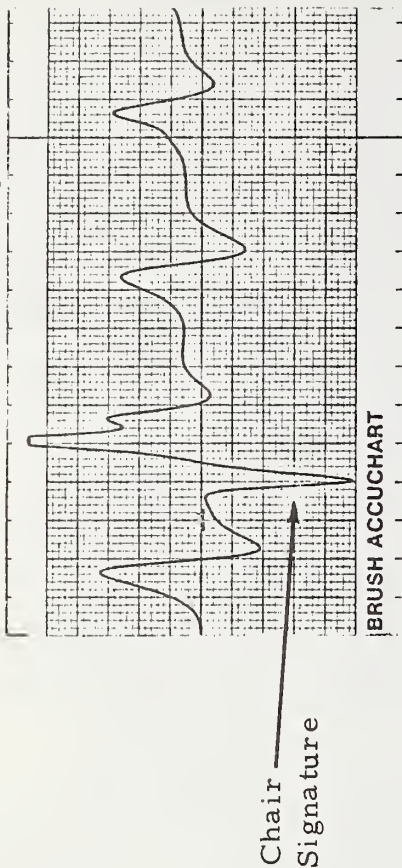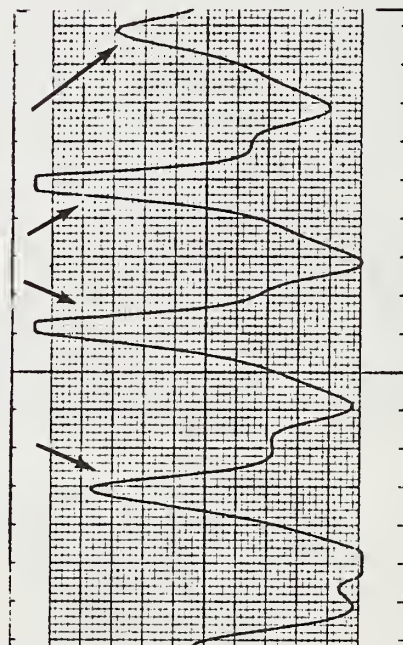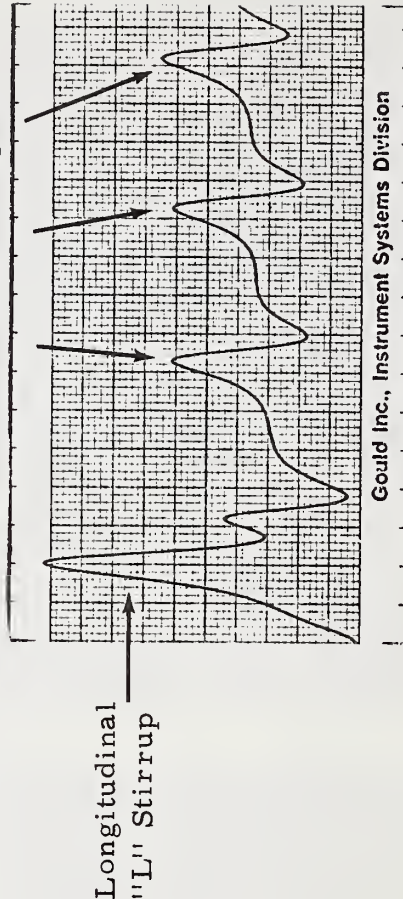
FIGURE 40. SELECTED INSPECTION RECORDS ILLUSTRATING DIFFERENT STIRRUP SIGNATURES FROM PRETENSIONED STRAND AND POST-TENSIONED BAR IN UTAH BRIDGE (S. L. C. Sixth South St.) GIRDERS AND CORRESPONDING RESPONSES FROM LABORATORY MOCKUPS

60

Girder 4, Span 35-36, North Bar

2. 0V typ
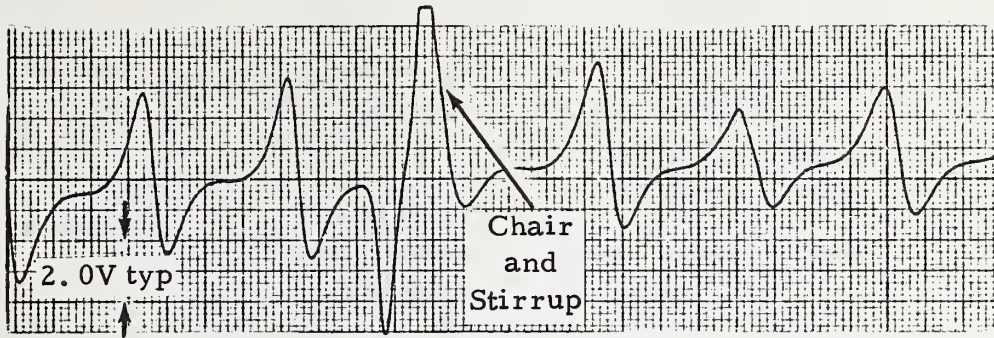
Chair
and
Stirrup

Laboratory Mockup, "L" Stirrups and Chair

Longitudinal
Stirrup

Transverse
Stirrups
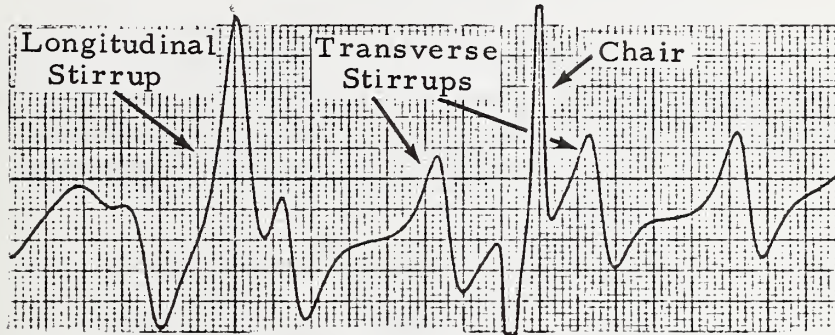
Chair

Laboratory Mockup, "L" Stirrups, Chair, and Bar End

Chair and
Bar End

Laboratory Mockup, "L" Stirrups, Chair, and Simulated Fracture

Chair and Simu-
lated Fracture
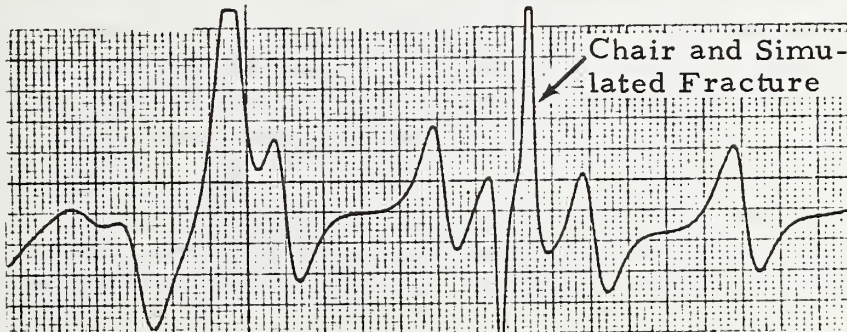
FIGURE 41.   MAGNETIC RECORDS SHOWING CORRESPONDING CHARACTER-
ISTICS BETWEEN SIGNATURES OBTAINED FROM THE FIELD
AND THOSE FROM LABORATORY MOCKUPS

61

The results presented in Figure 41 show a strong similarity between the laboratory mockup signatures and those obtained in the field. Furthermore, the results indicate that the signature from a fracture (or the end of the bar) can be completely "masked" by the presence of a chair signature; certainly, visual interpretation of the data with any degree of confidence is not possible without the aid of some other type of signature analysis or interpretation procedure. The large amplitude of the chair signature (which results from the fact that the feet of the chair are very close to the inspection magnet/sensor unit), undoubtedly accounts for this significant masking effect. The signature from a stirrup can also create a masking influence on a flaw signature (for example, see Figure 25) although the influence does not appear to be as severe as that from the chair (for the configurations investigated).

Recognizing the severe and complicating influence of signatures from steel configurational artifacts on the detection and recognition of flaw signatures, possibilities for discriminating against signatures from such artifacts have been considered. One possibility, that of "subtracting out" configurational steel signatures so that signatures from deterioration can be recognized, has been investigated on a preliminary basis. To facilitate this limited study, the previously described laboratory simulation tests included the recording of magnetic inspection signatures on analog magnetic tape to facilitate later analog-to-digital conversion of the signatures and further processing in the computations laboratory. The procedure used is functionally outlined in the block diagram of Figure 42. Briefly, the procedure consisted of playback of the analog signature, previously recorded on magnetic tape, through an A-to-D conversion system, then storing the digital information in a computer memory. Subsequently, the stored digital data from two different configurations were subtracted from each other, point by point, via a "subtraction program" prepared for use on an existing graphics terminal/calculator. The results of the subtraction process were then plotted in a format similar to the original inspection records and printed out in hard copy form. As an example, Figure 43 summarizes the results obtained by applying the above described process to records from several different steel configurations. The computer reproduced record at the top of Figure 43 shows typical signatures obtained with stirrups, a high-chair located intermediate between two stirrups, and a smooth continuous bar inside a flexible duct (similar to setup previously shown in Figure 41). The center record of Figure 43 shows the inspection signatures obtained with the same physical configuration as that used to obtain the upper record, but the chair was removed and a simulated bar fracture was added at the same location intermediate between the two stirrups. The lower record shows the result of physically placing the chair directly beneath the simulated fracture. Referring to

Field Evaluation System
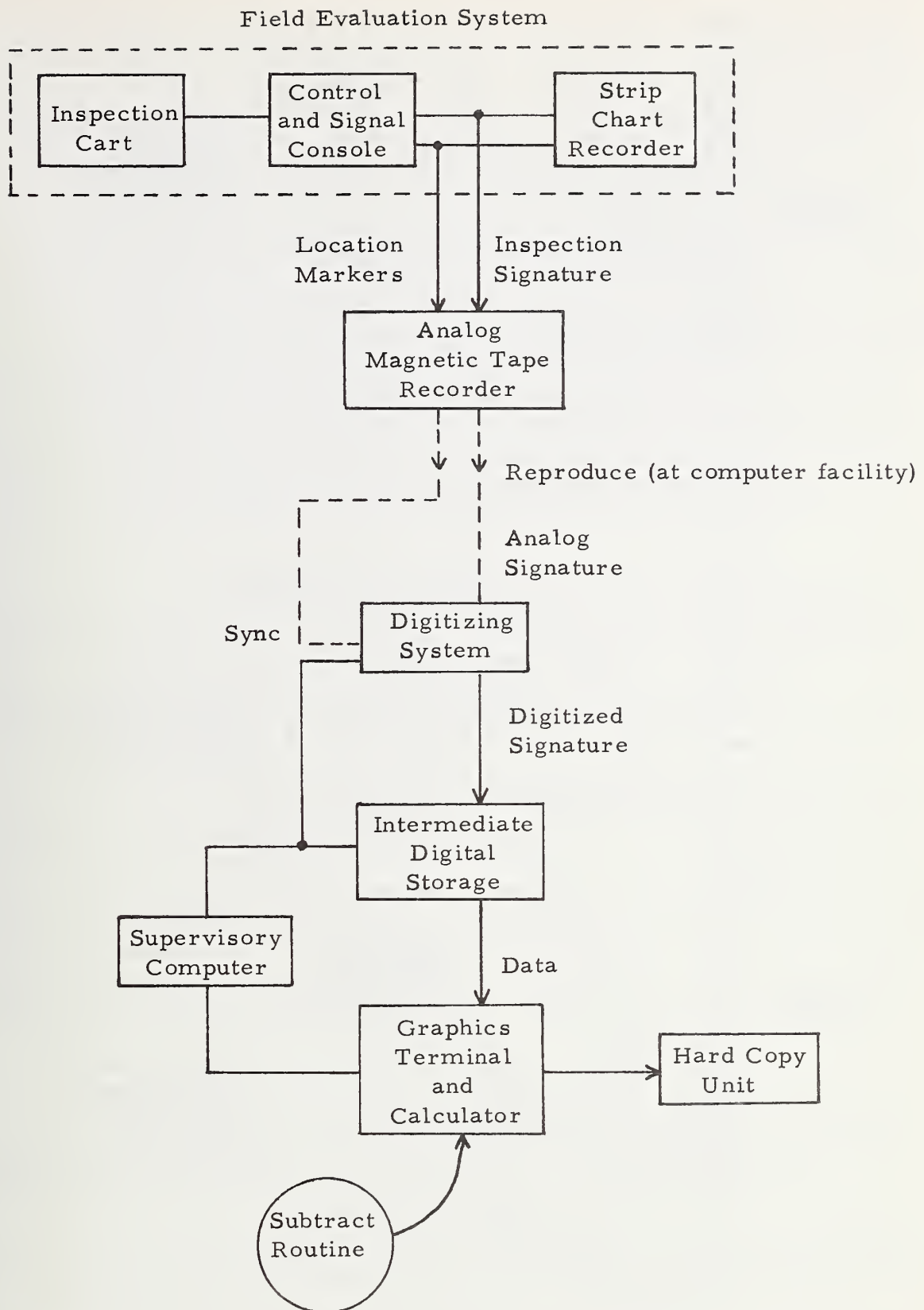
FIGURE 42. BLOCK DIAGRAM SHOWING PROCEDURE USED TO SUBTRACT MAGNET RECORDS
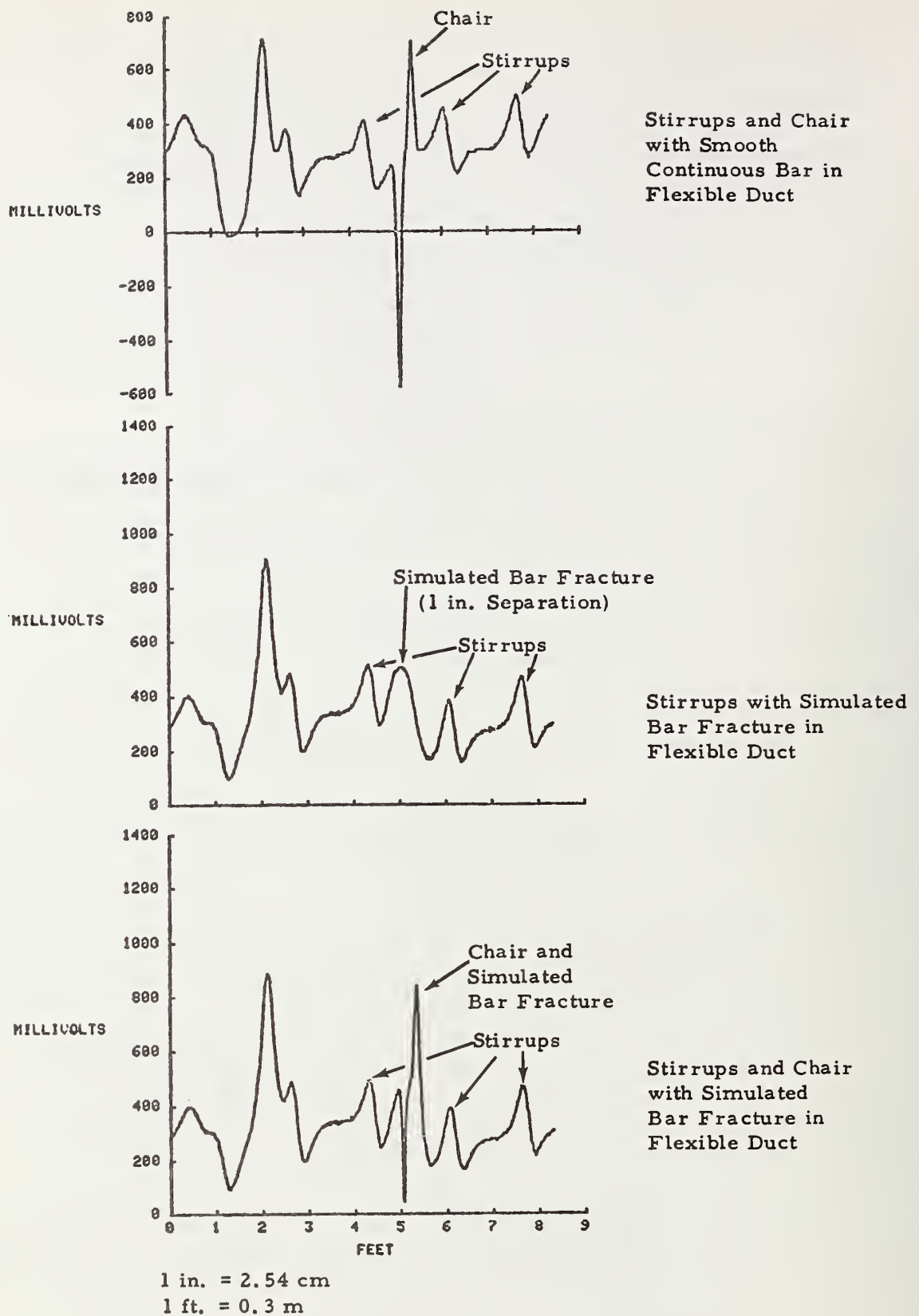
FIGURE 43. COMPUTER REPRODUCED RECORDS BEFORE SUB-
TRACTION

Figure 43 again through point-by-point computer subtraction of the entire record at the top from the entire record at the bottom of the figure, the result should be a record with a prominent signature caused by the simulated bar fracture with the influence of the stirrups and chair removed. The record at the top of Figure 44 shows the results of such a point-by-point subtraction process of the upper and lower records in Figure 43. The record previously shown in the center of Figure 43 is repeated at the bottom of Figure 44 to permit a visual comparison between the simulated bar fracture signature obtained as a result of the subtraction process and that obtained from the scan of a physical setup in which the chair was not present. (The upward-going peak near the left end of the top record in Figure 44 is associated with bar-end effects; the relatively large amplitude upward-going spike on the signature attributed to the fracture is a result of inaccuracies in the chair signature subtraction setup.) These results, although preliminary, are extremely encouraging in that they provide a means for significantly reducing the influence of configurational artifact signatures on the overall inspection record so that the potential detection capability of the magnetic inspection method can be better realized.

Based on the insight gained from laboratory simulation of the field configurations inspected at the Salt Lake City site, the recorded field data were re-examined. Particular emphasis was placed on the re-evaluation of the data recorded from girder 7 of Span 28-29, North bar, since this bar was a prime suspect for fracture (because the retaining nut was not seated in the end retaining plate at the bent 28 end). Re-examination of the record (Figure 33) from this North bar yielded no conclusive indications of a fracture, although several other signatures were identifiable as suspect for containing fracture signature components; however, all such suspect signatures appear to be dominantly controlled by the presence of stirrup and/or chair signatures. At this time it is not possible, with confidence, to select a specific signature location on the North bar of girder 7, Span 28-29, which indicates fracture. It is firmly believed, however, that with adequate development of signature analysis and interpretation networks and procedures, the point of fracture in this bar can be detected and located with the magnetic inspection approach.

5. Assessment of Equipment Performance

Based on the limited operating experience obtained in the field at the Salt Lake City site, the following observations are made regarding the performance of the magnetic inspection equipment.

An initial checkout of the equipment using a reference specimen (refer to Operator's Manual for details) at the field destination
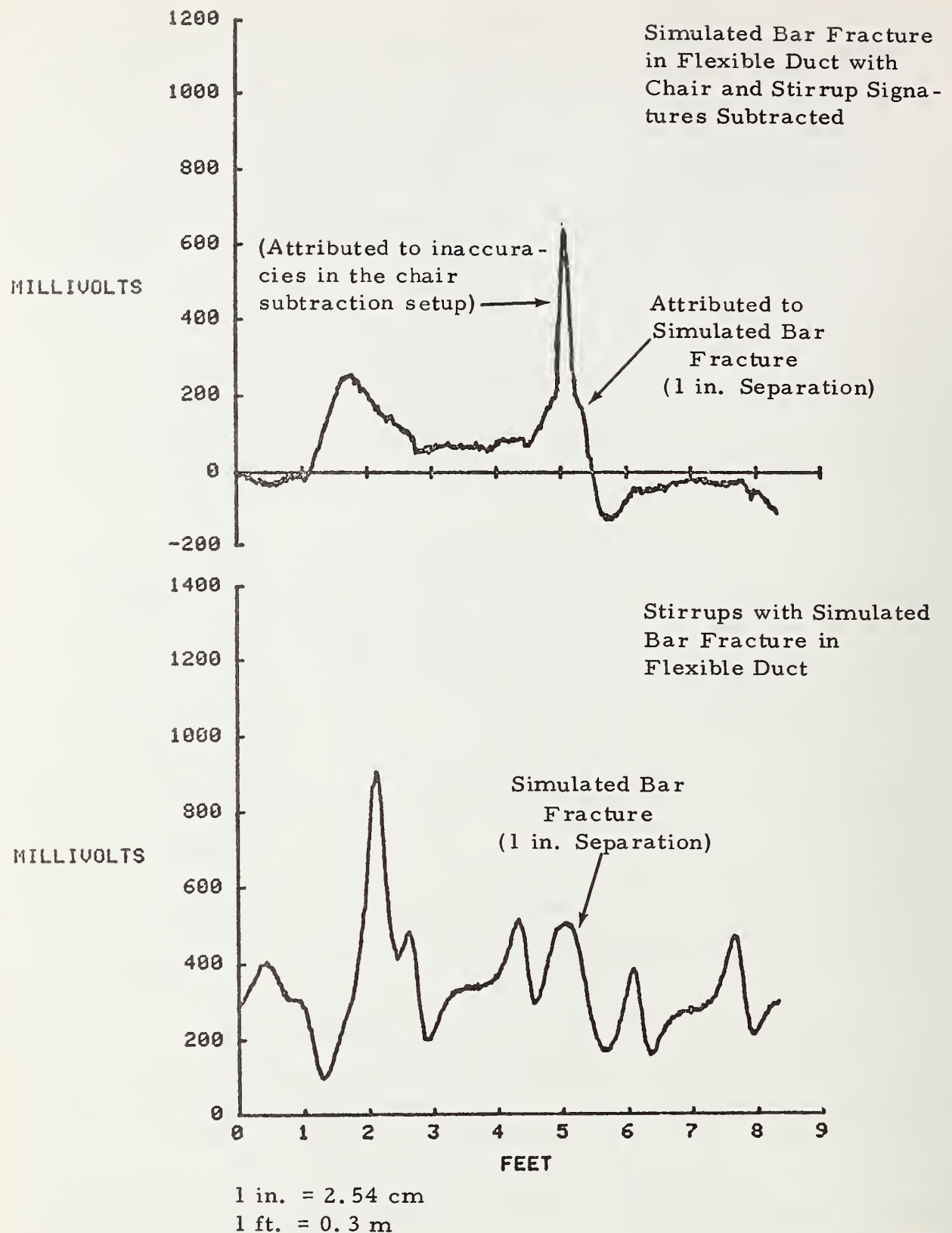
FIGURE 44. COMPUTER REPRODUCED RECORDS ILLUSTRATING RESULTS
OF SUBTRACTION PROCESS

confirmed satisfactory system operation. No equipment performance problems were encountered as a result of handling and shipping. Equipment response under field conditions was equivalent to that in the laboratory; excellent repeatability was obtained in both the laboratory and the field. Anomalous signatures in the field data established the presence of steel elements in bridge girders which were neither shown on the plans nor known to be present. Furthermore, characteristic signatures in the field data indicated the transverse steel stirrup configuration for the post-tensioned girders to be different than that shown on the bridge girder plans.

The selection of access and handling equipment to install and set up the inspection equipment on a girder was found to be extremely important to achieving an efficient inspection. For example, field experience at Utah established that use of a hydraulically actuated scissor-lift was significantly more effective than that of scaffolding (refer to photographs in Figure 28). With the scaffolding, considerable difficulty was encountered in lifting the hangers, track, and inspection cart upon the scaffold platform; additionally, the maneuverability and safety of personnel on the platform was minimal. Actual use of a hydraulically actuated scissor-lift (with a platform ~ 6-ft (1.8m) x 12-ft. (3.6m) greatly facilitated setup, movement, and installation of the inspection system; it is estimated that the overall inspection could be speeded up by a factor of two to three using scissor-lift type access equipment. The track assembly approach for longitudinally scanning girders is functionally adaptable to a variety of configurations in the field.

While the magnetic inspection equipment is basically adequate, for field operation, moderate modifications to several operating functions would be desirable. Each of these areas is briefly discussed below. It was found in the field trials that end-to-end coupling of the track assemblies resulted in a faster inspection (particularly when the length of the girder is significantly greater than the length of the track). Although such track coupling was accomplished via C-clamps and flat clamping plates in the field, provisions for a quick-connect/disconnect track-to-track coupling would reduce the setup time required to conduct an inspection. The preliminary prototype inspection cart incorporates provisions for manually selecting one of three inspection longitudinal scan speeds. The least speed, 2 in./s (5cm/s), was included because this speed was used during all preliminary laboratory investigations. In order to reduce the time required for scanning, two additional higher speeds, 5 in./s (12.7cm/s) and 10 in./s (25.4cm/s), were included. Tests show that operationally the equipment is the most functional at a scan speed of 5 in./s (12.7cm/s). Modification of the inspection cart drive speed-changing/

coupling system to a single speed unit would reduce inspection cart weight by almost 20 lbs (8kg); accordingly, significantly improved equipment installation characteristics would result. Finally, minor modifications to the remote cable system are desirable to further ruggedize the assembly and facilitate quicker setup and subsequent movement of the inspection system to adjacent locations.

D. Criteria for Field Use

1. General

Only a limited field evaluation of the preliminary NDE inspection equipment was conducted; accordingly, only a preliminary outline of criteria for field use of this equipment is possible at this time. Clearly, the experience gained from the Utah field evaluation and the existence of structural steel details in bridge structural members which are either not on the construction drawings or do not conform to the construction drawings indicate that data interpretation in the field may be impossible in some cases unless electronic record processing is developed. Significant development efforts should be undertaken and completed before comprehensive field evaluations are undertaken and such efforts should place greatest emphasis on signature analysis and interpretation. Minor modifications and improvements to the existing preliminary NDE equipment are also desirable and would be cost-effective via improved operational efficiency thereby increasing the actual inspection time available for data acquisition. More recent field evaluations conducted at Manufactured Concrete, Inc. (see Appendix IV) tend to confirm the comments above. Additional details regarding further development are presented in Section IV - Conclusions and Recommendations, of this report.

2. Procedures for Field Use (Preliminary)

Although field use data and experience are as yet extremely limited, the following general steps are outlined as significant feastures of a viable field use criteria; brief comments are included as appropriate. The Operator's Manual as well as this report are identified as reference documents.

a. Inspection Log and Forms

An inspection log, book, or file should be completed for each structure inspected. All notes, comments, diagrams, schedules, data logs, etc. pertaining to the inspection should be retained in this log or file. Forms should be developed for standard entries to ensure a record of all pertinent information.

b.   Pre-Site Visit

The importance of this tep cannot be over emphasized and the detailed nature of such a visit can vary widely depending upon the situation and how well one is acquainted with the structure to be inspected. It is essential that the environmental and accessibility features of the site be noted, and that handling and access equipment requirements as well as the number and type of personnel needed to assist in performing the inspection be estimated. As part of this step, consideration should also be given to the possibility of minimizing inspection costs by customizing the configuration of the track assembly to reduce the overall equipment installation time required for setup at each scan location. Suspect or critical locations should be identified for particular emphasis during inspection.

c.   Establish References

Maps or diagrams should be prepared to establish geographical and structural reference points and directions. It is important to establish a methodical approach for identifying the bridge structural members and elements, and locations inspected, as well as their relationship to existing landmarks or bench marks. Existing plans, sketches, or diagrams should be used as applicable.

d.   Prepare Data Forms and Data Logging Procedures

Preparations need to be made in advance for indicating the regions to be inspected, and the method to be used to identify and log the recorded data according to physical location on the structure, date, operator, etc. The data form and logging should use nomenclature consistent with that employed in the member location scheme.

e.   Establish an Inspection Schedule

This step assures that critical locations receive emphasis during inspection and preparation of an inspection schedule ahead of time assures that an efficient, effective inspection is conducted at minimum cost. It also permits each member of the inspection team to be informed both from the standpoint of the overall effort as well as specific task responsibilities.

f.   Conduct Inspections

Pre-inspection preparation should include checking of the inspection equipment and conducting cleaning and maintenance as

69

required. The Operator's Manual should be referred to for operation and checkout of the equipment. It is recommended that the equipment be operationally checked using the reference specimen (see Operator's Manual) at least one time each inspection day. Using a properly prepared inspection schedule, as inspections are conducted each item should be checked off as it is completed.

g.   Data Interpretation

As the inspection of each scan setup location is completed, signature analysis and interpretation should be completed prior to removal of the inspection setup from that location; locations on each member being inspected corresponding to suspect signatures should be marked in a suitable manner (the corresponding signature should also be marked on the inspection record in each case). Marked locations should be noted on the inspection diagram so that flaw occurrence patterns, if any, can be identified.

h.   Flaw Confirmation

If applicable or desirable, other techniques or methods should be employed to confirm the existence and extent of steel deterioration in the regions identified during the magnetic inspection. Supplementary methods to be used could be additional critical visual inspections and/or removal of concrete cover in the local region of interest.

III.   SUMMARY OF TECHNICAL BASIS FOR SELECTION AND
        DEVELOPMENT OF MAGNETIC METHOD

        A.   Design and Development of Preliminary Inspection Equipment

                Upon completion of a laboratory investigation of the magnetic
field method, which yielded very encouraging results (see Appendix I,
Interim Report), design and evaluation of a preliminary inspection equip-
ment was undertaken. From preliminary experimental results using
electromagnet and permanent magnet approaches for magnetization and
discussions with the Contract Manager, it was decided to initiate design
based on an electromagnet having approximately the same size and weight
as that used during the laboratory assessment phase. (Results of the
limited permanent magnet investigations are briefly summarized later
in this section of the report.) Assumed criteria used for design follows:

        i)   Total weight of inspection cart - 500 lbs. (230 kg)

        ii)   Transverse carriage weight - 300 lbs. (140 kg)

        iii)   Maximum grade of beam to be inspected - 5%

        iv)   Scanning speed range   2-10-in./s (50-250mm/s)

        v)   Maximum track deflection - 1/8-in. (3mm)

As a parallel effort to the detailed equipment mechanical and electrical
design, limited design studies were conducted in an attempt to reduce the
overall size and weight of the electromagnet required to obtain flaw
responses at least equivalent to those obtained in the initial laboratory
assessment phase. As a result of these efforts it was possible to improve
flaw detection sensitivity while reducing the weight of the electromagnet
by approximately a factor of 2. Figure 45 summarizes the results obtained
during the electromagnet development effort, and the significant features
are the use of large area pole plates and magnetic material in the vicinity
of the sensor (probe). The potential capability of the magnet method using
the new electromagnet design is indicated by the significant results in
Figure 46; the signature from a simulated fracture (0.5-in., 1.3cm
separation), without duct, for an equivalent concrete coverage of 9.5-in.
(24cm) is readily detectable above the electronic noise level of the system.

                An accelerated performance schedule required that the detailed
equipment design parallel the magnet design studies and as a consequence
some over design of the inspection carriage and cart components and
assembly resulted. Nevertheless, the total weight of the inspection cart

71
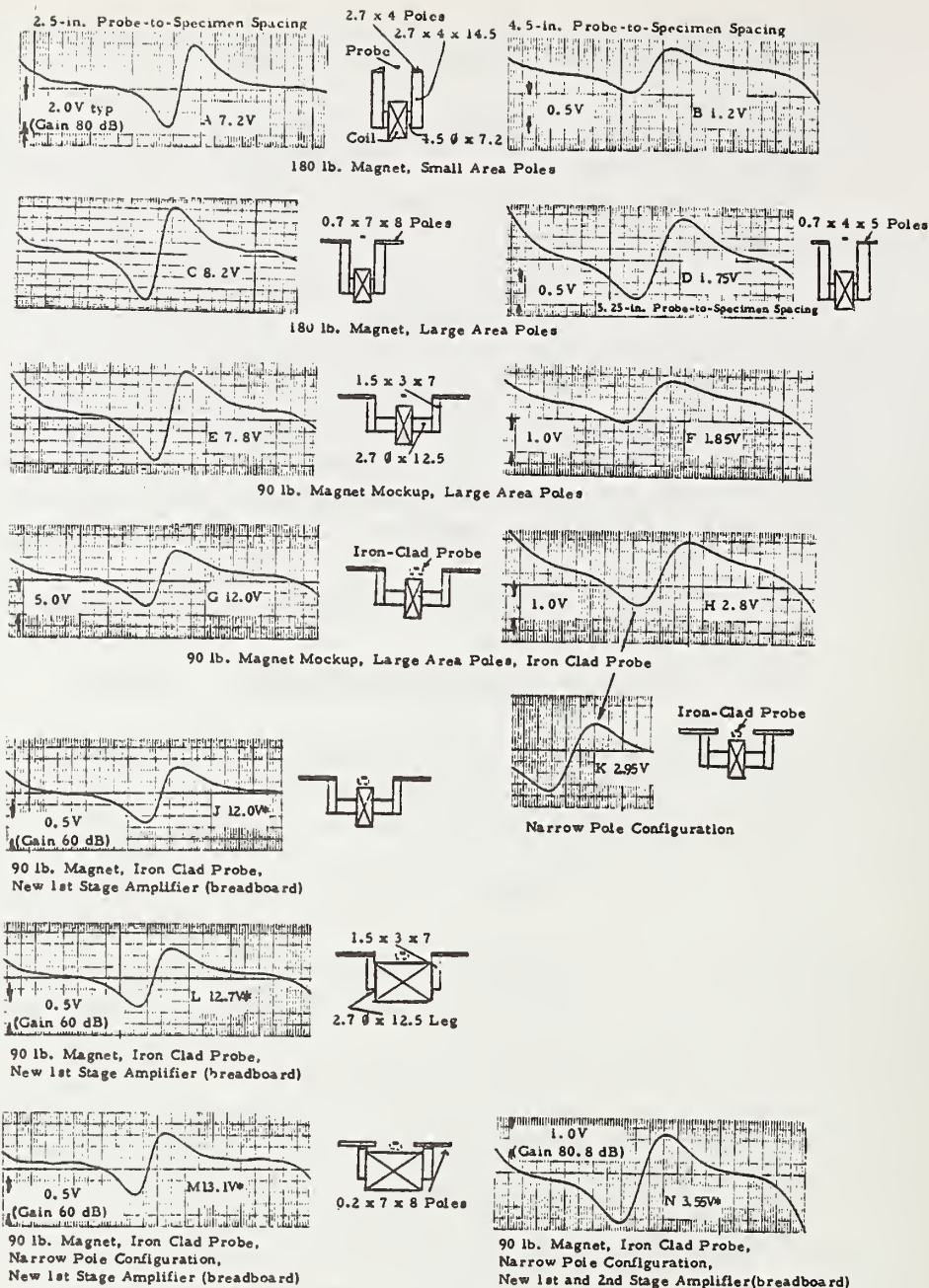
FIGURE 45. MAGNETIC SIGNATURES FROM A SIMULATED FRACTURE (0.5-in. (1.3cm) end separation) OF A 1-IN. (2.5cm) Ø BAR ILLUSTRATING SIGNIFICANT FEATURES OF ELECTROMAGNET DEVELOPMENT

72

10-in. Probe-to-Specimen Spacing
(no duct)

Ends of
Specimen

~ 10 in.

0. 4V

0. 2V
(Gain 80. 8 dB)
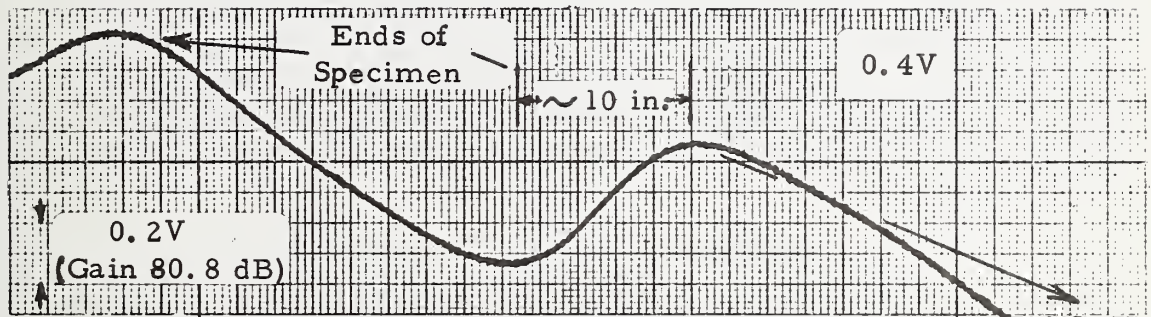
90 lb. Magnet, Iron Clad Probe,
Narrow Pole Configuration,
New 1st and 2nd Stage Amplifier (breadboard)

1 pound = 2. 2kg   1 inch = 25mm

FIGURE 46. MAGNETIC SIGNATURE FROM A SIMULATED
FRACTURE (0. 5-in. (2. 5cm) end separation) OF
A 1 INCH (2. 5cm) Ø BAR FOR EQUIVALENT
CONCRETE COVERAGE OF 9. 5 INCHES (24cm)
(without duct)

73

is approximately 260 lbs. (118 kg) versus the original design criteria value of 500 lbs. (230 kg), a considerable reduction in weight. In field applications, weight is always a significant consideration and is a particularly important factor in the case of components and units which must be handled and installed on the structural element to be inspected.

Initial laboratory evaluation data were acquired to characterize response of the equipment for the three manually selectable scan speeds and at several electromagnet excitation current levels. Signature amplitude data from both transverse stirrups and simulated bar fracture (0.5-in., 1.3cm, end separation) were monitored and analyzed as a function of scan speed, 2, 5, and 10-in. per second (5, 12.7, and 25.4-mm per second, respectively). Both the stirrup and fracture signature amplitudes were found to be independent of speed, as anticipated; essentially all subsequent data were obtained at a scan speed of 5-in. per second (12.7-mm per second); this medium scan speed was selected for general use because the dynamics of scan starting and stopping was smoother and a convenient strip chart presentation was obtained.

Inspection data were obtained also from both transverse stirrups and simulated fracture (0.5-in., 1.3cm, separation) at three different values of excitation current for the electromagnet, 0.5, 1.0, and 2.0 Amperes (design current). Figure 47 presents a graph of the flaw and stirrup signal amplitudes as a function of magnetizing current, and these results indicate the design current of 2 Amperes is adequate to provide a strong magnetic field in the steel (1-in. (2.5cm) ∅ bar) under inspection for a concrete coverage of 3.5-in. (9cm); the knee of the magnetization curve appears to be at approximately 0.7 Ampere.

During the initial checkout of the 90-lb. magnet design, the preliminary specimen mock-up configuration was used to evaluate the sensitivity capabilities of the magnetic method. The results previously presented in Figure 46 indicate that an excellent signal-to-electronic noise ratio is obtained from a simulated fracture with 0.5-in. (1.3cm) end separation and a specimen-to-magnet/sensor spacing as great as 10-in. (25cm) (equivalent to 9.5-in. of concrete coverage). It is pointed out that the record in Figure 46 was obtained with a recording sensitivity one order of magnitude (factor of 10) greater than that used for recording most of the laboratory evaluation data. Furthermore, the data in Figure 46 indicate the electronic noise to be on the order of two orders of magnitude less than (1/100) typical stirrup signal amplitudes obtained from the Texas Type "C" test beam. Importantly, these sensitivity limitation results strongly indicate excellent potential for the magnetic inspection method to detect deterioration of the prestressing steel in concrete bridge structural members.

74
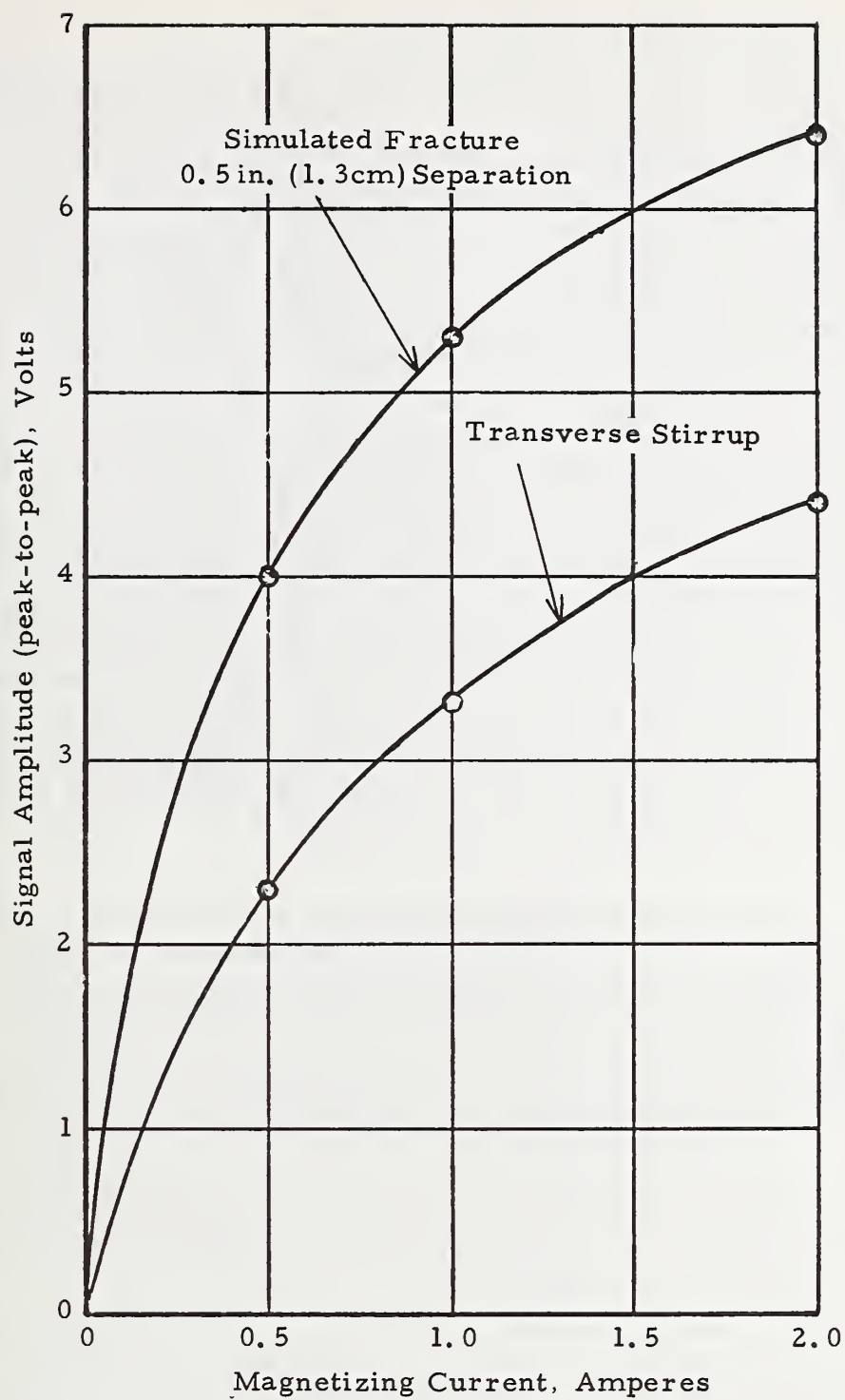
FIGURE 47. TYPICAL MAGNETIC SIGNATURE RESPONSE AS A
FUNCTION OF APPLIED MAGNETIC FIELD

75

B. Other Design Considerations

Early in the preliminary equipment design the feasibility of a strand/bar magnetic "tracking" approach was explored. The tracking concept envisioned a mechanism based on the magnetic field approach which would facilitate automatic transverse positioning of the magnet/sensor unit under a preselected element (strand or bar) as the element was longitudinally scanned. Such a device would greatly facilitate the future development of equipment to inspect draped strands or bars. It was determined that essentially no change in the vertical component of the applied magnetic field occurred as a function of the transverse position of the steel element; however, a relatively slow change in the horizontal field component as a function of transverse position of the steel was observed. In the case of parallel elements (strands or bars) the change in signal with transverse position was so broad relative to the spacing between the elements (even for spacings as great as 6-in. (15cm)) that the individual elements could not be unambiguously resolved. Accordingly, further investigation of the approach was terminated. It is suggested that a supplementary magnet/sensor unit having small area poles might provide adequate resolution for tracking.* Alternatively, automatic tracking might be achieved using optical techniques to follow the path of the element "predrawn" on the surface of the concrete bridge members. The preliminary inspection equipment incorporates provisions for the operator to remotely change the transverse position of the inspection head; a digital readout of position is provided.

Before proceeding with the design of the inspection equipment based on the use of an electromagnet, the feasibility of using permanent magnets was investigated on a limited basis. Use of permanent magnets to develop the magnetic method for field application would significantly reduce power requirements and might possibly provide significant weight reduction. The investigations were conducted using permanent magnets which were readily available; namely, cylindrical (1-in., 2.5cm-diameter x 6-in., 15cm length) Alnico magnets and Samarium Cobalt discs (1-in., 2.5cm diameter x 3/8-in., 1cm length) magnets. Tests were conducted using the magnets in a number of configurations and encouraging results were obtained initially; however, after about a 2-week testing period it was determined that a significant loss in detection sensitivity occurred. It is anticipated that the sensitivity loss occurred as a result of aging effects and demagnetization effects of grouping the magnets. Figure 48 illustrates typical results using a laboratory electromagnet (from the initial laboratory investigations) and essentially the same configuration of permanent

---

* A similar approach with small separation between magnet poles might also provide adequate resolution of steel artifacts (having small concrete coverage) to facilitate precise longitudinal positioning for coincidence - subtraction of artifact signatures.

180 lb. (82 kg) Electromagnet
Simulated Fracture (0.5 in., 1.3cm separation)
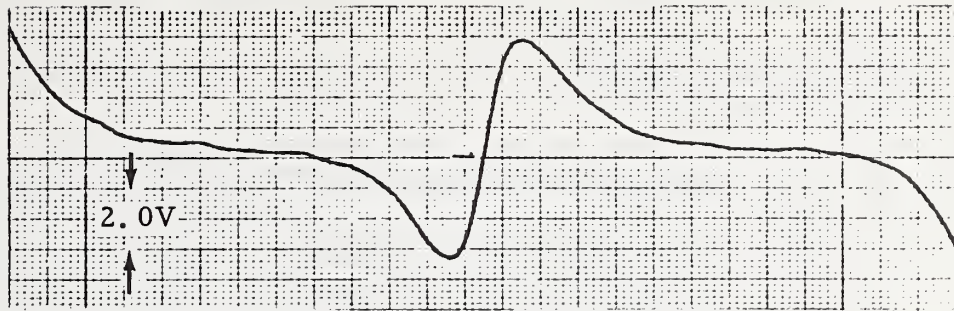
2.0V

Alnico Permanent Magnets (4 each)
Simulated Fracture (1.0 in., 2.5cm separation)

1.0V

Alnico Permanent Magnets (4 each)
Simulated Fracture (1.0 in., 2.5cm separation)

1.0V
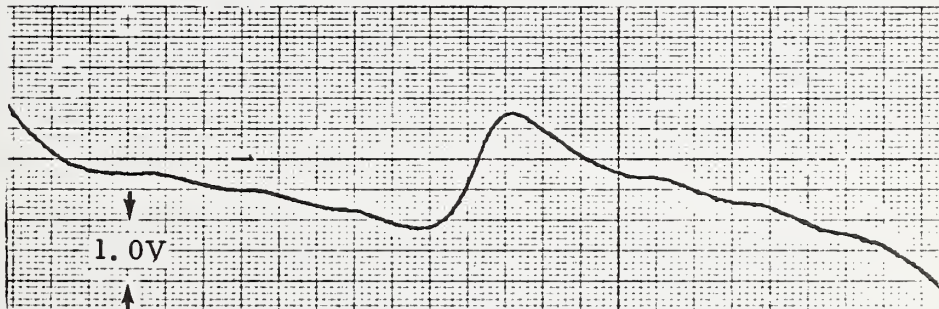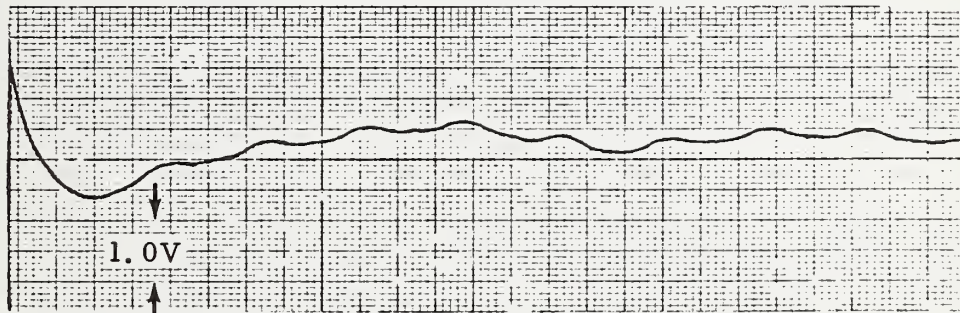
Probe-to-specimen spacing 2.5 in. (6.4cm), typical

FIGURE 48. MAGNETIC RECORDS COMPARING RESULTS USING AN
ELECTROMAGNET AND PERMANENT MAGNETS FROM
SIMULATED FRACTURE IN 1 IN. (2.5cm) ∅ HIGH
STRENGTH BAR IN RIGID DUCT

77

magnets over about a 10-day interval. After reviewing and discussing these comparative results between the electromagnet and permanent magnet approaches with the Contract Manager, the decision was made to continue development of magnetic inspection equipment based on an electromagnet design for the following reasons:

    i)   lack of repeatable results using permanent magnets,

    ii)   long delivery time anticipated for permanent magnets of the required configuration, and

    iii)   the ability to readily make changes in magnetic field strength using an electromagnet.

Certainly, the use of permanent magnets, as a long-range development option, should not be eliminated from consideration; such a development effort, if undertaken, however, should include careful consideration of the stability of permanent magnets as a function of aging, mechanical handling, temperature environment, etc.

C.   Technical Basis for Selection of Magnetic Method

A brief summary of the technical basis for selecting the magnetic field method for further development is presented here. The reader is referred to Appendix I for a comprehensive treatment of the rating and assessment of 15 NDE methods and the subsequent laboratory investigation of the magnet field method.

A state-of-the-art literature search and review pertaining to the detection of deterioration in reinforcing steel in prestressed concrete structures were conducted. Both Government and industrial indexes were searched using a strategy based on intersecting sub-sets of the three descriptors, i) nondestructive testing, ii) concrete, and iii) corrosion. As a result of this computerized search, selected manual searches, and personal communications, 72 documents were identified which were related to the overall program. Based on information contained in the identified documents and input from Southwest Research Institute personnel, having a broad background in related nondestructive inspection problems, 15 NDE methods with possible applicability to the subject inspection problem were identified and are listed below.

Acoustic Emission	Electromagnetic, Nonlinear
Eddy Current	Electromagnetic, Reflection
Electrical Resistance (Concrete)	Electromagnetic, Time-Domain
Electrical Resistance (Steel)	Reflectometry

Half-Cell Potential	Radiography
Holography	Strain-Gage
Magnetic Field	Thermal
Mossbauer	Ultrasonic Scattering

A formal assessment of these 15 method was undertaken based on analysis of information contained in documents from the published literature, the NDE background of the assessment team members, the detailed definition of the problem, and information input by the Contract Manager and from other cognizant FHWA personnel.

From the assessment, it was the concensus of the team that all 15 methods offered only marginal promise for detecting flaws when the reinforcing steel was inside a steel duct. Of the 15 methods, the most promising was the magnetic field and at least a limited experimental evaluation of this method was warranted. Results were unexpectedly good, even with the test bar inside a steel tube; accordingly, it was decided to undertake a comprehensive evaluation of the magnetic field method.

In the laboratory investigation of the magnetic field method, a simulated beam and an existing magnetic circuit, Hall-effect probes, amplifiers, power supplies, etc., were utilized. The simulated beam consisted of a wooden super-structure mounted on four nonmetallic wheels in which a matrix of steel rod or strand specimens containing manufactured flaws and unflawed steel items could be arranged in various configurations. The magnetic field was applied via a DC current excited electromagnet and the simulated beam was mechanically moved past the magnetizing circuit - Hall-effect probe inspection head; recordings of the signal output from the Hall-effect probe were made using a strip-chart recorder. The following parameters were explored on a preliminary basis:

(1) Flaw size and configurational parameters including length, section loss, orientation of nonsymmetrical flaws and separation of simulated fracture surfaces;

(2) Influence of adjacent unflawed steel items;

(3) Scan path with respect to centerline of flawed steel items;

(4) Type of duct;

(5)   Type of reinforcing steel;

(6)   Transverse rebars;

(7)   Probe-to-specimen spacing;

(8)   Magnetizing field strength.

The investigations were carried out using 5-ft. (1.5m) lengths of 0.5-in. (12.5mm) strand (7-wire) and 1-in. (25mm)-diameter ASTM A722 Type I and Type II bars; a range of simulated flaws consisting of reduced cross-sectional areas of various lengths was obtained by machining.

The following conclusions resulted from this preliminary experimental investigation of the magnetic field method, and it was recommended that development of an inspection equipment based on this method be undertaken.

(1)   Good overall sensitivity to loss-of-section.

(2)   Excellent overall sensitivity to fracture even with relatively small end separation (on the order of 0.01-in., 0.25mm).

(3)   Relatively minimal degradation of signal response in the presence of steel duct.

(4)   Presence of reinforcement adjacent to flaw had only a slight influence on flaw signal, if adequate magnetization was provided.

(5)   Configurational artifacts, i.e., helical band on the duct, thread-like protrusions on Type II bar, etc., and structural features, i.e., rebars, bar-duct contact, etc., have relatively minor negative type influences on flaw detectability.

(6)   Probe-to-reinforcement spacing, both vertical and transverse, is a significant parameter influencing overall magnetic response.

(7)   Magnetizing field strength required is a function of steel section to be inspected and the distance from the magnet and probe to the steel element under inspection.

80

IV.   CONCLUSIONS AND RECOMMENDATIONS

A.   Conclusions

Both laboratory and field evaluations of the magnetic inspection equipment have established the following features and capabilities of the method:

1.   Excellent agreement between results in the laboratory and the field for similar configurations of reinforcing steel.

2.   Good sensitivity to the details of the configuration of steel within approximately 6-in. (15cm) of the girder surface scanned.

3.   Good sensitivity to loss-of-section and fracture in post-tensioning steel bars (1- and 1-3/8-in., 2.5 and 3.5-cm diameter) in flexible and rigid steel or non-metallic duct for concrete coverages up to 6-in. (15cm), based on simulated flaws.

4.   Good sensitivity to loss-of-section and fracture in pre-tensioning strand (0.5-in., 1.3-cm diameter) for concrete coverage of 2 to 3-in. (5-7.5cm), based on simulated flaws.

5.   Excellent signal-to-noise ratio; the electronic noise level is two orders of magnitude below the amplitude range of the dominating signatures.

6.   Signatures from configurational details that are closer to the detector (having less concrete coverage) tend to "mask" signatures from flaws (loss-of-section and fracture) in steel elements in the same region but deeper (farther from the detector).

7.   Significantly reduced "masking" influence of stirrups for outermost strands (strands adjacent to transverse vertical faces, or sides of beam) in Texas Type "C" beams (stirrups do not extend into this region); accordingly, greater sensitivity to loss-of-section and fracture in strand is obtained in this region.

8.   Excellent possibilities for improved flaw (deterioration and/or fracture) recognition in the presence of reinforcement steel details (stirrups, chairs, etc.) based on the results of limited signature enhancement/recognition investigations (see Appendix IV).

81

Realization of the full potential capability of the magnetic method is dependent on development of techniques for discriminating between signatures from deterioration and those from a variety of reinforcement details. For nearly all other NDE methods even more difficult (perhaps insoluble in some cases) signature interpretation problems associated with the overall steel configuration in field structural members would be anticipated. In retrospect, if the fifteen candidate NDE methods were currently reassessed, the magnetic method would still be selected as the best approach for detecting steel deterioration and fracture in prestressed concrete members. Accordingly, recommendations for further development and evaluation work are made below.

B.   Recommendations

Results from laboratory and field evaluations strongly indicate the need for developing signature enhancement/recognition approaches before further field tests are conducted. Magnetic field distribution and/or electronic signal analysis approaches appear as very promising solutions for the flaw signature discrimination problem. Accordingly, each of these approaches is briefly described and discussed below.

Conceptually, the magnetic field distribution approach for discriminating steel deterioration signatures from reinforcement steel configurational details consists of the use of an array of magnetic field sensors, rather than a single sensor, to scan the structural member and to detect the presence of flaws using "pattern recognition" approaches to aid in interpreting the magnetic field distribution data obtained. It is recommended that preliminary laboratory investigations be conducted utilizing an array of sensors. Results would be evaluated on the basis of visual analysis of recordings made from selected array combinations for various structural steel element configurations (flaws, stirrups, chairs, etc.).

In addition to sensor arrays, the use of modern digital signal processing and analysis techniques offer great promise for the enhancement and recognition of flaw signatures in the presence of "masking" signals from steel reinforcement elements. This signal analysis approach consists of scanning a region of a beam, simultaneously digitizing the sensor(s) analog output and storing the digital information in memory. Subsequently, the stored digital information is analyzed using one or more analysis techniques. Correlation analysis is one very powerful technique and is particularly applicable to the problem at hand because the signatures from a given configuration of steel for scans over the same region are highly repeatable. For example, it is possible to recognize the presence

82

of certain signature content (from characteristic configurational steel elements such as stirrups, chairs, hold-downs, etc.) in a scan by conducting auto- and cross-correlation tests on the complete signature pattern from that scan. Those regions of the scan record showing a high degree of correlation, indicating nearly identical conditions and little or no deterioration, could then be eliminated from further analysis; subsequently, attention could be concentrated on those regions not showing high correlation since these would most likely be associated with deterioration. The correlation results could also be used to implement a "differencing process" by which signatures of no further interest could be removed from the scan record via point-by-point subtraction. Correlation analyses could also be conducted using functions constructed from signatures representative of known combinations of structural elements (stirrup and chair, stirrup and flaw, chair and flaw, etc.). In any event, the analysis could incorporate provisions to compare the actual configuration of steel (via interpretation of magnetic records) with that expected (via existing plans). Importantly, it is anticipated that a more effective flaw signature enhancement/recognition capability would be obtained by carefully combining the sensor array and electronic signal analysis approaches.

Subsequent to the investigation, development, and laboratory evaluation of the signature interpretation approaches, it is recommended that a field evaluation be conducted again at the Sixth South Street Viaduct in Salt Lake City, Utah, to confirm the flaw discrimination capability of the signature interpretation approach(es). Based on the previous field evaluation conducted in Utah, modifications to the existing inspection equipment are also desirable to make the system more readily adaptable to the field environment. While, basically, the existing magnetic inspection system is adequate for field operation, modification of the drive coupling and track rail coupling units would facilitate more effective use of the system in the field. Such efforts would be cost effective because the significantly improved operational efficiency would increase the actual inspection time available for data acquisition.

Contingent on the degree of success of the magnetic field inspection system to assess the flaw problems in the Sixth South Viaduct, it is recommended that at least three to four additional one-week field evaluations be conducted. Preferably, field sites should be selected which differ widely in accessibility and environmental problems so that experience can be gained for assessing the overall logistics of the inspection system installation and operational approaches. Each field evaluation should be preceded by a pre-site visit of one to two days to coordinate personnel and handling equipment problems and to delineate any special field problem areas. Such

83

pre-site visits would be cost effective since the subsequent one-week field evaluation effort could be significantly more productive (considering the number of program personnel involved as well as the support personnel and equipment which must be supplied by the State).

APPENDIX I

INTERIM REPORT, MARCH 1977
DETECTION OF FLAWS IN REINFORCING STEEL-IN
PRESTRESSED CONCRETE BRIDGE MEMBERS
(Exhibit)

TABLE OF CONTENTS

LIST OF ILLUSTRATIONS

iv

I. INTRODUCTION

A. Background

About 25 years ago, a new bridge structural design was introduced, that of prestressed concrete. In recent years, the use of prestressed concrete bridges has been widespread and such design now incorporates a variety of structural configurations. Basically, however, prestressed concrete bridge structural members are of two general types, pretensioned and post-tensioned. Pretensioned construction usually consists of 7-wire strand (on the order of 1/2-in. (1.3 cm) diameter) arranged in a matrix on 2-in. (5 cm) centers, the strands being pretensioned prior to casting the concrete members. Pretensioned members are produced at a plant site because of the special fabrication facilities and tooling required. In the case of the post-tensioned configuration, ducts, usually metal, are cast in a specified location and configuration in the concrete member; the reinforcing strand, rod, or bar is usually tensioned on-site and grouting material is introduced to fill the space between the reinforcement and the duct.

The load-carrying capability of prestressed bridge structural members is directly dependent upon the strength of the steel reinforcement rods, bars, or strands; hence, the integrity of the steel is of primary concern and is dependent upon one or more of the following factors:

(1) Quality of manufactured reinforcement material - governed by dimensional tolerances and presence of metallurgical type flaws such as voids or impurities.

(2) Corrosion deterioration as a result of field environment.

(3) Fracture failure - result of over stress (caused by loss of section due to corrosion deterioration) or by impact loading (as a result of construction or vehicular impact.

In recent years, there is growing evidence that deterioration of the steel as a result of corrosion does occur; furthermore, such deterioration does critically affect the structural strength. Currently used inspection procedures rely heavily on rust staining, cracking, and spalling of the concrete as an indicator that a problem exists in the reinforcing steel. Apparently, deterioration and even fracture of the reinforcement can occur without being preceded by visual evidence on the external surfaces of the concrete members. For example, the Sixth South Viaduct structure

in Salt Lake City consisting of 192 beams, presently, has 21 bars known to be fractured. A photograph of two of the fractures is shown in Figure 1. In this case, the presence of corroded and fractured post-tensioning rods was determined only from i) the loose rods and end-nuts during a visual inspection, and ii) the loud noise generated by one of the rods breaking which was overheard by people in the area who reported it to the State. There are no cracks or significant rust stains visible on these particular girders.

It is evident that presently available inspection methods for assessing the condition of reinforcing steel, in situ, in prestressed concrete bridge members are not adequate. The objective of the subject program is to develop a practical nondestructive method for detecting flaws in the reinforcement of prestressed concrete highway bridge members.

B.   Definition of the Problem

The overall objective of the program as stated in the previous section of this report involves the consideration of several flaw categories and an accompanying broad spectrum of mechanisms:

    i)   voids - manufacturing flaw

    ii)   corrosion deterioration - loss of material by electrolytic processes, stress corrosion cracking, and hydrogen embrittlement

    iii)   fracture - overload due to impact, gross loss of section, notch sensitivity, brittle fracture mechanisms such as stress corrosion cracking and hydrogen embrittlement.

Certainly from an overall point of view, the problem at hand is extremely broad both from the standpoint of mechanisms and also because of a wide variety of structural designs. Before the first significant step, that of assessing nondestructive inspection (NDE) methods with possible applicability to the problem,could effectively be undertaken, it became apparent that a more precise definition of the problem was required. Furthermore, the definition must include detailed immediate goals accompanied by a set of priorities relating to both mechanisms and structural design categories. In order to achieve adequate problem definition, the following steps were taken:

    (1)   A review of current literature was conducted relating to the corrosion of steel in reinforced concrete structures.

FIGURE 1.   OVERALL VIEW OF TWO FRACTURES FROM SIXTH
SOUTH VIADUCT STRUCTURE IN SALT LAKE CITY

(2)   Personal contacts were made with highway and bridge
        engineers in several states where corrosion problems
        were known to exist.

(3)   Conferences were held with cognizant FHWA personnel.

The paragraphs which follow in this section summarize definition of the
problem.

Review of the current literature, which is briefly summarized in
the section that follows, showed that the bulk of investigative work con-
cerning the corrosion of reinforcing steel was aimed predominantly at
material loss in the reinforcement (accompanied by cracking and spalling
of the concrete) with much less emphasis on stress corrosion cracking
and/or hydrogen embrittlement mechanisms. The literature, however,
did reflect an increasing concern about the possible role of stress
corrosion and hydrogen embrittlement mechanisms with the wider use of
high strength steels. Based on the literature review and personal contacts
with bridge and highway engineers in Utah and Florida, it was decided that
emphasis should be placed on the selection, rating, and investigation of NDE
methods for detecting substantial loss of steel section by corrosion and
for detecting fracture of reinforcing rods, strands, wires,and bars. This
problem definition was agreed on in conferences with cognizant FHWA
personnel and included the following:

(1)   Primary sensitivity goals are the detection of i) 10% or
        greater loss of area due to corrosion of steel, ii) fracture
        of rod or strand, iii) fracture of one or more wires in
        a strand.

(2)   Both ducted and non-ducted steel configurations (pre-
        tensioned and post-tensioned) are to be considered.

(3)   Regarding structural configurations, priority is to be
        given to the lower row of steel components along the
        tension flange in "I" and box beams.

(4)   Low priority is to be given to the detection of voids, of
        the order of 1/8-in. (3 mm) diameter in steel bars (this
        void size is within cross-sectional area tolerance band
        for manufacture of the bars).

As a result of several interacting factors associated with problem
definition and establishment of meaningful and realistic deterioration detection
goals, the program is presently about 9 to 10 months behind schedule but is
on a well directed course with goals related to currently known field problems.

C.   Corrosion of Reinforcing Steel in Prestressed Concrete

In view of the fact that corrosion is such a dominant factor for the deterioration of steel in a field environment, it will be of benefit to the reader to briefly summarize here pertinent information gleaned from the literature review.

Background

With few exceptions, concrete, because of its alkalinity, forms a protective environment for reinforcing steel.[25,42,45,46]*   The chemically protective nature of the concrete may be only an initial condition, however, and careful consideration must be given to what takes place once a structure has been completed and put into service.   Steel in prestressed bridge structural members is vulnerable to corrosion for several reasons:

(1)   Concrete is permeable[45,42,25] and even in the absence of cracks or spalls reinforcing steel can undergo corrosion from de-icing salts, salt water, salt water atmospheres, and/or air pollutants in the vicinity of industrial complexes permeating the concrete cover over the steel.

(2)   Cracking or loss of concrete cover over the reinforcing steel for whatever reason   (overload cracks, freeze-thaw cracks, cracks due to design difficulties, vehicular impacts, etc.), provides an opening for corrosive atmospheres directly to the reinforcing steel.

(3)   On prestressed structural elements, especially post-tensioned ones, the ends of the structure are particularly vulnerable to corrosion because of the inherent configuration.   The susceptibility of the ends of girders or beams in the post-tension case is greater because of the necessity to grout the ends after the tensioning has been completed. In addition, if the region between the reinforcing steel and the surrounding duct is not adequately grouted, the entire length of the reinforcing steel becomes susceptible to corrosion.

Nature of Corrosion

Generally, the corrosion of steel in concrete appears to be electrolytic or galvanic in nature.[25,42,47] Since there are many excellent

_____

* Superscript numbers in parentheses refer to References in Appendix C.

treatices on galvanic corrosion, the subject will not be treated in depth
in this report. It is important, however, to recognize that the dominate
features of this process are the formation of anodic and cathodic regions
in the presence of an electrolyte (in the case of bridges this is usually
a chloride), with the loss of metal occurring at the anode where the
steel goes into solution. Usually, the anodic region is small compared
to the cathodic region and the loss of material is in the form of severe
pitting.[46,47] A number of investigators have stated that the corrosion
process requires not only the presence of an electrolyte but also of
oxygen; this factor places importance upon the texture of the concrete
as well as the occurrence of pore space or voids in the vicinity of the
steel.[46,25]

Investigations have been conducted which cover a wide range of
factors influencing the effect of corrosion on the strength of steel.[25,48,
45,49,28] The influence of a corrosive environment on the structural
strength of steel has several facets, and there is some evidence [46]
that prestressing the steel in tension may accelerate the rate for intensity
of metal removal by corrosion. While electrochemical action results in
a reduction in cross-sectional area of the steel, what is more significant
is the notch effect produced by the pit nature of the corrosion. [46]
Importantly, the notch effect not only influences the ultimate strength but
also the ductility of the steel. [46]

While it is not intended to discuss them here, other possible
corrosion related mechanisms of failure which could be present are stress
corrosion and hydrogen embrittlement. However, these brittle fracture
mechanisms do not appear to be worthy of concern in prestressed bridge
structures at this time. A number of stress corrosion and hydrogen
embrittlement laboratory investigations have been conducted on bridge
steels [25,28,46,50]; thus far, the results appear to be contradictory.

Some Results of the Corrosion of Steel in Concrete

It has been widely accepted that the corrosion products occupy
slightly more than twice the volume of the steel present prior to corro-
sive attack which can produce pressures of the order of 5,000 psi
(3.5×10^7 Pa) in the concrete.[25,47] This volumetric expansion of
corroding steel results in the cracking and spalling of concrete
surrounding the reinforcing steel. The degree of corrosion necessary to
cause cracking and spalling of the concrete appears to vary widely; e.g.,
in the laboratory it has been shown to vary from 1 to 30 mils (0.025 to
0.75 mm) of material loss necessary to cause cracking.[48] It seems
that in most instances, cracking of the concrete caused by corrosion of
the steel is accompanied by visible signs of rust staining on the exterior

6

surface of the concrete but instances have been reported of the formation of a brown stain prior to cracking.[25,45]

Numerous laboratory and field investigations of the corrosion phenomena have been conducted using the half-cell potential method. This method can distinguish between passive and active states of corrosion which has provided some fundamental insight into the corrosion process. For example, investigations[48,51] have reported that under some circumstances the half-cell potential alternates between passive and active values. There appears to be consistency, however, in that the potential changes from passive to active and remains active sometime (more than several weeks) before cracking of the concrete around the steel occurs. Other investigations involving multiple wire strands[49] have shown a tendency for more severe corrosion of the internal center strand than for the surrounding strands. To summarize the reported findings, there appears to be general agreement with regard to the following:

(1)   It is not necessary to have cracking or spalling of the concrete in order to have corrosion of the steel take place.

(2)   It appears that at some point during the corrosion process of the steel, cracking of the surrounding concrete will take place which will eventually be accompanied by spalling of the concrete.

(3)   The depth of corrosion necessary to initiate cracking and/or spalling varies widely.

(4)   Concrete cracking, due to corrosion of the steel, is accompanied by (or may be preceded by) the appearance of rust stains on the exterior surface of the concrete in the vicinity of the steel.

Observations in the field[27] have noted cracking of the concrete in line with some rebars (and ducts) wherein corrosion in the stirrup section has appeared to lead to corrosion of the rebars. This perhaps emphasizes the importance of adequate concrete coverage over stirrup sections as well as the main structural steel members. It was also noted in on-site observations that the concrete cracking along the rebar ducts near the middle of the beam was not accompanied by rust staining.

Results reported, although scattered, indicate that the rate of corrosion can vary widely. In the laboratory, rates from a mean rate of 35 mils/yr (0.88 mm/yr) to a maximum of 138 mils/yr (3.45 mm/yr) have been reported.[48] In a California bridge less than 10 years old[52], a mean rate of metal loss of 29 mils/yr (0.725 mm/yr) (range of 7 to 80 mils/yr

or 0.18 to 2.0 mm/yr for a 10 to 90% frequency) was observed. These results were noted for the No. 4 reinforcing steel in the bridge deck. Another investigator[45] estimates a 6 to 10 mils/yr (0.15 to 0.25 mm/yr) metal loss rate under field conditions which he compares to a 7 to 35 mils/yr (0.18 to 0.88 mm/yr) rate for a bridge in England without concrete cover. To establish some perspective, based on an average metal loss rate of 30 mils/yr (0.75 mm/yr) from corrosion, a 1/2-in. (1.3 cm) diameter rebar would lose 10% of its original cross-sectional area in about 10 months.

Studies have also been conducted to determine the effect of crack width in the concrete on the rapidity of corrosion of the steel. It is important here to recognize that this relates to the influence of cracking in concrete and the corrosion of steel where the initial crack formation is not a result of the corrosion process. The studies have shown that cracks as narrow as 0.004 inch (0.1 mm) result in rapid corrosion of the steel.[25] Most investigators indicate that the corrosion rate of steel once it is unprotected by the concrete (such as in the presence of cracks and spalling) would be significantly greater.

II. RATING AND ASSESSMENT OF METHODS

A state-of-the-art literature search and review related to the detection of deterioration of reinforcing steel in prestressed concrete structures were conducted. Both Government and industrial indexes were searched using a strategy based on intersecting sub-sets of descriptors pertaining to i) nondestructive testing, ii) concrete, and iii) corrosion. As a result of this computerized search, other selected manual searches, and personal contacts, 72 documents have been identified which are related to the overall problem. Numerous other documents which provide background information related to applicable nondestructive inspection methods also have been identified for use during the method assessment task.

Based on information contained in the identified documents and input from Southwest Research Institute personnel having a broad background in related nondestructive inspection problems, 15 NDE methods with possible applicability to the subject inspection problem were identified. The assessment of these 15 methods was undertaken based on analysis of information contained in documents from published literature, the NDE background of the assessment team members, information input by the Contract Manager as well as other cognizant FHWA personnel. As pointed out in the introduction of this report, specific program objectives, NDE method sensitivity goals, and inspection priorities (regarding structural configurations) were established and agreed upon through suggestions, comments, and meetings with FHWA personnel. The establishment of specific objectives and goals was crucial to the effective and meaningful assessment of the 15 NDE methods which follow:

Acoustic Emission
Eddy Current
Electrical Resistance (Concrete)
Electrical Resistance (Steel)
Electromagnetic, Nonlinear
Electromagnetic, Reflection
Electromagnetic, Time-Domain
  Reflectometry
Half-Cell Potential

Holography
Magnetic Field
Mossbauer
Radiography
Strain-Gage
Thermal
Ultrasonic Scattering

All documents identified during the search phase of the assessment effort were given a cursory review and each categorized according to the inspection method(s) discussed in each document; those documents providing overall background to the problem were also recognized. Each method was rated by a member of the assessment team using a worksheet(s)

and accompanying instructions (See Appendix B for worksheet format, instructions, and completed worksheets for each method assessed). Briefly, the worksheet provided a rating of each method based on the following parameters:

      (1)   Sensitivity, no duct or nonmetallic duct;

      (2)   Sensitivity, metallic duct;

      (3)   Adaptability to field use;

      (4)   Instrumentation factors.

From the detailed information contained in the completed worksheets, a composite comparative rating chart (see Table I) was constructed based on the following parameters:

      (1)   Sensitivity, no duct or nonmetallic duct;

      (2)   Sensitivity, metallic duct;

      (3)   Ability to accommodate field environment;

      (4)   Ability to access inspection areas;

      (5)   Potential for development within scope for the contract.

A discussion of the composite rating chart (Table I) is presented here; for a more detailed examination of ratings for a particular method, along with critical comments, the reader is referred to Appendix B. The composite rating in Table I utilizes graduations of color (shades of gray) to illustrate a rating code because it facilitates a more effective overall assessment and comparison of the individual methods. In general, the darker the shade (the greater the density) the better the performance of the method for that particular parameter; a legend is presented in the chart which annotates the meanings of the density rating. Briefly, the composite rating chart indicates the following:

Without Duct or With Nonmetallic Duct

Magnetic field and radiography were the only promising methods with any significant quantitative capability for corrosion detection, or partial or total fracture detection. Electromagnetic non-linear and reflection methods as well as ultrasonic scattering methods appear to offer some possibilities, but would require

10

considerable laboratory effort initially to estimate feasibility.

In addition, the electromagnetic nonlinear method does not offer much promise of being quantitative. While the methods commented on thus far do not include those requiring penetration of the concrete, even if penetration of the concrete were considered as a viable option, the added methods for serious consideration, for example electrical resistance, do not offer significant promise in terms of detection sensitivity.

With Metal Duct

Only the magnetic field method offers significant promise; if penetration of the concrete is considered operationally unacceptable, the remaining methods have little capability. As in the no-duct case, even if penetration of the concrete is considered a viable approach, the capability of methods added for consideration is rather poor.

For the reader wishing to gain somewhat greater insight into the applicability of each of the methods to the inspection problem at hand, it is recommended that the "remarks" in the worksheets of Appendix B for each of the methods be perused and that the description of methods in Appendix A be reviewed.

Based upon the results of the literature study assessment of the 15 methods, the decision was made to conduct a limited experimental evaluation of the magnetic field method. The objective of this experimental effort was to define in somewhat greater detail the capability of the magnetic field method, including an initial appraisal of the influence of factors, such as metallic duct, stirrup rebars, multiple strand or bar matrix configuration, etc. on flaw detectability. The experimental work conducted is described and the results obtained are discussed in the section which follows.

11

GLOSSARY OF TERMS IN TABLE I

1.0   Methods: Self-explanatory

1.1   No.: Self-explanatory

1.2   Description: Self-explanatory

2.0   Sensitivity: Pertains to the effectiveness of a method to determine the condition of reinforcing steel in prestressed concrete.

2.1   No Duct or Nonmetallic Duct: Rating relates to pre-tensioned configuration for no duct or sheath over the reinforcing steel or a nonmetallic duct post-tensioned configuration.

2.1.1   Corrosion: Relates to the detection of the loss of section due to corrosion. Sensitivity for various thickness of concrete coverage categories indicates influence of coverage on detection.

2.1.2   Fracture: Relates to the detection of the fracture of reinforcement rod or strand. Fracture may be a result of overload because of reduced section due to corrosion or the result of mechanical damage from impact.

2.1.2.1   Total: Detection of fracture of total strand, or rod, or bar.

2.1.2.2   2-4 Wires: Detection of fracture of 2 to 4 wires in a strand.

2.1.2.3   1 Wire: Detection of fracture of 1 wire in a strand.

2.1.3   Voids: Detection of voids 1/8-inch (3 mm) diameter or larger occurring in bar during fabrication.

2.2   Metallic Duct: See 2.1 except reinforcement rod, bar, or strand is within a metallic duct (usually steel). Rating generally relates to post-tensioned configuration.

2.2.1   See 2.1.1

2.2.2   See 2.1.2

2.2.2.1   See 2.1.2.1

2.2.2.2   See 2.1.2.2

2.2.2.3   See 2.1.2.3

3.0   Accommodate Field Environment: Rating indicates ability of each method to accommodate to operation under field conditions.

4.0   Access Inspection Area: This rating indicates the capability of each method to assess anticipated bridge inspection regions because of size, shape or weight of instrumentation package or sensors. Requirement to have opposing sides accessible or penetrate concrete (and duct) is indicated by note.

5.0   Potential for Development (within scope of contract): Rating indicates probability that the method can be developed within the scope and funding of the present contract. The scope includes a breadboard system, evaluation of the breadboard in the laboratory and the field, breadboard system update (or fabricate preliminary prototype system), and field use criteria development.

TABLE 1. SUMMARY OF RATINGS OF INSPECTION METHODS

1.0 METHODS		2.0 SENSITIVITY			3.0 ACCOMMODATE FIELD ENVIRONMENT	4.0 ACCESS INSPECTION AREA	5.0 POTENTIAL FOR DEVELOPMENT
1.1 NO.	1.2 DESCRIPTION	2.1 NO DUCT OR NON-METALLIC DUCT	2.2 METALLIC DUCT				

2.1 NO DUCT OR NON-METALLIC DUCT sub-columns: 2.1.1 CORROSION; 2.1.2 FRACTURE (2.2.2.1 TOTAL, 2.2.2.2 24 WIRE, 2.2.2.3 1 WIRE); 2.1.3 VOIDS — each with sub-headings <3", 3'-6", >6"

2.2 METALLIC DUCT sub-columns: 2.2.1 CORROSION; 2.2.2 FRACTURE (2.2.2.1 TOTAL, 2.2.2.2 24 WIRES, 2.2.2.3 1 WIRE); 2.2.3 VOIDS — each with sub-headings <3", 3'-3", 3'-6", >6"

1.1 NO.	1.2 DESCRIPTION
1	ACOUSTIC EMISSION
2	EDDY CURRENT
3	ELECTRICAL RESISTANCE (CONCRETE)
4	ELECTRICAL RESISTANCE (STEEL)
5	ELECTROMAGNETIC NON-LINEAR
6	ELECTROMAGNETIC REFLECTION
7	ELECTROMAGNETIC REFLECTOMETRY
8	HALF-CELL POTENTIAL
9	HOLOGRAPHY
10	MAGNETIC FIELD
11	MOSSBAUER
12	RADIOGRAPHY
13	STRAIN GAUGE (VIBRATION)
14	THERMAL
15	ULTRASONICS (SCATTERING)

*Amount of Concrete Coverage

Legend:

Typical
Density
Layout

Corrosion (2.1.1, 2.2.1)
- <10%
- <50%
- >50%
- 100%, Not applicable

Fracture, Voids (2.1.2-2.1.3, 2.2.2.1-2.2.3)
- Excellent
- Good
- Fair
- Poor, Not applicable

Accommodate Field Environment (3.0)
Access Inspection Area (4.0)
Potential for Development (5.0)
- Excellent
- Good
- Fair
- Poor

Notes:

1 Not quantitative.
2 Not detectable after it has occurred.
3 Must penetrate concrete (and duct).
4 Not applicable to existing bridges.
5 Feasibility not established.
6 Method primarily sensitive to grouting defects.
7 Requires access to both sides.

13

III. PRELIMINARY EXPERIMENTAL INVESTIGATION
OF MAGNETIC METHOD

A.   Apparatus

The limited experimental effort conducted consisted of a preliminary laboratory investigation of the magnetic field method using a simulated beam and existing magnetizing circuits, Hall-effect probes, amplifiers, power supplies, etc. A test bed was designed in conjunction with the simulated beam specimen to permit utilization of an existing mechanical drive system to provide scanning motion for the experiments conducted. The laboratory test setup is illustrated in Figure 2, along with annotation of the major system components. The test bed consists of a wooden frame over which the simulated beam can be moved on wheels for mechanical scanning of the beam specimen. The simulated beam is a wooden structure mounted on four nonmetallic wheels; nonferromagnetic fasteners and hardware were used throughout to eliminate possible interference with the magnetic data from flaws.

The simulated beam structure was designed such that the configuration of reinforcing steel components used could be modified easily and quickly to facilitate the investigation of a number of configurations. Two typical arrangements of reinforcing steel are illustrated in Figures 3 and 4. Typically, the steel elements examined were 5 ft. (1.5 m) in length. The scan drive had a total traverse capability slightly greater than the length of the steel specimens so the specimens could be scanned from end-to-end if desired. By adjusting the end bulkheads on the simulated beam structure or the height of the magnet, the spacing between the magnet and/or probe and any particular steel reinforcing component could be adjusted to a selected value in the range of 0.25 in. (0.64 cm) to ∼ 6 in. (15 cm). The probe was mounted with respect to the magnet such that the path along which the probe scanned a particular steel component could be varied in a transverse direction across the test bed; this permitted the probe to follow a scan path either directly below the steel component of interest or on a path off-center up to ∼ 1 inch (2.5 cm) off-center (by repositioning the magnet, greater off-center distances could be obtained). Figure 5 illustrates a typical arrangement for use in testing the influence of stirrup rebars on the magnetic signatures from simulated flaws; using the same basic approach, several different rebar reinforcing steel configurations were investigated. A comparison of Figure 6 with Figure 4 shows the manner in which a variety of pole tip configurations could be investigated for their influence on the signatures obtained from flaws.

FIGURE 2. OVERALL VIEW OF LABORATORY SETUP FOR MAGNETIC FIELD INVESTIGATIONS

15
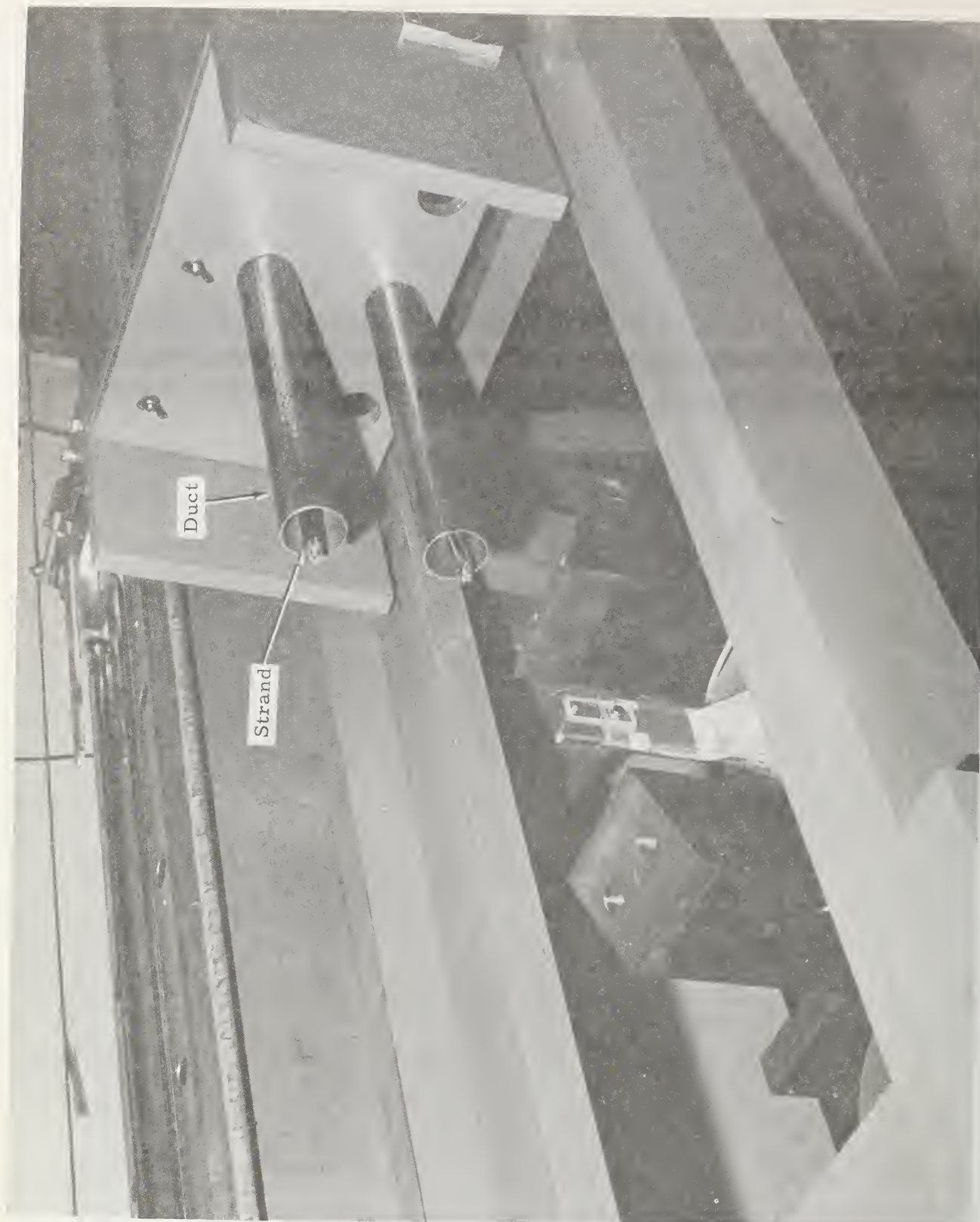
FIGURE 3. CLOSEUP VIEW OF SIMULATED BEAM WITH REINFORCING STRAND MATRIX

16

Strands

Magnet

Probe
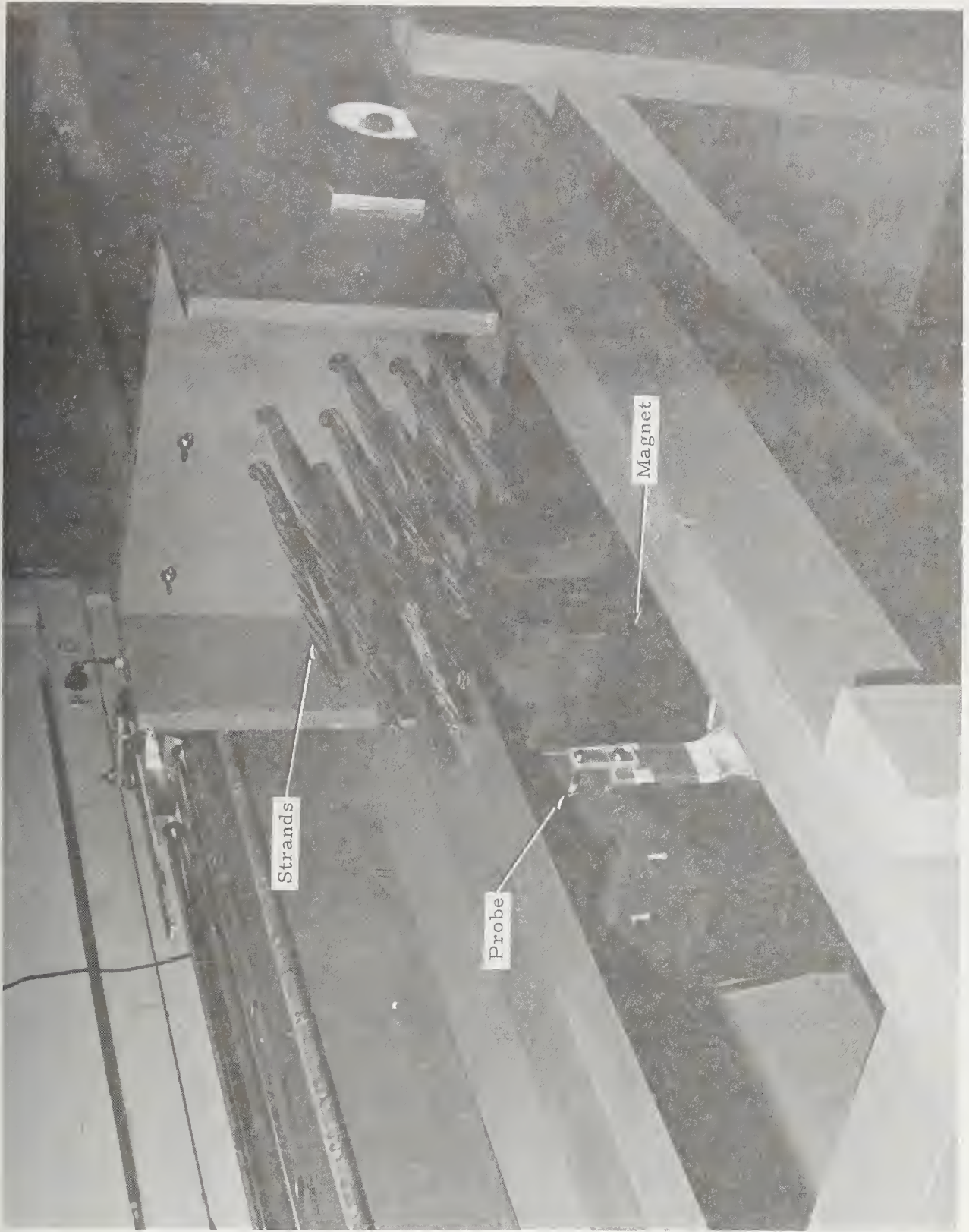
FIGURE 4. CLOSEUP VIEW OF SIMULATED BEAM WITH REINFORCING STEEL AND DUCT MOUNTED

17
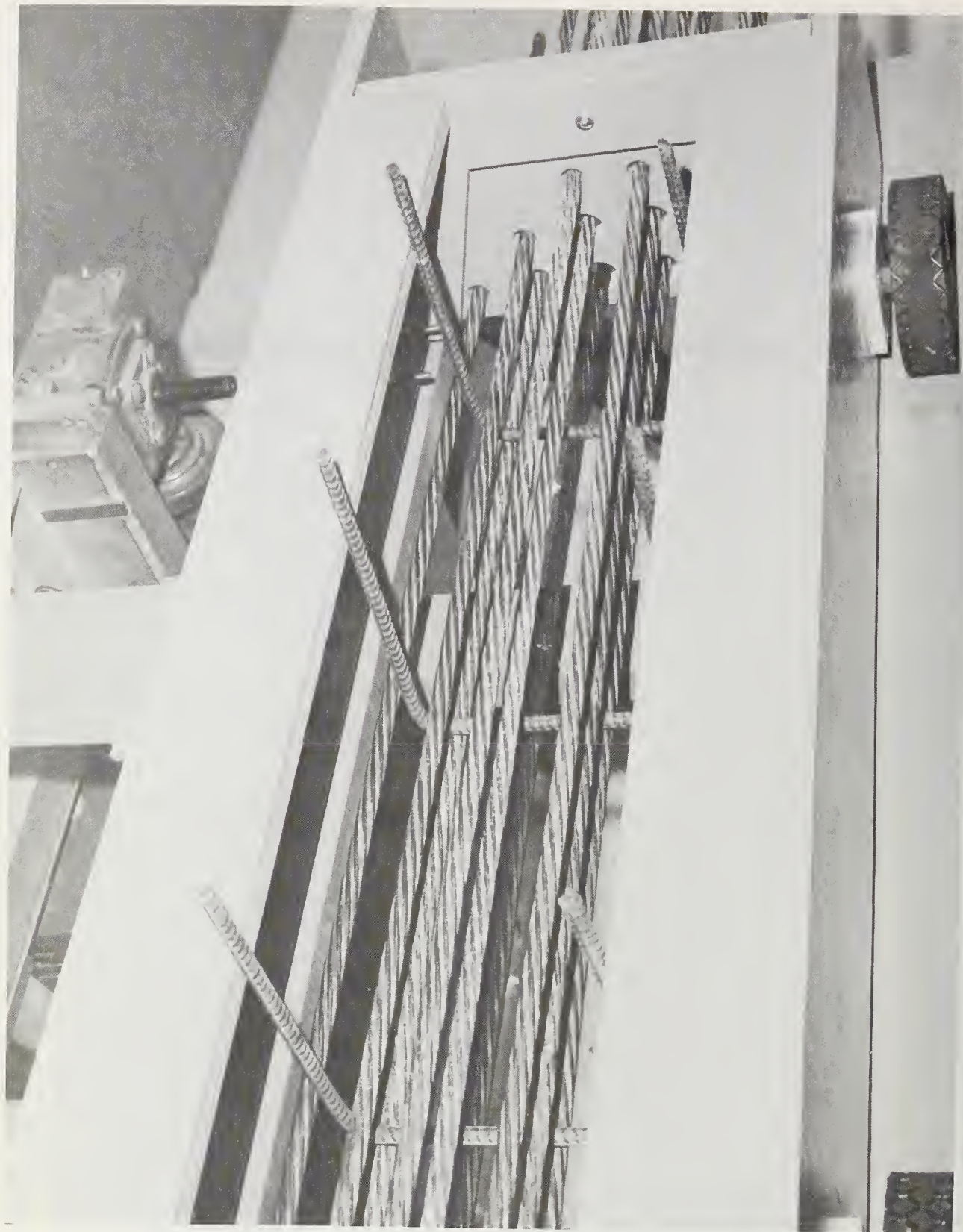
FIGURE 5. VIEW OF STRAND MATRIX WITH TRANSVERSE REBARS

18
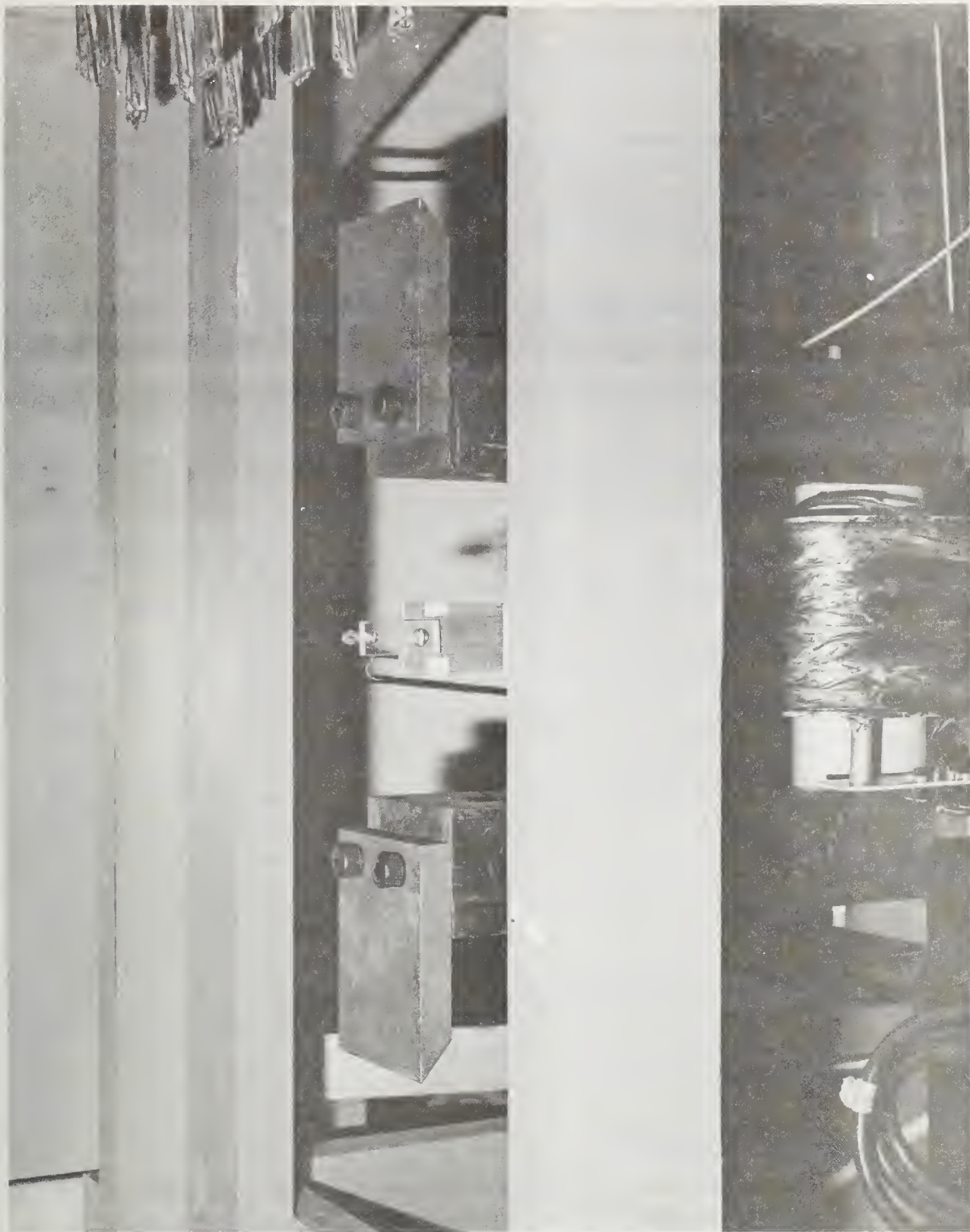
FIGURE 6. VIEW SHOWING ELECTROMAGNET WITH FLAT PLATE POLE TIPS

19

B.   Experimental Approach

The magnetic field investigations were conducted by inserting specimens containing manufactured flaws and unflawed steel sections in various configurations in the simulated beam specimen, applying a DC current to the electromagnetic, mechanically moving the simulated beam containing the test specimens past the magnet-probe head unit, and recording the signal output from the Hall-effect probe on a strip-chart recorder. Utilizing this general approach, the following parameters were explored on a preliminary basis:

(1)   Flaw size and configurational parameters including length, section loss, orientation of nonsymmetrical flaws and separation of simulated fracture surfaces;

(2)   Influence of adjacent unflawed steel members;

(3)   Scan path with respect to center line of flawed steel members;

(4)   Type of duct;

(5)   Type of reinforcing steel;

(6)   Transverse rebars;

(7)   Probe-to-specimen spacing;

(8)   Magnetizing field strength.

Table 2 summarizes the test specimen configurations including flaw sizes and shapes used in the subject investigations. Many of the specimens listed in Table 2 are shown in Figure 7 including typical sections of flexible and rigid duct. Closeup views of flaw test sections for many of the specimens are shown in Figures 8, 9, and 10. The amount of cross-section removed by machining (simulation of cross-section loss by corrosion) in terms of percentage of the original bar cross-section has been calculated for each flaw type and tabulated for the corresponding specimen in Table 2. The results of the numerous experimental investigations are presented in the section which follows.

C.   Experimental Results

Many typical recordings are presented in Figure 11 which illustrate typical signatures from duct, strand, bar, and rebars. A brief discussion

TABLE 2.
TEST SPECIMEN (Manufactured Flaws)

Flaw Configuration I
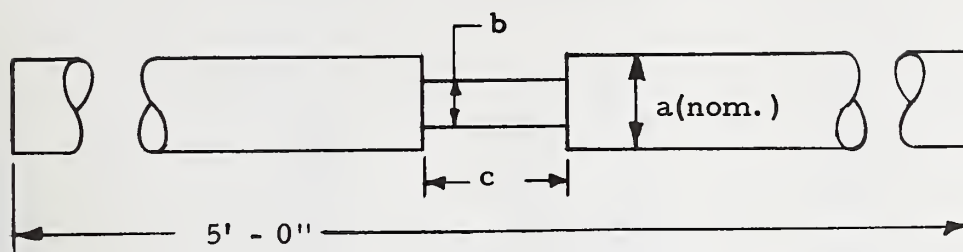
Flaw Configuration II
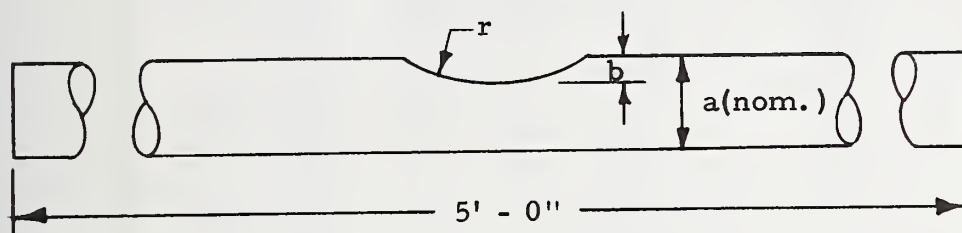
Specimen	Material	Flaw Conf.	a(in.)	b(in.)	c(in.)	r(in.)	% Area*
A	Strand, 7-wire	I	0.5	0.17	0.13	–	86
B	Strand, 7-wire	I	0.5	0.35	6.0	–	43
C	Strand, 7-wire	I	0.5	0.17	6.0	–	86
D	Cold Rolled Bar	I	1.0	0.25	0.13	–	94
E	Cold Rolled Bar	I	1.0	0.80	1.0	–	36
F	Cold Rolled Bar	I	1.0	0.80	6.0	–	36
G	Cold Rolled Bar	-	1.0	—	–	–	0
H	A722, Type I	II	1.0	0.20	–	1.0	14
I	A722, Type I	II	1.0	0.50	–	1.0	50
J	A722, Type II	II	1.0	0.50	–	1.0	50
K	A722, Type II	-	1.0	—	–	–	0
L	A722, Type I	I	1.0	0		–	100
M	Strand, 7-wire	I	0.5	2wire	variable	–	28
N	Strand, 7-wire	I	0.5	3.5wires	variable	–	50
P	Strand, 7-wire	I	0.5	0	variable	–	100
Q	A722, Type I	—	1.0	–	–	–	0

* % Area lost (removed); % Area remaining = 100% - % Area lost

NOTES: Typically, 5-ft. lengths of 2-5/8-in. diameter rigid and flexible duct
were used to simulate post-tension configurations.
1 inch = 2.54 cm
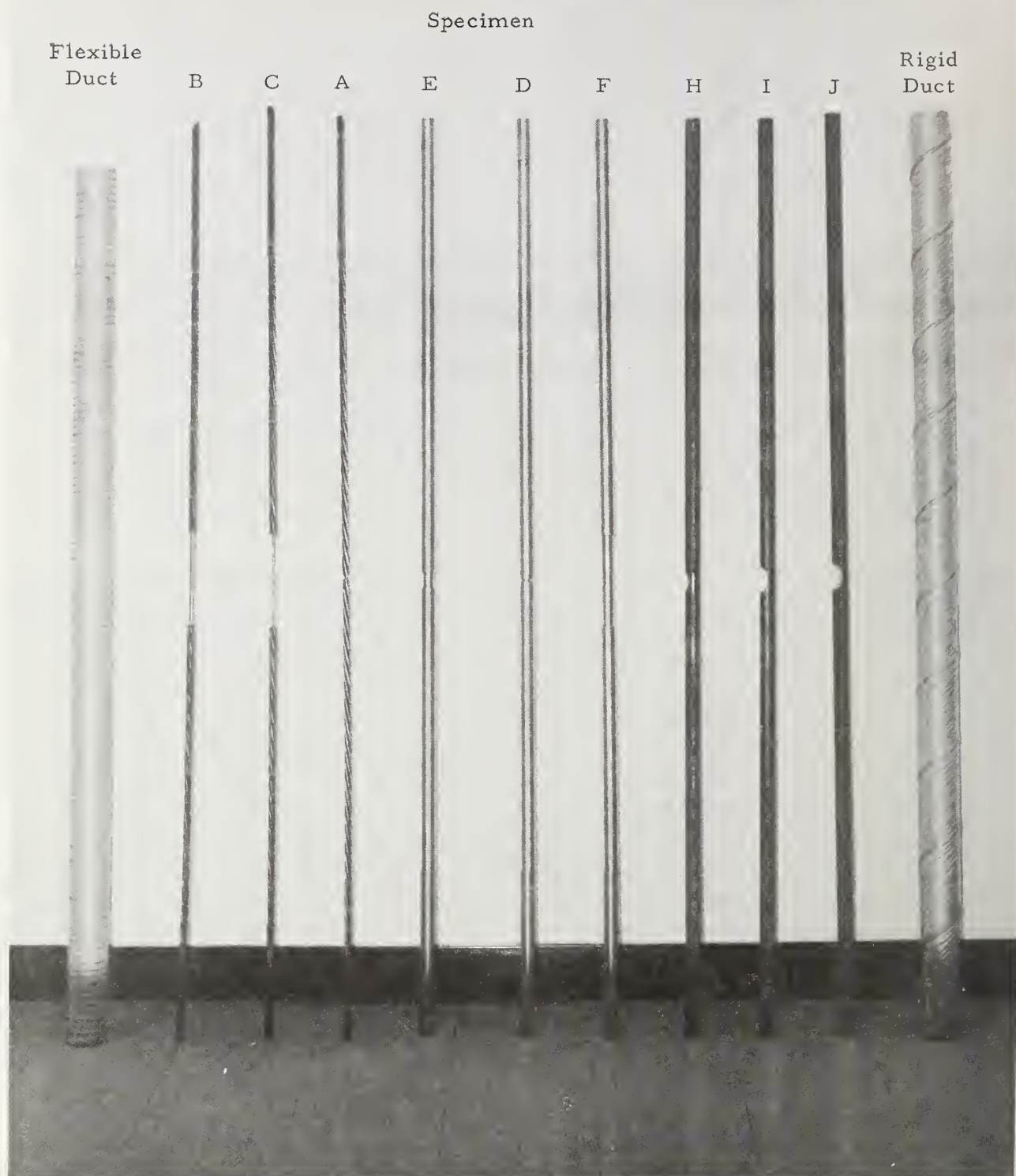
FIGURE 7. OVERALL VIEW OF TYPICAL TEST SPECIMENS

Specimen   A   C   B

FIGURE 8.   CLOSEUP VIEW OF STRAND SPECIMENS WITH MANU-
FACTURED FLAWS

23
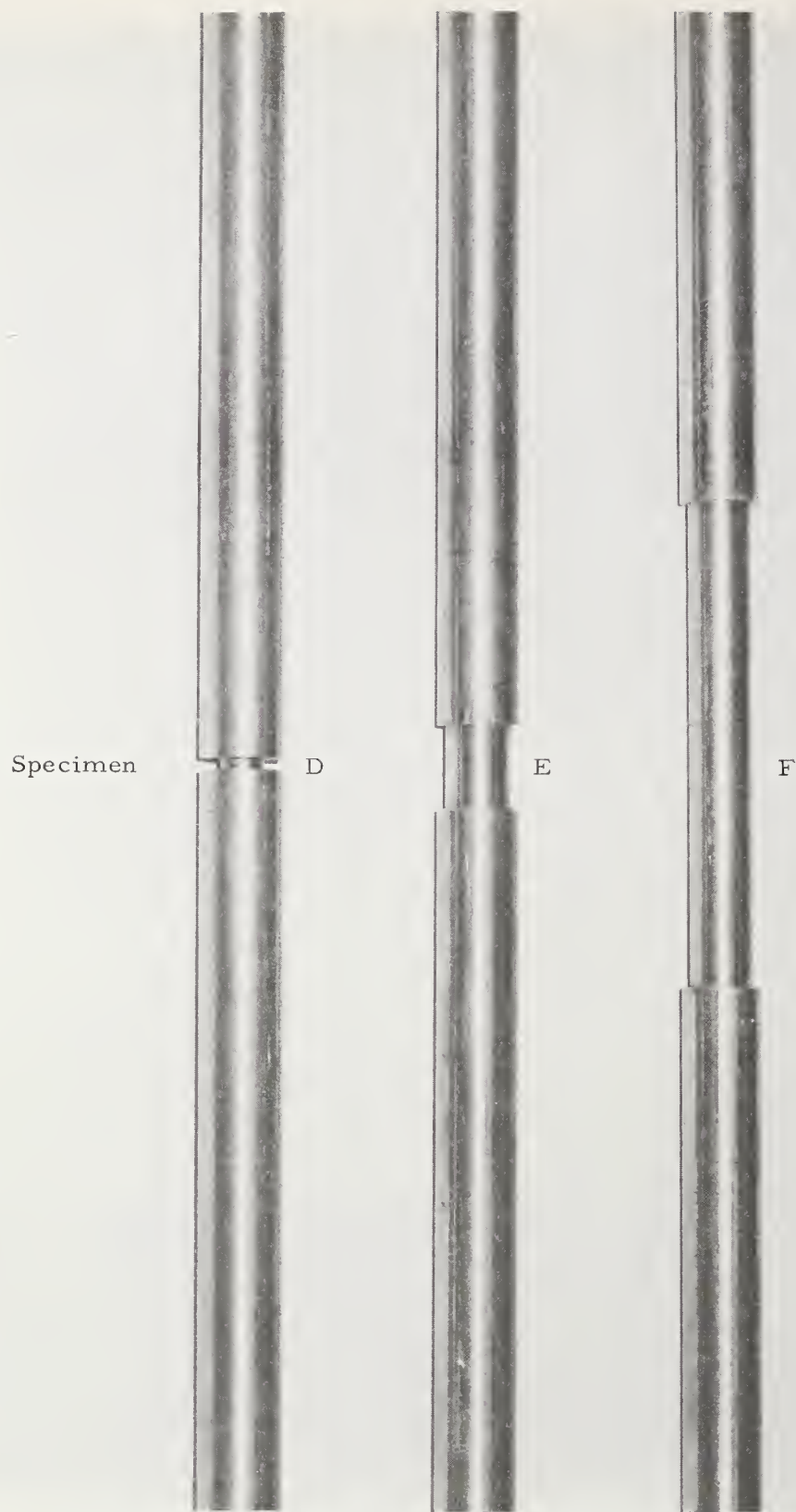
Specimen   D   E   F

FIGURE 9.   CLOSEUP VIEW OF CRS BAR SPECIMENS WITH MANU-
            FACTURED FLAWS
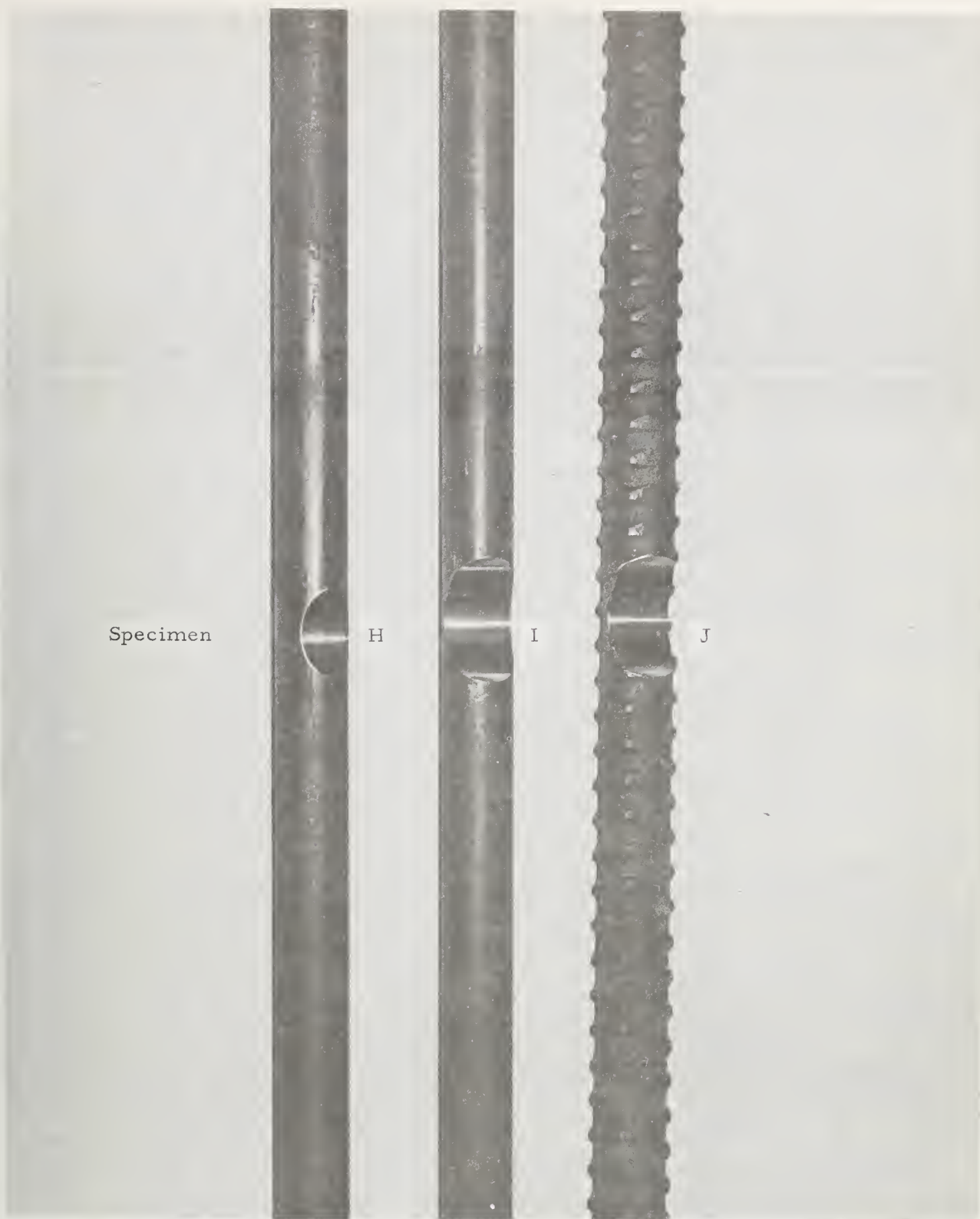
Specimen   H   I   J

FIGURE 10. CLOSEUP VIEW OF ASTM-A722 TYPE I AND TYPE II
BARS WITH MANUFACTURED FLAWS
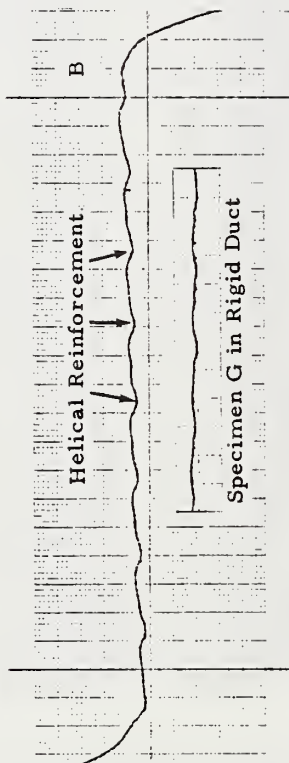
D

Rebar

Flaw

Rebar

2.0 V

1/2 in. φ strand (Specimen A), 3/8 in. φ rebars 20 in. apart and above specimen, 1.5 in. probe-to-specimen spacing, 2 amp.

E

Rebar

Rebar

2-5/8 in. rigid duct, no specimen, 3/8 in. φ rebars 20 in. apart and above duct, 2.5 in. probe-to-duct spacing, 3 amp.

F

Rebar

Flaw

Rebar

2-5/8 in. φ bar (Specimen D), rigid duct, 3/8 in. φ rebars 20 in. apart and above duct, 2.5 in. probe-to-specimen spacing, 3 amp.

A

1.0 V Typ.

2 in. typical

2-5/8 in. flexible duct, no specimen, 2.5 in. probe-to-duct spacing, 3 amp.

B

Helical Reinforcement.

Specimen G in Rigid Duct

2-5/8 in. rigid duct, no specimen (insert with specimen), 2.5 in. probe-to-duct spacing, 3 amp.

C

End of Specimen

End of Specimen
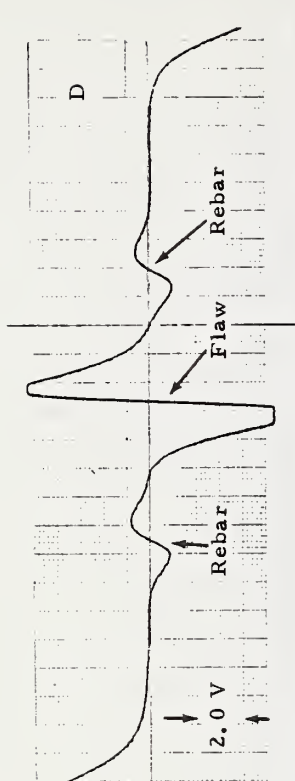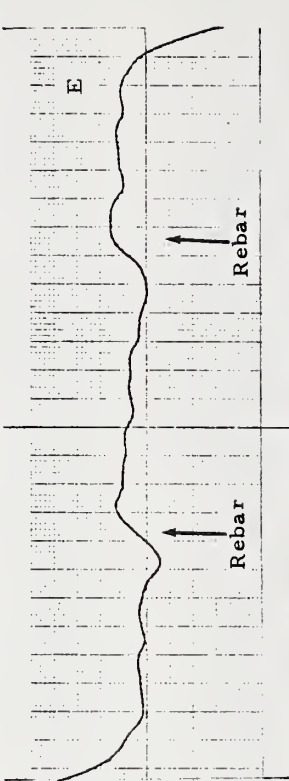
1 in. φ A722 Type II bar (Specimen K), no duct, 2.5 in. probe-to-bar spacing, 4 amp.

FIGURE 11. MAGNETIC RECORDS ILLUSTRATING TYPICAL SIGNATURES FROM DUCT, STRAND, BAR AND REBARS

26

of this figure is in order to acquaint the reader with the data presentation format. The vertical excursion in each record is proportional to the magnetic disturbance generated at the probe by the specimen and any attendant flaw conditions; generally, there is a large vertical excursion at each end of scan (see record C, Figure 11) caused by the demagnetizing effect of the specimen ends. The horizontal scale in each record is proportional to distance along the specimen, a typical scale of which is shown at the bottom of record A (Figure 11).

Further examination of the records in Figure 11 will acquaint the reader with typical features of magnetic field response. Record A was obtained from a length of flexible duct containing no reinforcing steel within it and with the probe located 2.5 inches (6.4 cm) below the center of the duct. Notice the relatively smooth line (other than the end effects) except for the signal departures pointed out by the arrows; these signal departures are caused by the fact that the flexible duct was not completely straight (the local spacing between the duct and the probe varies locally along the length of duct). Record B was obtained under conditions similar to record A except using a piece of rigid duct; notice the relatively straight base line with a periodic pattern of small bumps caused by the extra thickness of steel in the helically formed bead on the rigid duct. The signature insert within record B, obtained with a 1-inch (2.54 cm) diameter section of ASTM A722 Type I bar within the duct, shows that as reinforcing steel cross-section is added inside the duct it tends to smooth the influence from the helical bead on the duct. Interestingly, and fortunately, the helical thread-like protrusions on the ASTM A722 Type II bar (such as tradename Dywidag) does not produce any significant background signal (see record C). Record D, Figure 11, illustrates the influence of a flaw and also rebars(transversely oriented to the test specimen such as for stirrups). The rebars give the same polarity of signature, e.g., viewing from left to right downward going and then upward going, as the flaw; however, the amplitude of signature from the rebar is relatively small. The data in record E illustrates the combined effect of rebars along with a section of rigid duct but without reinforcing bar inside. It is pointed out that the distance from the probe to the rebar in the case of record E is considerably greater than that for record D; correspondingly, the signature from the rebar is significantly less in the case of record E. Record F, Figure 11, illustrates the combined magnetic response from a section of rigid duct containing a bar specimen with a manufactured flaw and two rebars transversely placed above the duct to either side of the flaw. The results illustrated in Figure 11 are very encouraging in that a relatively minor response is obtained from configurational artifacts of the typical steel members as compared to response from manufactured flaws.

To facilitate an overall view of the influences and interactions of the many test parameters on signatures from flaws, signature information from

the inspection records has been reduced and is presented in tabular and graphical form in this section of the report, and specific brief comments are made below about each of the presentations.

Table 3 - Influence of adjacent unflawed material on the signal obtained from a flawed specimen.

Results from specimen A indicate the influence of adjacent strands on the flaw signature amplitude is minimal. For specimen D the influence of flexible duct is less than that for rigid duct when adjacent bars are not present; the influence of neither duct is extremely significant. Specimen D results, however, do show the presence of adjacent bars on either side of the flawed specimen (4 in. or 10 cm spacing) do indicate a significant reduction in signal amplitude from the flaw; this reduction in signal amplitude may be caused by insufficient magnetization. The results from specimens E and F show a more pronounced effect of rigid duct on signal amplitude than for specimen D, perhaps because in the case of specimens E and F the flaws extend over a greater length. The apparent increase in flaw signal amplitude for specimen F inside a flexible duct is misleading and is probably the result of an inability to maintain the spacing between the probe and the specimen with sufficient repeatability for the "with" and "without" flexible duct tests.

Table 4 - Influence of the transverse position of probe scan along the specimen (vertical distance from the probe to the specimen remaining constant).

The results indicate approximately a 50% reduction in signal for the probe track 1-inch (2.5 cm) off-center [probe-to-specimen vertical spacing of 1.5 inches (3.8 cm)]. The reduction in signal amplitude appears to be essentially independent of the presence of steel adjacent to the flawed specimen and essentially independent of the flaw configuration (note the dimensions for specimen C are significantly different than those for specimen A, refer to Table 2).

Figure 12 - Signal amplitude as function of probe-to-specimen spacing.

The results from specimens A, B and L tend to indicate the same general functional relationship and it is one which is strongly dependent upon the spacing.

28

TABLE 3

INFLUENCE OF ADJACENT REINFORCEMENT ON FLAW SIGNATURE AMPLITUDE

Specimen	Relative Flaw Signature Amplitude								
	No. Adj. Strands				No Duct	Rigid Duct		Flexible Duct	
						No Adj. Bars	Two Adj. Bars	No. Adj. Bars	Two Adj. Bars
	0	1	2	11					
A	100%	95%	94%	88%	-	-	-	-	-
D	-	-	-	-	100%	85%	69%	96%	67%
E	-	-	-	-	100%	67%	-	-	-
F	-	-	-	-	100%	71%	-	111%	-

TABLE 4

INFLUENCE OF TRANSVERSE LOCATION PROBE SCAN TRACK ON FLAW SIGNATURE AMPLITUDE
(probe-to-specimen vertical spacing 1.5 in., 3.8 cm)

Specimen	Relative Flaw Signature Amplitude	
	Scan On-Center	Scan 1-in. Off-Center
A Only	100%	53%
A+1 adj. strand	100%	54%
A+2 adj. strands	100%	52%
A+11 adj. strands	100%	51%
C+11 adj. strands	100%	49%
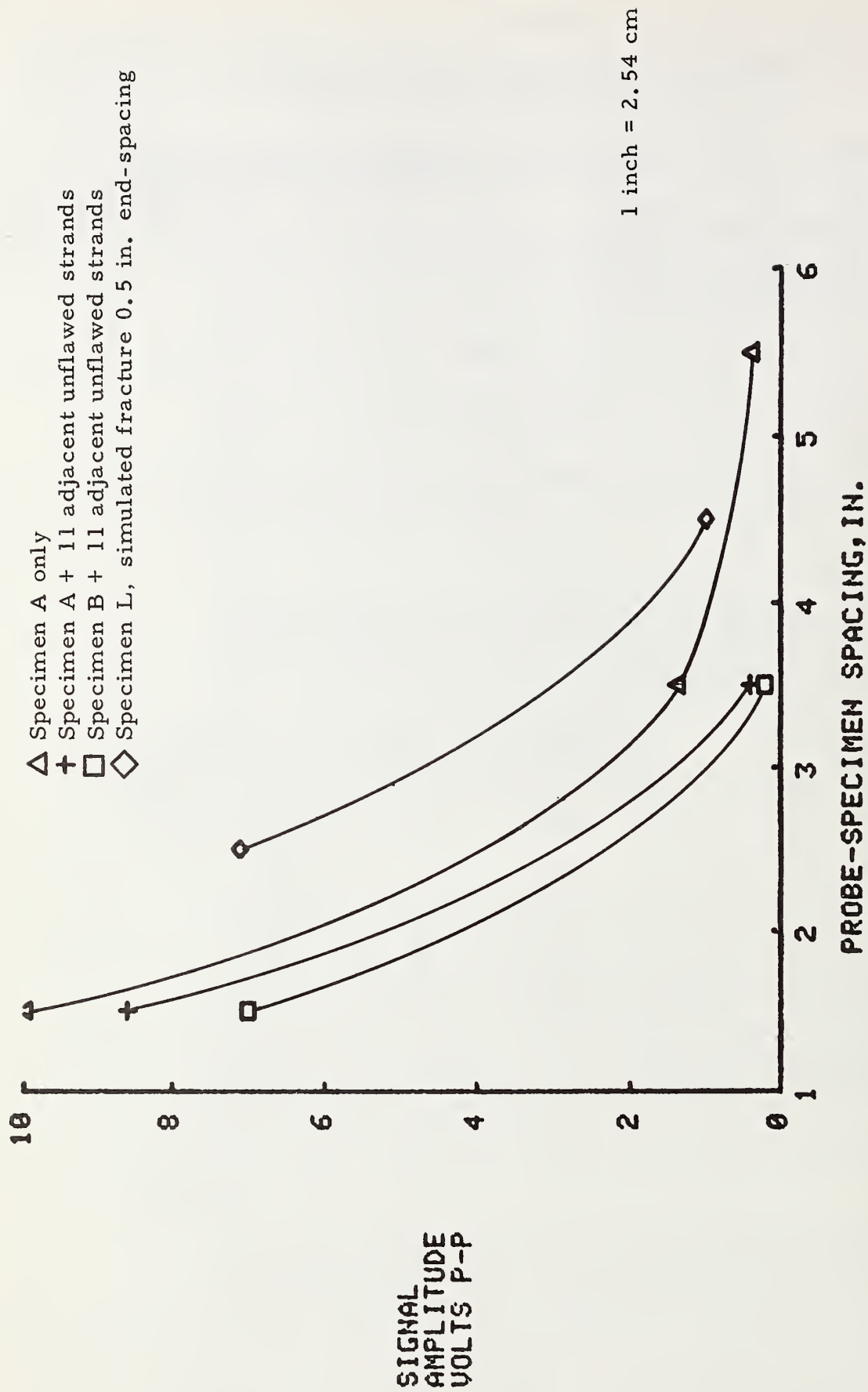
FIGURE 12.   GRAPH OF FLAW SIGNAL AMPLITUDE AS A FUNCTION OF PROBE-TO-
SPECIMEN SPACING (3 Amp)

△ Specimen A only
+ Specimen A + 11 adjacent unflawed strands
□ Specimen B + 11 adjacent unflawed strands
◇ Specimen L, simulated fracture 0.5 in. end-spacing

1 inch = 2.54 cm

PROBE-SPECIMEN SPACING, IN.

SIGNAL
AMPLITUDE
VOLTS P-P

<u>Figure 13</u> - Signal amplitude as a function of magnetizing current.

The data for specimen A with a 1.5-inch (2.8 cm) probe-specimen spacing shows a tendency towards saturation at higher magnetizing currents. The data for specimen B at a spacing of 2.5 inches (6.4 cm) and that for specimen A at 3.5 inches (8.9 cm), particularly, indicates significant further increases in signal amplitude would be obtained with greater applied field strength. Other preliminary results to be presented later in this section will indicate that by proper configuration of the magnetic circuit additional signal amplitude can probably be obtained without further increases in magnet power.

<u>Figure 14</u> - Signal amplitude as a function of flaw length.

The results from specimens D, E, F and L show an extremely rapid increase in signal amplitude for flaw lengths from almost zero up to the order of 1/8 inch (3 mm) and then a relatively slow additional increase in signal amplitude for greater flaw lengths. These results tend to indicate that deeply corroded regions would not have to extend over a great distance along the strand or bar to be detectable.

<u>Figures 15 and 16</u> - Signal amplitude as a function of loss of cross section.

The results from specimens B and C, Figure 15, indicate an almost linear relationship between signal amplitude and percent area lost; on this basis, liberty has been taken and a straight line relationship assumed with the other curves in Figures 15 and 16. The data point corresponding to specimens I and J, Figure 16, indicate a tendency for lower signal amplitudes from flaws not symmetrically distributed about the reinforcement cross-section (compare the data point from specimens I and J with those from specimens E and F in the same figure.

It is informative to now examine the records in Figure 17 because they indicate good sensitivity for detecting partial and total fracture in 7-wire strand even with relatively small separation of the fractured interfaces. The data in Figure 17 were obtained with the flaw specimen in a matrix of 11 additional unflawed strands. Figure 18 illustrates similar results for bar-type specimen in rigid duct with a probe-to-specimen

31
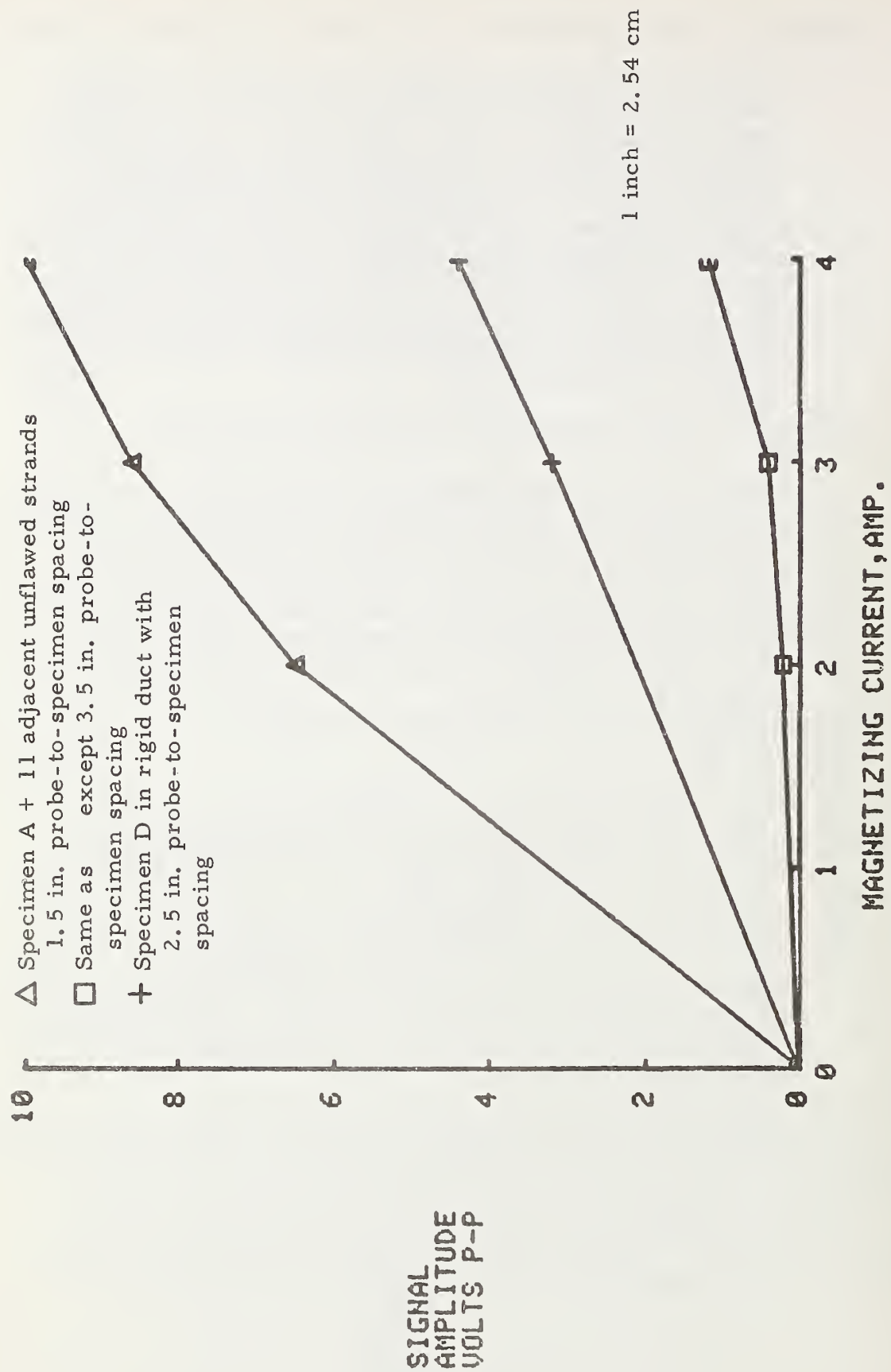
FIGURE 13. GRAPH OF FLAW SIGNAL AMPLITUDE AS A FUNCTION OF MAGNETIZING CURRENT

1 inch = 2.54 cm

△ Specimen A + 11 adjacent unflawed strands 1.5 in. probe-to-specimen spacing

□ Same as except 3.5 in. probe-to-specimen spacing

+ Specimen D in rigid duct with 2.5 in. probe-to-specimen spacing

SIGNAL AMPLITUDE VOLTS P-P

MAGNETIZING CURRENT, AMP.
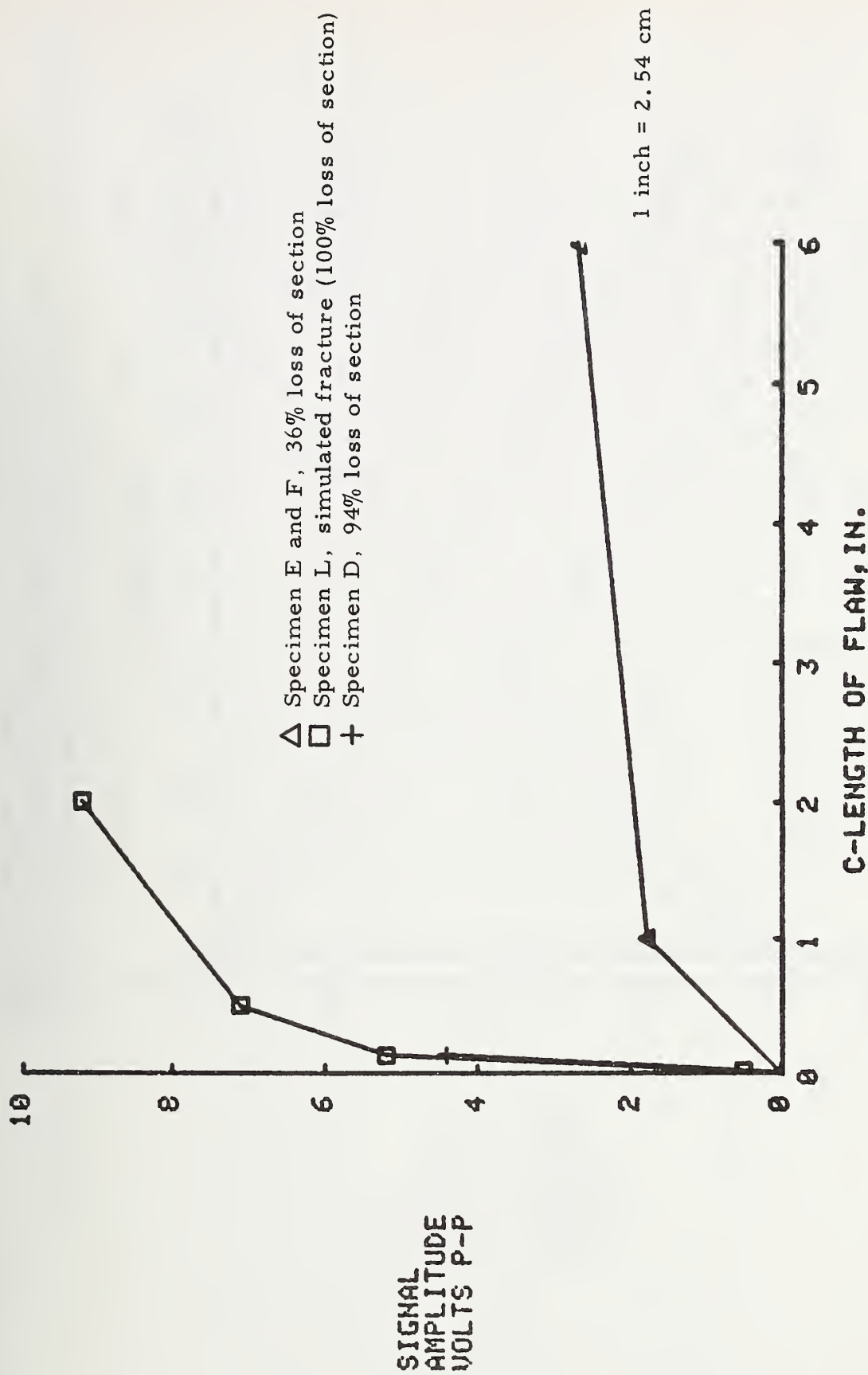
FIGURE 14. GRAPH OF FLAW SIGNAL AMPLITUDE AS A FUNCTION OF FLAW LENGTH (each specimen in rigid duct with 2.5-in. probe-to-specimen spacing, 4 Amp)

33
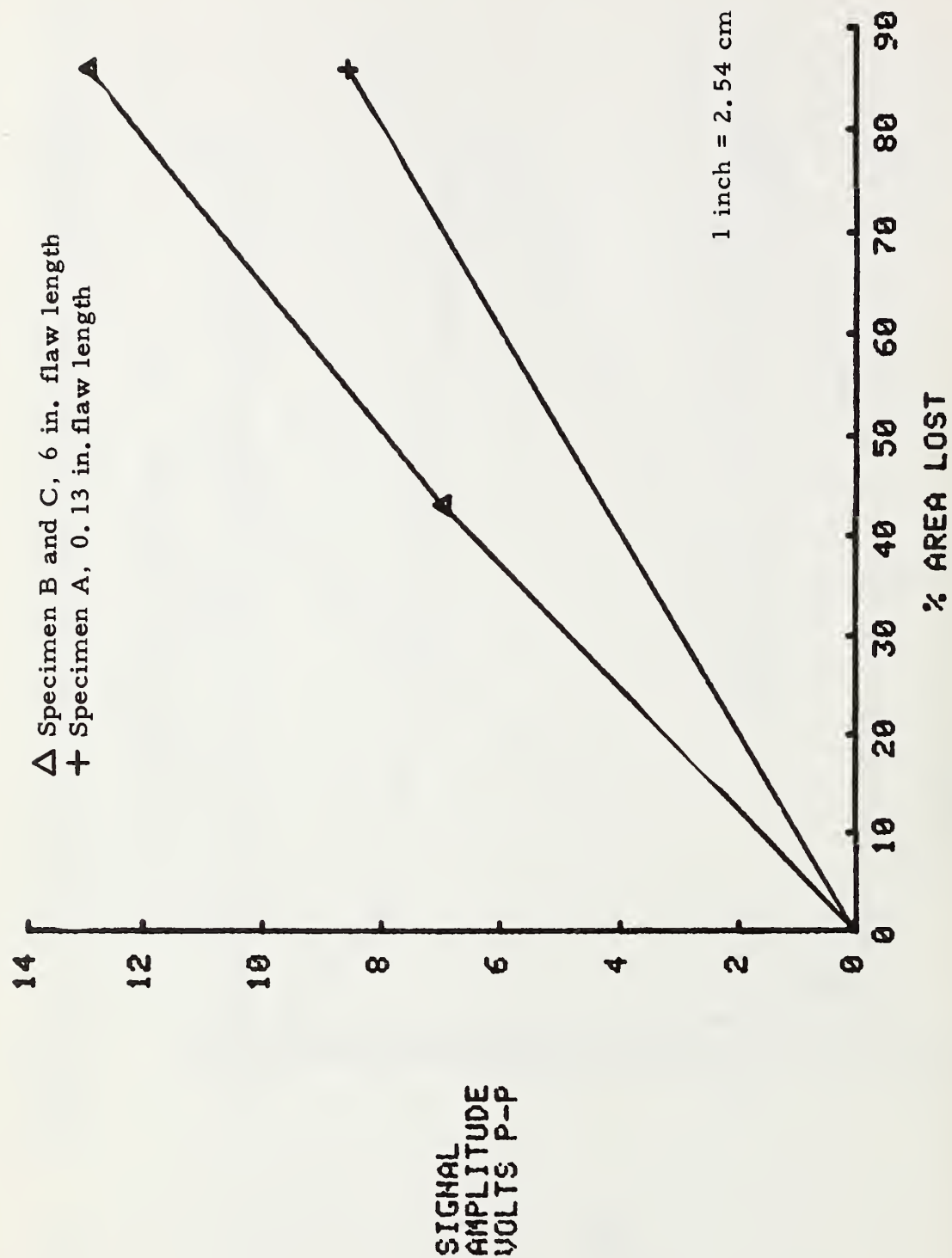
FIGURE 15. GRAPH OF FLAW SIGNAL AMPLITUDE AS A FUNCTION OF LOSS OF CROSS SECTION (each specimen with 11 adjacent unflawed strands, 1.5-in. probe-to-specimen spacing, 3 Amp)

34
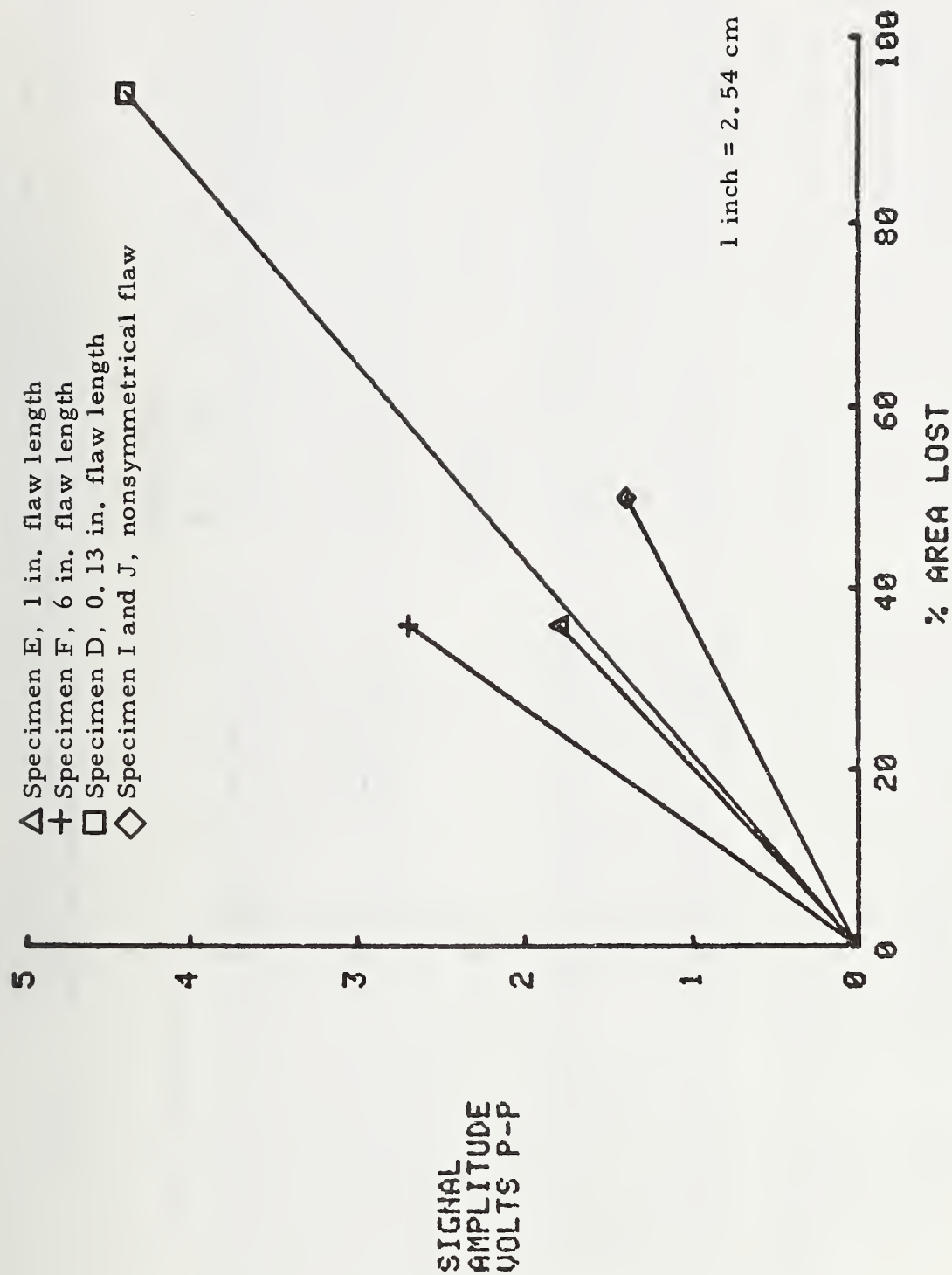
FIGURE 16. GRAPH OF FLAW SIGNAL AMPLITUDE AS A FUNCTION OF LOSS OF CROSS SECTION (each specimen in rigid duct, 2.5 in. probe-to-specimen spacing, 4 Amp)

35
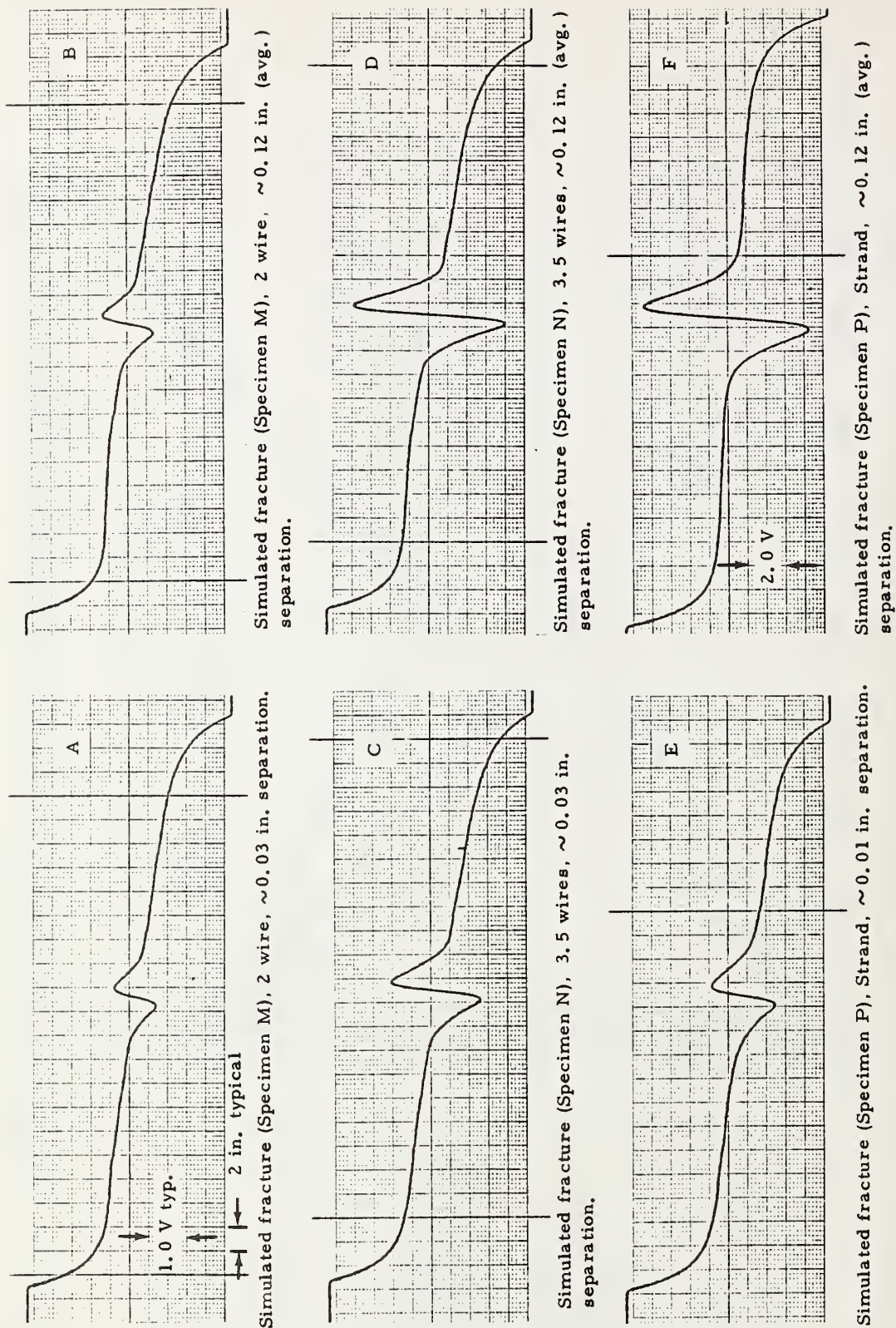
FIGURE 17. MAGNETIC RECORDS (3 Amp) ILLUSTRATING INFLUENCE OF WIRE FRACTURE AND END-SEPARATION ON SIGNATURE FOR SIMULATED FRACTURE OF 0.5 IN. φ 7-WIRE STRAND (Specimens M, N, P, plus 11 unflawed strands in test matrix, 1.5 in. probe-to-flaw strand spacing)

Simulated fracture (Specimen M), 2 wire, ~0.03 in. separation.

Simulated fracture (Specimen M), 2 wire, ~0.12 in. (avg.) separation.

Simulated fracture (Specimen N), 3.5 wires, ~0.03 in. separation.

Simulated fracture (Specimen N), 3.5 wires, ~0.12 in. (avg.) separation.

Simulated fracture (Specimen P), Strand, ~0.01 in. separation.

Simulated fracture (Specimen P), Strand, ~0.12 in. (avg.) separation.

1.0 V typ.

2 in. typ.

2.0 V

36
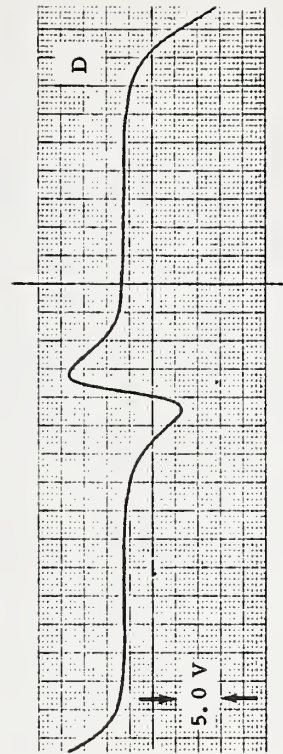
FIGURE 18.   MAGNETIC RECORDS (4 Amp) SHOWING INFLUENCE OF END-SEPARATION ON SIGNATURE
FOR SIMULATED FRACTURE OF A722 TYPE I (Specimen L), 1 IN. φ, HIGH STRENGTH BAR
CENTERED AND TOUCHING IN RIGID DUCT (2.5 in. probe-to-bar spacing)

Simulated fracture, ~ 0.005 in. separation, bar specimen
centered in rigid duct.

Simulated fracture, 0.13 in. separation, bar specimen centered
in rigid duct.

Simulated fracture, ~ 0.005 in. separation, bar specimen
touching bottom of rigid duct.

Simulated fracture, 0.13 in. separation, bar specimen touching
bottom of rigid duct.

37

spacing of 2.5 inches (6.4 cm). Records A and B at the top of Figure 18 illustrate the very rapid increase of signal amplitude for separations up to approximately 1/8 inch (3 mm) as commented on in the previous discussion of Figure 14. Records C and D illustrate the fact that if the bar is in contact with the duct in the region of the fracture, the magnitude of the signature is not reduced. As a matter of fact, a comparison of records C and D with A and B, respectively (Figure 18), indicate an increase of signal; however, this is probably a result of the reduced spacing between the probe and the bar specimen since the position of the duct was not altered in the experiment.

Figure 19, encouragingly, illustrates excellent detectability for post-tension bar fracture having end-separation with i) a significant cross-section of rebar directly over the fracture area (compare records A and B) and ii) good detectability of 0.5-inch (1.3 cm) separation with probe-to-specimen spacings as much as 6.5 inches (see record F, Figure 19). Furthermore, a comparison of records D and E in this figure illustrate that an almost 25% increase in signal amplitude was obtained by using flat plate-type pole tips versus the conventional wedge-type pole tips used almost throughout this investigation (refer to Figures 4 and 6 showing the two pole tip configurations). This preliminary indication of the influence of pole tip design on flaw signal response suggests that significant further improvements should be possible with additional design investigations.

Finally, Figure 20 presents magnetic signature results obtained in an attempt to inspect near the fractured end of one of the failed 1-3/8-in. (3.5 cm) diameter bars (see Figure 1) from the Sixth South Viaduct structure in Salt Lake City. The fracture specimen used in this experiment is uniformly corroded around the entire bar circumference within about 10 inches (25 cm) of the fracture; the corrosion rapidly tapers about the circumference and ends about 2 ft. (60 cm) from the fracture. The loss of section near the fracture is $\sim$8-10%. It is evident in record A (Figure 20) that no signature from the corrosion is detectable; the large signal from the bar ends makes it difficult to detect signature trends from the much lesser effects of corrosion. Next, a 1-3/8-in (3.5 cm) diameter steel bar, 20-in. (51 cm) length was placed adjacent to each end of the Utah sample to minimize the end "effect" signals (see record B, Figure 20). However, because of the unevenness of the ends, "gaps" of $\sim$ 0.05-0.10 in. ($\sim$ 1 to 2 mm) were present which produced the large signals observed. Record C, Figure 20, wherein the probe was scanned about 0.25 in. (0.64 cm) from the bar surface shows response from local corrosion pitting (pointed out by the arrows); but again, effective results cannot be obtained any closer than about 6-8 inches (15-20 cm) from the fracture because of
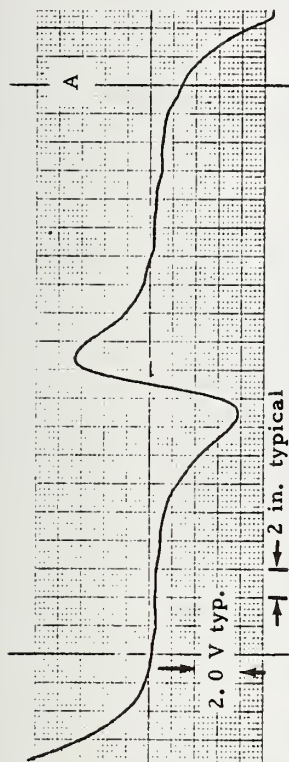
Simulated fracture, 0.5 in. separation, no transverse rebars, 2.5 in. probe-to-bar spacing.
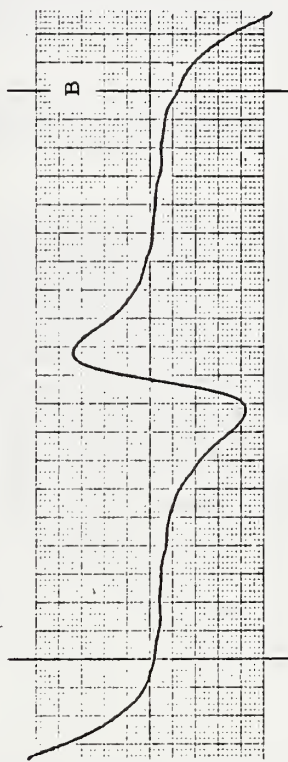
Simulated fracture, 0.5 in. separation, 3-3/8 in. φ rebars nested on top of duct over fracture, 2.5 in. probe-to-bar spacing.

Simulated fracture, 0.5 in. separation, 4.5 in. probe-to-bar spacing, standard pole tips.

Simulated fracture, 0.5 in. separation, 4.5 in. probe-to-bar spacing, plate pole tips.
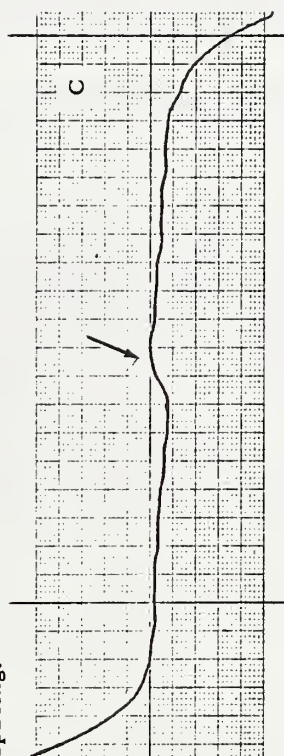
Unflawed bar with 3-3/8 in. φ rebars nested on top of duct, 2.5 in. probe-to-bar spacing.
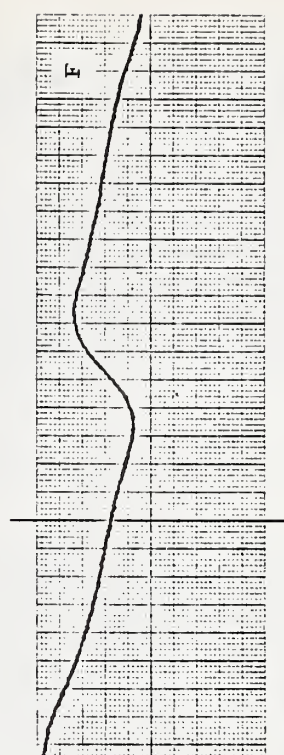
Simulated fracture, 0.5 in. separation, 6.5 in. probe-to-bar spacing, plate pole tips.

FIGURE 19.   MAGNETIC RECORDS (4 Amp.) SHOWING SIGNATURES FROM SIMULATED FRACTURE OF A722 TYPE I (Specimen L) 1 IN. φ, HIGH STRENGTH BAR CENTERED IN RIGID DUCT FOR PROBE-TO-SPECIMEN SPACINGS FROM 2.5 IN. TO 6.5 IN. WITH AND WITHOUT REBARS

39
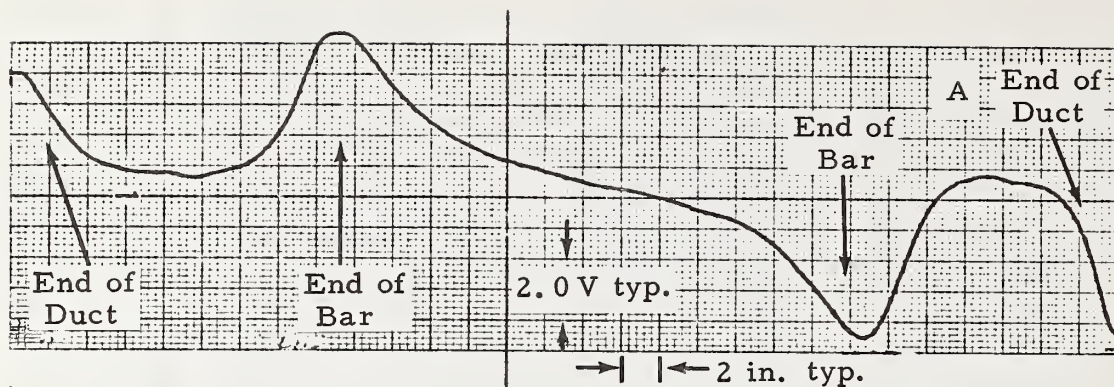
32-in. length Utah fractured bar, in rigid duct, 2.75-in. probe-to-bar spacing.
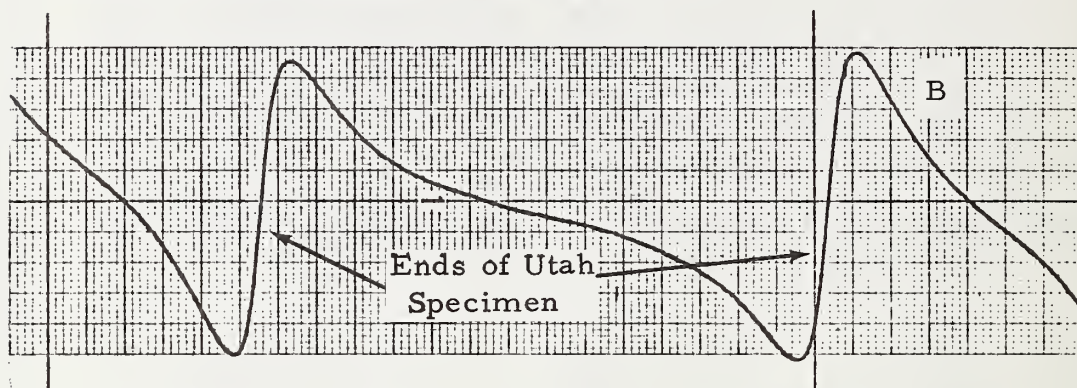
32-in. length Utah fractured bar with 20-in. length of steel bar adjacent each end, no duct, 2.0-in. probe-to-bar spacing.
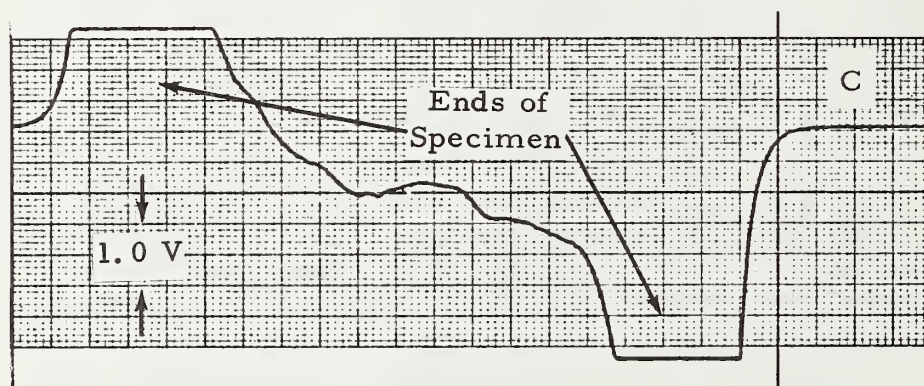
32-in. length Utah fractured bar, no duct, probe ~ 0.25 in. below bar surface.

FIGURE 20.   MAGNETIC SIGNATURES (3 Amp) FOR 32-IN. LENGTH FRACTURED BAR FROM SIXTH SOUTH VIADUCT, SALT LAKE CITY

40

end effects. Nevertheless, record B in Figure 20 further confirms the results previously shown in Figures 14, 18, and 19 - that very strong magnetic response should be obtained from fractured reinforcement even when inside steel duct and with thick concrete cover.

IV. CONCLUSIONS

The preliminary experimental investigation of the magnetic field method has established several important features about the capabilities of the method, namely:

(1)   Good overall sensitivity to loss-of-section.

(2)   Excellent overall sensitivity to fracture even with relatively small end-separation.

(3)   Relatively minimal degradation of signal response in presence of steel duct.

(4)   Presence of reinforcement adjacent to flaw has only a slight influence on flaw signal (if adequate magnetization is provided).

(5)   Configurational artifacts (helical band on duct, thread-like protrusions on Type II bar, etc.) and structural features (rebars, bar-duct contact, etc.) have relatively minor negative influences on flaw detectability.

(6)   Probe-to-reinforcement spacing (both vertical and transverse) is a significant parameter influencing overall magnetic response.

(7)   Magnetizing field strength required is a function of steel section to be inspected and the distance from the magnet to the steel element under inspection.

Importantly, corrosion specimens typical of field conditions, are needed to further evaluate the magnetic field approach and to realistically establish design parameters. Such specimens must have sections containing varying degrees of corrosion sufficiently far from the specimen ends to be useful. Additional experiments should be conducted using longer specimen lengths with realistic corrosion to confirm the results obtained from shorter specimen. Furthermore, experimental investigations should be conducted to explore approaches for more effective inspection in the vicinity of reinforcement ends.

V. RECOMMENDATIONS

On the basis of the results from the literature assessment of 15 NDE methods and the preliminary experimental investigations conducted using the magnetic field method, it is recommended that the magnetic field method be selected for development of a conceptual design followed by detailed design and fabrication of a breadboard unit. The conceptual design, however, should include sufficient laboratory work to realistically specify the overall concept in terms of power requirements, weight, scanning and tracking features, etc. On this basis, it is crucial that Tasks D, E, and F be more closely inter-related than originally envisioned under the subject contract. While the overall estimated effort required in Tasks D, E, and F (combined) remains the same at this time, it is recommended that Task D be extended to 2-1/2 months total in parallel with Task F and that Task E extend to end of Task D. It is estimated that the funds required in Task D will be approximately $3,000 greater than originally allocated and that the funds required in Task F will be diminished by an equal amount. The design review would, of course, be scheduled at the conclusion of Task E.

APPENDIX A
DESCRIPTION OF METHODS

ACOUSTIC EMISSION

Acoustic emission is a measure of the energy released as a solid material undergoes plastic deformation or fracture. In particular, it has been shown that the sources of acoustic emission from metals may include microslip[4], twinning[5], martensitic phase transformations[6], micro-crack nucleation[7], and crack propagation[1]. Part of this energy is converted into elastic waves which propagate through the material and which can be detected by the appropriate transducers. The first basic studies were performed in the late 1940's and early 1950's in the United States and Germany.[8, 9] One of the earliest reported engineering applications of acoustic emission was in the surveillance of Polaris missile chambers at Aerojet General Corporation in 1964, during hydrostatic testing.[10]

The bulk of recent studies has approached the problem of stress wave emission from one or the other of two extremes of the deformation spectrum. At one end, Fisher and Lally[4] have been able to show conclusively that recognizable acoustic emission can be obtained from preyield dislocation bursts which generate a total plastic microstrain of only 1×10^{-7}. In somewhat related work, Frederick, et al.[11, 12] have succeeded in relating variations in acoustic emission characteristics of a variety of metals and alloys with the variations in their stacking fault energies, which strongly affect dislocation mobility. At the other end, investigations have been based upon the much higher amplitude acoustic waves generated by macroscopic fatigue cracks, $\geqslant 0.25$ in. (0.64 cm) in length in precracked specimens or in pressure vessels.[1-3, 13] The latter work has been particularly related to the problems peculiar to nuclear pressure vessel design.

Usually acoustic emission is limited to those flaw-detection problems where cracks exist and loading of the crack region sufficient to produce crack extension is possible. Such a procedure necessarily presumes knowledge of the prior load history on the structure and a practical means for loading a structure which does not in itself damage the structure. Analysis of acoustic emission data from a complex structure such as a bridge is particularly difficult because of the emission from sources within the structure other than fatigue cracks (welds, bolts, rivets, joints, etc.). Recent field experiments conducted under an FHWA contract showed that on a steel bridge there was considerable low-level noise over a period of several weeks and that the use of multiple transducers with logic circuits provided at best a marginal indication of response from fatigue cracks known to be in the region being monitored. Whether the fatigue cracks were actually extended during the monitoring period was not confirmed since no other independent measurements or observations were reported.

Harris investigated the use of acoustic emission monitoring for the cables on the lift span of the Dunbarton Bridge.[14] In this work it was necessary to apply a load to the cables by a transverse force to stimulate acoustic emission. No results were confirmed that would indicate the potential of this method for detecting reinforcing steel deterioration. However, it was indicated that the attenuation between strands of the cable was high with a value of 24 dB being measured for adjacent strands. In this case, the term strands is used for the individual wires which make up each cable. Also, measurements of attenuation along the cable ranged from 1 to 5 dB/inch.

Laboratory experiments conducted using acoustic emission monitoring of wire-rope cables has shown that at high sensitivity settings the emission provided "ample warning of impending strand failure". Also it was indicated[16] that a one-to-one correlation was obtained between the number of broken wires and the number of events observed at a particular gain setting. During this investigation a variety of experiments were conducted; however, the cables were only 5-1/2 inch (14 cm) long between connections and the cables were 1/4 inch (0.64 cm) diameter, 7 x 19 stainless steel and 6 x 19 improved plow steel with wire rope core. Extraneous sources of noise included the end attachments, rubbing at one cable on the other, etc. There was no indication of the method by which the transducers were mounted for sensing the acoustic emission.

The relatively recent work of Bickle[15] explored the application of acoustic emission methodology for civil engineering applications and does indicate interesting potential applications. In one series of experiments acoustic emission from concrete beams without rebars and with rebars was conducted. While there were indications that differences in the emission were observed, the effort was primarily exploratory and does not provide a basis for knowing repeatability, variation from specimen to specimen, etc. It was suggested that the method could possibly provide a method of sensing rebar debonding in concrete elements.

Personal communications from the Utah State Highway Department indicated that fracture of a reinforcing strand was reported when a loud cracking noise was heard by people in the vicinity of a bridge in which several reinforcing strands are known to be fractured.

In summary, the foregoing indicates promise of acoustic emission methods for providing information on condition of reinforcing strands. However, the relatively high attenuation of the strands and the concrete overlay,

numerous potential extraneous noise sources, the necessity of loading beams to stimulate emission, and the fact that the method would probably not provide an indication of strand deterioration until most of the section is lost places acoustic emission low in the assessment ranking. However, acoustic emission monitoring should not be completely discounted, since arrays of inexpensive transducers permanently affixed to each bridge element and transmitting data to central receivers for overall monitoring of the bridge structure, could possibly become economically and operationally practical in the future.

EDDY CURRENT

Eddy current methods depend on the electromagnetic induction of electric currents in metals by a coil carying alternating currents. These eddy currents cause the impedance of the exciting coil or any pickup coil in close proximity to change as a function of the material characteristics. A number of factors influence the eddy current characteristics, including magnitude and frequency of the exciting alternating current, electrical conductivity, magnetic permeability, configuration of the part, relative position of the coils and the part, and more importantly, the presence of discontinuities or inhomogeneities in the material. [18] Eddy current inspection techniques have been widely used, and the American Welding Society [19] describes the application, principles of operation, advantages, and precautions for using eddy currents to examine welds. Automated weld followers and inspection devices are described by Smith and McMasters [17] and Forster [20].

There are two general approaches to eddy current testing. [18, 21, 22] The first of these may be called the single-coil approach. Here, properties of the test article are inferred from the effects on relative amplitudes and phases of the voltage and current flowing in a wire coil (the "probe"). The second approach is to introduce a second sensor. Properties of the test article are inferred from the effects of eddy currents on the secondary sensor. In the above approaches, the sensors may be constructed for either "absolute" or "differential" sensing. Recently, a new eddy current instrument, referred to as the magnetic reaction analyzer [17], has been developed which utilizes a Hall effect element, instead of coil type probe, to sense the magnetic reaction fields. When an inspection is performed at a fixed test frequency, any material discontinuity that alters the conductivity or thickness (geometry) of the item under test will be reflected in the magnetic field sensed by the Hall probe. In practice a test frequency is chosen to penetrate the material to the desired inspection depth. The depth to which inspection can be performed may be adjusted, using a variable of test frequency, and when necessary

47

the excitation coil diameter. On large parts large-area excitation coils facilitate deep penetration and can tolerate what is considered unusually large lift-off variations (1/4 inch (0. 64 cm) in steel). However, it is doubtful that the method is useful for inspecting reinforcing steel with the amount of concrete coverage present on bridge structural beams. Other influencing factors such as the possible presence of magnetite in the concrete agregate could further reduce the useful sensitivity of the instrument.

In general, performance of an eddy current approach would probably be similar to that obtained from pachometer-type instruments[23, 24] used to locate reinforcing steel in bridge decks. Such instruments utilize low frequency magnetic field excitation coupled with a impedance-change measurement. Experience has shown such instruments to be influenced by the presence of magnetite; furthermore, the sensitivity of such instruments to loss of steel due to corrosion or fracture has been rated poor.

ELECTRICAL RESISTANCE OF CONCRETE

It has been shown that electrical resistivity measurements can be used as a nondestructive method for the determination of pavement thickness and depth to reinforcing steel.[26] The resistivity test, used for many years in subsurface exploration work throughout the country, involves a measurement of the resistance to the passage of an electric current through the material undergoing testing. The test is made by using four electrodes equally spaced in a line on the surface of the material being tested. The nature of the test is such that the effective depth (penetration of the applied current) is approximately equal to the electrode spacing for a particular setting of the electrodes.

Four small plastic tubes, plugged with stiff clay and filled with a saturated solution of copper sulphate into which a copper wire is inserted, are used in the test. The clay, with the help of a wetting of the concrete surface with ordinary tap water, provides for a suitable contact for the electrical circuits with the pavement surface. Most materials have a characteristic resistivity and the test procedure, which involves all material from the surface to the depth involved for a particular electrode setting, will produce resistivity values which will trend toward higher or lower resistivity values depending upon the fundamental resistivity of the second layer (the base course in the case of pavement thickness tests).

The presence of a conducting material such as steel reinforcing bars affects the resistivity test as the depth of test reaches the layer of steel reinforcement. Results have shown an average variation in the resistivity

measurements of depth to steel of 8. 6% (0. 35 inch, 0. 90 cm) for 110 tests.[26]
One factor likely affecting the measurement of depth to reinforcing steel is
the failure to always locate a test point directly above a steel bar.

Another aspect of resistivity measurements is based on the fact that
concrete, like soils, normally has a fairly high resistance; and one might
expect if low resistances were measured, it might be an indication that a
corrosive environment existed within the concrete[25]. Observations have
indicated that when the resistivity is above 60, 000 ohm-cm, no corrosion
occurred; for resistivities below 60, 000 ohm-cm, corrosion was detected--
generally, the lower the resistivity the greater the corrosion of the steel.
Because water content affects the resistivity, such measurements need to
be made while the spans were wet. Also, measurements must be made on
a grid pattern to be certain that local anodic areas are being monitored.
The resistivity of anodic areas was found to be always lower than that of
cathodic regions. It has been quoted[25] that--"It should be strongly em-
phasized that this resistance approach would need considerably more study
before it could be recommended for determining when serious corrosive
conditions existed in a bridge structure." Importantly, the resistivity
approach in concrete does not directly assess the condition of the steel but
only indicates that corrosive conditions are present.

ELECTRICAL RESISTANCE OF STEEL

If penetration of the concrete (and duct) in a prestressed member is
considered, a measurement of the resistance of the steel might be a viable
method for determining corrosion or fracture of the steel. Such an approach
has been proposed to determine continuity[27, 28] by making electrical
contact to the ends of reinforcing bars and measuring resistance of the bars
by forcing a known current through the bar and measuring the resulting
potential drop across the bar.

To establish contact with the steel bar, a hole was drilled through the
concrete beam and the duct after which a small spot, approximately 1/4 inch
(0. 64 cm) in diameter and 0. 030-0. 040 inch (0. 75-1. 0 mm) deep was drilled
on the surface of the bar for electrical contact. Bronze electrodes were
tightened against the bar by means of threaded devices. A DC current
(10 ampere) was forced through the bar and monitored with an ammeter.
If loose or faulty contact occurred, the current reading would fluctuate;
adjustment of electrodes was made until a constant current was obtained.
Bar resistance was determined by potentiometer measurement of the re-
sulting potential drop across the bar. Probably the greatest contributing
factor to variations in measured potential from bar to bar was differences

in contact between the electrode and the bar. The contact varied because of differences in hole location, variations in size and shape of the spots drilled on the bar, and variations in the angle that the hole was drilled.

Although it was initially reported[27] that the method showed some potential for detecting reduced sections in bars, laboratory investigation of the method showed that the spread in the data was so large as to make the method impractical for determination of reduced section dimensions in steel bars[28].

Resistance calculations using a simplified model tend to support the conclusion that the method is insensitive. For example, the presence of a 3 inch (7.6 cm)-long section with only 6% of the cross-section remaining in a 40 foot (12.2 m)-length of bar increases the total resistance only 10%; importantly, a 10% variation in resistance could result from dimensional tolerances alone on the bar. Similarly, a 50% reduction in bar cross-section over a two foot-length would only increase the resistance approximately 10%. The complicating factors of penetrating the concrete (and duct) and obtaining reliable contact as well as the influencing factors of contact between the bar and stirrups and/or duct and bar tolerances do not make the method appear promising.

ELECTROMAGNETIC INSPECTION METHODS

Electromagnetic techniques applicable to the problem of indirectly inspecting the integrity and load strength of prestressed concrete beams are of two basic types:

(1)   A high-resolution concrete-penetrating radar capable of indicating the physical status of steel rods and cables; and

(2)   Electromagnetic response to electrical nonlinearities associated with corrosion products resulting from deteriorated steel members.

The first method is a means for physically locating the sizing sections of the steel components of the beam, within practical limits of resolution, for the purpose of directly measuring changes in metallic cross-section and possibly detecting fracture conditions in the load carrying steel elements. The second method pertains specifically to the corrosion status of the steel elements and would utilize this information as an indirect empirical measure of the integrity of the reinforcing steel components of the beam.

50

In considering the applicability of these two techniques to the inspection of prestressed concrete beams, neither method is applicable to beams having tensioned steel rods or cables contained inside metallic conduit tubes. Electromagnetic energy appropriate for reflection or nonlinear response from a metallic structure cannot penetrate such conduit materials and, hence, the methods offer only a means for inspecting the physical status of the outer surface of the metal conduit, not the reinforcing steel member contained inside. If the conduit tubes used in the beam are non-metallic, both of the electromagnetic inspection methods mentioned above can readily penetrate such enclosures and may potentially function in the same manner as if the conduits were absent.

For the case where the tensioned steel members are enclosed in metallic conduits, a third electromagnetic inspection method is suggested, offering the capability of detecting voids in the grouting used to seal the enclosed reinforcing steel members. This method utilizes the fact that the steel rod or cable enclosed within a metallic tube forms an approximate coaxial structure crudely comparable with that of an electromagnetic coaxial transmission line. Thus, by applying time domain reflection testing concepts to such an imperfect transmission line the relatively large discontinuties resulting from air voids in the grouting injected to fill the annular space between the cable and the conduit may be detected and located in approximate position along the beam structure. Grouting voids are known to be highly susceptible locations for corrosion deterioration of prestressed concrete beams.

Electromagnetic Reflection Method

Electromagnetic reflection methods applicable to concrete beams are similar in concept to conventional radar ranging techniques with the exception that the atmospheric propagation medium is replaced by the concrete and the radar target sizes and detection ranges are reduced by several orders of magnitude. Electromagnetic wave propagation in concrete differs from propagation in air in that the propagation velocity is reduced by about 40-50% as a result of the higher permittivity of concrete and target range-dependent and frequency-dependent absorption losses occur because of the higher conductivity of concrete. The first of these differences is advantageous to small target detection and resolution because the wavelength of the target illuminating and reflected waves is reduced in direct proportion to the reduced propagation velocity. In regard to conductivity effects, electromagnetic absorption in dry concrete is relatively small, permitting useful penetration depths of several meters at wavelengths of a few centimeters (operating frequencies up to about 6 GHz). However, the presence of moisture and conducting mineral content in the concrete may reduce practical penetration depths to about one meter or less at wavelengths of a few centimeters.

51

Depth and size resolution of imbedded steel rods or cables is dependent upon the electromagnetic wavelength in the concrete. Thus, by reducing the operating wavelength (requiring increased operating frequency and signal bandwidth) the observed target reflection detail can be improved. This characteristic of the electromagnetic inspection method cannot be extended without limit, however, because of the frequency-dependent absorption effects in the concrete medium. That is, as the operating frequency is increased to obtain improvement in resolution, the useful penetration depth obtainable with a given operating source power is reduced and therefore the ability to adequately illuminate and detect the internally imbedded steel rod targets will ultimately impose the upper limit on operating frequency and resolution.

The radar cross-section of a cylindrical metallic reflector is dependent upon its diameter in terms of the illuminating wavelength. When the incident E-field is parallel to the axis of the cylinder, circulating currents are induced parallel to the axis and strong reflections occur. In this case, the backscatter cross-section per unit length is approximately equal to the illuminated half-circumference of the cylinder for cylinder diameters equal to the illuminating wavelength or larger. Because of the longitudinal circulation currents which are established on the cylinder with parallel E-field polarization, the reflections remain strong even when the cylinder diameter is small compared with the wavelength. When the incident E-field is perpendicular to the cylinder axis, the backscatter cross-section per unit length is approximately the same as that for parallel polarization orientation for diameters equal to or larger than the wavelength, but decreases rapidly (i.e., as inverse diameter cubed) for cylinder diameters smaller than the wavelength.

In regard to these radar cross-section characteristics, strong reflections may always be obtained from rods and cables which are thin compared with wavelength when the incident E-field is parallel to the rod axis; however, when the reflected signal strength is to be a measure of the effective cylinder diameter, the illuminating wavelength must always be equal to or less than the rod diameter being observed. Therefore, the polarization orientation of the incident wave is not important from a reflection cross-section viewpoint. This fact simplifies the practical scanning procedures required to inspect a concrete beam and will permit the radar transmitter and receiver antennas to be operated in a cross-polarized orientation to eliminate system self-interference feedover and avoid reflection responses from planar surfaces such as the air-concrete interface.

52

The electromagnetic inspection frequency required to yield a radar reflection whose strength is proportional to the diameter of a cylindrical rod target is

$$f = \frac{15k}{D_{cm}} \text{ GHz}$$

where: D_{cm} = rod diameter in centimeters;
            k = a numerical factor indicating the rod diameter in wavelengths where $k \gtrsim 1$.

Thus, for $k = 2$ the radar frequency must be 12 GHz for $D_{cm} = 2.5$ cm and 24 GHz for $D_{cm} = 1.25$ cm, corresponding to the diameters of typical steel reinforcing rods and cables, respectively. Penetration losses in concrete at these frequencies are estimated to be about 0.10 dB/cm indicating that a radar system having a total transmission loss capability of about 40 dB will be required to yield a useful reflection signal (20 dB signal-to-noise ratio) suitable for determining the relative diameters of typical reinforcing steel elements embedded 10 cm in concrete. Using small microwave antennas this performance capability will require a microwave source power of about 10 dBm.

The highest operating frequency and the total transmission loss capability estimated for the radar reflection method is considered to be attainable within the present state-of-the-art and can be achieved using either short pulse or wide bandwidth FM-CW radar system techniques. The accuracy of the method will depend largely upon the uniformity of the absorption losses within the concrete since variations of this parameter cannot be directly distinguished in the observed reflection signal strength. However, by means of signal analysis methods which evaluate the backscatter signal versus frequency, the variability caused by inhomogeneous absorption effects may potentially be processed out of the inspection data to yield information related only to the steel rod diameter and its embedded depth within the concrete beam.

Nonlinear Electromagnetic Response to Corrosion Deterioration

Electromagnetic reflections from conducting metallic targets may be interpreted as electromagnetic reradiation from the structure as a result of circulating currents induced in it by the incident wave. Conventional radar systems operate using a receiver tuned to the frequency of the transmitted signal since the predominant currents induced in a metallic target have the same frequency as the incident wave. However, if the metallic target has

53

nonlinear electrical properties, as may be caused by corrosion oxides on its surface, then the induced circulating currents flowing through the non-linear conduction paths will be distorted resulting in the generation of harmonics and intermodulation products. These new circulating current components, produced as a result of corrosion effects, will also reradiate from the structure and may be detected if the receiver is properly tuned for their reception.

Since the oxide coatings causing the nonlinearities will not necessarily rectify the induced currents, the bilateral nonlinear conduction effects will tend to generate odd-order distortion products. Thus, for an oxided metallic target illuminated by an electromagnetic wave, a small portion of the trans-mitter-induced energy will be converted to third- and higher odd-order harmonics and related odd-order sum and difference intermodulation products.

When this nonlinear response inspection technique is applied only to indicate the presence of corrosion, ie., the embedded depth and size resolution of the steel reinforcing members are not measured, the electromagnetic system need not operate at the high microwave frequencies required for the reflection inspection method described earlier. Instead the nonlinear response method can utilize CW electromagnetic transmission rather than pulsed or FM operation. The use of a continuously transmitting system can be most effec-tively implemented using a two-frequency system whereby the corrosion-related nonlinear distortion frequency is an odd-order intermodulation product not related to any of the residual harmonics which may be emitted directly by the CW source. Also, because a lower operating frequency will be employed, the incident wave would be linearly polarized parallel to the axis of the steel rods being inspected.

The practical feasibility and accuracy of this nonlinear response method for assessing corrosion status of steel reinforcing rods and cables is not predictable on the basis of presently available information. The method is basically an impirical measure of corrosion effects which may vary with different materials and environmental conditions. Laboratory tests have been performed in the past to confirm the existence of nonlinear reradiation as a result of natural corrosion oxides present on metal structures. Further, this effect is often a noticeable form of radio communication interference aboard ships and other locations where transmitters and receivers may be operating simultaneously on appropriately different frequencies.

Successful implementation of this inspection method will require that the transmitting source be thoroughly free of distortion frequency products intended to be observed from the nonlinear effects of the corroded steel elements

and that the receiver have exceptionally good linearity so that interfering distortion frequency products are not generated in the receiver as a result of the strongly reflected fundamental signal. Additionally, no nonlinear metallic structures or electrical connections should be associated with the source or receiving antennas or extraneously located in the same vicinity as the inspection system.

Time Domain Reflection Inspection

Time domain reflectometry, as conventionally applied to electromagnetic transmission lines, may be a practical means of locating grouting voids and complete breaks in steel rods and cables contained in metallic conduit enclosures. The approximate coaxial structure of this type of concrete beam reinforcement configuration may potentially support the propagation of guided electromagnetic energy in the form of TEM waves. When an electromagnetic impulse is introduced at a given location on a transmission line structure of this type, distinctive reflections are produced by any variations in the characteristic impedance of the line. With a general knowledge of the conduit tubing internal diameter and the diameter of the steel reinforcing rod or cable which it contains and a typical value of the relative dielectric constant of the grouting material, the nominal impedance and propagation velocity of the coaxial structure can be determined. Analysis of the amplitudes, polarities and time delays associated with the observed impulsive reflections will yield sufficient information to determine the presence of air voids in the grouting, the length of such voids, and the approximate positions of the voids along the concrete beam.

While this inspection technique cannot reveal direct information on the physical status of the load-carrying steel members of concrete beams, the detection and size assessment of grouting voids as described above may yield useful data which could guide the application of other more specific inspection processes. Additionally, since the time domain reflection technique may be applicable to cable and conduit structures containing uncured grouting materials, this measurement method may be well suited for use in monitoring the initial grouting process to ensure that no voids remain in the reinforcement conduits of beams used in newly constructed highways and bridges.

Application of this method will require separate electrical contact with the conduit tubing and the enclosed steel rod or cable. Access to these elements may be gained by an appropriate drilling process capable of intercepting the embedded conduit and penetrating the conduit to permit electrical contact with the internal load-carrying steel member.

In an article[42] on the repair of spalling bridge decks, John Kliethermes states... "With a high degree of confidence, it can now be said that most spalling results from the expansive forces associated with corrosion. It can also be said that the predominant cause of corrosion is the salt that is absorbed by the concrete" and that "the corrosion of reinforcing steel is the result of an electrochemical process whereby corrosion cells are created by variable amounts of chloride, oxygen and moisture along the length of the reinforcement. These cells produce a flow of electric current between two half-cells, the anode and the cathode. The corrosion cell may be minute with the anode and cathode microscopically spaced, such as seen when steel corrodes in air, or they may be spaced several feet, as frequently found in bridge decks."

The electrical potential difference between the anodic half-cell and cathodic half-cell may be measured via a voltmeter. However, the difference in measured voltage between the two unstable half-cells is not too meaningful because the electrical activity will change as the electrolyte changes. Therefore, in order to compare readings over a period of time, a standard reference half-cell that retains a constant electrical potential must be used. The reference most commonly used is a copper/copper sulfate half-cell. It is comprised of a plastic tube with a porous plug inserted in one end, a pure copper rod, and a solution of saturated copper sulfate. The plastic tube is filled with the copper sulfate solution, and then the copper rod is inserted. The copper rod is stable in a copper sulfate solution, and therefore, its potential remains constant regardless of changing conditions. To compare the electrical potential of the reference half-cell to that of steel embedded in concrete, the (half-cell) copper electrode and steel must be connected. This is usually accomplished by making a positive electrical connection to the top mat of reinforcing steel and by providing a moisture junction through the concrete between the copper rod and the reinforcing steel at the point where the potential value is to be determined. A voltmeter is placed in the completed electrical circuit to measure the electrical potential difference.

The values of potential difference measured can vary with variations in conductivity of the concrete and the means for making contact to the steel[44]. Even wider variations have been observed when measurements are made without direct electrical connection to the steel[43]. However, the same potential gradient contours (but not potential levels) have been noted regardless of whether or not direct connection was made to the steel[43].

The best measure of half-cell potential is via direct connection
to the steel and there is generally good agreement that a potential difference
of -0.35 volt or greater (more negative) is an indication of corrosive
activity. In practice, however, potentials have been noted to fluctuate
between active and passive levels over a period of weeks[44]. It is,
therefore, difficult to ascertain the condition of reinforcing steel by a
single potential reading; in any case, the method is not quantitative unless
a potential history is maintained and a rate of corrosion is predicated.
Application of the half-cell potential method to bridge structural members
vs. decks also involves other implementation considerations such as potential
probe orientation difficulties, adequate wetting of concrete members,
achieving electrical connection to steel, etc. The method will not
distinguish between corrosive environments surrounding a duct vs. the
reinforcing steel in the duct.

HOLOGRAPHY

Optical interference holography consists essentially of illuminating an
object to be examined with a portion of the beam from a coherent optical
radiation source (laser) causing the scattered beam from the object to
interfere with a reference beam obtained from the same source and
recording the resulting interference pattern by means of a photographic
emulsion which is subsequently developed. The resulting negative is
a diffraction pattern, and, when it is reilluminated with a suitable coherent
light source, a three-dimensional "like" image of the original object is
reconstructed. If the reconstructed image is superimposed on the original
object, it is then possible to observe interference fringes in those regions
where small displacements exist on the surface of the object which did not
exist at the time the hologram was made. This two-beam method has been
credited to Leith and Upatnieks[29]. In many cases, a second approach is
used which consists of a double or possible multiple exposure of the
emulsion to the irradiation scattered from an object when the object is
successively photographed in one position and then in a slightly distorted
position (as that caused by an applied mechanical load or a temperature
change). Reillumination of this multiple exposure then reconstructs the
image with interference fringes appearing which correspond to the
relative displacement of the object's surface for the two exposures.
Optical interference holography has been used to detect flaws in many
types of bonded structures[30]. These approaches have been used also
to study the deformation of components under load[31], as well as fatigue,
fatigue cracking, and stress-corrosion cracking[32-34, 35].

Regardless of application, the method works by comparisons of
surfaces in two different states of stress or load. Because it is a surface
effect, holography cannot directly be used to locate corroded or fractured
tensioning members imbedded in prestressed concrete. Indirectly, it may

be used to identify areas on the exposed surface of the concrete which contain high or anomalous stress distributions[40]. Areas so defined may reflect the presence of a broken tensioning member beneath the surface, provided the concrete structure in question can be loaded sufficiently to cause a change in the surface stress distribution.

In practice, the method is at best difficult to instrument in the field. The bridge environment dictates the use of extremely high power laser pulses of exceedingly short duration for creation of the hologram. Such lasers are both expensive and bulky in addition to being somewhat of a safety hazard. Also, the interference fringe pattern obtained will be very difficult to interpret, as it will reflect the total change in stress distribution, containing components attributable to mounting geometries and loading in addition to the components attributable to the steel tensioning members.

MAGNETIC FIELD

The common principle of magnetic field methods is the detection of magnetic field anomalies in a relatively uniform magnetic field where these anomalies are caused by material inhomogeneities such as voids, inclusions, cracks, chemical desegregations, etc. Two broad categories of problems exist. In one, a relatively uniform magnetic flux is established in a region essentially filled with a ferromagnetic material, the region is then scanned with a sensitive, high resolution magnetometer (probe) to detect local anomalies caused by varying permeability produced by voids, discontinuities and locally stressed regions. In the other, a relatively uniform magnetic field is established in an extended volume containing only a small or local region of ferromagnetic material, such as magnetometer surveys for submarines. In the reinforcing strand deterioration or fracture problem, the steel is only a fraction of the volume being examined and yet it is desirable to detect anomalies caused by local flaws in the steel. Accordingly, it is a case intermediate between the preceeding cases.

Several instruments[62], for example Pachometer, Covermeter, Ferrometer, Pribor IZS and FEMETR, operating on magnetic principles, have been developed for measuring either the distance of reinforcing bar to the surface of concrete when the diameter of the reinforcing bar is known, or to measure the diameter of a bar when the thickness of the concrete covering the bar is known. FHWA has made rather extensive evaluations of the Pachometer principle and has concluded that the accuracy "and reliability of the system proved excellent"[24]. The instrument, of course, is designed for making measurements of concrete cover over reinforcing bars and in discussions with one of the FHWA investigators, it was indicated that the method probably was incapable of detecting loss of section from deterioration. One of the other instruments (not identified) was investigated[63] and it was indicated that while the instrument could measure cover and also obtain a

reasonable measurement of rod diameter when a single rod was involved, proximity of adjacent rods in a typical deck or beam configuration produced significant errors. For example, for a 1-3/8 inch (3.5 cm) rod diameter with a 2 inch (5 cm) concrete cover, the indicated rod size was 9/16 inch (1.4 cm), and for a 1-3/8 inch (3.5 cm) diameter rod with 2-1/2 inch (6.4 cm) coverage, the indicated size was 5/8 inch (1.6 cm) diameter. Accordingly, it is judged that this particular magnetic field instrument operating from the basis of "comparing the fixed electromagnetic characteristics of a reference transformer with the variable ones of a measured transformer (probe)" offers little promise for detecting reinforcement steel deterioration.

As indicated earlier, the present problem is generically between that of a region completely filled with ferromagnetic material and of a region with only a small fraction of magnetic material. Since extensive prior investigations[57-61], both experimental and analytical, demonstrated excellent sensitivity and resolution of magnetic perturbation for the detection of minute flaws and fatigue cracks, it is possible that the magnetic field methods when adapted for the reinforcing steel deterioration problem can provide good detection capability. The unknown influence of distance between the magnetizing source and the material to be magnetized, limited fill factor of the steel occupying the region being magnetized, and complexities of the steel configuration would require extensive investigation before capabilities and limitations and advantages and disadvantages of the method could established.

MOSSBAUER EFFECT

The possibility of using the Mossbauer effect to assess the state of corrosion of steel has been proposed. The Mossbauer effect[36] is the resonant absorption of gamma rays by atomic nuclei. The energy (or wavelength) of nuclear gamma rays is extremely well defined. Very small effects upon nuclear energy levels, such as those produced by the magnetic and electric fields arising from orbital and conduction electrons, can shift the nuclear energy levels by an amount which destroys resonant absorption. This can be counteracted by shifting the energy of the incident gamma rays through the Doppler effect produced by putting the gamma ray source in motion. The resonant absorption rate as a function of source velocity produces a Mossbauer "spectrum", the features of which may be interpreted in terms of changes in the magnetic and electric field environment of the target nuclei. Because the local electric field environment of iron nuclei in corrosion products differ from the environment in undamaged steel, it is, in principle at least, feasible to employ the Mossbauer effect in measurements of corrosion. The equipment required is basically a radioactive source of gamma rays (Co^{57} in this case), a servo-controlled velocity transducer to move the source, a gamma ray detector, and a multichannel pulse height analyzer. No field-worthy equipment as such appears to be available, and this approach to fatigue crack detection will not be considered for further evaluation in the present program.

59

RADIOGRAPHY

Radiography is based upon the attenuation of a beam of penetrating radiation by a specimen[22]. Discontinuities in an otherwise homogeneous specimen are revealed by the change in attenuation which they produce. Film radiography uses photographic films to record a "shadowgram" or radiograph of the transmitted radiation. The detectability of a flaw in an otherwise homogeneous specimen depends upon the differential in film density (i.e., contrast) which it produces. The geometrical size of the flaw (as projected on the radiograph) is also important since low contrast images of small size are more difficult to discern by visual inspection than larger images of comparable contrast. The most important parameters influencing the detectability of the image of the flaw on the final radiograph are:

(1)   Beam quality, which in turn depends upon

   (a)   The degree of collimation of the incident radiation
   (b)   The absence of multiple scattering (diffusion) of radiation in the specimen

(2)   Exposure, which depends upon the product of

   (a)   Radiation source strength
   (b)   Duration of exposure (sec.)

(3)   Effective source size (which contributes to geometrical unsharpness of the image)

(4)   Film-to-focus distance

(5)   Film-to-specimen distance

(6)   Film characteristic curve and speed

(7)   Presence and type of image intensifying screens (lead foil or fluourescent powder)

(8)   Physical stability of source, specimens, and film cassette during exposure

(9)   Uniformity of film development

(10)   Visual acuity and expertness of film interpreter.

In the usual industrial or field environment, a radiographic sensitivity of 2 percent is ordinarily considered good. By convention, "2-percent sensitivity" means that, if a penetrameter (made of the same material as the specimen) whose thickness (T) is 2 percent that of the specimen and which contains a circular hole whose diameter is twice the thickness of the penetrameter (2T), is placed in contact with specimen (on the source side) and the assembly is radiographed for a fixed set of conditions, the image of the 2T-hole in the penetrameter can be unambiguously discerned by a qualified radiograph reader. Under carefully optimized conditions, 0.7-percent radiography can be achieved; this means the image of a 1T-hole in a penetrameter, the thickness of which is 1 percent of the specimen thickness, can be discerned[37].

In terms of applicability to the inspection of bridges which are in unrestricted service, the following general observations may be made:

(1)   Normal vibration would require the use of fast-pulse X-ray sources. These are available but may have inadequate total exposure for the thicknesses of concrete required.

(2)   Thicknesses of concrete of interest would probably require X-ray units capable of 600 KV and upward;

(3)   A clearance of 2 to 3 ft between the X-ray source and the area to be radiographed would be necessary;

(4)   Skills required are high;

(5)   The health hazard associated with radiation requires a considerable safety program.

Currently available nonfilm radiographic methods (X-ray, T.V., etc.) have resolution inferior to film. Digital image enhancement, though greatly increasing crack detectability, is not yet economic for large-scale application.

While some work on the use of gamma radiography in the inspection of reinforced concrete has been reported,[41] personal communications have indicated the cost to be prohibitive for bridge inspection and the expected resolution to be poor. The decision to use or not use radiography should be based mainly on there being no viable alternative method.

STRAIN GAGE

The vibrating wire principle for the measurement of strain in concrete provides a means of making long term studies of dams or pressure vessels since they exhibit good stability over a number of years[39]. It has been

61

reported that long term measurements of strain could be made to better than 1 x 10⁻⁶. The principle of the vibrating wire gage relies on the mesurement of the natural frequency of a wire under tension. Any change of tension causes a corresponding change of frequency. By considering the gage length, properties of the wire and the design of the gage, a relationship between strain and frequency can be expressed.

The gage generally consists of the wire, end clamps, a spacer tube enclosing the wire, and an electromagnet for plucking and measuring the signal from the wire. A gage length of at least four times the largest aggregate size is necessary to avoid excessive errors. The design of the gage should be such that the strain field around it is not upset by the presence of the gage. Ideally, the stiffness of the gage should match that of the concrete it replaces. By the choice of a suitable material for the tube, its diameter and thickness, a particular stiffness can be obtained. It has been demonstrated that the gage factor, for vibrating wire gages, is affected when cast in concrete. Accordingly, the practice has been adopted to encapsulate all gages in concrete before use to offer mechanical protection and to calibrate a sample of the production lot. The gage factors thus obtained are then used for all gages in the production lot. If the coefficient of expansion for the gage is different from that of the concrete in which it is cast, a temperature correction will be required.

The frequency of the vibrating wire may be measured by balancing the signal with a second signal of known frequency or by using a standard frequency meter. In most cases, to improve the accuracy, the frequency is obtained by timing a known number of cycles-- usually 100.

In the pressure vessel applications, several hundred vibrating wire strain gages have been used[39]. While such an array of strain gages in a bridge might very well be used to monitor the serviceability of the bridge, it is difficult to see how this method could be retrofitted to existing bridges.

THERMAL

Thermal methods, in general, as applied to the detection of defects fundamentally consist of establishing a heat-flow or thermal gradient in the region of the material being examined and then measuring the local temperature disturbances caused by the presence of a flaw. Implementation of the method involves two general areas: (1) establishing a heat flow in the part and (2) detecting local temperature differences.

Inspection of reinforced concrete would necessitate the use of an active test system in which the component under test must be raised or lowered in temperature with respect to its surroundings to establish a heat flow in the region under inspection. To establish a favorable heat flow pattern, it is often necessary to bring the part into thermal contact with an appropriate arrangement of thermal sources, heat sinks, conductors, and insulators.

The second area to be considered in thermal testing is the sensing or measuring of the local temperature differences which indicate the presence of a flaw. Both contact and non-contact methods are available for such temperature sensing. In recent years, the greatest emphasis has been on the use of non-contacting methods (predominantly infrared radiation techniques) for temperature measurement because contact methods, in themselves, alter the heat flow at the part surface under test, and they do not readily lend themselves to automation. To obtain good sensitivity with the infrared method, however, a uniform surface emissivity is required, and it is, therefore, extremely important to maintain the test surface uniformly clean and free of contaminating liquids or solids.

In the case of reinforced concrete inspection, the thermal diffusivity of the concrete cover and inconsistencies in the thermal conductivity of the bond between reinforcing cables and the concrete would effectively destroy the sensitivity and resolution of thermal techniques. For a post-tensioned beam the presence of a duct (especially metal) around the reinforcing rod would cause further diffusion of the thermal energy, thus diminishing the sensitivity even further. Even in the case of clean exposed metal surfaces, the sensitivity of thermal methods has been limited to the detection of larger flaws[38]. Thermal techniques have generally been found to have relatively poor resolution when compared with other techniques even when applied on specimens having thermally "good" surfaces. The technique generally involves the use of complex and expensive instrumentation.

ULTRASONICS

Ultrasonics consists of using high-frequency, mechanical vibrations, introduced into a part by means of a transducer, to observe the interaction of this acoustical energy with discontinuities in the part material. A number of different techniques such as through-transmission, resonance, pulse-echo, etc., are used for specific applications, with the pulse-echo technique being the most widely used. In ultrasonics, an acoustic pulse is launched into the sample and propagates as a wave, which, depending on the method of excitation, may vibrate the material in various modes. Modes commonly used are longitudinal (compressional), shear (transverse), plate (Lamb) and surface (Rayleigh). The pulse travels through the material at its mode's characteristic speed of sound; upon encountering a reflecting interface or discontinuity, the pulse is reflected and eventually travels back to the initiating transducer or another appropriately placed transducer. The distance from the transducer to the flaw can be estimated by using the transit time of the acoustic energy and the characteristic speed of sound, and the received pulse or signal amplitude provides a qualitative indication of the relative size of the reflecting area.

Propagation of ultrasonic energy through any given material is a function of the grain size of the material and the wavelength of the acoustic energy. Frequencies on the order of several megacycles are commonly used in steel, but these frequencies will not propagate any appreciable distance through concrete. Ultrasonic inspection of concrete, therefore, is performed at much lower frequencies, in the range of a few tens of kilocycles[53]. These frequencies will propagate adequately through concrete (and steel), but their wavelengths are so long in steel that the inspection resolution obtained is poor.

Ultrasonic pulse velocity measurements in concrete have been used to assess its quality,[53, 54, 55] but the experiments have shown that it is virtually impossible to detect even the presence of the steel reinforcing members,[56] much less extract any information regarding the condition of the steel.

On the other hand, there is a possibility that ultrasonic scattering may be used to estimate the degree of corrosion present on reinforcing members, provided access to both sides of the concrete is possible. The method essentially would treat the steel reinforcing rod as a cylindrical lens whose focal length is a function of the diameter of the rod and the ratio of the acoustic velocities of the steel and the concrete. An ultrasonic wave passing across the rod has some of its energy deflected off axis by the lens effect. The presence of corrosion products, probably possessing an acoustic velocity differing from that of either steel or concrete, would act to change the focal length of the lens. These effects could be monitored by measurement of the ultrasonic energy distributions on the side of the concrete member opposite the transmitting transducer. The presence of more than one steel reinforcing strand would, of course, complicate the measurements.

APPENDIX B

(Worksheets have been omitted for brevity - see Interim
Report for Method Rating Worksheets)

APPENDIX C

REFERENCES

1. Dunegan, H. L., Harris, D. O., and Tatro, C. A., "Fracture Analysis by Use of Acoustic Emission," Engineering Fracture Mechanics, I, p. 105, 1968.

2. Dunegan, H. L., and Harris, D. O., "Acoustic Emission-a New Nondestructive Testing Tool," Ultrasonics, 7, p. 160, 1969.

3. Harris, D. O., Dunegan, H. L., and Tetelman, A. S., "Prediction of Fatigue Lifetime by Combined Fracture Mechanics and Acoustic Emission Techniques," Dunegan Research Corp. Technical Bulletin DRC-105.

4. Fisher, R. M., and Lally, J. S., "Microplasticity Detected by an Acoustic Technique", Canadian Journal Physics, 45, p. 1147, 1967.

5. Frederick, J. R., "Use of Acoustic Emission in Nondestructive Testing", U. S. Air Force, Contract No. F33615-68-C-1703 ARPA Order No. 1244, May 1969.

6. Liptai, R. G., Dunegan, H. L., and Tatro, C. A., "Acoustic Emissions Generated During Phase Transformations in Metals and Alloys", International Journal Nondestructive Testing, 1, p. 213, 1969.

7. Kerawala, J. N., "An Investigation of the Behavior of the Acoustic Emission from Commercial Ferrous Materials", Phd. D. Thesis, University of Michigan, 1965.

8. Mason, W. P., McSkimin, J. H., and Shockely, W., "Ultrasonic Observation of Twinning in Tin", Physics Reviews, 73, No. 10, 1948.

9. Schofield, B. H., Bareiss, R. A., and Kyrala, A. A., "WADC Technical Report 58-194", Astia Document No. AD 1555674, 1958.

10. Green, A. T., Steele, R. K., and Lockman, C. S., "Acoustic Verification of Structural Integrity of Polaris Chambers", Society, Plastics Engineers, Atlantic City, N. J., January 1964.

11. Frederick, J. R., "Acoustic Emission as a Technique for Nondestructive Testing", Materials Evaluation, p. 43, February 1970.

12. Agarwal, A. B. L., Frederick, J. R., and Felbeck, D. K., "Detection of Plastic Microstrain in Aluminum by Acoustic Emission", Metallurgical Transactions, 1, p. 1069, 1960.

13.   Crimmins, P. P., "Correlation of Stress-Wave Emission Characteristics with Fracture in Aluminum Alloys", George C. Marshall Flight Center, NASA Contract NAS 8-21405, June 1969.

14.   Harris, D. O., "Acoustic Emission Monitoring of Lift Span Cables on Dumbarton Bridge", Dept. of Public Works, Division of Bay Toll Crossings, State of California, Dec. 1972.

15.   Bickle, L. W., and Smiel, A. J., "Applicability of Acoustic-Emission Techniques to Civil Engineering Research", New Mexico Univ., Albuquerque, Eric H. Wang Civil Engineering Research Facility Air Force Weapons Lab., Kirtland AFB, New Mexico, 102p., June 1975.

16.   Harris, D. O., and Dunegan, H. L., "Acoustic Emission Testing of Wire Rope", Materials Evaluation, pp. 1-6, January 1974.

17.   Smith, G. H., and McMaster, R. C., "Inspection and Tracking of Welds Using the New Magnetic Reaction Analyzer", Proceedings of the 5th International Conference on Nondestructive Testing, The Queen's Printer, Ottawa, pp. 108-113, 1969.

18.   Pasley, R. L., and Birdwell, J. A., "Eddy Current Testing", Nondestructive Testing-A Survey, Chapter 5, NASA-SP-5113, C. Gerald Gardner, Technical Editor, 1973.

19.   Anon., Welding Inspection, American Welding Society, New York, p. 223, 1968.

20.   Forster, F., Proceedings of 5th Conference on Nondestructive Testing, The Queen's Printer, Ottawa, p. 209, 1969.

21.   Hochschild, R., Electromagnetic Methods of Testing Metals, Progress in Nondestructive Testing, Vol. 1, The MacMillan Company, New York, pp. 59-109, 1959.

22.   McMaster, R. C., Nondestructive Testing Handbook, The Ronald Press Company, New York, 1963.

23.   Anon., "R" Meter - Technical Information, James Electronics, Inc.

24.   Moore, K. R., "Rapid Measurement of Concrete Cover on Bridge Decks", Public Roads, Vol. 39, No. 2, Sept. 1975.

25. Moore, D. G., Klodt, D. T., and Hensen, R. J., "Protection of Steel in Prestressed Concrete Bridges", Research sponsored by American Assoc. of State Highway Officials in cooperation with the Bureau of Public Roads; Highway Research Board, Div. of Engineering, National Research Council, National Academy of Sciences-National Academy of Engineering, 1970.

26. Moore, R. W., "Electrical Resistivity Instruments for Measuring Thickness and Other Characteristics of Pavement Layers", Federal Highway Administration, Washington, D. C. Materials Div., p. 59, August 1972. Prepared by Soils and Exploratory Techniques Group

27. Gould, R. W., Hummel, R. E., and Lewis, R. O., "Electrical Resistance as a Measure of Reinforcing Bar Continuity Sunshine Skyway Bridge", Progress Report 1, Dept. of Materials Science and Engineering, University of Florida, Gainesville, Florida 32611, June 29, 1973.

28. Gould, R. W., "Detection and Prevention of Re-bar Failure in Concrete Structure", Final Report, College of Engineering Materials Science and Engineering, University of Florida, Gainesville, Florida 32611, January 30, 1975.

29. Leith, E. N., and Upatnicks, J., "Reconstructed Wavefronts and Communication Theory", Journal of the Optical Society of America, Vol. 52, No. 10, 1962.

30. Harris, W. J., and Clauss, F. J., "Inspecting Bonded Structures by Laser Holography", Metal Progress, Vol. 100, No. 2, August 1971.

31. Alwang, W. G., Burr, R. and Cavanaugh, L. A., "Holographic Measurement of Compressor Blade, Turbine Blade and Airframe Panel Vibration Distribution", Society of Automotive Engineers, International Automotive Engineering Congress, Detroit, Michigan, January 1969.

32. Leith, E. N., and Vest, C. M., "Investigation of Holographic Testing Techniques,", Contract No. DAAG46-69-C-0017, April, 1970.

33. Marom, E., and Mueller, R. K., "Nondestructive Early Fatigue Detection", Proceedings of 6th Symposium on Nondestructive Evaluation of Components and Materials, 1967.

34. Marom, E., "Electro-optical Noncontacting Techniques for Sonic Fatigue Tests", AFFDL-RE-69-95, December 1969.

35. Friesem, A. A., and Vest, C. M., "Detection of Microfractures by Holographic Interferometry", Applied Optics, Vol. 8, No. 6, June 1969.

36. Wertheim, G. K., Mossbauer Effect: Principles and Applications, Academic Press, New York, 1964.

37. Anon., "Making a Radiograph", Radiography, Vol. IV, NASA CR-61215 (N68-28787).

38. Kubiak, E. J., Johnson, B. A., and Taylor, R. C., "Dynamic Infrared Detection of Fatigue Cracks (Discussion)", Proceedings 5th International Conference on Nondestructive Testing, 1967.

39. Hornby, I. W. and Notltingk, B. E., "Application of the Vibrating-Wire Principle for the Measurement of Strain in Concrete", Cent. Electr. Res. Lab., Leatherhead, Surrey, England, Experimental Mechanics, Vol. 14, No. 3, pp. 123-128, March 1974.

40. Anon., "Holographic Detection of Cracks in Concrete", A. Luxmoore, Univ. Coll, Swansea, Glamorgan, Wales; Non-Destructive Testing (London), Vol. 6, No. 5, pp. 258-263, Oct. 1973.

41. Tassios, T. and Oeconomou, C., "Contribution to the Gamma Radiography of Reinforced Concrete Structures", National Tech Univ., Athens, Greece, Material Constr., Material Struct., Vol. 4, No. 20, pp. 101-106, Mar-Apr 1971.

42. Kliethermes, J. C., "Repair of Spalling Bridge Decks", Highway Research Record, No. 400, pp. 83-92, 1972.

43. Stratfull, R. F., "Half Cell Potentials and the Corrosion of Steel in Concrete", California State Div. of Highways, Materials and Research Dept., 32p. Report No.: CA-HY-MR-5116-7-72-42, M/R-635116-7, Prepared in Cooperation with Federal Highway Administration, Washington, D. C., November 1972.

44. Clear, K. C. and Hay, R. E., "Time-to-Corrosion of Reinforcing Steel in Concrete Slabs", Vol. 1 Effect of Mix Design and Construction Parameters, Federal Highway Admin., Washington, D. C. 105p. April 1973.

70

45.   Lewis, D.A., and Copenhagen, W.J., "The Corrosion of Reinforcing Steel in Concrete in Marine Atmospheres", The South African Industrial Chemist, Oct. 1957.

46.   Rehm, G., "Corrosion of Prestressing Steel," General Report submitted at FIP Symposium on Steel for Prestressing, Madrid 1968.

47.   Tremper, B., Beaton, J.L., and Stratfull, R.F., "Corrosion of Reinforcing Steel and Repair of Concrete in a Marine Environment", Highway Research Board Bulletin 182, 1957.

48.   Spellman, D.L. and Stratfull, R.F., "Laboratory Corrosion Test of Steel in Concrete", California State Div. of Highways, Materials and Research Dept., Report No.: M/R-635116-3, 44p., Sept. 1968.

49.   Roshore, E.C., "Durability and Behavior of Prestressed Concrete Beams", Technical Report No. 6-570, Report 3, Laboratory Tests of Weathered Pretensioned Beams., Army Engineer Waterways Experiment Station, Vicksburg, Miss., Oct. 1976.

50.   Snape, E., "Roles of Composition and Microstructure in Sulfide Cracking of Steel", NACE Conference, Cleveland, Ohio, 1968.

51.   Spellman, D.L. and Stratfull, R.F., "Concrete Variables and Corrosion Testing", California State Div. of Highways, Materials and Research Dept., Report No.: M/R-HRB-635116-6, 50p. Prepared in cooperation with Federal Highway Admin., Washington, D.C., January 1972.

52.   Spellman, D.L., and Stratfull, R.F., "Chlorides and Bridge Deck Deterioration", Highway Research Record No. 328, 1970.

53.   Bellini, P.X., "Sonic Testing of Reinforced Concrete", Ohio Dept. of Transportation, Columbus, Youngstown State Univ., Ohio, Dept. of Civil Engineering, Federal Highway Admin., Washington, D.C., Report No.: OHIO-DOT-01-74, 130p., December 1973.

54.   Anon., "Nondestructive Testing of Concrete", No. 378, 7 reports, Highway Research Board, Div. of Engineering, National Research Council, National Academy of Sciences - National Academy of Engineering, Washington, D.C., 1972.

55.   Moore, W. M., "Detection of Bridge Deck Deterioration", Summary Report of Research Report No. 130-9, Study 2-18-68-130, Dec. 1972.

56.   Scholar, C. F., "Performance of Ultrasonic Equipment for Pavement Thickness Measurement and Other Highway Applications", Final Report, July 1970.

57.   Barton, J. R., and Kusenberger, F. N., "Magnetic Perturbation Inspection to Improve Reliability of High Strength Steel Components", ASME Design Engineering Conference 69-DE-58, New York, May 1969.

58.   Barton, J. R., and Kusenberger, F. N., "Fatigue Damage Detection", Metal Fatigue Damage, Mechanism, Detection, Avoidance and Repair, STP495, pp. 193-201; 210-212, American Society for Testing and Materials, 1971.

59.   Kusenberger, F. N., "Low Cycle Fatigue Damage Detection in Model Pressure Vessel", Proceedings of 5th Annual Symposium on Nondestructive Evaluation of Aerospace and Weapons Systems Components and Materials, 1965.

60.   Kusenberger, F. N., and Barton, J. R., "Development of a Prototype Equipment for the Automatic Detection of Fatigue Damage in Helicopter Transmission Gears", Proceedings of 7th Symposium on Nondestructive Evaluation of Components and Materials in Aerospace, Weapons Systems and Nuclear Applications, April 1969.

61.   Kusenberger, F. N., Lankford, J., Jr., Francis, P. H., and Barton, J. R., "Nondestructive Evaluation of Metal Fatigue," AFOSR Scientific Report AFOSR-TR-71-1965, April 1971.

62.   Brunarski, L. and Karminski, A., "The Magnetic Method for Measuring the Diameter and the Depth of Reinforcement Below the Surface of Concrete", published in Proc. 7th Int. Conf. on NDT; Warsaw, Poland, Polish Soc. Mech. Eng.; Vol. 1, D-28, 4 pp. June 1973.

63.   Saucier, K. L., "Evaluation of an Instrument to Detect Presence, Size and Depth of Steel Embedded in Portland-Cement Concrete", Army Engineer Waterways Experiment Station, Vicksburg, Miss, Report for 1964-1965.

APPENDIX II

FCP RESEARCH REVIEW CONFERENCES, PROGRAM REVIEWS, AND OTHER PRESENTATIONS

1.   FCP Research Review Conference Presentations

        University Park, Pennsylvania   23 September 1976
        Atlanta, Georgia   4 October 1977

2.   Program Technical Review (FHWA, Washington Offices)
                        13-14 December 1976
        Participants:

        Craig Ballinger   FHWA
        Charles Galambos   FHWA
        Stan Gordon   FHWA
        Charles McGogney   FHWA
        Emile Paulette   FHWA
        Walter Podolney   FHWA
        John Barton   SwRI
        Felix Kusenberger   SwRI
        Anthony Leone   Consultant (SwRI)

3.   Program Technical Review (FHWA, Washington Offices)
                        18 March 1977
        Participants:

        Charles Galambos   FHWA
        Charles McGogney   FHWA
        Jerar Nishanian   FHWA
        Robert Varney   FHWA
        John Barton   SwRI

4.   Program Oral Review (Southwest Research Institute)
                        18-19 April 1977
        Participants:

        Charles McGogney   FHWA
        John Barton   SwRI
        Felix Kusenberger   SwRI
        Anthony Leone   Consultant (SwRI)

5. Program Design Review (Southwest Research Institute)
                        31 Aug. -1 Sept. 1977

    Participants:

    Charles McGogney   FHWA
    John Barton   SwRI
    Felix Kusenberger   SwRI
    Armando DeLosSantos   SwRI
    Ruell Solberg   SwRI
    Anthony Leone   Consultant (SwRI)

6. Field Site Conference (Salt Lake City, Utah)
                        11 November 1977

    Participants:

    C. McGogney   FHWA
    R. Sharp   FHWA
    R. Frost   FHWA
    M. Godfrey   FHWA

    R. Behling   Utah DOT
    A. Bloomfield   Utah DOT
    D. Christensen   Utah DOT
    P. Panos   Utah DOT
    A. Peikes   Utah DOT
    F. Bennet   Utah DOT

    F. Kusenberger   SwRI
    G. Ferguson   SwRI
    A. Leone   Consultant (SwRI)

7. Presentation (Southwest Research Institute)
                        11 January 1978

    Participants:

    N. Clary   FHWA
    G. Bolyard   FHWA
    H. Taylor   FHWA
    H. Gale   FHWA
    W. Lindsay   FHWA
    G. Love   FHWA
    J. Viner   FHWA
    J. Ahlskog   FHWA
    J. Wentworth   FHWA
    J. Hatton   FHWA

II-2

APPENDIX III

PERSONNEL CONTRIBUTING TO OVERALL PROGRAM EFFORT

The following personnel, listed according to organizational affiliation have provided guidance and have technically contributed to the subject program.

Department of Transportation
Federal Highway Administration

Washington Headquarters

C. Ballinger	C. McGogney
C. Galambos	J. Nishanian
M. Godfrey	E. Paulette
S. Gordon	W. Podolney
C. Hartbower	R. Varney

Region 4, Atlanta, Georgia

R. Hove

Region 8, Denver, Colorado

R. Sharp

Utah Division, Salt Lake City, Utah

R. Frost

State Departments of Transportation

Florida

H. Burns	J. Roberts
R. Rodriguez	

Utah

R. Behling	D. Christensen
F. Bennet	P. Panos
A. Bloomfield	A. Peikes

McDonough Brothers Incorporated

J. McDonough, Jr.

University of Florida

M. Self

Southwest Research Institute

A. DeLosSantos   A. Leone (Consultant)
G. Ferguson   R. Solberg

APPENDIX IV

FIELD EVALUATION CONDUCTED AT MANUFACTURED CONCRETE, INC.
SAN ANTONIO, TEXAS

A.   General

The field evaluations at Manufactured Concrete, Inc. in San Antonio,
Texas (formerly McDonough Brothers, Inc.) were undertaken subsequent
to the field work at Salt Lake City, Utah (see Section II. C. 1 of this report).
The decision to conduct a second field evaluation was based on the anomalous
signatures obtained from the post-tensioned girders on the Sixth South
Street Viaduct at Salt Lake City, and the related problems of interpreting
magnetic signature records for the detection of fracture and deterioration
of the prestressing steel elements. The anomalies were later correlated
with the presence of unanticipated steel elements. Importantly, the
selection of a second field test site was based on the availability of Texas
Type "C" girders for inspection since the laboratory work was conducted
on a 20-ft. (6m) test beam having the Type "C" configuration. This approach
would permit direct comparison of field inspection results with those
previously obtained in the laboratory. Fortunately, a large group of
80-ft. (24m) Type "C" girders were available at Manufactured Concrete,
Inc., the fabricators of the 20-ft.(6m) test beam used in the laboratory
study. Approval to handle and inspect the girders was obtained from the
State of Texas and the City of San Antonio by FHWA, and an inspection
schedule was immediately developed which was commensurate with the
short-term availability of the girders prior to their delivery to the customer
(City of San Antonio).

B.   Site Description

Figure IV-1 shows an overall view of the inspection site and girder
setup, provided through the excellent support of Manufactured Concrete, Inc.
Figure IV-2 shows a view of a Type "C" girder being installed
for inspection. The site layout accommodated the setup of three girders
simultaneously using available steel reinforced concrete blocks as temporary
piers to support each end of the 80-ft. (24m) girder approximately 5-ft. (1.5m)
above ground level. Girders were transported from the production storage
location to the test site and set up using the special handling equipment shown
in Figure IV-2. Subsequent to inspection, each girder was returned to storage.
Ten (10) 80-ft. (24m) span girders were inspected over approximately 60-ft.
(18m) of their span. Inspection, including transport of the inspection
equipment to the test site, initial setup, teardown, etc. was completed in a
5-day period. Figure IV-3 illustrates views of the inspection equipment
installed on each of two different girders, one of which was previously

FIGURE IV-1. OVERALL VIEW OF FIELD SITE AT MANUFACTURED CONCRETE, INC. (formerly McDonough Brothers, Inc., San Antonio, Texas) SHOWING THREE TYPICAL 80-FOOT (24m) TYPE "C" GIRDERS SET UP
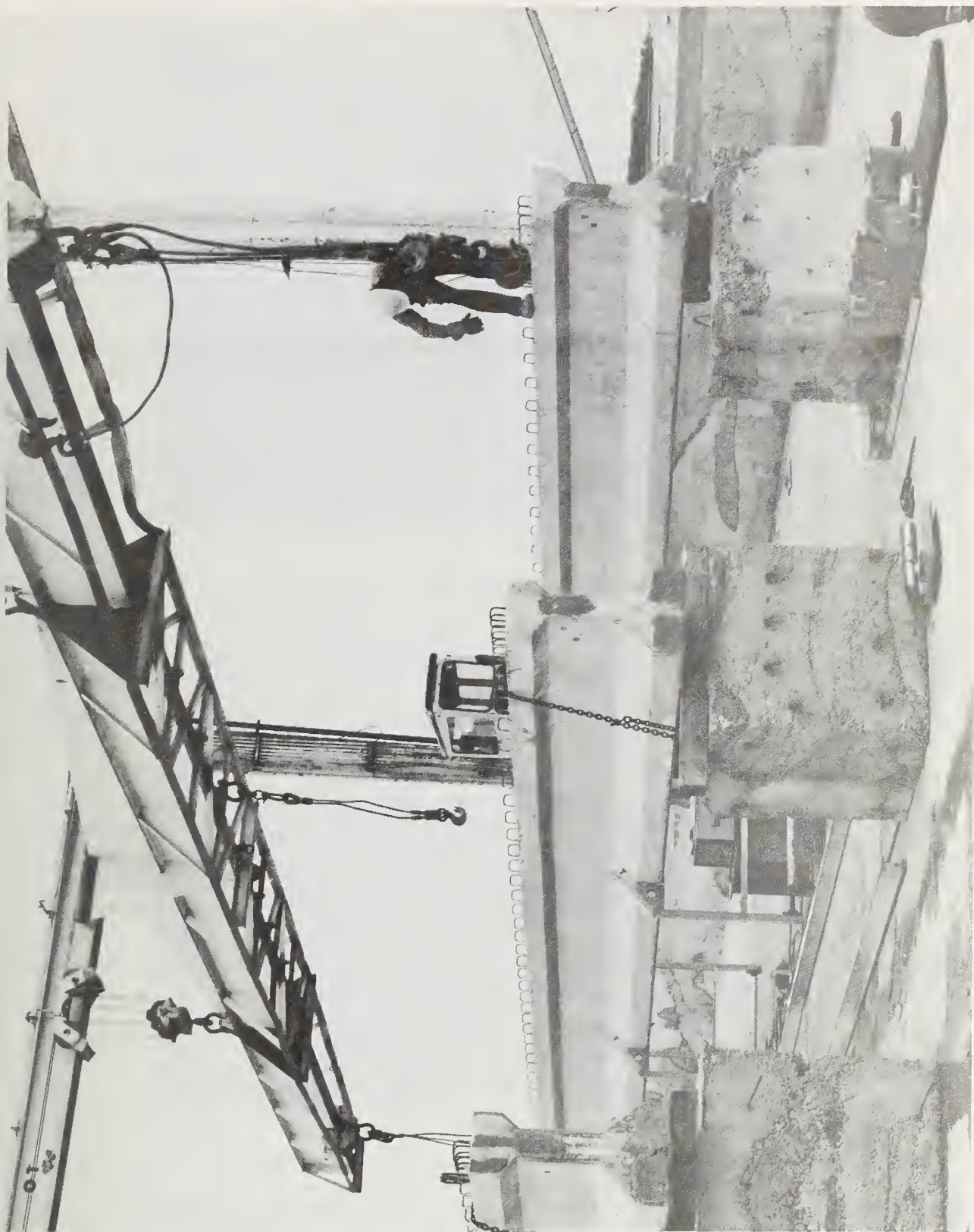
IV-2

FIGURE IV-2. VIEW OF 80-FOOT (24m) TYPE "C" GIRDER BEING SET UP FOR INSPECTION

IV-3

A. View of Typical Inspection Setup on Production Girder

B. View of Inspection Setup on Reject Girder

FIGURE IV-3. VIEWS OF MAGNETIC INSPECTION EQUIPMENT INSTALLED
ON GIRDERS AT MANUFACTURED CONCRETE, INC. (formerly
McDonough Brothers, Inc., San Antonio, Texas)

IV-4

rejected because of severe honeycomb type defects (see Figure IV-4). As will be explained in detail later in this section of the report, the reject girder was utilized for special tests in which strand deterioration and fracture and separation were simulated in the field. Figure IV-5 presents plans showing the structural details of the Texas Type "C" girders inspected. A comparison of the details in Figure IV-5 with those of the test beam in Figure 10 of the body of this report shows corresponding structural details, except that i) the center two columns of strands for the 80-ft. (24m) girders are draped while those of the test beam are not, and ii) the detailed configuration of the holdown fixtures in the two cases was different (not shown).

C. Inspection Procedures and Results

Typically, inspections were initiated approximately 8-ft. (2.4m) from one end of a girder and the first group of scans extended approximately 34-ft. (10m) along the length of the girder; this initial scan group was set up by using 24-ft. (7.6m) and 15-ft. (4.6m) track lengths placed end-to-end. Subsequently, the 25-ft. (7.6m) length of track was moved ahead of the 15-ft. (4.6m) track section and again placed end-to-end to facilitate an additional 34-ft. (10m) scan group overlapping the first scan group approximately 10-ft. (3m). In this manner, ~60-ft. (18m) of each 80-ft. (24m) girder was inspected. For each scan group, the inspection head was transversely positioned under each strand so that a total of 10 transverse locations at 2-in. (5cm) intervals was scanned. On records to be discussed, T = 2.0 is a scan track located coincident with the outermost strand in the flange; T = 4.0 is the adjacent strand, T = 6.0 the next adjacent, etc.

Figure IV-6 shows typical magnetic inspection records over approximately a 25-ft. (7.6m) length of scan on a production girder for four adjacent transverse scan tracks. Note the relatively smooth trace (absence of stirrups signals) in Record A at the top of Figure IV-6 and the increasing amplitude of the stirrup signals in Records B, C, and D. An examination of the structural details in Figure IV-5 indicates that the stirrups (R-bars) end beneath the lower row of pretensioned strand between the T = 4.0 and T = 6.0 (Records B and C) transverse positions; correspondingly, the signals from the stirrups (R-bars) are significantly more pronounced in Records C and D than they are for Records A (essentially no stirrup signature) and B (Figure IV-6). The plans specify a stirrup spacing of 1-ft. (30cm) and the records in Figure IV-6 indicate, typically, a 1-ft. (30cm) spacing although there is evidence of unequal spacing (see Record C). The records in Figure IV-6 indicate that the spacing between the bottom of the R-bar stirrup and the lower surface of the girder, i.e., coverage over the R-bar, is uniform because of the uniform amplitude of the stirrup signal.
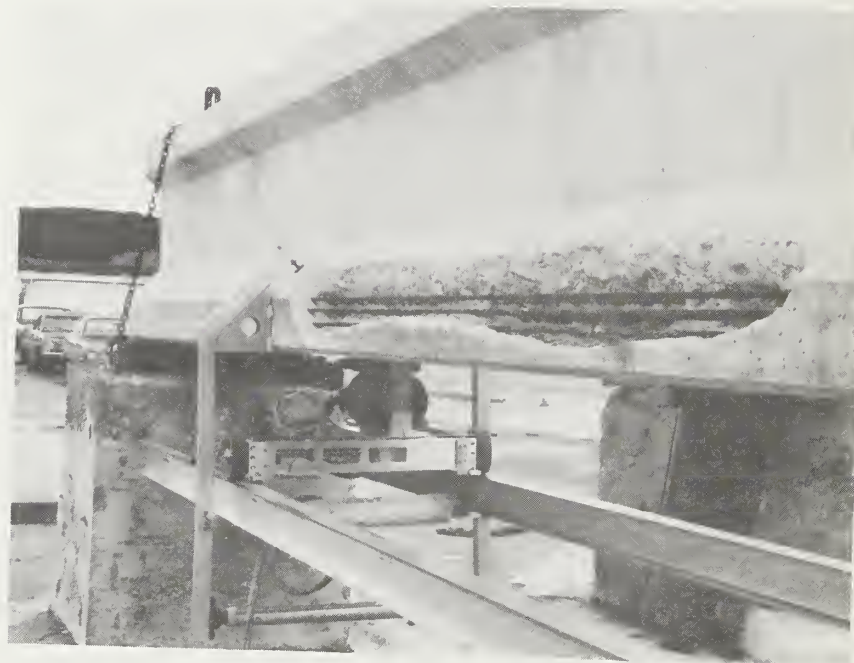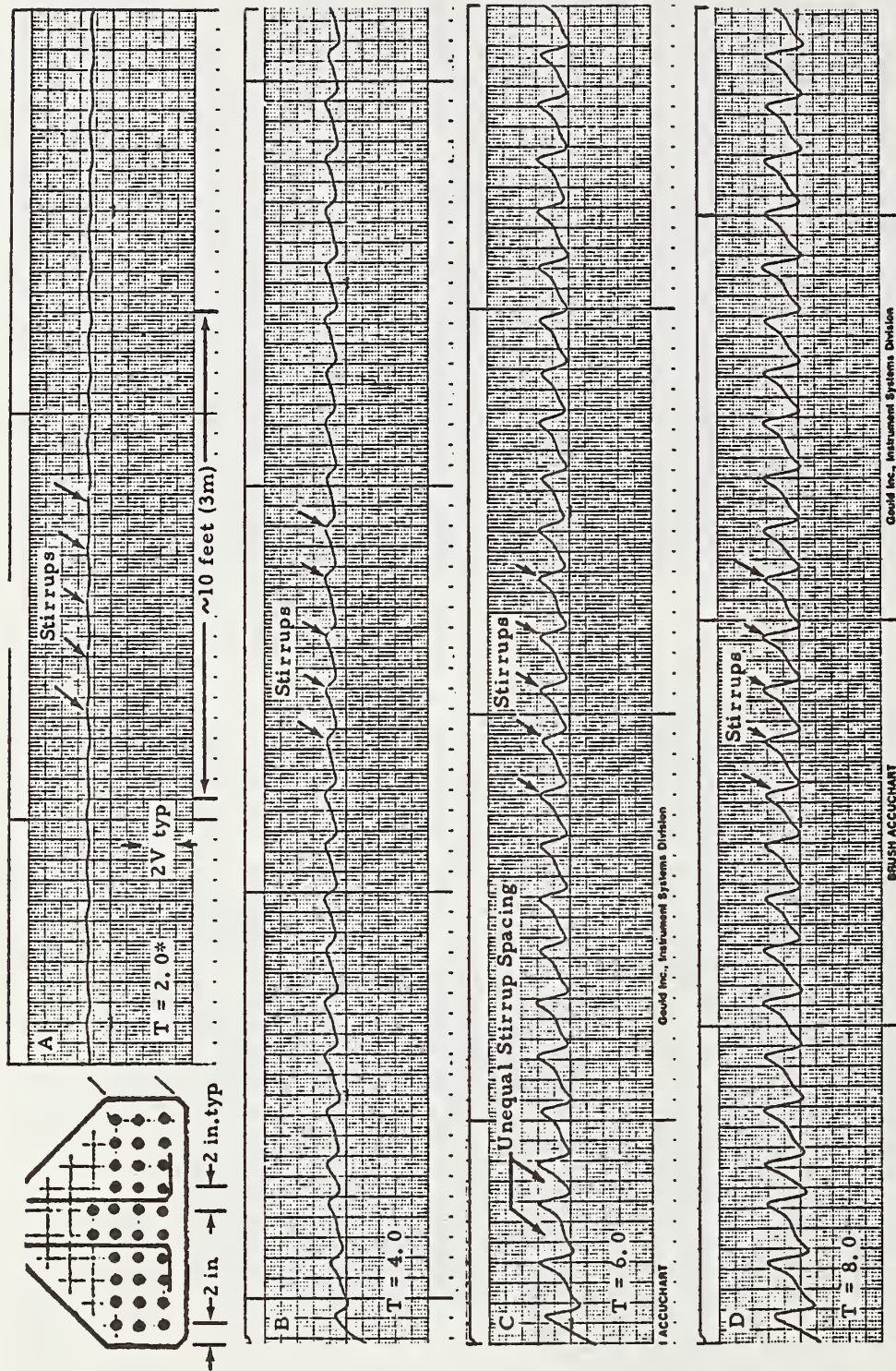
IV-5

FIGURE IV-4. VIEWS SHOWING "HONEYCOMB" AREAS ON REJECT
GIRDER [D-3(C-3A), Cast 7-26-77]

FIGURE IV-5. DRAWINGS FOR GIRDERS INSPECTED AT MANUFACTURED CONCRETE, INC.
(Formerly McDonough Brothers, Inc.)

FIGURE IV-6. TYPICAL MAGNETIC INSPECTION RECORDS FROM 80-FOOT (24m)[1]-TYPE "C" GIRDER AT MANUFACTURED CONCRETE, INC. (B-4C-5A, Cast 12-30-77).

* T = transverse position of scan from girder face, in inches; 1 in. = 2.54cm

Figure IV-7 presents selected inspection records near mid-length on another production girder showing unequal stirrup spacing in this region; this type of stirrup spacing pattern was noted on approximately 30% of the production girders inspected. Since the plans specify the quantity of R-bars (see Figure IV-5) it is anticipated that the closer R-bar spacing near mid-span on the girder represents the reduction in spacing necessary to achieve the total quantity specified; this condition undoubtedly results because of the accumulation of tolerances on the nominal 1-ft. (30cm) spacing of the R-bars during steel "tieup".

For purposes of comparison, Figure IV-8 illustrates typical magnetic inspection records from the laboratory test beam at transverse positions of 6.5, 8.5, and 10.5-in. (16, 22, 27-cm, respectively) from one face of that beam. A direct comparison of records from essentially the same transverse positions in the laboratory and the field (Figures IV-7 and IV-8) show good correspondence in the signature response from stirrups. The amplitude of the stirrup signatures in the case of the laboratory test beam (see Figure IV-8) appears to be slightly greater than that for the production girders; this is anticipated since the bottom of the R-bars for the test beam are slightly closer to the lower surface of the beam (less concrete coverage) because the pretensioned strand was housed in 9/16-in. (1.4cm) I.D. PVC tubing and the R-bars located against the O.D. of the PVC tubing (on production girders the R-bars are located against the bottom of the pretensioned strand). Again referring to Figures IV-7 and IV-8, specifically, Record C in each case, it is evident that the signature from the "holdown" for the production girder is lower in amplitude and different in shape to that obtained from the test beam. Investigation established that the physical configuration of the holdown in the test beam was different from that used in the production girders such that significantly different magnetic signatures would be anticipated.

As is evident from the foregoing discussions, there is excellent agreement between the results obtained in the laboratory from the 20-ft. (6m) section of Type "C" test beam and those obtained in the field from the 80-ft. (24m) production girders. In the case of the field girders, however, a few anomalous signatures were obtained at random locations on some girders which could not be correlated with any structural features on the manufacturing drawings. A typical example of such anomalous signatures is shown in Record B of Figure IV-9. Such anomalous signatures were also noted on the reject girder (girder containing the honeycomb defect) and the signature locations were physically marked on the girder. These locations were subsequently excavated using a pneumatic hammer - short pieces of 16-ga. soft iron wire were noted in each of the two locations excavated. Such wire is used to "tie" the transverse steel
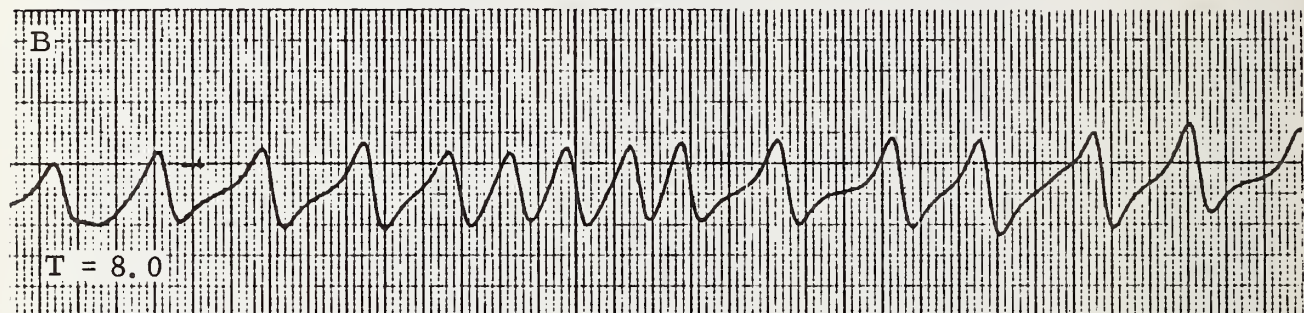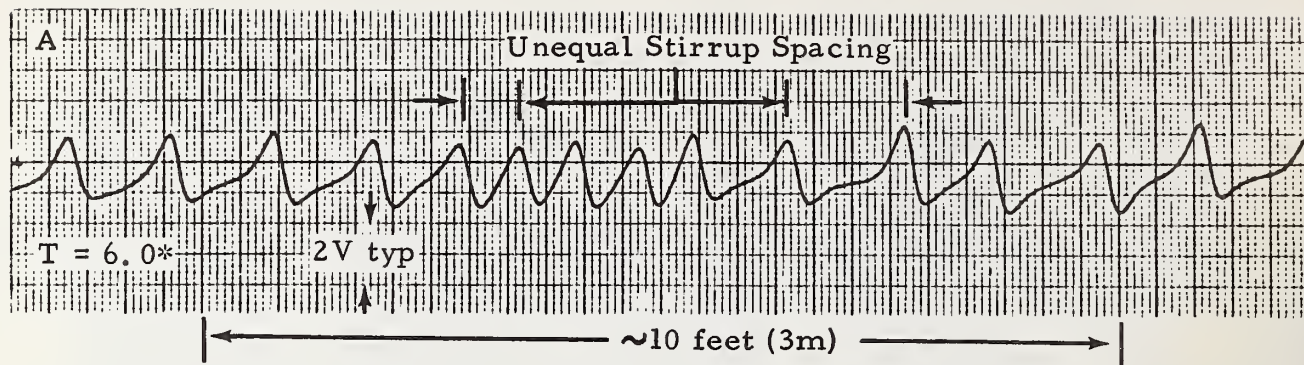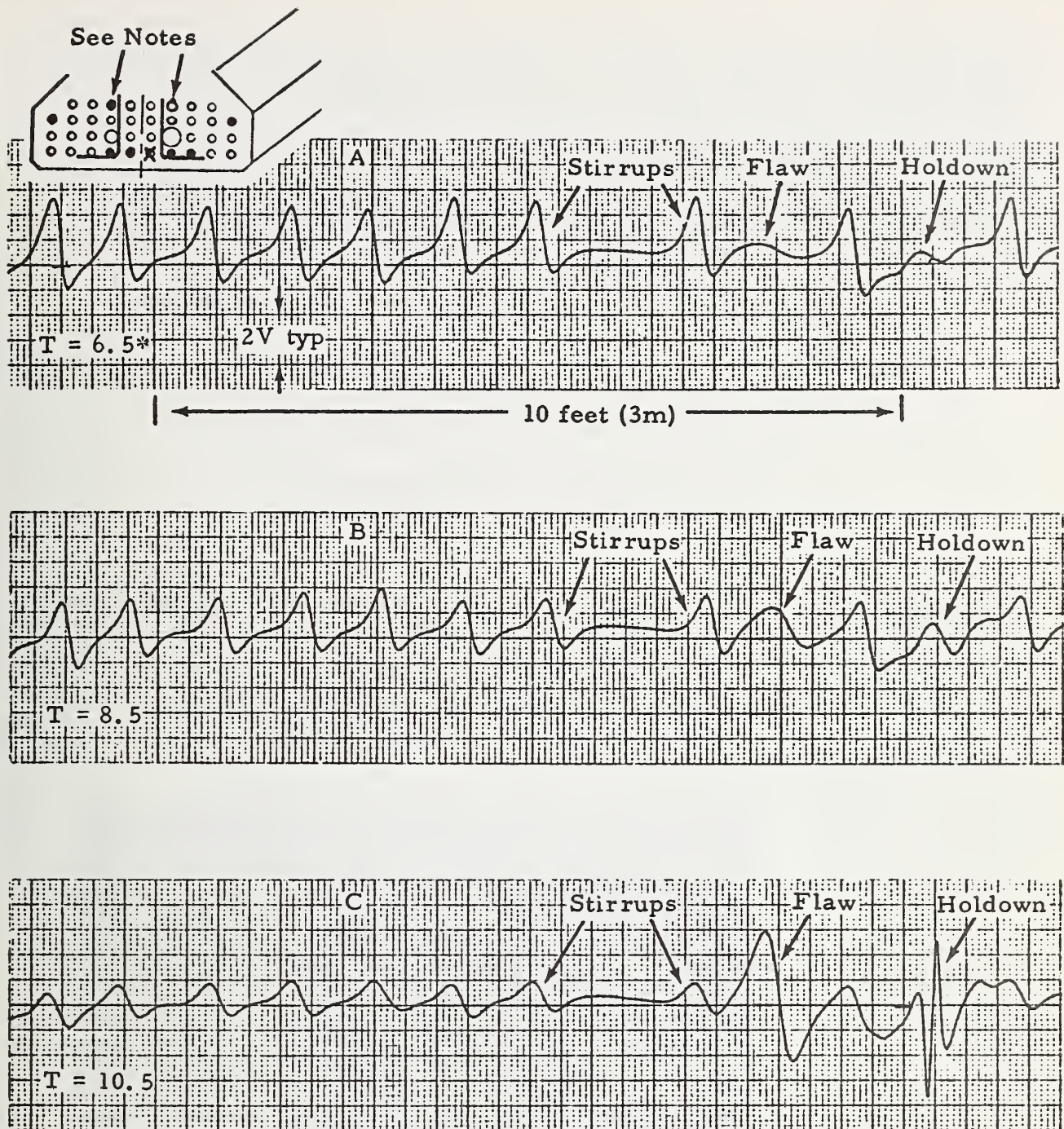
IV-9
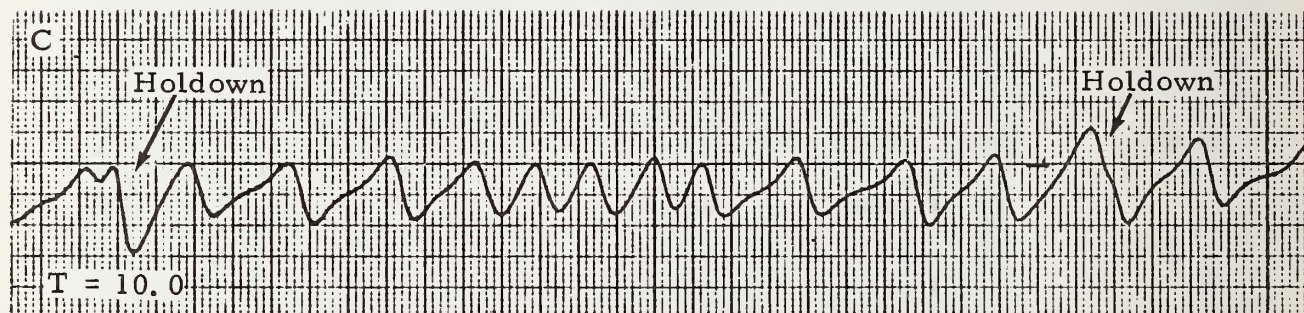
* T = Transverse position of scan from girder face, in inches;
   1 in. = 2.54cm

FIGURE IV-7.MAGNETIC INSPECTION RECORDS FROM 80-FOOT (24m)
          TYPE "C" GIRDER SHOWING "STIRRUP" AND "HOLDOWN"
          SIGNATURES NEAR CENTER OF GIRDER (C-2C-2A,
   Cast 12-29-77)

Notes: x Flawed strand - 6 of 7 wires removed over 2 in. length
  • Unflawed strand
  * T = Transverse position of scan from girder face in
     inches; 1 in. = 2.54cm

FIGURE IV-8. TYPICAL MAGNETIC INSPECTION RECORDS IN THE LABORA-
   TORY FROM TYPE "C" TEST BEAM, 20-FOOT (6m) SECTION

IV-11

A. Signatures from Soft Iron "Tie Wire" (16 ga) Mockup Tests on Girder

Longitudinal Axis of Girder
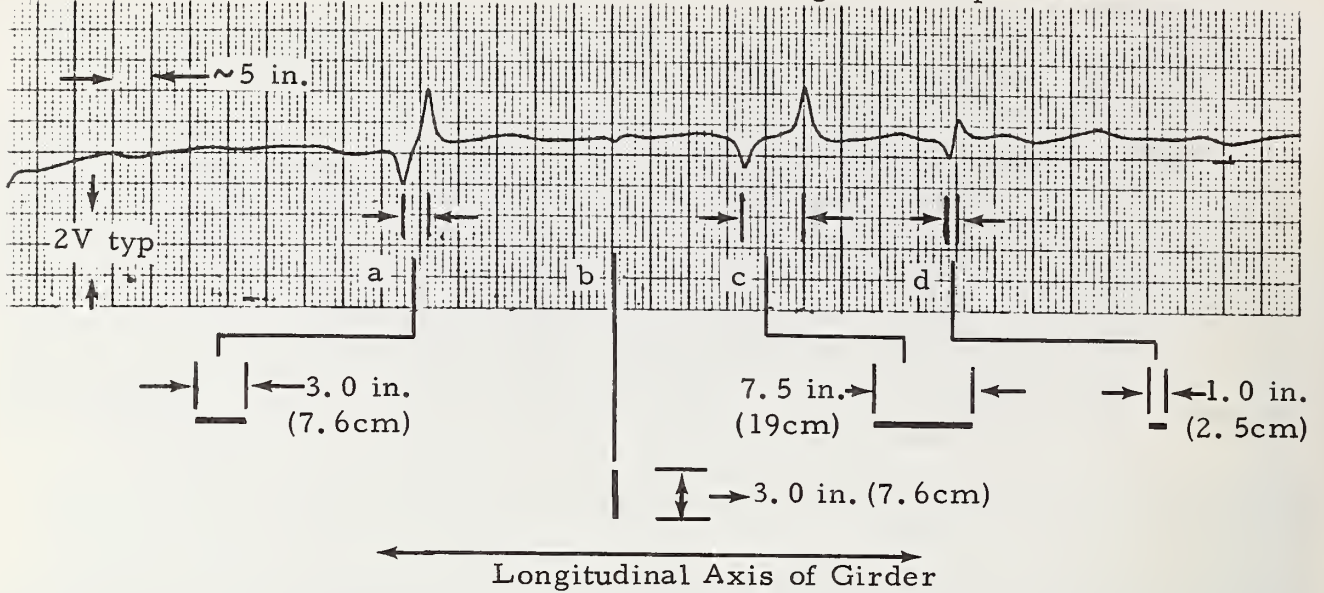
B. Signature Corresponding to Visual Indication of "Tie Wire" Scrap
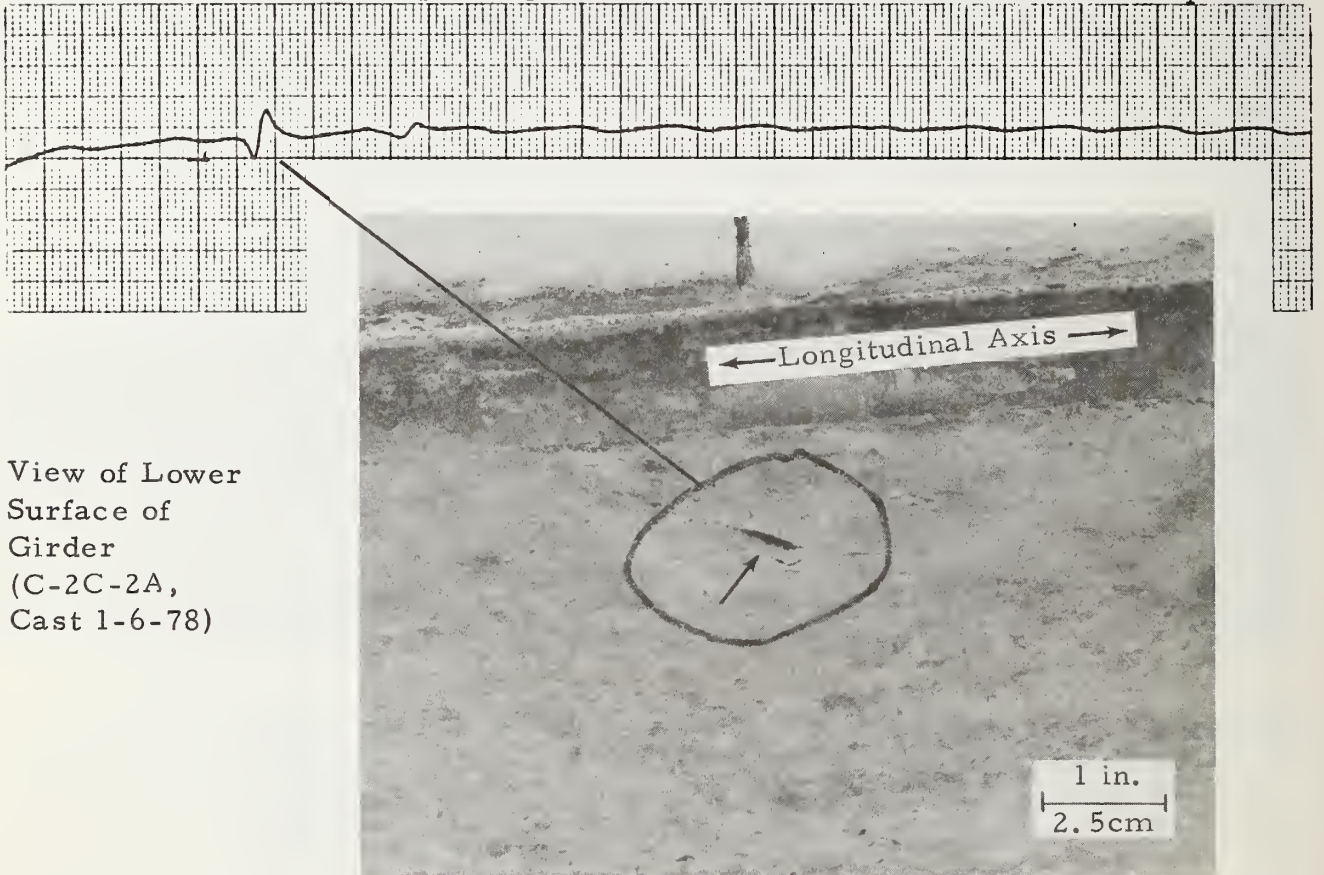
View of Lower
Surface of
Girder
(C-2C-2A,
Cast 1-6-78)

FIGURE IV-9. MAGNETIC SIGNATURES FROM SOFT IRON "TIE WIRE"
SCRAP PIECES CAST IN LOWER SURFACE OF GIRDER

IV-12

to the prestressing steel during fabrication, the excess wire is cut off, and the soffit is cleaned with a jet of air to remove the scrap. The tie wire scraps were located very near the surface but were covered with a very thin coating of concrete. In subsequent inspections of other girders, visual inspection at locations corresponding to such signatures as those shown in Record B of Figure IV-9, disclosed, in some cases, the presence of wire scrap; one such case is illustrated by the photograph and record at the bottom of Figure IV-9.

To further confirm signature features from such sources as wire scrap, mockup tests were conducted near the honeycomb end of the reject girder by attaching known lengths of wire in each of two orientations along the bottom surface of the girder; subsequently, an inspection scan was made over the path of the specimens. Record A at the top of Figure IV-9 illustrates the results obtained from various lengths of "tie wire" scrap ranging from 1-in. (2.5cm) to 7.5-in. (19cm) in each of two orientations with respect to the longitudinal axis of the girder. The signature from wire "d" (1-in., 2.5cm, length) correlates well with the more dominant signature shown in Record B below in the same figure. Note that signatures from samples "a" and "c" indicate that the horizontal distance between the downward- and upward-going peaks appear to correlate well with the length of the sample. Also note that in the case of the sample oriented transverse to the axis of the girder (and scan direction) wire "b", a very small signature amplitude is obtained compared to that from the same sample length but oriented parallel to the axis of the girder (wire "a"). Continuing to examine the data in Figure IV-9, Record A, it is pointed out that the signature polarity (as viewed from left-to-right) is downward-going and then upward-going which is opposite to that obtained from a deterioration type flaw (fracture or loss-of-section). This "opposite polarity" type signal is indicative of the presence of a piece of ferromagnetic material (iron or steel) with no connecting ferromagnetic material in the immediately adjacent region. Importantly, the evaluation of these signatures, including the details of their features, would be considerably more difficult if they were located in a transverse position where larger amplitude stirrup signatures were present.

Field evaluations were also conducted on simulated fracture, and loss-of-section in strand using the reject girder. Concrete was excavated from the region surrounding a pretensioned strand at several locations; subsequently, an acetylene torch was used to either completely cut through a strand to simulate a separated fracture or to partially cut a strand section to simulate loss-of-section due to corrosion. Photographs

IV-13

of the typical flaws fabricated are shown in Figure IV-10, and the corresponding magnetic signatures obtained from scanning these regions are shown in Figures IV-11 and IV-12. Magnetic records were also obtained before flaw fabrication. Figure IV-11 shows typical results obtained from flaws "a", "b", and "c". Results obtained from the flaws fabricated in the production type girder containing pretensioned strands are in good agreement with the laboratory results obtained from the test beam containing <u>untensioned</u> strand. It is pointed out in Record A of Figure IV-11 that the horizonal distance between the upward-going and downward-going peaks (peak separation) from flaw "a" is greater than that from flaw "c" in Record B of the same figure, as was anticipated, since flaw "a"is in a second-row strand while flaw "c" is in a first-row strand (see sketch at upper left in Figure IV-11). Note the signatures from the scrap wire pointed out in Record B; these signals were present before the flaws were fabricated as shown in Record C. It is also pointed out that as the inspection head is transversely positioned beneath strands adjacent to the flawed strand, the flaw signature becomes correspondingly smaller in amplitude as anticipated. Figure IV-12 shows additional results, from flaws "d" and "e", both simulating strand fracture with end separation of approximately 1-in. (2.5cm). Again, these results are in agreement with those previously obtained in the laboratory. Note the difficulty of recognizing the presence of flaw signatures on scan records for the various scan track locations (transverse) where the stirrup signature amplitudes are significant (see Records A and B in Figure IV-12).

D.   Cursory Flaw Signature Enhancement Investigations

        The one-week evaluation conducted at Manufactured Concrete, Inc. on ten unerected girders dramatically demonstrated the inherent capabilities of the magnetic method to assess configurational features and the structural condition of the prestressing steel in concrete bridge beams. These recent evaluations, however, also confirm the need for signature enhancement and signature analyses if the full potential of the magnetic method is to be realized. Because of continuing interest in our nation's bridge inspection problems and confidence in the capabilities of the magnetic method for the inspection of prestressed concrete bridge structural members, Southwest Research Institute undertook cursory signature enhancement investigations with the approval of and at no cost to the Government. These investigations and the encouraging results obtained are briefly summarized below.
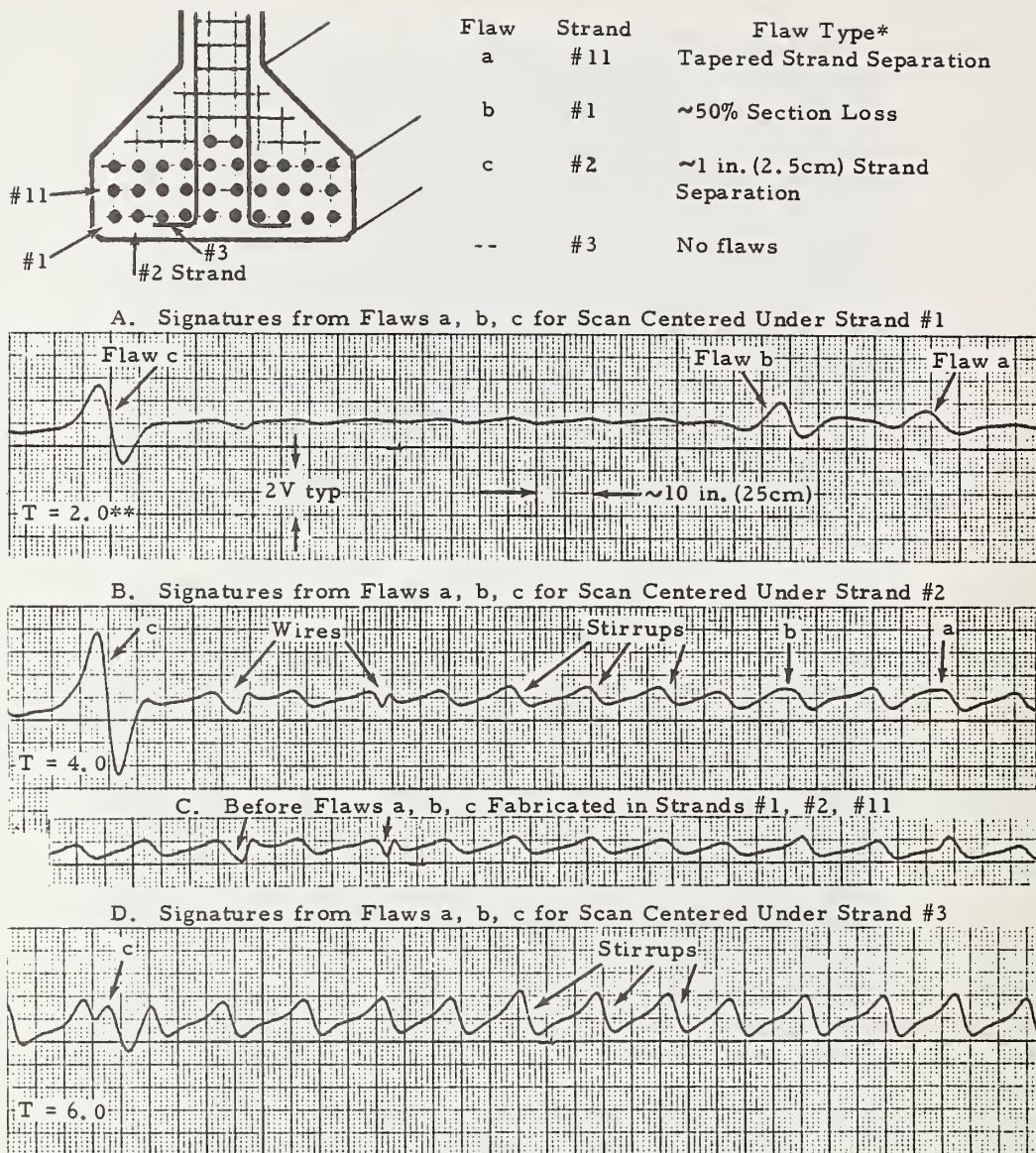
A. Flaw a - Tapered Strand Separation

B. Flaw b - ~50% Strand Section Loss

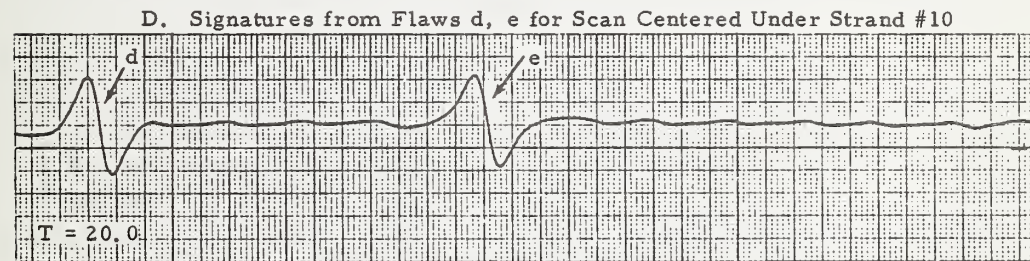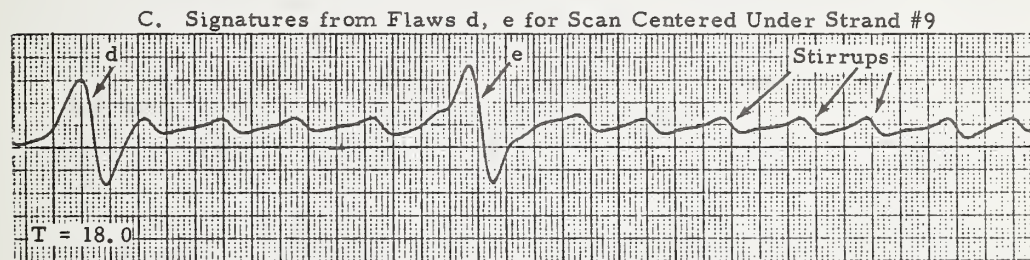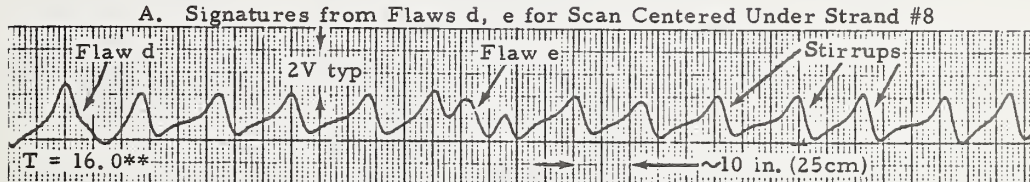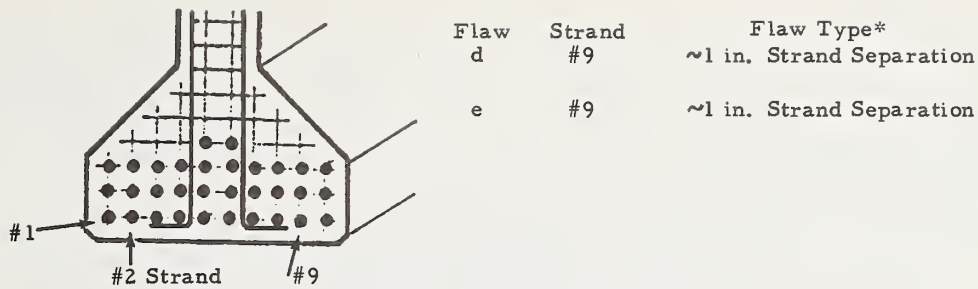C. Flaws c, d, e - ~1 in. Strand Separation

Note: See Figure IV-11 and IV-12 for magnetic signatures from flaws

FIGURE IV-10. PHOTOGRAPHS OF FLAWS FABRICATED IN PRETENSIONED
STRANDS OF REJECT GIRDER [D-3(C-3A), Cast 7-26-77]

FIGURE IV-11. MAGNETIC RECORDS SHOWING SIGNATURES FROM FLAWS FABRICATED IN STRANDS OF REJECT GIRDER [D-3(C-3A), Cast 7-26-77]

Flaw	Strand	Flaw Type*
d	#9	~1 in. Strand Separation
e	#9	~1 in. Strand Separation

A. Signatures from Flaws d, e for Scan Centered Under Strand #8

Flaw d   2V typ   Flaw e   Stirrups

T = 16.0**   ~10 in. (25cm)

B. Before d, e Fabricated in Strand #9

C. Signatures from Flaws d, e for Scan Centered Under Strand #9

d   e   Stirrups

T = 18.0

D. Signatures from Flaws d, e for Scan Centered Under Strand #10

d   e

T = 20.0

Notes: *   See Figure IV-10 for photographs of flaws
       ** T = Transverse position of scan from face of girder,
           in inches; 1 in. = 2.54cm

FIGURE IV-12. MAGNETIC RECORDS SHOWING SIGNATURES FROM FLAWS
FABRICATED IN STRANDS OF REJECT GIRDER [D-3(C-3A),
Cast 7-26-77]

IV-17

The signature enhancement investigations were aimed at evaluating the configurational characteristics of plant-produced Type "C" girders; namely, the periodic, uniform amplitude which is characteristic of stirrup signatures and the low amplitude of stirrup signatures for scans beneath the outermost strands (e.g., record A, for T = 2.0, Figure IV-6) were considered. Tests were conducted on the laboratory Texas Type "C" test beam for 1/2-in. (1.3cm) strand containing manufactured flaws inserted in the T = 2.0 location; the results of these tests are shown in Figure IV-13. The top record in Figure IV-13 shows the stirrup signatures obtained over an 8-ft. (2.4m) scan with a vertical sensitivity ten times greater than that normally used in previous laboratory and field test data recording. The gentle downward curvature of the baseline from left to right in all records of Figure IV-13 results from magnetic "end effects". The second record from the top in Figure IV-13 shows the signatures obtained from flaws manufactured in one wire of 7-wire strand; importantly, flaw B, a fractured wire (simulated) with an end separation of only 0.05-in. (∿1.25mm), is detectable with prior knowledge of the stirrup signatures (compare records A and B in Figure IV-13 for "before" and "after" flaw conditions, respectively). The record B of Figure IV-13 shows also that a fractured wire with 0.25-in. (6.3mm) end separation (flaw A) is readily recognizable in the presence of the periodic stirrup signatures of lower uniform amplitude. Record C in Figure IV-13 illustrates that signatures from more subtle flaws which simulate minimal corrosion deterioration are almost undetectable. Record D in Figure IV-13 shows the outstanding signature obtained from a more severe simulated flaw at the significantly increased sensitivity used in this test. Photographs of flaws A, B, and E are shown in Figure IV-14.

Certainly, the flaw signatures in Figure IV-13 illustrate the excellent sensitivity of the magnetic method where there is minimal influence from structural steel details such as stirrups. Signature enhancement tests were also conducted on the higher sensitivity data previously presented in Figure IV-13. Such tests consisted of digitizing the signatures from scanning an unflawed strand and flawed strands (containing flaws A and B) and, subsequently, subtracting the two scans point-by-point (hereafter referred to as a "differencing process"). Reconstructed analog versions of the digitized scan data before and after the "differencing process" are illustrated in Figure IV-15. The lower trace shows that the fracture of a single wire in a 7-wire strand with an end separation of 0.05-in. (∿1.25mm) is readily detectable and illustrates the potential improvements which could be achieved by further reducing the influence of stirrup signatures through application of modern data processing techniques.

A modification of the "differencing process" was applied also to field data records from the evaluations conducted at Manufactured Concrete, Inc. and these results are very encouraging. Strip chart recordings from the reject
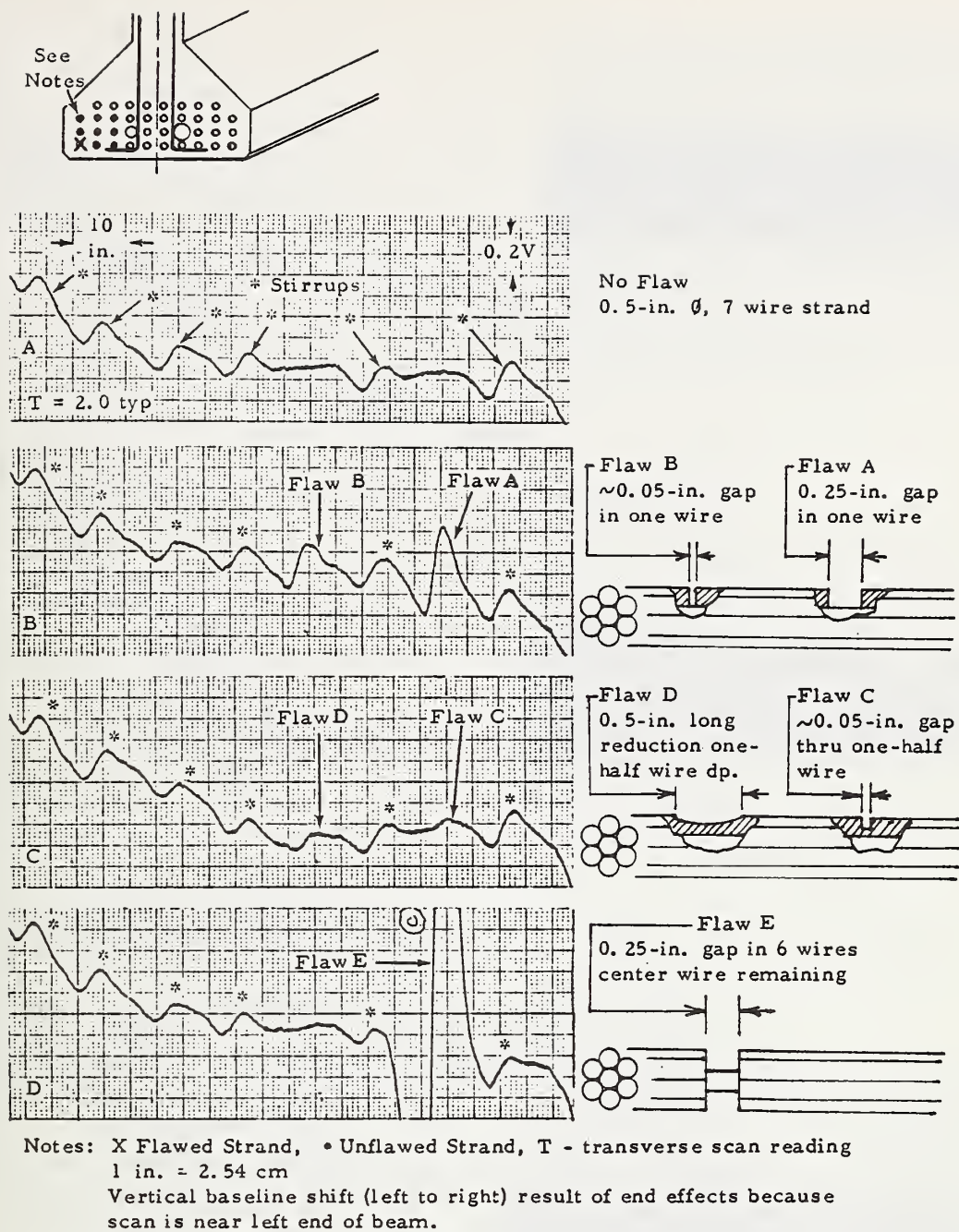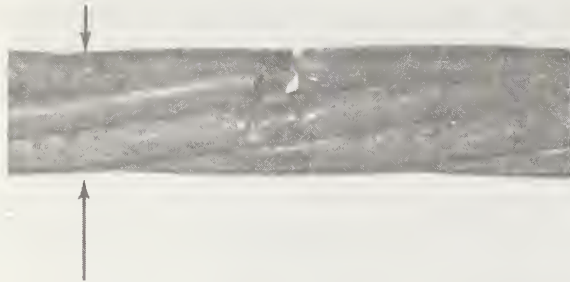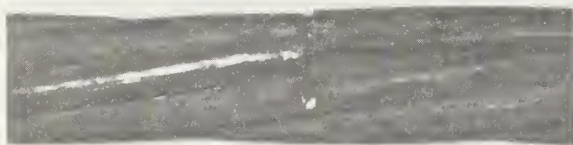
IV-18

Notes: X Flawed Strand, • Unflawed Strand, T - transverse scan reading
1 in. ≈ 2.54 cm
Vertical baseline shift (left to right) result of end effects because
scan is near left end of beam.

FIGURE IV-13.   HIGH SENSITIVITY MAGNETIC RECORDS
ILLUSTRATING INFLUENCE OF STIRRUP
SIGNATURES ON DETECTION OF SMALL
FLAWS

IV-19

0.5-in. (1.3cm) diameter, typ.

Flaw A

1/4-in. (0.64cm) Gap
in 1 Wire

Flaw B

Saw Cut, ∼ 0.05-in.
(∼ 0.13cm) Gap in
1 Wire

Flaw E

1/4-in. (0.64cm) Gap
in 6 Wires

See Figure IV-13 for flaw signatures

FIGURE IV-14.   PHOTOGRAPHS OF TYPICAL FLAWS
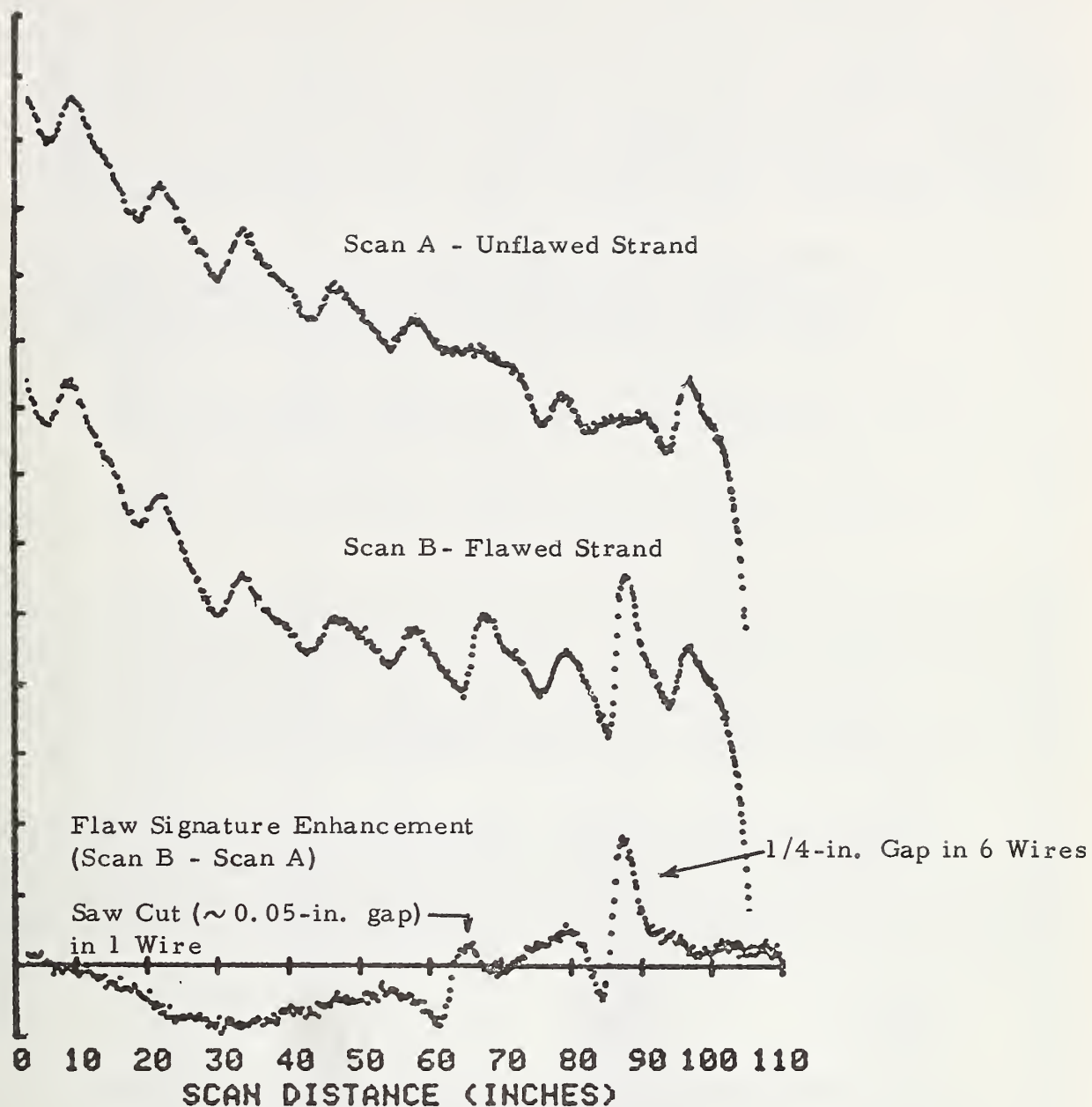FABRICATED IN 7-WIRE STRAND

IV-20

FIGURE IV-15.   DIGITIZED HIGH SENSITIVITY RECORDS SHOWING
SIGNATURE ENHANCEMENT FOR SMALL FLAWS

IV-21

girder, after the introduction of flaws, were digitized in the laboratory for scans at five different transverse locations. A reproduction of the reconstructed digitized signatures are presented in Figure IV-16; comparison of these records for T = 2.0, 4.0 and 6.0 with the original analog records previously shown in Figure IV-11 illustrates the fidelity of the digitized signature. A reproduction of the digitized signatures from T = 6.0 and 8.0 is repeated at the top of Figure IV-17 for reference purposes in the following discussion. The modified differencing process consisted of:

i) adjusting the vertical amplitude of the T = 6.0 record, on a point-by-point basis, such that the average amplitude of the stirrup signatures was equal to that for the stirrup signatures from the adjacent scan location, T = 8.0;

ii) subsequently the T = 8.0 record was subtracted, point-by-point, from the normalized T = 6.0 record; and

iii) the result was reconstructed in analog form as shown at the bottom of Figure IV-17.

This bottom record in Figure IV-17 illustrates a dramatic increase in the detectability of a flaw signature; compare the signature pointed out by the arrow in the lower record of Figure IV-17 with the corresponding signature in the top record of the same figure. Importantly, these signature enhancement results were obtained on field data without prior knowledge of the "before flaw" condition.

Although the recent signature enhancement investigations described above were limited, the results obtained are extremely encouraging and illustrate the significant potential improvements in capability of the magnetic method to assess deterioration of the prestressing steel in concrete bridge structural members.

E.   Summary

A comparison of the overall signature response was obtained between production Type "C" girders in the field using the magnetic inspection equipment with those obtained from a Type "C" test beam in the laboratory. The agreement was excellent. Such signature agreement is noted for the response from the overall configuration of the structural steel elements as well as for response from simulated flaws (fracture and loss-of-section). Signatures obtained on production girders not previously observed from the laboratory test beam are the result of either the presence of minor, superfluous, non-structural items (wire scrap) or holdowns of a different physical configuration which produce a different magnetic response. The results of recent signature enhancement investigations are very encouraging and provide a viable approach for improving the magnetic detection of flaws in the pretensioning strands of Type "C" girders.
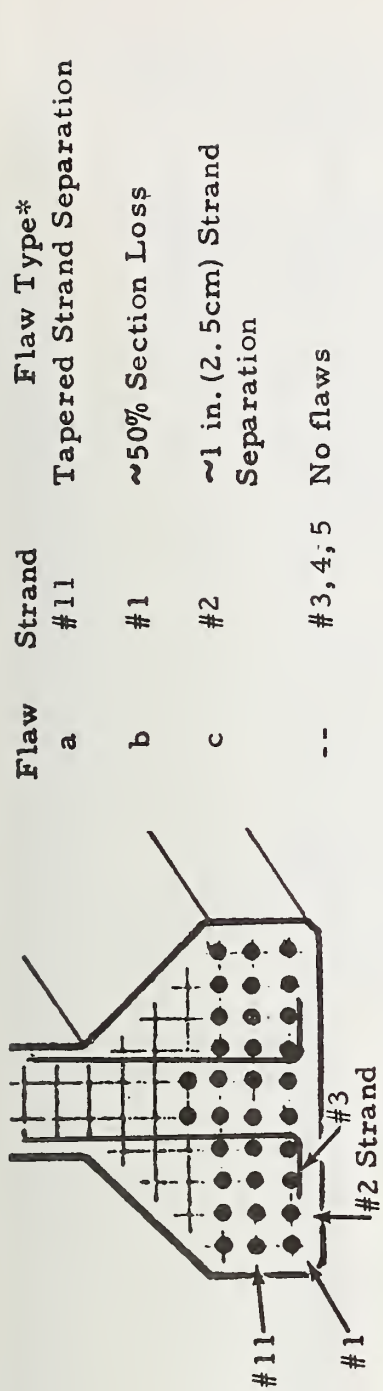
Flaw	Strand	Flaw Type*
a	#11	Tapered Strand Separation
b	#1	~50% Section Loss
c	#2	~1 in. (2.5cm) Strand Separation
--	#3,4,5	No flaws

Digitized Signatures for scans centered under Strands #1, #2, #3, #4, and #5
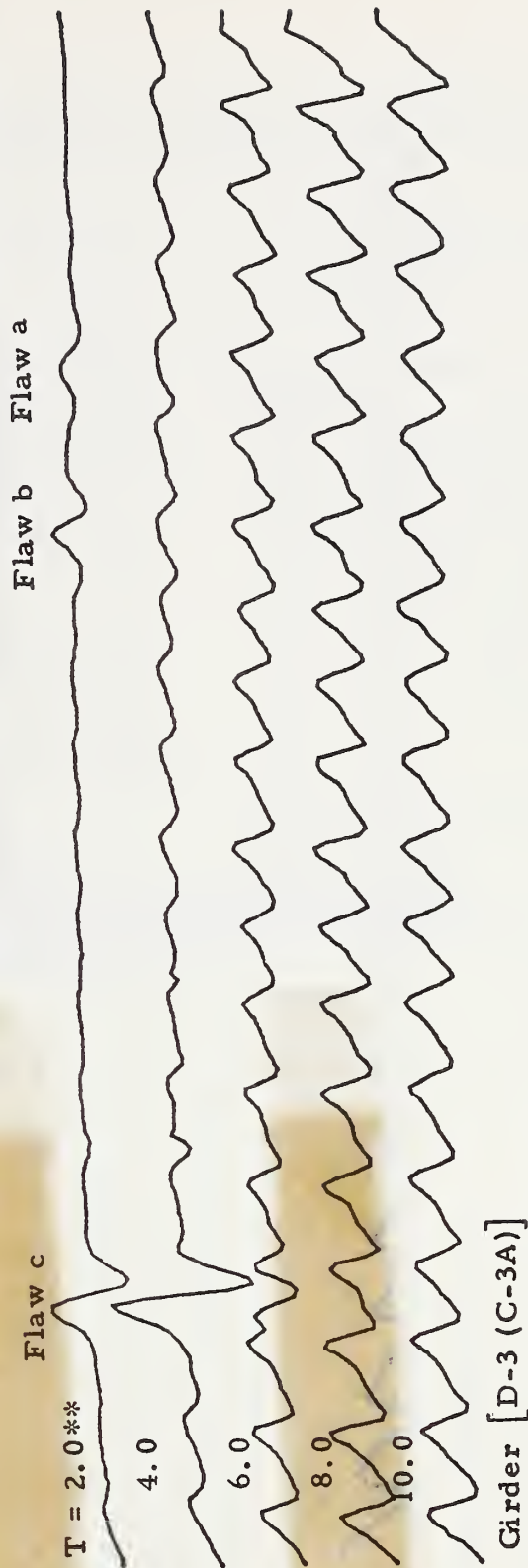
Girder [D-3 (C-3A)]

Notes: * See Figure IV-10 for photographs of flaws

      ** T = Transverse position of scan from face of girder, in inches; 1 in. = 2.54cm

FIGURE IV-16. DIGITIZED SIGNATURES FROM FLAWED AND UNFLAWED STRANDS OF REJECT GIRDER [D-3 (C-3A), Cast 7-26-77]

IV-23

Signatures "Before" Enhancement

Signature "After" Enhancement

T = 6.0**

Girder [D-3 (C-3A)]

Notes: * Arrows indicate flaw signature; all other signals are from stirrups
        ** T = Transverse position of scan from face of girder in inches (1 in. = 2.54cm);
        see Figure IV-16

FIGURE IV-17. SMALL FLAW SIGNATURE "BEFORE" AND "AFTER" ENHANCEMENT

Form DOT F 1720.2
FORMERLY FORM DOT F 17

TE 662 .A
81-08
Kusenberge
Detection
reinforci

FEDERALLY COORDINATED PROGRAM (FCP) OF HIGHWAY RESEARCH AND DEVELOPMENT

The Offices of Research and Development (R&D) of the Federal Highway Administration (FHWA) are responsible for a broad program of staff and contract research and development and a Federal-aid program, conducted by or through the State highway transportation agencies, that includes the Highway Planning and Research (HP&R) program and the National Cooperative Highway Research Program (NCHRP) managed by the Transportation Research Board. The FCP is a carefully selected group of projects that uses research and development resources to obtain timely solutions to urgent national highway engineering problems.*

The diagonal double stripe on the cover of this report represents a highway and is color-coded to identify the FCP category that the report falls under. A red stripe is used for category 1, dark blue for category 2, light blue for category 3, brown for category 4, gray for category 5, green for categories 6 and 7, and an orange stripe identifies category 0.

FCP Category Descriptions

1. **Improved Highway Design and Operation for Safety**

    Safety R&D addresses problems associated with the responsibilities of the FHWA under the Highway Safety Act and includes investigation of appropriate design standards, roadside hardware, signing, and physical and scientific data for the formulation of improved safety regulations.

2. **Reduction of Traffic Congestion, and Improved Operational Efficiency**

    Traffic R&D is concerned with increasing the operational efficiency of existing highways by advancing technology, by improving designs for existing as well as new facilities, and by balancing the demand-capacity relationship through traffic management techniques such as bus and carpool preferential treatment, motorist information, and rerouting of traffic.

3. **Environmental Considerations in Highway Design, Location, Construction, and Operation**

    Environmental R&D is directed toward identifying and evaluating highway elements that affect the quality of the human environment. The goals are reduction of adverse highway and traffic impacts, and protection and enhancement of the environment.

4. **Improved Materials Utilization and Durability**

    Materials R&D is concerned with expanding the knowledge and technology of materials properties, using available natural materials, improving structural foundation materials, recycling highway materials, converting industrial wastes into useful highway products, developing extender or substitute materials for those in short supply, and developing more rapid and reliable testing procedures. The goals are lower highway construction costs and extended maintenance-free operation.

5. **Improved Design to Reduce Costs, Extend Life Expectancy, and Insure Structural Safety**

    Structural R&D is concerned with furthering the latest technological advances in structural and hydraulic designs, fabrication processes, and construction techniques to provide safe, efficient highways at reasonable costs.

6. **Improved Technology for Highway Construction**

    This category is concerned with the research, development, and implementation of highway construction technology to increase productivity, reduce energy consumption, conserve dwindling resources, and reduce costs while improving the quality and methods of construction.

7. **Improved Technology for Highway Maintenance**

    This category addresses problems in preserving the Nation's highways and includes activities in physical maintenance, traffic services, management, and equipment. The goal is to maximize operational efficiency and safety to the traveling public while conserving resources.

0. **Other New Studies**

    This category, not included in the seven-volume official statement of the FCP, is concerned with HP&R and NCHRP studies not specifically related to FCP projects. These studies involve R&D support of other FHWA program office research.